WNT signalling driven up-regulation of microRNAs in medulloblastoma

By

Mr. Kedar Yogi

[LIFE09200904006]

Tata Memorial Centre (TMC),
Kharghar, Navi Mumbai – 410210.

A thesis submitted to the
Board of Studies in Life Sciences
In partial fulfilment of requirements

For the Degree of
DOCTOR OF PHILOSOPHY
Of
HOMI BHABHA NATIONAL INSTITUTE

April 2016

HOMI BHABHA NATIONAL INSTITUTE

Recommendations of Viva Voce Committee

As members of Viva Voce committee we certify that we have read the dissertation prepared by Mr. Kedar Narsinha Yogi entitled "WNT signalling driven up-regulation of microRNAs in medulloblastoma" and recommend that it may be accepted as fulfilling the thesis requirement for the award of Degree of Doctor of Philosophy.

S.N. Dalal — 20/4/2016

Chairman: Dr. Sorab Dalal — Date:

Shirsat — 20/4/2016

Guide: Dr. Neelam Shirsat — Date:

Sanjay Gupta — 20/4/16

Member: Dr. Sanjay Gupta — Date:

Pritha Ray — 20.4.16

Member: Dr. Pritha Ray — Date:

K. Somasundaram — 20/04/16

External Examiner: Dr. K. Somasundaram — Date:

Final approval and acceptance of thesis is contingent upon candidate's submission of final copies of thesis to HBNI.

I/We hereby certify that I/We have read this thesis prepared under my/our direction and recommend that it may be accepted as fullfulling the thesis requirement.

Date: 20th Apr. 2016

Place: Navi Mumbai

Shirsat

Signature

Dr. Neelam Shirsat

STATEMENT BY AUTHOR

This dissertation has been submitted in partial fulfilment of requirements for an advanced degree at Homi Bhabha National Institute (HBNI) and is deposited in the Library to be made available to borrowers under rules of the HBNI. Brief quotations from this dissertation are allowable without special permission, provided that accurate acknowledgement of source is made. Requests for permission for extended quotation from or reproduction of this manuscript in whole or in part may be granted by the Competent Authority of HBNI when in his or her judgment the proposed use of the material is in the interests of scholarship. In all other instances, however, permission must be obtained from the author.

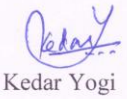

Kedar Yogi

Date: 20/4/2016

Place: Navi Mumbai

DECLARATION

I, hereby declare that the investigation presented in the thesis has been carried out by me. The work is original and has not been submitted earlier as a whole or in part for a degree /diploma at this or any other Institution / University.

Kedar Yogi

Date: 20/4/2016

Place: Navi Mumbai

List of Publications arising from the thesis

Article:

1. MiR-148a, a microRNA upregulated in the WNT subgroup tumors, inhibits invasion and tumorigenic potential of medulloblastoma cells by targeting Neuropilin1

Kedar Yogi, Epari Sridhar, Naina Goel, Rakesh Jalali, Atul Goel, Ali Asgar Moiyadi, Rahul Thorat, Pooja Panwalkar, Atul Khire, Archya Daspgupta, Prakash Shetty, and Neelam Vishwanath Shirsat, **Oncoscience**. 2015 Mar 2; 2(4):334-48. eCollection 2015. PMID: 26097868

Conferences:

1. **Participated and presented** abstract titled '**Role of miR-148a up-regulated in WNT subgroup medulloblastomas**' as a poster presentation at **XXXVI All India Cell Biology Conference and International Symposium on "Stress Adaptive Response and Genome Integrity (SARGI)** held on 17-19th October 2012 at Bhabha Atomic Research Centre (BARC), Mumbai

2. **Participated and presented** abstract titled **'Role of miR-148a in WNT subgroup Medulloblastoma'** as an **oral presentation** at **9th National Research Scholars Meet in Life Sciences (NRSM)** held at Advanced Centre for Treatment, Research and Education in Cancer (ACTREC) on 18-19th December 2014

3. **Participated and presented** abstract titled **'miR-148a functions as tumour-suppressor microRNA in medulloblastoma cell lines by targeting Neuropilin1'**, **as a poster presentation** at **AACR special series conference "Advances in Brain Cancer Research"** held on 27-30th May 2015 at Washington D.C.

Others

1. miR-148a functions as tumor-suppressor microRNA in medulloblastoma cell lines by targeting Neuropilin1. [abstract]. Kedar Narsinha Yogi, Epari Sridhar, Naina Goel, Rakesh Jalali, Atul Goel, Aliasgar Moiyadi, Rahul Thorat, Pooja Panwalkar, Atul Khire, Archya Dasgupta, Prakash Shetty, Neelam Shirsat. In: Proceedings of the AACR Special Conference: Advances in Brain Cancer Research; May 27-30, 2015; Washington, DC. Philadelphia (PA): AACR; Cancer Res 2015;75(23 Suppl):Abstract nr B41.

Dedicated

To

Aai, Baba and Tai

ACKNOWLEDGEMENT

I always believed that PhD degree although awarded to oneself, is essentially teamwork with contributions of many directly or indirectly shaping up one's "Thesis work". I wish to thank all such people who have been part of my work and last six years of PhD tenure at ACTREC.

I wish to express deepest gratitude to my mentor Dr. Neelam Shirsat whose scientific expertise, critical understanding of the field has helped me grow as a researcher and in successfully completing the assigned project.

ACTREC has been a self equipped and multi-facility centre for cancer research, Thanks to the former Director Dr. Rajiv Sarin, former Dy.Director Dr. Surekha Zingde and current Director Dr. Shubhada Chiplunkar and Dy.Director Dr.Sudeep Gupta. I also wish to thank them for the support and encouragement that I got while organising National Research Scholars Meet and resolving issues taken up by Students Council of ACTREC. I sincerely thank ACTREC for providing me the fellowship, Sam Mistry Fund (TMC) and HBNI for travel fellowship.

I would like to extend my appreciation to Doctoral committee members- Dr. Rita Mulherkar (Former chairperson), Dr. Pritha Ray, Dr. Sanjay Gupta and Dr. Sorab Dalal (Current chairperson) for their critical comments, suggestions and much needed dose of encouragement during entire PhD tenure.

I am grateful to Dr.Sridhar for taking out time from his TMH work to contribute towards histopathological analysis in my thesis work. His ever-accommodating nature and enthusiasm about the project was of immense importance. I wish to thank Dr. Rahul thorat for his technical expertise, scientific support and more importantly enthusiasm he carried while standardising intracranial injections in mice. I have thoroughly enjoyed working

with person of his character and spirit. I would also extend my appreciation to Dr. Abhijit De for his generous help with learning animal imaging technique.

I would also like to thank our clinical collaborators Dr. Rakesh Jalali, Dr. Ali, Dr. Prakash Shetty, Dr. Tejpal Gupta, Dr. Atul Goel and Dr. Naina Goel for providing tissue samples and clinical data. I also thank Dr. Archya Dasgupta who took untiring efforts to collect patient survival data.

I wish to thank Mr. Uday Dandekar (common instrument facility), Dr. Ingale sir and technicians Mahesh and Shashi (Animal House facility), Mr. Prakash Chavan (Histology facility) for their proficient assistance. I also thank staff members Vaishali, tanuja (microscopy facility), Mr. Naresh and Mrs. Sharada (Sequencing facility), Mrs. Maya (program office) and staff at Departments of Photography, IT, Administration, Accounts, Steno pool and SCOPE for their help and support.

I believe that “It’s the journey that is more important and not the destination”, and as a corollary to this famous quote I think it’s the people that surround you who make the journey wonderful. My journey would have not been as enjoyable as it was, had it not been with fantastic people at shirsat lab. Thanks to Anantji, Umesh and sadaf for their excellent support during these years. I especially thank anantji for all his technical help and being the nucleus for most of our lab jokes. Amit, Saumil, Pratibha, Shailendra and Dr.Sulochana have been great seniors in teaching each and every detail of lab work and helping me with number of things on and off the bench. Thanks to all of you. Special thanks to Ratika, who has been always a last resort for resolving many scientific and non scientific problems I encountered. I am equally grateful to my lab and batchmate Pooja for tolerating my irritating nature and sharing good time at work. I have thoroughly enjoyed working with my earlier Labmates-Atul, Vahbiz, Sandeep dukare, Sanket, Annada, Shreyas, Current juniors-Satish, Shalaka, Raikamal, Harish, Akash, Shweta, Purna and

aditi; my trainees- Heran, Swapnil, Bhavani and Helpers Ram and sharad. I will remember and cherish all the good time spent with all of you, for long. Thanks for being part of wonderful memories at shirsat lab.

My time in ACTREC has been very pleasant thanks to my ‘official’ batchmates Rupa, Shafqat, Sushmita, Priyanka, Pooja, Shrikanta, Snehal, Madhura, Tanmoy, Bhanu, Rubina and ‘unofficial’ batchmates Avinash, Sandeep kothivale, Kaushal, Abira and Manish. I will cherish fun time with you all. I also thank Nikhil, Bhavik and Gopal for the time spent together in chatting, watching cricket matches and especially cooking at Parijat. Heartfelt thanks to my roommates Ajit, Ramkumar, Ajay making Room No.44, Kanchan a second home for me. I have found great friends in seniors Ratika, Ajit Chande, Amitabha, Dilip, Dimpu, Cheryl, Sumeer and Hemant. Time spent with them had been a true stress buster.

My immediate senior and dear friend Manohar has given me immense support and showed great deal of understanding, in all good and difficult times I faced at ACTREC. We have shared lot of great moments with each other and my special thanks to him for being himself.

This thesis would not have been possible without endless support, understanding, love and care from my family. Thank you Aai, Baba and Tai!

CONTENTS

Homi Bhabha National Institute

Ph. D. PROGRAMME

1. Name of the Student:	Kedar Narsinha Yogi
2. Name of the Constituent Institution:	Tata Memorial Centre**,** Advanced Centre for Treatment, Research and Education in Cancer
3. Enrolment No. :	LIFE09200904006 (18th August 2009)
4. Title of the Thesis:	**"**WNT signalling driven up-regulation of microRNAs in medulloblastoma
5. Board of Studies:	Life Sciences

SYNOPSIS

Introduction

Medulloblastoma (MB), an embryonal tumor of the cerebellum, is the most common pediatric malignant brain tumor, pathologically classified as a WHO grade IV tumor[1]. Standard treatment includes surgical resection, followed by cranio-spinal radiation and chemotherapy. Advances in surgical and radiation techniques have improved the 5-year

survival rate to about 80% for average risk patients and 55-76% for high risk patients[2]. Genome wide expression profiling studies have identified four core molecular subgroups of medulloblastomas namely WNT, SHH, Group 3 and Group 4 that are not only distinct in underlying biology but also differ in clinical characteristics like age related incidence, presence of metastasis and survival. We have earlier reported differential microRNA expression in the four molecular subgroups with the WNT subgroup having the most distinctive expression profile [3]. A number of microRNAs like miR-193a, miR-148a, miR-23b, miR-224-452 cluster and miR-365 are specifically up-regulated in the WNT subgroup tumors as compared to normal cerebellar tissues and other subgroups of medulloblastoma[3]. In the present project therefore, studies were carried out to investigate if the WNT subgroup specific miRNA expression is due to the direct activation by β-catenin-TCF complexes or indirectly through transcription factor like MYC, a WNT signalling target gene. WNT subgroup medulloblastomas have been reported to have lowest incidence of metastasis at diagnosis (< 10%) and highest survival (90% - 95% ten year overall survival) among all the four subgroups [4]. miR-148a is one of the microRNAs up-regulated in WNT subgroup tumors. MiR-148a is known to be down-regulated as a result of promoter hypermethylation in various cancers and has been shown to act as tumor-suppressive/ metastasis suppressive miRNA [5]. In the present study the effect of miR-148a expression on medulloblastoma cell growth and malignant behaviour was investigated in detail.

Objectives

1) To determine if the expression of the WNT subgroup specific miRNAs is directly or indirectly regulated by the WNT signaling pathway.

2) To study the role of WNT subgroup specific miRNA, miR-148a in proliferative, migratory and tumorigenic potential of medulloblastoma cells.

Methodology

Medulloblastoma Tumor tissues and cell lines: Medulloblastoma tumor tissues were obtained with the approval of the Institutional Review Board. All the medulloblastoma cases studied were treated as per the standard practices with surgery followed by radiation (with the exception of less than 3 yr old children) and chemotherapy. Three medulloblastoma cell lines *viz.* Daoy, D283 and D425 were used in the present study.

RNA and DNA extraction: RNA was extracted from fresh frozen and FFPE medulloblastoma tumor tissues using Ambion Recover All RNA extraction kit while the genomic DNA was extracted using Qiaamp DNA mini kit.

Transfection of medulloblastoma cells with synthetic miRNA mimics:D283 cells were transfected with 50 nM of miR-148a mimic, or siGLO (a RISC-free control siRNA) or a siRNA negative control (Dharmacon) as per the manufacturer's protocol.

Transduction of medulloblastoma cells with miRNA expressing lentiviral vectors*:* The genomic region encoding miR-148a was PCR amplified from normal human lymphocyte DNA and cloned in pTRIPZ, a doxycycline inducible lentiviral vector. Daoy, D425 and D283 medulloblastoma cell lines were transduced with the pTRIPZ-miR-148a lentiviral particles and stable polyclonal populations were selected in the presence of puromycin. The cells transduced with lentiviral particles of empty pTRIPZ vector were used as a control.

Real time RT-PCR analysis and Molecular Classification of Medulloblastomas*:* MiR-148a expression was determined by real time RT-PCR analysis using the Taqman assay (Applied Biosystems) with *RNU48* as a control house-keeping small RNA, while NRP1 NRP1 was measured by SYBR Green real time RT-PCR assay using *GAPDH* as a house-keeping control gene. Relative Quantity (RQ) was estimated as RQ = $2^{-(Ct\ test - Ct\ control)}$ X

100. Molecular classification of Formalin Fixed Paraffin Embedded (FFPE) tumor tissues was carried out using real time RT-PCR as described[6].

MTT Reduction Assay: 500 or 1500 cells of Daoy and D425 cell lines respectively, were seeded per well of a 96-well micro-titer plate. The cell growth was evaluated by MTT assay at intervals of 3 days for the total period of 12 days[7].

Clonogenic Assay and Radiation sensitivity determination*:* 1000 cells were plated per 55 mm plate. For assessing radiation sensitivity, the cells were irradiated at a dose of 4 Gy. The medium was changed 24 h later and the cells were allowed to grow for 6-8 days until microscopically visible colonies formed. The cells were fixed by incubation in chilled methanol: acetic acid mixture and the counted after staining with 0.5% crystal violet.

Soft Agar Colony Formation Assay: 7500 Daoy cells or 1000 D425 cells were seeded in DMEM /F-12 medium supplemented with 10% FBS containing 0.3% agarose over a basal layer of 1% agarose in DMEM/F-12 supplemented with 10% FBS. The cells were incubated for about 3-4 weeks and the colonies formed were counted.

Tumorigenicity Assay and *in vivo* imaging*:* 5 X 10^6 Daoy / D425 cells transduced with pTRIPZ-miR-148a construct and cells transduced with empty pTRIPZ vector were injected subcutaneously in two flanks of a BALB/c Nude mouse following doxycycline induction for 72 h. Size of the tumors developed was measured using Vernier caliper at regular intervals over a period of 1-2 months. D283 polyclonal populations transduced with pTRIPZ-miR-148a construct were transfected with a pcDNA3.1 vector expressing firefly luciferase and 2 x 10^5 cells were injected into the cerebellum of BALB/c Nude mice using small animal stereotaxic frame. The tumor growth was monitored by *in vivo* bioluminescence imaging on 1st and 4th week post intracranial injection using IVIS Spectrum *in vivo* imaging system and analysed using "Living Image" software.

Invasion Assay*:* 50,000-75000 Daoy or D283 cells were seeded in 200 µl of plain DMEM in the upper chamber of 8-um pore size transwell inserts (BD Biosciences) coated with Matrigel^{TM}, placed in a 24 well micro-titre plate, with 750 µl of DMEM supplemented with 10% FBS in the lower chamber. These cells were allowed to migrate for 36-56 h and were labelled with Calcein AM (Life technologies). Non-invaded cells from the upper chamber were removed by wiping with a cotton bud. The inserts were photographed and fluorescence intensity of the labelled cells was measured using a fluorescent reader.

Luciferase Reporter Assay: Putative promoter regions of the select miRNAs were cloned upstream to firefly luciferase cDNA in a promoter-less luciferase reporter vector pGL3b. Co-transfection of the promoter constructs with or without activating mutant beta-catenin or MYC expression constructs and EGFP expression plasmid was done using Calcium phosphate BES buffer method in HEK293 cells. The promoter activity was evaluated by measuring luciferase activity normalised by EGFP fluorescence. For identification of miR-148a targets, the 3'-UTRs of predicted miR-148a target genes were cloned downstream to firefly luciferase cDNA in a pcDNA 3.0 vector. HEK 293T cells were transfected with the 3'UTR luciferase reporter plasmid, miR-148a expression vector and EGFP expression vector by Calcium phosphate BES buffer method. Luciferase activity was assessed from the total protein extracted from the transfected HEK293T cells and was normalized against the EGFP fluorescence measured using Mithras LB940 multimode reader.

Immunohistochemical Analysis*:* 5 µm sections of FFPE medulloblastoma tissues or subcutaneous tumor tissues were deparaffinized, rehydrated and the antigen retrieval was done as per the protocol (www.cellsignal.com). The FFPE sections was blocked using 3% Bovine serum albumin (BSA) and incubated with anti-NRP1 (Cell signalling) antibody, while subcutaneous tumor sections were incubated with anti-mouse CD31 antibody

followed by incubation with the peroxidase conjugated secondary anti-rabbit IgG. The bound peroxidase signal was detected using 3, 3-' Diaminobenzidine as a substrate. The sections were scored on the basis of the intensity and percentage of positive cells by a neuropathologist blinded to the molecular subgroup or survival data.

Statistical analysis*:* The significance of the difference in miR-148a expression in the WNT subgroup tumors as compared to other medulloblastomas or differences in performances of miRNA expressing stable cells as compared to the vector control cells were determined by the Student's t test using GraphPad Prism v 5.0. Kaplan-Meier survival analysis was done using GraphPad Prism version 5.01 software and the significance of the difference in the NRP1 high and NRP1 low groups was determined by the Log-Rank test.

Results

Objective 1

Putative promoter regions, putative transcription start sites (TSSs), Transcription factor binding sites (TFBSs) for β-catenin-TCF/LEF and/or MYC transcription factors and presence of CpG island in the upstream region from the start (+1) of pri-miRNA sequence were identified by online RNA Polymerase II promoter prediction softwares like Proscan, Promoter 2, First exon finder and Core Boost_HM. Further, known Expressed sequence tags (ESTs), Chromatin immunoprecipitation (ChIP) data available on UCSC web-portal was utilized to corroborate the findings of promoter prediction programs.

Identification of putative promoter regions and determination of promoter activity upon exogenous expression of MYC and mutant beta-catenin

MiR-224 lies in the intron of GABRE gene. The upstream (-1500 to +28) region of the *GABRE* gene showed 50 fold ($p < 0.0001$) higher promoter activity while miR-365 upstream region (-1200 to +99), showed ~5 fold ($p < 0.001$) higher promoter activity than

the promoter less pGL3 basic vector. Putative TSSs for miR-193a lie between -700 to -850 from pri-miR-193a. The region covering -4169 to -599 bp upstream to pri-miR-193a and -1749 to -369 upstream to pri-miR-148a showed 8 fold and 4 fold ($p < 0.001$) higher promoter activity than the pGL3 basic vector respectively. None of the promoter constructs for the four miRNAs showed induction on co-transfection with mutant β-catenin expressing vector or in the presence of Lithium chloride, known WNT signaling activator, despite the presence of putative TCF/LEF binding sites in these constructs. MiR-193a and miR-148a promoter constructs showed 2 to 4 fold induction ($p < 0.001$) of the promoter activity on co-transfection with MYC expressing construct. Further, site directed mutagenesis of the putative MYC binding site in the miR-148a promoter construct abolished the induction of the promoter activity by MYC transcription factor.

Effect of histone deacetylation and CpG demethylation on miRNA expression in medulloblastoma cell lines

Medulloblastoma cell lines belonging to group 3 have high expression of MYC but negligible expression of miR-193a and miR-148a. Bisulphite sequencing of 250 bp upstream region to pri-miR-148a, known to be hyper-methylated in various malignancies[5, 8] was performed from the genomic DNA of four medulloblastoma cell lines Daoy, D425, D283 and D341 and tumor tissues belonging to four molecular subgroups of medulloblastoma. All the four medulloblastoma cell lines showed around 80-100% of the CpGs to be methylated. Tumor tissues belonging to SHH (2/3), Group 3 (1/3) and Group 4 (3/3) showed more than 50% CpGs methylated while WNT (1/1) did not show any methylated CpGs. This suggests that miR-148a expression is downregulated as a result of CpG methylation in non-WNT medulloblastomas.

Objective 2

Two stable inducible polyclonal populations expressing *miR-148a* were used for studying the effect of miR-148a expression on growth and malignant behavior of medulloblastoma cell lines Daoy, D425. D283 cells transiently transfected with miR-148a mimic were also studied in addition to the stable doxycycline inducible polyclonal population. The polyclonal populations expressed miR-148a at levels comparable to that in the WNT subgroup or higher, upon doxycycline induction.

Effect of miR-148a expression on proliferation, clonogenic potential, radiation sensitivity and anchorage-independent growth of medulloblastoma cells.

MiR-148a expression resulted in 30-45% and 57-64% growth inhibition ($p < 0.0001$) of Daoy and D425 cells respectively. MiR-148a expression was found to reduce clonogenic potential of Daoy cells by 35-40% ($p < 0.0001$). No further reduction in colony formation was observed in soft agar colony formation assay indicating no effect of miR-148a expression on anchorage independent growth. Irradiation at a dose of 4 Gy reduced clonogenic potential further by 33-47% with or without induction of miR-148a expression, indicating no effect in radiation sensitivity upon miR-148a expression. Clonogenic potential of semi-adherent D425 cells was found to be reduced by 30-50% ($p < 0.0001$) upon miR-148a expression as judged by soft agar assay.

Effect of miR-148a expression on invasion potential of medulloblastoma cell lines

MiR-148a expression brought about 60-70% reduction ($p < 0.0001$) in the invasion potential of polyclonal populations of Daoy cell line while invasion potential of D283 cells was found to be inhibited by about 35-43% ($p < 0.0001$), upon miR-148a expression either in a stable inducible manner or in a transient manner using synthetic miR-148a mimic.

Effect of miR-148a expression on *in vivo* tumorigenicity and angiogenesis

The size of the subcutaneous tumors formed by Daoy and D425 was significantly reduced by 45-60% and 50-80% ($p < 0.05$) respectively, while D283 cells stably expressing miR-

148a and firefly luciferase, showed 25 fold reduction ($p < 0.0001$) in the bioluminescence (average radiance) upon doxycycline induction compared to the un-induced cells when injected stereotactically in cerebellum of nude mice. Subcutaneous tumor sections of miR-148a expressing Daoy cells showed significant decrease ($p < 0.05$) in total number of CD31 positive blood vessels and number of CD31 positive hotspots than that of vector control cells indicating angiogenesis inhibition.

Identification of protein-coding gene targets of miR-148a

The 3'-UTRs of the putative target genes *viz. ARHGAP21, B4GALT5, MMP15, ROBO1, NRP1, TMSB10* and two known miR-148a target genes *ROCK1* and *DNMT1* were cloned downstream to luciferase cDNA in the reporter vector. Luciferase activity of the cells expressing *ROCK1, DNMT1, NRP1 and, MMP15* constructs was found to be significantly reduced by 30-50% ($p < 0.0001$) in the presence of miR-148a expression. NRP1 3'UTR construct with mutant miR-148a binding site in presence of miR-148a expression, failed to show reduction in the luciferase activity further confirming it as a miR-148a target. Western blot analysis showed reduction in the protein levels of NRP1, ROCK1 and DNMT1 upon miR-148a expression in Daoy and D283 cells. MiR-148a was found to target only the full length NRP1 isoform of 120 kDa and not the 80 kDa soluble antagonist isoforms.

Reversal of miR-148a mediated reduction in the invasion potential and tumorigenicity of medulloblastoma cells upon exogenous NRP1 expression

Upon doxycycline induction of miR-148a expression, the cells with exogenous NRP1 expression showed marginal (~20%) reduction in the invasion potential unlike the 60-80% reduction seen in parental miR-148a expressing Daoy cells. Further, subcutaneous injection of miR-148a expressing Daoy cells transfected with NRP1 cDNA formed tumors of size comparable to the control un-induced cells even after doxycycline induction of

miR-148a expression. Thus, restoration of NRP1 expression was found to rescue the reduction in invasion potential as well as tumorigenicity brought about by miR-148a expression.

Correlation of NRP1 expression with molecular subgroups and overall survival

NRP1 expression was studied in a total of 93 medulloblastoma FFPE tissues by immunohistochemical analysis. Majority (75%) of the WNT subgroup medulloblastomas showed no detectable NRP1 expression. On the other hand, only 23% Group 3 tumors lacked NRP1 expression. Kaplan Meier analysis of 62 medulloblastoma cases, showed that tumors with moderate or high NRP1 expression had significantly poorer overall survival ($p = 0.0349$) than those having no detectable or low NRP1 expression with a hazard ratio 6.06.

Summary and conclusions

In the present study, promoter regions of miR-193a, miR-148a, miR-365 and miR-224 were identified by using luciferase reporter assay. Promoter activity of miR-193a and miR-148a was found to be induced in the presence of MYC suggesting up-regulation of expression of these two miRNAs as a result of activated WNT signalling pathway. The medulloblastoma cell lines belonging to Group 3 have high expression of MYC, but negligible expression of miR-148a and miR-193a. Bisulphite sequencing of CpG island region upstream to miR-148a coding region showed that this region was methylated in medulloblastoma cell lines and some of the non-WNT medulloblastoma tissues, indicating promoter CpG methylation as a likely cause of down-regulation of expression of this miRNA in non-WNT medulloblastoma tumor tissues. Expression of miR-148a at levels comparable to those in the WNT subgroup medulloblastomas or higher was found to inhibit growth and bring about reduction in the clonogenic potential, invasion potential and tumorigenicity of medulloblastoma cells. Neuropilin 1 was identified as a novel miR-

148a target gene in medulloblastoma. Rescue of miR-148a mediated inhibition in invasion and in vivo tumorigenicity on restoration of NRP1 expression, highlighted the importance of NRP1 as a key miR-148a target gene in medulloblastoma. Furthermore, NRP1 expression in medulloblastomas was found to be associated with poor survival, with little or no expression in majority of the WNT tumors, indicating its usefulness as marker for prognostication. The tumor suppressive effect of miR-148a expression accompanied by the down-regulation of NRP1 makes miR-148a an attractive therapeutic agent for the treatment of medulloblastomas.

References

1 Polkinghorn, W. R. & Tarbell, N. J. Medulloblastoma: tumorigenesis, current clinical paradigm, and efforts to improve risk stratification. *Nature clinical practice. Oncology* **4**, 295-304, doi:10.1038/ncponc0794 (2007).

2 Rossi, A., Caracciolo, V., Russo, G., Reiss, K. & Giordano, A. Medulloblastoma: from molecular pathology to therapy. *Clinical cancer research : an official journal of the American Association for Cancer Research* **14**, 971-976, doi:10.1158/1078-0432.CCR-07-2072 (2008).

3 Gokhale, A. *et al.* Distinctive microRNA signature of medulloblastomas associated with the WNT signaling pathway. *Journal of cancer research and therapeutics* **6**, 521-529, doi:10.4103/0973-1482.77072 (2010).

4 Kool, M. *et al.* Molecular subgroups of medulloblastoma: an international meta-analysis of transcriptome, genetic aberrations, and clinical data of WNT, SHH, Group 3, and Group 4 medulloblastomas. *Acta neuropathologica* **123**, 473-484, doi:10.1007/s00401-012-0958-8 (2012).

5 Lujambio, A. *et al.* A microRNA DNA methylation signature for human cancer metastasis. *Proceedings of the National Academy of Sciences of the United States of America* **105**, 13556-13561, doi:10.1073/pnas.0803055105 (2008).

6 Kunder, R. *et al.* Real-time PCR assay based on the differential expression of microRNAs and protein-coding genes for molecular classification of formalin-fixed paraffin embedded medulloblastomas. *Neuro-oncology* **15**, 1644-1651, doi:10.1093/neuonc/not123 (2013).

7 Mosmann, T. Rapid colorimetric assay for cellular growth and survival: application to proliferation and cytotoxicity assays. *Journal of immunological methods* **65**, 55-63 (1983).

8 Hanoun, N. *et al.* The silencing of microRNA 148a production by DNA hypermethylation is an early event in pancreatic carcinogenesis. *Clinical chemistry* **56**, 1107-1118, doi:10.1373/clinchem.2010.144709 (2010).

Publications in refereed journal:

a. **Published** – NA

b. **Accepted - MiR-148a, a microRNA upregulated in the WNT subgroup tumors, inhibits invasion and tumorigenic potential of medulloblastoma cells by targeting Neuropilin**
Kedar Yogi, Epari Sridhar, Naina Goel, Rakesh Jalali, Atul Goel, Ali Asgar Moiyadi, Rahul Thorat, Pooja Panwalkar, Atul Khire, Archya Dasgupta, Prakash Shetty, and Neelam Vishwanath Shirsat, Oncoscience. (Advance publication online on 2nd March 2015)

c. **Communicated** –NA

d. **Other publications** –

Confrences attended/ Oral or Poster presentations

1) K. Yogi, N. Shirsat, Role of miR-148a up-regulated in WNT subgroup medulloblastomas, **Poster session** presented at XXXVI All India Cell Biology Conference and International Symposium on "Stress Adaptive Response and Genome Integrity (SARGI) held on 17-19th October 2012 at Bhabha Atomic Research Centre (BARC), Mumbai.

2) **Oral Presentation** of abstract titled "Role of miR-148a in WNT subgroup Medulloblastoma at 9th National Research Scholars Meet in Life Sciences (NRSM) held at Advanced Centre for Treatment, Research and Education in Cancer (ACTREC) on 18-19th December 2014.

Signature of Student

Date 09/04/2015

Doctoral Committee:

Sr. No	Name	Designation	Signature	Date
1	Dr. Sorab Dalal	Chairman		9/4/2015
2	Dr. Neelam Shirsat	Guide/Convener		9.4.2015
3	Dr. Sanjay Gupta	Member		9.4.2015
4	Dr. Pritha Ray	Member		9.4.15

Forwarded through,

Dr. S.V. Chiplunkar
Director ACTREC
Chairperson,
Academic & Training Programme

Dr. S. V. Chiplunkar
Director
Advanced Centre for Treatment, Research & Education in Cancer (ACTREC)
Tata Memorial Centre
Kharghar, Navi Mumbai 410210.

Dr. K. Sharma
Director, Academics
T.M.C.

PROF. K. S. SHARMA
DIRECTOR (ACADEMICS)
TATA MEMORIAL CENTRE
PAREL, MUMBAI

List of Figures

List of Tables

List of Abbreviations

5'-Aza CdR: 5' Aza deoxycytidine

APC: Adenomatous polyposis coli

AR: Analytical Reagent

ATP: Adenosine triphosphate

BCOR: BCL6 corepressor

BES: *N*,*N*-*bis*(2-hydroxyethyl)-2-aminoethanesulfonic acid)

Blbp: Brain Lipid Binding protein

CCDS: Consensus coding DNA sequence

CGH: Comparative genomic hybridization

CGNP: Cerebellar granule neuron progenitors

ChIP: Chromatin immunoprecipitation

CSI: Craniospinal irradiation

DAB: 3,3'-diaminobenzidine

DEPC: Diethyl pyrocarbonate

DGCR8: Digeorge syndrome chromosomal region 8

DMEM: Dulbecco's Modified eagle medium

DMEM-F12: Dulbecco's Modified eagle medium-Nutrient mIxture F-12

DMSO: Dimethyl sulphoxide

DNA: Deoxyribonucleic acid

DNMT: DNA methyl transferase

dNTP: deoxy nucleotide triphosphate

DPE: Downstream promoter element

DTT: Dithiotreitol

EDTA: Ethylenediaaminetetraacetic acid

EGL: External granule layer

ELISA: Enzyme Linked Immunosorbant Assay

ENCODE: Encyclopedia of DNA elements

EST: Expressed sequence tags

FBS: fetal Bovine Serum

FDA: Federal Drug Administration

FFPE: Formalin fixed paraffin embedded

GFAP: Glial fibrillary Acidic Protein

GFP: Green Fluorescent Protein

GSK3β: Glycogen synthase kinase 3β

H&E: Haemtoxyline and Eosin

HDAC: Histone Deacetylase

HGF: Hepatocyte growth factor

LCA: Large cell anaplastic

LEF: Lymphoid enhancing factor
LR: Laboratory Reagent
LRP: Lipoprotein receptor related protein
M-MLV: Moloney Murine Leukemia Virus
mRNA: messenger RNA
MOPS: 3-(*N*-morpholino)propanesulfonic acid
MTT: 3-(4,5-Dimethylthiazol-2-yl)-2,5-Diphenyltetrazolium Bromide
MVD: Macrovascular density
NCOR: Nuclear receptor corepressor 1
NRP1: Neuropilin1
PBS: Phosphate Buffered Saline
PCR:Polymerase chain reaction
PEG: Polyethyleneglycol
PET: Paired end ditaging
PNET: Primitive neuroectodermal tumours
PNK: Polynucleotide kinase
PRC: Polycomb repressive complex
PVDF: Polyvinylidine fluride
RE: Restriction enzyme
RISC: RNA induced silencing complex
RNA: Ribonucleic acid
RT-PCR: Reverse transcriptase PCR
RT: Room tempearature
SAP: Shrimp Alkaline Phosphatase
SDS: Sodiumdodecylsulphate
SHH: Sonic Hedgehog
SNP: Single nucleotide polymorphism
snRNAs: Small nucleolar RNAs
SWI-SNF: SWItch sucrose nonfermentable
TAE: Tris Acetate EDTA
TB: Transformation buffer
TBST: Tris buffered saline and Tween-20
TCF: T-cell factor
TE: Tris EDTA
TFBS: Transcrition factor binding site
TGFβ: Transforming growth factor β
TRE: tetracycline responsive element
tRNA: transfer ribonucleic acid
TSS: Transcription start site
UCSC: University of California SantaCruz

UNG: Uracyl N glycosylase

UTR: Untranslated region

WGS: Whole genome sequencing

Chapter 1: INTRODUCTION

Medulloblastoma, an embryonal tumour of the cerebellum is the most common pediatric brain tumour and represents approximately 20% of all brain tumours that affect children up to 14 years of age [1]. Medulloblastoma typically arises in the roof of posterior fossa and grows in cerebellar vermis, fills the fourth ventricle and can invade the floor of ventricle to involve brainstem. These tumours also have tendency of spreading through cerebrospinal fluid to craniospinal axis. Approximately 30% of the children show metastasis at diagnosis. All medulloblastomas are pathologically graded as grade IV, the highest grade of malignancy as per the world health organisation (WHO) guidelines owing to their aggressive and malignant nature [1].

Risk stratification of medulloblastoma patients is based on the clinical parameters that include age at diagnosis, presence of metastasis and extent of post operative residual tumour. Patients less than 3 years of age or those with ≥ 1.5 cm^2 post operative residual tumour or metastasis at diagnosis are classified as high risk while all others are included in standard risk group. Current treatment regimen is trimodal and involves surgery followed by cranio-spinal irradiation (CSI) and chemotherapy. Five year event free survival of standard risk patients has been improved to more than 80%. However, patients at a high risk of recurrence (aged < 3 years or with significant residual disease following surgery, large cell/anaplastic medulloblastoma, or metastatic disease) have lower survival rates. Further, neuro-cognitive sequelae in the survivors are one of the most devastating side effects of current treatments. These side effects occur most often in young patients who are treated with craniospinal irradiation. Thus, understanding of molecular pathogenesis of these tumours is required for development of novel therapeutic strategies that would help improve survival of high risk patients and decrease the side effects of the current therapy to standard risk patients.

Gene expression profiling studies of medulloblastomas have identified four distinct molecular subgroups that not only differ in their expression profile, but also differ in their clinical

characteristics like overall survival rates[9]. Two subgroups are associated with aberrant hyperactivation of WNT and SHH signalling pathway and hence named as WNT and SHH respectively. Hyperactivation of WNT and SHH signalling pathways was known to occur in medulloblastomas associated with two familial cancer syndromes namely Turcot's and Gorlin's syndrome wherein germline mutations in WNT and SHH signalling pathway genes predispose patients to multiple malignancies. The remaining two subgroups are called Group 3 and Group 4 as no signalling or developmental pathways are not yet been identified to be associated with these two subgroups. Group 3 and 4 have overlapping gene expression profile which involves number of transcription factors involved in brain development. Group 4 tumours have higher expression of neuronal differentiation genes, while many Group 3 tumours display retina specific gene expression. The patients with WNT subgroup tumours have the best prognosis with overall survival rates exceeding 90% and show the least incidence of metastasis. While Group 3 patients have the worst survival rates of ~ 60% and highest incidence of metastasis and hence regarded as the worst prognosis subgroup amongst all the other subgroups of medulloblastoma. SHH and Group 4 tumours have been known to have intermediate prognosis with current treatment regimen [10].

MicroRNAs (miRNAs) are class of small non-coding RNAs that function by regulating expression of protein coding genes at post-transcriptional level. Single microRNA is believed to effectively control expression of 10-100 genes. It has been now established that several types of tumours show aberrant expression of different microRNAs as compared to their normal counterparts and that the miRNAs can play either oncogenic or tumour suppressive role in various malignancies depending upon the genes that they target[11]. MiRNA profiling in parallel to protein coding gene expression profiling of medulloblastomas done previously in our lab reported that the WNT subgroup tumours show the most distinct miRNA profile with significant over-expression of several miRNAs like miR-193a, miR-148a, miR-23b,

miR-224-452 cluster and miR-365 in comparison to other subgroup tumours and normal cerebellar tissues [3]. WNT subgroup tumours as well as the worst prognosis Group 3 medulloblastomas have overexpression of proliferation related genes including the oncogene MYC. WNT subgroup medulloblastomas also overexpress a number of TGF-beta signalling pathway genes that are indicators of poor prognosis[3]. Therefore, the molecular basis of the excellent survival of the WNT subgroup medulloblastomas is not explained by the expression profile of the protein-coding genes. MiRNA profiles of the WNT subgroup tumors on the other hand, is distinct with over expression of a number of miRNAs like miR-193a that have been shown to have tumour-suppressive activity in other cancers[12, 13]. It is thus likely that the distinctive miRNA profile of the WNT subgroup medulloblastomas plays major role in excellent survival rates of these tumours. MiR-148a is a miRNA that is known to be downregulated in various cancers, is overexpressed in the WNT subgroup tumors. Aim of the present study therefore was to delineate the role of miR-148a, one of the WNT subgroup specific miRNAs, in malignant behaviour of medulloblastoma cell lines and to determine whether expression of the WNT subgroup specific miRNAs is regulated directly or indirectly at transcriptional level by WNT signalling pathway.

Objectives

1) To determine if the expression of the WNT subgroup specific miRNAs is directly or indirectly regulated by the WNT signaling pathway.

2) To study the role of WNT subgroup specific miRNA, miR-148a in proliferative, migratory and tumourigenic potential of medulloblastoma cells.

Briefly the study presented in this thesis includes

- Determination of modulation of the promoter activity of the WNT subgroup specific miRNAs on activation of the WNT signalling pathway. .
- Effect of miR-148a expression on proliferation, anchorage independent growth, clonogenic potential, invasion potential and tumorigenic potential of medulloblastoma cell lines.
- Delineation of the molecular mechanism underlying miR-148a mediated inhibition of growth and invasion potential of medulloblastoma cells by identification of protein coding genes targeted by miR-148a. Evaluating the significance of the expression of NRP1, a novel miR-148a target gene, in medulloblastoma tumour tissues by correlating the expression with the molecular subgroups and overall survival.

Chapter 2: REVIEW OF LITERATURE

2.1 Medulloblastoma: Brief history, nomenclature and epidemiology

In 1925, Bailey and Cushing identified a novel tumour type, localised to the cerebellum, and distinct from gliomas, the most common malignant brain tumours[14]. The authors postulated that these undifferentiated tumours arise from a hypothesized central nervous system (CNS) precursor cell called a medulloblast and hence was named as "medulloblastoma"[15]. Although the existence of such a cell has never been proved, the name medulloblastoma has stuck with sub-class of a broad category of tumours known as embryonal tumours. In the intervening years since its initial description, the tumour has been well described and both the means of diagnosis and therapeutic strategies have greatly improved. By definition, it arises in the posterior fossa (a region of the brain that contains the brainstem and cerebellum), usually from the roof of the fourth ventricle, and presents as a midline tumour (Figure 2.1). More commonly in older children, the tumours can also arise in a cerebellar hemisphere.

Medulloblastoma is the most common malignant brain tumour of childhood, accounting for ~20% of all paediatric brain malignancies[16]. Approximately 70% of the cases occur in childhood (3 to 15 years of age), with 10-15% cases in infants (< 3 years of age). There is a bi-modal distribution in age of incidence, with peaks at 3-4 years and 8-9 years of age with the incidence of medulloblastoma in males 1.5-2 times higher than in females. [16]

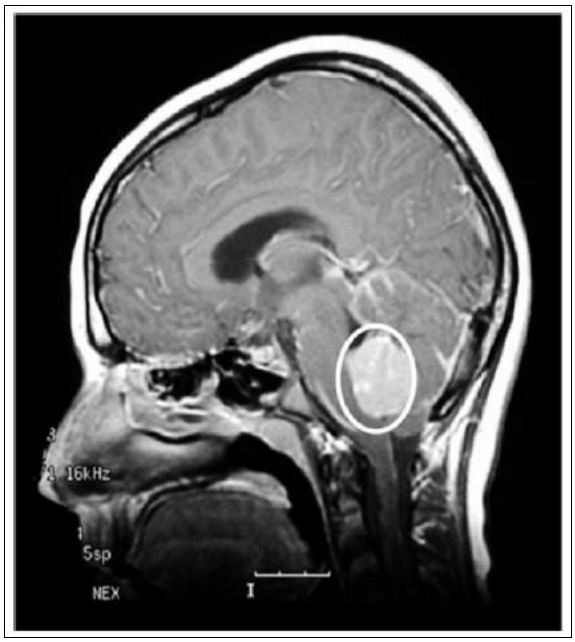

Figure 2.1: Sagital MRI following gadolinium injection shows dense white medulloblastoma tumour marked in circle[17]

The WHO classifies medulloblastoma as one of the five embryonal tumours, each of which share a primitive 'embryonal' cellular morphology, and is classified as grade IV owing to its aggressive behaviour[1]. Classification of such tumours has been a source of great controversy, with many in the past considering medulloblastoma and supratentorial primitive neuroectodermal tumours to be indistinguishable other than their anatomic location, and, as such, they were collectively called primitive neuroectodermal tumours or 'PNETs'. Microarray based expression profiling analysis by Pomeroy *et al* clearly showed that medulloblastoma constitutes a distinct tumour type with a distinguishable molecular profile, and is distinct from PNETs as well as Atypical teratoid and rhabdoid Tumours (AT/RT)[18].

Based on histological appearance, five variants of medulloblastoma are recognized: (a) the classical variant medulloblastoma, in which the cells occasionally display features of neuroblastic differentiation; (b) desmoplastic medulloblastoma, in which tumour cells commonly show neurocytic differentiation, and are surrounded by a collagen-rich extracellular matrix; (c) large-cell anaplastic medulloblastoma (LCA), associated with poor

prognosis and short survival; and finally (d) the melanotic and (e) medullomyoblastoma variants, which are less common[2].

2.2 Risk stratification and treatment of medulloblastoma

Current risk stratification for the selection of patients for the differential treatment regimens stratifies patients in two categories i.e. (1) Standard or average risk and (2) High risk based on three factors (a) age at diagnosis, (b) extent of resection and (c) Chang metastasis staging. Medulloblastoma patients aged above 3 years with gross-total or near total resection, without CSF metastases, and, in most trials, with non-anaplastic and non-large-cell histological subtype have been considered as 'standard-risk' (or 'average-risk') disease, while all other patients including infants i.e. children below 3 years are considered as 'high-risk'[10].

The treatment of medulloblastoma is trimodal with surgery being a primary mode of treatment followed by chemotherapy and cranio-spinal irradiation (CSI). Standard-risk patients receive'reduced-dose' CSI of 23.4 Gy with a localized boost to the posterior fossa to a total of 55.8 Gy, combined with concurrent single-drug chemotherapy followed by a multi-drug chemotherapy regimen. The addition of adjuvant chemotherapy allowed the dose of CSI to be reduced from earlier recommended 36.0Gy to 23.4Gy without a significant decrease in survival, as demonstrated by an event-free survival of 67–81% at 5 years, while better preserving neurocognitive function[10]. This regimen has also benefited from addition of maintainance chemotherapy following localised boost which involves vincristine, cisplatin and lomustin or cyclophosphamide. Nevertheless, loss of neuro cognitive function has been observed to still occur, especially in younger patients.[1, 10] Protocols for high-risk patients generally include 'full-dose' CSI of 36.0 Gy with a similar localized boost to the posterior fossa with concurrent single-drug chemotherapy and a more aggressive adjuvant regimen. With this treatment regimen, survival rates in the high-risk category are found to be lower (43–70% of five year event free survival), with a degree of compromise in neurocognitive

function[1]. Higher survival rates of upto 60-70% as either overall survival or progression free five year survival have been obtained with intense chemotherapy regimens and alternative radiotherapy fractionation schedules.

However the current strategy of clinical risk stratification has been found to have several shortcomings. (1) The disease recurs in 20–40% of standard risk patients indicating incorrect classification, resulting into delay in giving more aggressive therapy. (2) Current risk stratification fails to identify many patients who meet high-risk clinical criteria, but who could have been cured with low-risk treatment regimens, and thus avoiding unnecessary neuro cognitive decline and other side effects. (3) By categorizing patients into only two risk categories, current clinical risk stratification inappropriately simplifies the true heterogeneity of tumour behaviour, consequently hindering efforts to titrate treatment more accurately[10]. Therefore the challenges posed in identification of favourable prognosis and lower prognosis group of patients have been addressed partly by the current advances in understanding molecular heterogeneity of this disease and hence will prove beneficial in near future in better treatment design.

2.3 Molecular genetics in medulloblastoma and deregulated signalling pathway

Genetic alterations in common oncogenes / tumour suppressor genes, like *EGFR* mutation / amplification, $p16INK^{4A}$deletion are relatively rare in medulloblastoma [19]. The most common genetic alteration reported in medulloblastoma is the isochromosome 17q (i17q), a rearrangement that is brought about by the simultaneous loss of chromosome 17p and gain of 17q. Isochromosome 17q occurs in around 40-50 % of tumours and has been found to be associated with an unfavorable prognosis [20].

Medulloblastoma was thought to be a cancer originated from aberrant regulation of developmental pathways because of its prevalence in children and occurrence in the part of brain i.e. cerebellum that develops postnatally. It was also postulated that the presence of

both glial and neuronal differentiation markers in these tumours could be because of their cell of origin being neural stem cells, suggesting cause of tumourigenesis lying in deregulated cerebellar development[17]. Molecular analysis of two familial human cancer syndromes namely Gorlin's syndrome and Turcot's syndrome, whose patients have predisposition to develop medulloblastoma, provided valuable evidence for the role of deregulated signalling pathways like SHH and WNT which play crucial roles in cerebellar development, in medulloblastoma genesis. Germline mutations in *PTCH1 (PATCHED1)* gene that encodes for a membrane-bound receptor in the Sonic Hedgehog (SHH) pathway were identified in patients with Gorlin syndrome. Affected Individuals primarily developed basal cell carcinoma and in some cases medulloblastoma [21]. In type II Turcot syndrome, affected individuals were found to possess germline mutations in Adenomatous Polyposis Coli (*APC)*, a tumour suppressor gene that negatively regulates cytoplasmic β-catenin expression, which is the key effector of the WNT signaling pathway. These patients showed predisposition towards developing colorectal cancers and medulloblastoma [22].

2.3.1 WNT signalling pathway

The Wnt1 gene, originally named Int-1, was identified in 1982 as a gene activated by integration of proviral DNA of mouse mammary tumour virus in an attempt to identify genes that could cause breast cancer. The fly Wingless (wg) gene, which controls segment polarity during larval development, was later shown to be a homolog of Wnt1. The name WNT hence was derived from the fusion of Wingless and int-1[23]. Later studies in Xenopus and Drosophila established that Wnt ligands, a family of secreted cysteine-rich glycosylated proteins, signal by two pathways: canonical (Wnt-1, Wnt-3a and Wnt-8) and non-canonical (For ex. Wnt-4, Wnt-5a) [24]. The key signalling cascade intermediate in WNT signalling pathway is β-catenin (Figure 2.2). In absence of WNT proteins binding to WNT receptors Frizzled (Fz) and coreceptors like LRP5/6, cytoplasmic β-catenin is sequestered by what is

called as destruction complex. This destruction complex involves Axin-1 which acts as a scaffolding protein for APC, Casein kinase-1 and GSK3-β proteins. GSK3- β phosphorylates β-catenin which is recognised by E3-ubiquitin ligase β-TRCP which further targets it to proteasomal mediated degradation. The activation of WNT signalling cascade is initiated by binding of Wnt ligands to the frizzled and LRP5/6 receptor complexes. This recruits AXIN-1 to the membrane with the help of dishevelled thus destabilising destruction complex. Cytoplasmic β-catenin pool thus stabilized enables nuclear accumulation of β-catenin which then binds to TCF/LEF family of DNA binding proteins. In absence of β-catenin, these proteins bind to Groucho family of proteins and repress target gene expression , while in complex with β-catenin, TCF/LEFs activated transcription of target genes like MYC, CCND1[25]. Mutations in the WNT pathway genes *CTNNB1 (*β-catenin gene), *APC*, and *AXIN1* have been identified in approximately 10 % of sporadic medulloblastomas in mutually exclusive manner [4]. β-catenin nucleo-positivity has been reported to be a predictor of favorable outcome in medulloblastomas with mutations in *CTNNB1* being present exclusively in these nucleo-positive tumours[26].

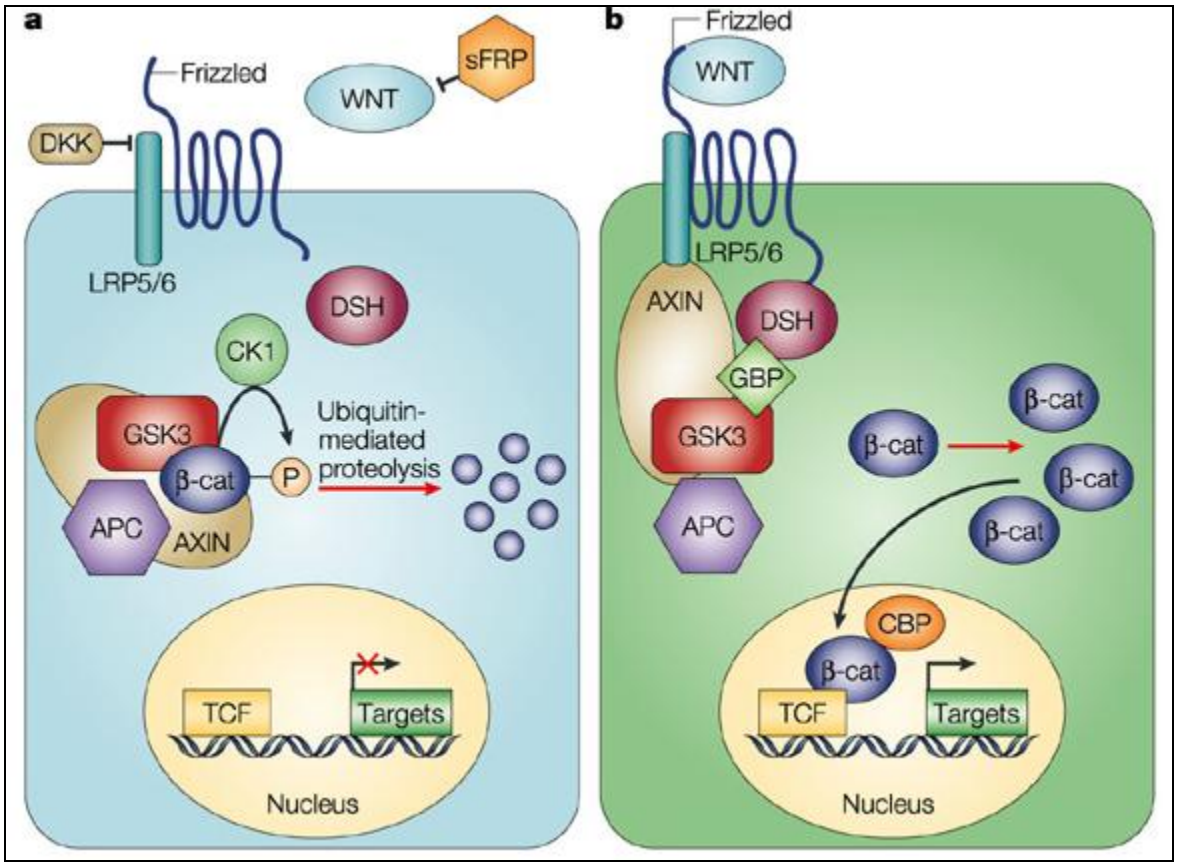

Figure 2.2: The canonical WNT signaling pathway. a) In absence of WNT ligand (Inactive). (b) In the presence of WNT ligand (Active) [27].

2.3.2 SHH signalling pathway

Hedgehog signalling pathway has been shown to have profound effect in embryonic development with involvement in stem cell maintainance, proliferation and differentiation. Early studies in drosophila and mouse cell culture models established the mechanism of hedgehog signal transduction pathway. In both vertebrates and invertebrates, binding of hehdgehog ligand to patched receptor (PTCH1) relieves repression mediated by smoothened (SMO) and activates signalling cascade that ultimately drives activation of transcription factor family composed of Gli1-3 leading to expression of specific target genes[28]. While in absence of hedgehog ligand, PTCH1 represses the activity of smoothened (Figure 2.3) [29]. The SHH pathway in addition to its many important roles, controls the normal development of the external granular layer (EGL) of developing murine cerebellum. SHH produced by

Purkinje cells results in induction of GLI family of transcription factors in cerebellar granule neuron precursor cells through activation of target genes like *Cyclin D1* (*CCND1), N-Myc (MYCN)* as a result of which these cells proliferate to form external granule layer during cerebellar development[30]. Mutations in SHH pathway genes (PTCH1, SMO, SUFU) have been identified in 25% of medulloblastoma in mutually exclusive manner [4].

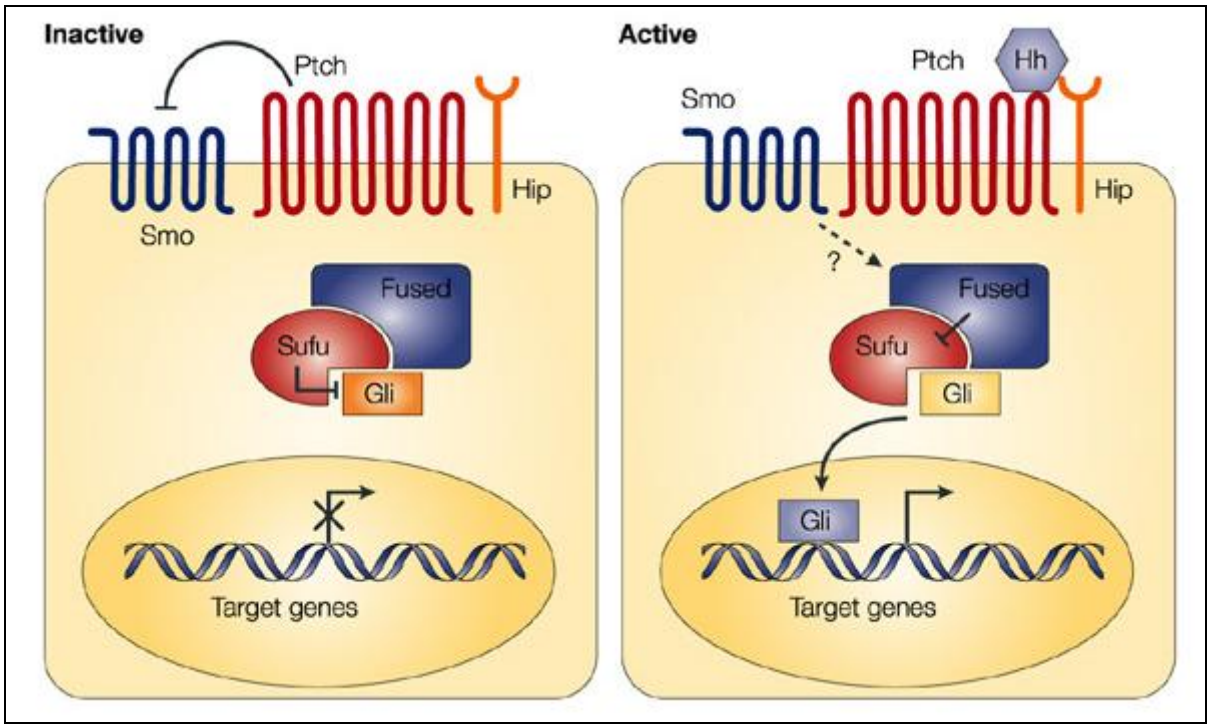

Figure 2.3: SHH signalling pathway[30]

2.4 Expression profiling and current consensus in medulloblastoma subgrouping

Microarray based gene expression profiling, Array CGH and SNP profiling studies of medulloblastomas performed by various groups has revolutionised the understanding about medulloblastoma as a disease and has led to identification molecular subgroups of medulloblastoma.

In 2006, Thompson *et al*, were first to introduce concept of transcriptionally discrete subgroups of medulloblastoma describing five distinct subgroups in a cohort of 46 cases. Most notable subgroups out of these were the ones associated with activated WNT or SHH signalling pathways [31, 32]. In 2008, Kool *et al* essentially recapitulated earlier findings in a

seperate cohort of 62 cases and showed clear segregation of WNT and SHH subgroups unlike as in study by Thompson *et al*, while other three subgroups were shown to be closely related to each other. A strong correlation between patient age, gender, histology and molecular subgroups was shown by this study. In 2010, independent studies by Northcott *et al* on 103 cases and cho *et al* on 194 cases segregated their tumour series into four and six subgroups respectively[9, 33]. Concurrent with the study by Northcott *et al.* in 2010, our group also identified 4 molecular subgroups of medulloblastoma by performing gene expression profiling of 19 medulloblastomas using Affymetrix Gene 1.0 ST array. These four molecular subgroups closely matched those reported in Northcott *et al* study. Strikingly, the WNT tumours have been observed to be more common in cohort from our group as compared to that reported by other groups [3].

Differences in number of subgroups and their nomenclature reported by various groups were resolved in a meeting held at Boston in 2012 and **current consensus was made on the number and names of the molecular subgroups of medulloblastoma which are namely WNT, SHH, Group 3 and Group 4**[4]. This reaffirmed the fact that medulloblastoma is not a single disease entity but is composed of four molecular subgroups that differ in their underlying biology, clinical presentation and demographics.

2.4.1 WNT subgroup

Demographics and clinical characteristics: This group accounts for roughly 10-15% of all medulloblastomas. WNT subgroup patients are often older children and adults with the median age at diagnosis of ~10 years [34]. The male to female ratio in the WNT subgroup patients is 1:1. Histologically they are generally of classic morphology with very rare cases of large cell anaplastic morphology. The prevalence of metastasis at diagnosis is found to be 9-15% and is the least amongst all the four subgroup tumours [34]. With current treatment regimen, these subgroup patients show > 90% overall survival and survival rates of the

patients with metastasis at diagnosis are found to be almost equivalent to the non metastatic ones [4]. Hence the WNT subgroup is regarded as the best prognosis subgroup and is currently considered for treatment de-escalation to avoid treatment related side effects [10].

Genomic and molecular characteristics: As mentioned earlier, WNT subgroup tumours show hyperactivation of the WNT signalling pathway as a result of somatic mutations in the *CTNNB1* gene encoding β-catenin that occurs in more than 90% of these tumours. These mutations result in making β-catenin resistant to proteasomal degradation leading to its increased nuclear accumulation. A minority of the WNT subgroup tumours carries an inactivating mutation in the WNT signalling inhibitor genes *APC* or *AXIN1* [10]. Novel missense mutations in *CDH1*, a gene that is involved in sequestering β-catenin at the membrane have also been reported in the WNT subgroup tumours that do not harbour mutations in *CTNNB1*, *APC* or *AXIN1* [35]. Lack of sequesteration of β-catenin by mutant CDH1 has been shown to promote WNT signalling in adult cancers [36]. Mutual exclusivity of these mutations to the mutations found in β-catenin suggests that *CDH1* is another target gene when mutated can result in activation of WNT signalling pathway. As compared to other subgroups, the genome of the WNT subgroup tumours is relatively stable. Somatic copy number variations are infrequent in the WNT subgroup tumours with the exception of monosomy 6, observed in over 75-85% of the WNT subgroup tumours [4, 37]. Whole genome/exome sequencing data has identified recurrent mutations in *DDX3X* (50%), *SMARCA4* (26%), *TP53* (16%), *KMT2D (12.4%)*, *ARID1B* and *CREBBP* in the WNT tumours. Many of these genes like *SMARCA4*, *CREBBP*, *ARID1B* and *KMT2D* encode proteins that are known chromatin modifying genes that may cooperate with mutant β-catenin in tumourigenesis of the WNT subgroup medulloblastomas [34, 35, 38].

Mouse model and cell of origin: Gibson *et al* generated mouse model for WNT subgroup medulloblastoma, where tumours resembling human WNT subgroup tumours with respect to

expression profile and anatomical location arose from lower rhombic lip/dorsal brain stem progenitor cells upon expression of stabilised allele of *CTNNB1* under Blbp promoter along with homozygous deletion of TP53. However these tumours arose at relatively longer latency period and lower penetrance (15%). CGNPs that belong to cerbellar hemisphere were not found to give rise to such tumours following similar genetic changes, suggesting CGNPs not being the cell of origin for WNT subgroup tumours, unlike what seen for SHH and Group 3 mouse models (discussed in respective subgroup sections ahead). This study further showed that these progenitor cells from dorsal brain stem include mossy fibre neuron precursors which could be probable cell of origin for the WNT subgroup tumours [39]. Consistent with the differences in probable cell of origin of WNT and SHH tumours, the anatomical location of these subgroups in humans and in the mouse model was found to be different. WNT subgroup tumours were found to be located in IV ventricle and infiltrating dorsal surface of brainstem, while SHH tumours were distributed away from brainstem and within the cerebellar hemispheres[39].

2.4.2 SHH Subgroup

Demographics and clinical characteristics: SHH subgroup accounts for 28% of all sporadic medulloblastomas. SHH subgroup tumours include tumours with all the three histologic variants with many having desmoplastic histology or extensively nodularity while others are classic and few have large-cell-anaplastic morphology. Age distribution in this subgroup is biphasic with peak incidence in the infants/very young children (< 3 years) and adults (> 16 years) amongst those affected, with male to female ratio of 1.5:1. These tumours are located often in the cerebellar hemispheres and rarely at midline [34]. SHH subgroup patients are heterogenous in survival rates with some having excellent survival while other in particular those with large cell anaplastic histology and/or presence of metastasis at diagnosis or *MYCN* amplification having poor pronosis. Overall SHH subgroup patients have an intermediate

outcome with overall survival rates of 60-80%, with metastasis at diagnosis in ~20% of patients [4, 34].

Genomic and molecular characteristics: 25% of SHH tumours show somatic mutations in one of the genes of the SHH pathway (*PTCH1*, *SUFU*, or *SMO*) that results into hyperactivation of SHH signalling pathway [4]. Approximately 30-40% of all SHH subgroup tumours are characterized by loss of chromosome arm 9q, which harbors the *PTCH1* gene[9, 33, 40]. A subset of SHH tumours show amplification of SHH signalling targets like *GLI2* or *MYCN* and are associated with poor prognosis [37]. A recent study on somatic copy number alterations (SCNAs) in 1087 medulloblastomas has shown presence of additional 'SHH subgroup enriched' SCNAs like amplifications of *MDM4* (9%) and *PPM1D* (8.3%), and focal deletions of *TP53* (29%) and 'SHH subgroup restricted SCNAs' which include amplifications of IGF signalling genes viz. *IGF1R* (6%), *IRS2* (9.4%), PI3K genes like *PIK3C2G* (2.6%) and *PIK3C2B* (9%), and deletion of *PTEN* (9.8%)[37]. SHH subgroup restricted SCNAs are particularly important in consideration for targeted and combinatorial therapies as many of these genes have been currently investigated as therapeutic targets in other solid tumours and are likely to help in treatment in case of acquired resistance to SHH signalling inhibitors like vismodegib, as seen in phase II studies [37, 38].

Mouse models and Cell of origin: Cerebellar granule neuron progenitor cells (CGNPs) that proliferate in response to SHH secreted by Purkinge neurons during development of cerebellum are believed to be the cell of origin for this subgroup of medulloblastomas [41]. Heterozygous deletion of *PTCH1* gene resulted in development of sporadic murine medulloblastoma with 14% incidence rate, which could be increased to 95% in the background of heterozygous deletion of *TP53* or to 30-40% with homozygous or heterozygous deletion of *Ink4c* or *Kip1* and to ~ 60% with homozygous deletion of *Hic1*. These genetically engineered mouse models successfully achieved spontaneous generation of

SHH activated subset of medulloblastomas in mice that closely resembled human SHH subgroup medulloblastomas [41]. Second generation of SHH mouse models utilised CGNPs specific promoters to either drive Cre-lox system to knockout *Ptch1* [42] or to drive constitutively active *Smo* in ND2A-SmoA hemizygous mouse model, proved CGNPs to be cell of origin for SHH subgroup medulloblastomas [43, 44].

2.4.3 Group 3

Demographics and clinical characteristics: Group 3 medulloblastomas account for 27% of all sporadic medulloblastomas with male: female ratio of 2:1. These tumours are almost exclusively found in infants and children, rarely in adolescents and not in adults [38]. Majority of the tumous are of classic histology while of all the four subgroups, most cases of large-cell anaplastic medulloblastomas belong to this group. Group 3 patients have high incidence of metastatic disease at diagnosis (~ 40-45%) and it is even higher in infants, classifying most of these tumours as high risk medulloblastomas. The five year and ten year survival rates in infants are 45% and 39% respectively, while in children the rates are 58% and 50%. Thus Group 3 patients have the lowest survival rates amongst four subgroups [34]. Therefore, this subgroup has been known as the worst prognosis subgroup and development of new targeted therapies and treatment strategies specific to this subgroup is urgently required.

Genomic alterations: Group 3 and Group 4 tumours have been found to have overlapping gene expression profiles with no clear association to deregulation of any particular signalling pathway as in WNT or SHH tumours. However Group 3 tumours do show over-expression of proliferation related genes like *MYC, CCND2*, TGFβ1 signalling components, retinal specific genes like *CRX, IMPG2* and other genes like *NPR3* [3, 4]. Genetic alterations like amplifications of genes that are part of TGFβ signalling pathway like *ACVR2A, ACVR2B* and *TGFBR1*, TGFβ signalling pathway target *OTX2* and recurrent deletions of TGFβ inhibitor

genes like *CD109* and *FKBP1A*, collectively account for ~20% of Group 3 tumours indicating involvement of deregulated TGFβ signalling pathway and hence could be rationale therapeutic target for this poor prognosis subgroup. Isochromosome 17q characterised by deletion of 17p and gain of 17q is the most frequent genetic alteration in Group 3 and Group 4 with 26% of Group 3 tumours showing i17q. The other frequent alterations like 1q (35%), 7 (55%), and 12q gains (17%), and 11, 16q deletions (50%) [4, 45-47]. However functional implications of these alterations in pathogenesis of Group 3 tumours are not yet known. MYC and OTX2 are the two proto-oncogenes whose focal amplification is seen in 12-16% and 7% of Group 3 tumours and are found to be mutually exclusive. Both MYC amplifications and. Isochromosome 17q have been shown to be poor prognostic indicators in Group 3 patients, in addition to large cell anaplastic (LCA) histology as mentioned earlier [48, 49]. In addition to variety of chromosomal alterations, occurrence of widespread chromothripsis in the absence of *TP53* mutations resulting in potentially functionally significant fusions like MYC-PVT1 and of phenomenon like enhancer hijacking i.e. repositioning of active enhancer regions close to known oncogenes like *GFI1* or *GFI1B* further highlight the unstable nature of genome in Group 3 tumours [37, 50]. However, enhancer hijacking is not specific to Group 3 tumours unlike MYC-PVT1 fusions which have been shown to occur in 60% of MYC amplified Group 3 tumours. These studies also therefore emphasize the possible functional significance of the chromosomal structural alterations in tumourigenesis of Group 3 tumours, unknown till now. However many Group 3 tumours that do not possess these aberrations, have been shown to possess recurrent somatic copy number variations in chromatin modifier genes like chromatin remodelling proteins encoded by *SMARCA4*, *KMT2D*, and *CHD7*; and a variety of mutations in the lysine-specific demethylase (*KDM*) gene family (*KDM6A*, *KDM3A*, *KDM4C*, *KDM5B*, and *KDM7A*) as shown by whole genome sequencing analysis [34, 35].

Hence studies on the functional role of mutations in these genes become important to understand the underlying biology of a subset of Group 3 tumours.

Mouse models and Cell of origin: Two independent studies by Pei *et al* and Kawauchi *et al* generated mouse models for the most aggressive subgroup of medulloblastoma i.e. Group 3 by forced expression of MYC in either Prom1+/Lin- stem cells isolated from postnatal cerebellum or CGNPs in the background of mutant *TP53* [51, 52]. MYC over-expression or amplifications are well known in Group 3 Medulloblastoma, while monoallelic loss of *TP53* is also noted in Group 3 tumours that exhibit isochromosome 17q [9, 33]. However since these tumours were found to be more immature or undifferentiated than normal stem cells and as they did not show any CGNP lineage specific gene expression, lineage commitment is not required for the development of these tumours [53]. Further these tumours showed over-expression of PI3K/Akt/mTOR pathway genes and down-regulation of FOXO target genes like that found in human Group 3 tumours and therefore can be efficiently targeted by PI3K inhibitors[51, 52]. Considering worst prognosis of these tumours and lack of Group 3 specific targeted therapy, development of such mouse models will in future facilitate preclinical stage testing of drugs specific to Group 3 tumours.

2.4.4 Group 4

Demographics and Clinical characteristics: As a group, these are the most common medulloblastoma (~ 34%), occurring at all ages, however are rare in infants [32]. As in Group 3 tumours, classic and LCA histology is seen in Group 4 tumours, however proportion of tumours with LCA histology is much less as compared to Group 3. Highlighting feature of these subgroup tumours is the skewed distribution of gender, with disease occurring 3 times more often in males than in females. Prevalence of metastasis at diagnosis is 35-40% with five year survival rate of ~75% [34]. Therefore this subgroup is regarded to have intermediate prognosis with patients responding better to the treatment than Group 3.

Genomic and molecular characteristics: Similar to Group 3, no germline mutations or existence of deregulated signalling pathway has been shown to predispose individuals to the development of Group 4 tumours or to have any direct association with Group 4 tumour biology [34, 47]. These tumours are known to show over-expression of neuronal differentiation genes like *GRM8, KCNA1* and *UNC5D* and glutamergic pathway genes unlike Group 3 tumours [3, 32, 47]. Although isochromosome 17q is found in both Group 3 and 4 tumours, its more defining feature of Group 4 tumours as it occurs in ~66-80% of these tumours and remains associated with poor prognosis even in this subgroup [32, 45]. Other chromosomal aberrations enriched in Group 4 are gains of chromosomes 7 (47%), 12q (20%), 18 (16%), and deletions of 8p (41%) and 10q (15%) [4]. Taken together, these findings suggest that genome of Group 4 tumours similar to Group 3 is unstable. Whole genomic sequencing (WGS) analysis have identified genes that are recurrently mutated and/or altered in copy number that are known to overlap between Group 3 and 4 tumours. These include mutations affecting the KDM family members, *OTX2* amplifications, *DDX31* deletions, *CHD7* mutations, activation of *GFI1*/*GFI1B* expression, and *KMT2D* and *KMT2C* mutations. Unlike Group 3 tumours, these subgroup tumours are known to have preferential amplification or overexpression of *MYCN* than *MYC* [34, 35, 54]. The most frequent mutation in Group 4 tumours is mutation in *KDM6A* gene that occurs in 13% of Group 4 tumours. Functionally these mutations result in prevention of H3K27 demethylation, thus most likely resulting into preservation or initiation of stem cell like state in these tumour cells [35]. The most frequent focal somatic copy number alteration that occurs in 10% of Group 4 tumours is a single copy gain on 5q23.2 on *SNCAIP* gene. Although, the functional significance of this alteration is not yet known, mutual exclusivity of SNCAIP duplications to the other most common alterations in Group 4 namely *MYCN* and *CDK6* amplifications and their occurrence

along with i17q indicates their possible role as one of the driver alterations underlying Group 4 tumourigenesis. [37, 47].

Mouse model and cell of origin: Swartling *et al* in 2010, generated a novel medulloblastoma mouse model, called as GTML (double transgenic for Glt1-tTa and TRE-MycN/luciferase) by expressing MYCN through tTA-TRE syetem under glutamate transporter 1 promoter. These tumours were derived from cells belonging to developing posterior hindbrain that show activity of Glt1 promoter [55]. They further reported the GFAP positive neural stem cells from hindbrain to be cell of origin but found that they can give rise to tumours that resemble either Group 4 or SHH subgroup of human medulloblastomas, in response to N-myc depending upon the time of tumour initiation [55, 56]. Hence although gene expression profile of GTML tumours matches closely to human Group 4 medulloblastoma, it is still unclear whether this model system faithfully recapitulates human Group 4 medulloblastoma phenotype. Tables 2.1 and 2.2 below depict major clinical, genomic and molecular alterations across subgroups of medulloblastoma.

Subgroup / Characteristics	WNT (~10%)	SHH (~30%)	Group 3 (~25%)	Group 4 (~35%)
Sex ratio	1:1	1.5:1	2:1	3:1
Age distribution	Older children & adults	Infants,children and adults	Infants and young children	Older children and yound adults
Histology	Classic, very rarely LCA	Classic > desmoplastic > LCA	Classic > LCA	Classic, rarely LCA
Metastasis at diagnosis	5-10%	15-20%	40-45%	35-40%
Overall survival	~95%	~75%	~50%	~75%
Probable cell of origin	Lower rhombic progenitor cells	CGNPs of EGL	CD133+ neural stem cells/CGNPs	Unknown

Table 2.1: Clinical characteristics of four molecular subgroups of medulloblastoma.
The table shows the distinct demographics, clinical features characteristic of each subgroup, adapted from [47] Percentages in paranthesis indicates percentage contribution of indicated subgroup tumours in all medulloblastomas.

Subgroup / Characteristics	WNT	SHH	Group 3	Group 4
Expression Profile	WNT signalling	SHH signalling	MYC signature Retinal signature	Neuronal signature
Cytogenetic (- Loss, + gain)		3q+, 9p+	1q+, 7+, 17q+, 18+	4+, 7+, 17q+, 18+
	6-	9q-, 10q-, 14q-, 17p-	8-, 10q-, 11-, 16q-, 17p-	8-, 10-, 11-, 17p-, X-
Most Frequently mutated genes	CTNNB1 (90.6%) DDX3X (50%) SMARCA4 (26.3%) MLL2 (12.5%) TP53 (12.5%)	PTCH1 (28%) TP53 (13.8%) MLL2 (12.6%) DDX3X (11.7%) MYCN (8.2%) BCOR (8%) LDB1 (6.9%) TCF4 (5.5%) GLI2 (5.2%)	MYC (16.7%) PVT1 (11.9%) SMARCA4 (10.5%) OTX2 (7.7%) CTDNEP1(4.6%) LRP1B (4.6%) MLL2 (4%)	KDM6A (13%) SNCAIP(10.4%) MYCN (6.3%) MLL3 (5.3%) CDK6 (4.7%) ZMYM3(3.7%)

Table 2.2: Genomic and molecular characteristics of molecular subgroups of medulloblastoma. The table shows the distinct demographics, clinical features characteristic of each subgroup, adapted from [47]. Percentages in paranthesis indicate percent occurrence of the mutations in indicated genes within indicated subgroup tumours.

2.5 Epigenetic modifications and their subgroup specific nature in medulloblastoma

Recently the epigenome of medulloblastoma tumours has been extensively studied using whole genome or whole exome sequencing, copy number and expression analysis with a specific attention to subgroup specificity and/or enrichment of (1) presence of histone modifications like H3K27 and H3K4 trimethylation, (2) mutations in histone code modifier genes like KDM family of proteins and SWI-SNF complex proteins, and (3) over-expression of genes like EZH2, HDAC2 that play crucial role in regulating global profile of histone modification like histone methylation and acetylation [35, 57, 58]. WGS analysis done by Robinson *et al* revealed that Group 3 and Group 4 tumours show enrichment of H3 Lysine27-trimethylation (H3K27me3), a histone code associated with transcriptional repression and disruption in maintainance of H3 Lysine4-trimethylation (H3K4me3), a transcriptional activation histone mark [35, 59]. This global histone modification phenotype was shown to be as a result of (1) gain or over-expression of EZH2, (H3K27me3 writer enzyme), (2) inactivating mutations in genes like *KDM6A* and *UTY* that are involved in maintainance of H3K27me3, (3) inactivating mutations in genes like *CDH7* and *ZMYM3* that are involved in H3K4me3 associated transcriptional activation, resulting in disruption of H3K4me3 associated transcriptional activation [35]. The authors suggested that enrichment of aforementioned mutations in chromatin modifiers results in an epigenetic state similar to stem cells and that it is characteristic of Group 3 and 4 tumours unlike WNT and SHH tumours that show significantly lesser H3K27me3 mark. [35]. The study from Dubuc *et al* further suggested that the K4+/K27- tumours do better than K4+/K27+ tumours in their overall survival [57].

Although H3K27 trimethylation enriched phenotype is not seen in SHH subgroup medulloblastomas, these subgroup tumours along with Group 3 and Group 4, have been shown to over-express class I histone deacetylase HDAC2 as compared to WNT subgroup

and normal cerebellum[60]. It is also known that Shh induced HDAC activity is required for CGNP hyperplasia in *in vitro* primary culture as well as in a medulloblastoma mouse model [61]. Whole exome analysis of medulloblastoma has found out recurrent mutually exclusive mutations in genes involved in NCOR and BCOR chromatin modifying complexes specifically in SHH subgroup [62], again pointing towards subgroup specific nature of disruption observed in chromatin remodelling.

WNT subgroup tumours on the other hand showed enrichment of mutations in genes like *SMARCA4*, *CREBBP*, *TRRAP* and *MED13*, which are known to bring about chromatin remodelling in cooperation with their binding partner β-catenin, a driver gene known for WNT subgroup tumours[35]. Taken together, these findings suggest aberrant regulation in chromatin modifiers across all subgroups of medulloblastoma as a result of mutations in genes mainly belonging to NCOR, SWI-SNF complexes and KDM-PRC family. Further investigation into the functional implication of these mutations is required.

DNA methylation is another epigenetic modification that has profound effect on transcriptional regulation of genes. Whole genome bisulphite sequencing analysis of medulloblastoma tissues has revealed that DNA Methylation profiles vary across subgroups with global hypomethylation in WNT and Group 3 tumours as compared to other subgroups and normal cerebellum [58, 63]. The overall CpG methylation rate was reported to be lowest in the WNT subgroup tumours [58]. Since regulation of DNA methylation and histone codes like histone lysine methylation and histone acetylation is tightly linked with each other and is implicated in transcriptional regulation of different genes [64], further investigation into their subgroup specific nature and collective functional implications will further strengthen the understanding about molecular mechanism underlying pathogensis of different subgroups of medulloblastoma.

2.6 MicroRNAs: The new way of regulation

The Central dogma of molecular biology states that genetic information is transferred from DNA to RNA and then from RNA to protein. Several exceptions to the central dogma were subsequently noted including the process of reverse transcription and identification of non-coding RNAs including microRNAs. MicroRNAs (miRNAs) are small, evolutionary conserved, single-stranded, non-coding RNA molecules that bind target mRNA to prevent its translation by either inhibition of translation or via targeting it for degradation.

2.6.1 Brief history

MicroRNAs, originally discovered in *Caenorhabditis elegans***,** are found in most eukaryotes, including humans. The first miRNA lin-4 was discovered in 1993 by the joint efforts of Ambros and Ruvkun's laboratories [65, 66]. *Lin-4,* was identified in *Caenorhabditis elegans* through a genetic screen for defects in the temporal control of post-embryonic development. Most genes identified from the mutagenesis screens were protein-coding, but *lin-4* was found to encode a 22-nucleotide non-coding RNA that contained sequences partially complementary to 7 conserved sites located in the 3′-UTR of the *lin-14* mRNA. This complementarity was both necessary and sufficient to inhibit the translation of the *lin-14* mRNA. Almost 7 years after the finding of the first miRNA, let-7, also required during *C. elegans* larval development, was identified in the year 2000 [67]. The finding that let-7 was conserved across species from flies to humans [68] and targets the *RAS* oncogene homolog in *C. elegans* [69], triggered a search for microRNAs in diverse species including humans. There are currently 2588 annotated miRNAs in human genome. Since each miRNA is predicted to regulate expression of hundreds of genes, miRNA biogenesis is critical in controlling protein coding gene expression [70, 71].

2.6.2 MicroRNAs: biogenesis

MiRNAs are single stranded RNAs, ~20 to 22 nucleotides long and are generated from endogenous short hairpin shaped transcripts [71, 72]. MiRNA coding genes are located throughout the genome, with some housed within introns of protein coding gene (intragenic), while some in noncoding RNA (ncRNA) transcription units (intergenic miRNAs). Lee *et al* in 2004 showed that miRNA encoding genes are transcribed by RNA polymerase II in form of primary transcripts (pri-miRNAs) which contain 5' cap structures as well as poly-A tails at 3'end by demonstrating inhibition of miRNA expression upon treatment with alpha amanitin and direct binding of RNA pol II to miRNA promoter regions [73]. Since then, vast majority of miRNAs are shown to be transcribed by RNA polymerase II either as part of host gene transcripts in case of intragenic miRNAs or as individual transcription units in case of intergenic miRNAs [71, 74]. In some cases of intragenic miRNAs, there is a direct correlation observed in expression between the host gene and miRNA, however expression of host gene and miRNA can also be differentially regulated with use of alternate promoters and regulated processing [75, 76].Very few miRNAs that are close to Alu repeats have been shown to be transcribed by RNA Pol III [77]. Many miRNA precursors which are found in clusters are transcribed in form of polycistronic transcripts from a single promoter, while intragenic miRNA clusters are processed from parent gene transcript via alternative splicing mechanism.

RNA Pol II transcription of the genomic region encoding miRNA gives rise to a capped polyadenylated primary miRNA transcript that may contain multiple stem loop / hairpin structures corresponding to multiple miRNAs (in case of miRNA cluster) and are typically therefore > 1000 bp long. The miRNA biogenesis from such a primary transcript is a multistep process comprising of three main events: cropping, nuclear export and dicing. The enzyme Drosha / DGCR8 crops the pri-miRNA at the stem and releases a hairpin-structured

60-100 nucleotides long precursor-miRNA (pre-miRNA) with a ~2-nt 3' overhang. DGCR8 is a double-stranded RNA-binding protein that recognizes the proximal ~ 10 bp of the pri-miRNA hairpin stem, positioning the catalytic sites of the RNase III enzyme Drosha to facilitate cropping. The ~2-nt 3' overhangs of the pre-miRNA are further recognized by Ran-GTP and the export receptor Exportin-5 enabling its nuclear export. Subsequently, another RNase III enzyme, Dicer processes the pre-miRNA in the cytoplasm to release a ~ 22 nucleotide miRNA: miRNA* duplex (* indicates passenger complementary strand). This miRNA duplex is then loaded into an RNA induced silencing complex (RISC), which includes argonaute protein that unwinds the duplex. The mature single stranded miRNA then binds to complementary sites in the mRNA target to regulate gene expression. The mechanism of inhibition depends on the degree of miRNA-mRNA complementarity (imperfect or perfect) that results in either inhibition of protein synthesis or mRNA degradation (Figure 2.4).

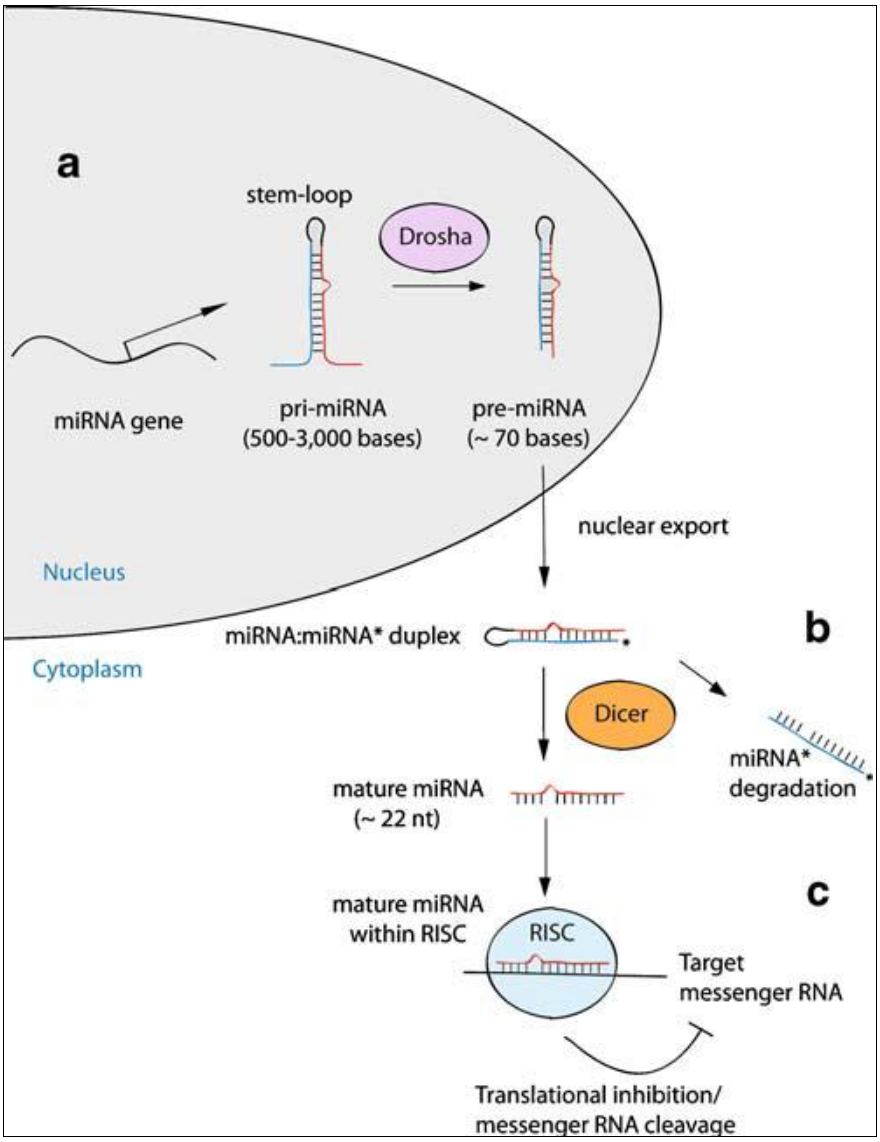

Figure 2.4: Biogenesis and function of miRNAs, a) transcription and cropping of miRNA transcripts in nucleus, b) dicing of pre-miRNAs into mature miRNAs and their functional process [78].

2.6.3 MiRNA target identification

The most important region of mature miRNA for target mRNA recognition is the sequence between 2 to 8 nucleotides of its sequence and is known as the seed region [79]. Binding sites for these seed sequences of miRNAs are most commonly found in 3'-untranslated regions (3'UTRs) of target mRNAs in animal cells. The target prediction for each miRNA depends upon following key factors: (1) complementarity of seed sequence- search for perfect complementarity of 6 nucleotides (2-7) of miRNA to the 3'UTR sequence over yields greater

prediction specificity over 7nt motif (2-8 nucleotides), (2) conservation of seed sequence/miRNA binding site in 3'UTR across species – 3'UTRs with highly conserved binding sites increases predictive efficiency, and (3) influence of UTR context – it has been observed that identical miRNA binding site can mediate repression in one UTR but not in others. Such a type of site efficacy is found to be governed by (a) positioning of binding site 15nt from stop codon, (b) positioning away from centre of long UTRs, (c) A-U rich nucleotide composition near the site and (d) proximity of two binding sites for co-expressed miRNAs [80]. Several computational target prediction programs namely TargetScan (v6), Pictar, RNA22, miRanda, DIANA-microT, microInspector and RNAhybrid are developed on the basis of the above mentioned variables that govern predictive efficiency for miRNA bindng sites. MiRNA registry maintained at www.miRBase.org collectively maintains putative and validated targets of all annotated miRNAs.

2.6.4 MicroRNAs in cancer

The early evidence that microRNAs could have potential role to play in cancer came from the first miRNAs discovered in *C.elegans* and Drosophila i.e. lin-4 and let-7 respectively that were found to control proliferation and apoptosis of cells. Thus their deregulation could contribute to diseases like cancer with aberrant proliferation as key feature. Secondly, it was noticed that miRNA genes were located in fragile sites in the genome which are commonly amplified or deleted in cancers. As more and more miRNAs were discovered in humans, malignant tumours and tumour cell lines of different cancers were found to have deregulated expression of miRNAs compared to their normal tissue counterparts. The first known report of deregulation of miRNA in cancer showed deletion of miR-15a and miR-16-1 in chronic lymphoid leukaemia suggesting their role as tumour suppressors [81]. Let-7 family of miRNAs was the first group of miRNAs that was shown to possess tumour suppressive activity. Loss or reduction in let-7 expression in lung cancer was shown to increase

expression of RAS proto-oncogene thus promoting cell growth and in turn tumourigenesis [69]. Subsequent studies showed that microRNAs can play both kinds of roles i.e. they either can be oncogenic or tumour suppressors. In 2005, two independent studies showed that the six miRNAs belonging to miR-17-92 cluster located on commonly amplified region in B-cell Lymphoma are over-expressed in tumours and could accelerate c-Myc induced tumourigenesis in mice [82]. Further studies by O'donnel *et al* revealed that miR-17-92 inhibits E2F1, whose expression is induced by c-Myc like that of miR-17-92 itself in lung cancer and thereby suggested that miR-17-92 cluster is induced by c-Myc to fine tune expression of E2F1[83]. A single miRNA may regulate various un-related target genes and thereby control different cellular processes depending upon its target gene expression in that tissue type [78].

2.6.5 Aberrant expression of microRNAs in medulloblastoma and their functional significance

First report of miRNA deregulation in medulloblastoma was that of brain enriched miR-124a to be downregulated in medulloblastomas. MiR-124a was shown to target CDK6, one of the markers for adverse prognosis in medulloblastomas [84]. The first global miRNA profiling of medulloblastoma was carried out by Ferretti *et al* by Taqman qRT PCR-based profiling of 248 miRNAs on a small cohort of primary medulloblastomas (n = 14), reporting consistent down-regulation of a number of miRNAs in tumours as compared to normal cerebellum. Further, two miRNAs downregulated in medulloblastomas viz. MiR-9 and miR-125a were shown to inhibit medulloblastoma cell growth and impair anchorage independence by targeting pro-proliferative truncated form of neurotrophin receptor TrkC [85].

MicroRNA profiling in parallel to protein coding gene expression profiling study done on 19 medulloblastomas by our group, for the first time showed that the miRNA profile differs across the four molecular subgroups as well as in comparison to normal cerebellar tissues,

with the WNT subgroup having distinct signature of several up-regulated miRNAs like miR-193a, miR-224/miR-452 cluster, miR-183/miR-96/miR-182 cluster, miR-148a, miR-23b/27b/24-1 cluster and miR-365 (Figure 2.5) [3]. MiRNA profiling could segregate tumours in almost identical four molecular subgroups as identified by the protein coding gene expression profiling. A follow-up study from our group showed that 21 marker real time-RT PCR assay that included 9 miRNAs and 12 genes could classify medulloblastomas into the four subgroups in a cohort of 101 primary medulloblastomas (Figure 2.6) and additional validation cohort of completely un-related 34 primary medulloblastomas from DKFZ, Germany. This study highlighted robustness of use of miRNAs as markers for molecular classification of medulloblastomas apart from distinct signature of overexpressed miRNAs in WNT subgroup tumours. The assay is particulary useful for classification of archival formalin fixed paraffin embedded (FFPE) tissues due to the fact that miRNAs being small in size are less susceptible to degradation during formalin fixation [6].

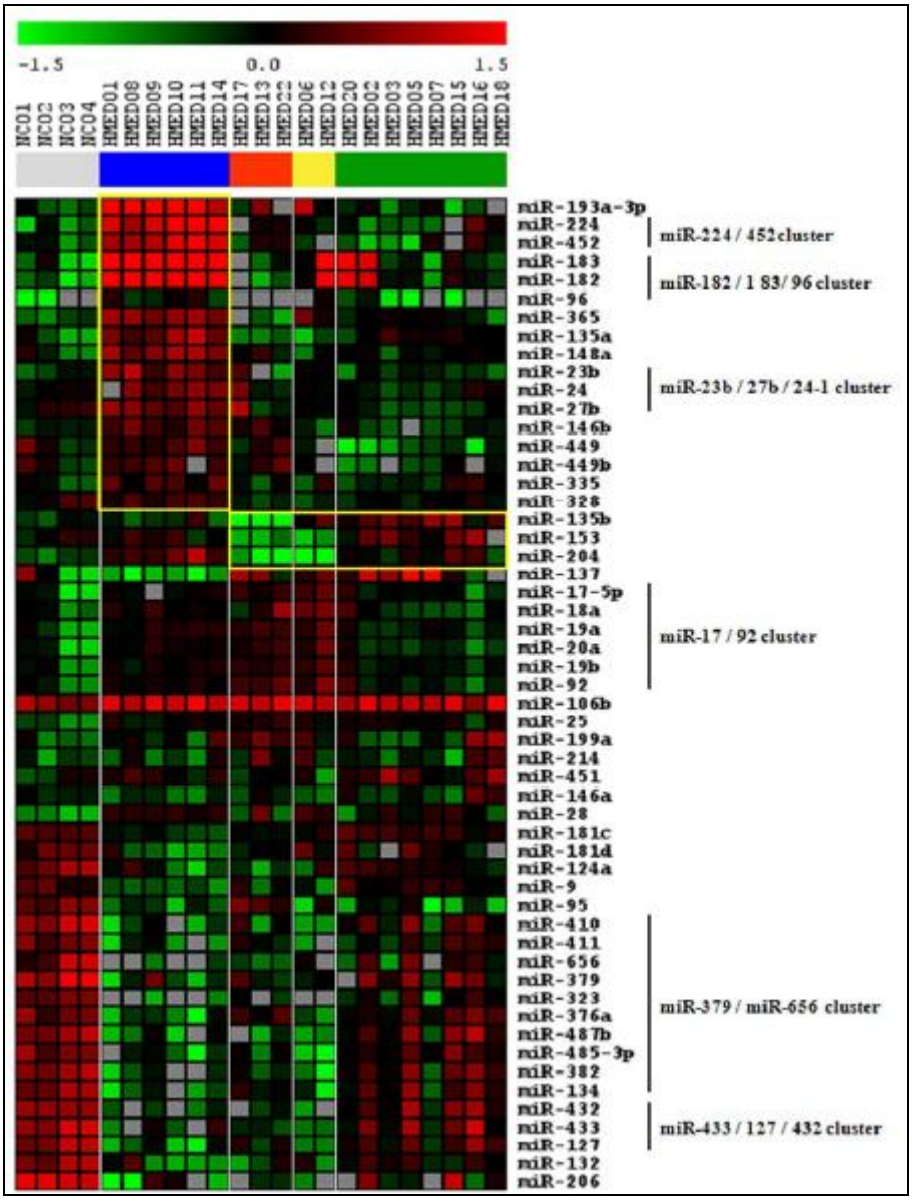

Figure 2.5: Heat map showing significantly differentially expressed miRNAs in four molecular subgroups of medulloblastoma and normal cerebellar tissues using SAM analysis. Grey: normal, blue: WNT, red: SHH, yellow- Group 3 and green: Group 4. The miRNAs within the yellow box represent the most significantly differentially up or down-regulated miRNAs in each of the subgroups. [3]

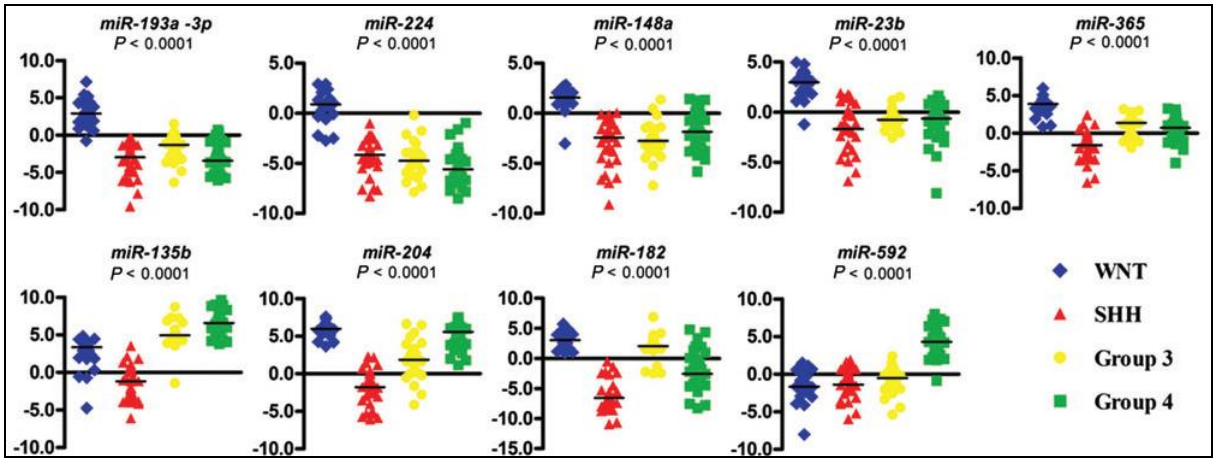

Figure 2.6: Validation of differential miRNA expression in 101 medulloblastoma by Real time-RT PCR as a follow up study. Scatter dot plot represents Log 2 transformed relative quantity expression values (Y-axis) of indicated miRNA across four subgroups (X-axis) indicated as blue: WNT, red: SHH, yellow- Group 3 and green: Group 4. [6]

Two independent studies by Northcott *et al* and Cho *et al* also studied miRNA expression along with protein coding gene expression profiling of medulloblastomas. Both of these studies showed subgroup specific differential expression, however neither of these studies reported distinct over-expression of miRNAs in WNT subgroup. This is most likely because of either less number of WNT tumours in these cohorts or low sensitivity or specificity of oligonucleotide based arrays they utilised. Nevertheless, over-expression of miR-193a, miR-224-452 cluster, miR-23b-27b-24-1 cluster and miR-183-96-182 cluster were also found in WNT subgroup medulloblastoma from Northcott *et al* series of tumours [86].

Many of these miRNAs aberrantly regulated in medulloblastomas have been characterised for their function and the genes they target. Northcott *et al* reported miR-17-92 cluster to be up-regulated in SHH medulloblastoma and to act as a positive effector of SHH mediated proliferation, suggesting growth advantage to those tumours having miR-17-92 overexpression or amplification [86]. Increased expression of the miR-183-96-182 cluster was shown to be restricted to non-SHH medulloblastomas, with miR-182 as significantly up-

regulated miRNA in metastatic tumours compared to non-metastatic ones [87, 88]. Knockdown of entire cluster of miRNAs resulted in enrichment of genes associated with apoptosis and dysregulation of PI3K-mTOR signalling axis [87]. Mir-182 was specifically found to promote cell motility/invasion and leptomeningeal spread and tumourigenesis *in vivo,* in SHH subgroup mouse models [87, 89]. MiR-34a, another miRNA downregulated in medulloblastomas, upon reintroduction in medulloblastoma cell lines has been shown to impair proliferation, invasion and survival by targeting c-MET [90] and induce apoptosis, senescence and chemosensitization by down-regulating DLL-1 and MAGE-A with concomitant increase in expression of p53 and its targets [91, 92]. Given the downregulation and robust tumour suppressive role of miR-34a across several malignancies, reintroduction of miR-34a in target tumour cells through synthetic mimics loaded in lipophilic nanoparticles is currently being tested in Phase I clinical trials [93]. Table 2.3 depicts the list of experimentally evaluated miRNAs and the functional implication of their expression in medulloblastoma as studied by *in vitro* or *in vivo* experiments.

Previous study from our lab has reported that ectopic expression of WNT subgroup specific miR-193a-3p and miR-224 in Daoy medulloblastoma cell line inhibits proliferation, anchorage independent growth and increase radition sensitivity respectively [3]. Given the fact that WNT subgroup tumours have the best prognosis amongst all the subgroups despite aberrant hyperactivation of pro-proliferative WNT signalling pathway, determination of role of other miRNAs over-expressed specifically in WNT subgroup medulloblastomas is warranted.

Type of study	MicroRNAs	Targets	*In vitro/ in vivo*	Functional relevance
Over-expression of miRNAs	miR-124	CDK6, SLC16A1	*In vitro*	Anti-proliferative
	miR-199b-5p (Up in metastatic vs non-metastatic)	HES1	*In vitro and in vivo*	Anti-tumourigenic
	miR-125b, miR-324-5p, miR-326	Not known	*In vivo*	Anti-proliferative
	miR-9, miR-125 (Down)	t-Trkc	*In vitro*	Anti-proliferative, pro-apoptotic
	miR-17-92 (Up in SHH)	ptch1	*In vivo*	Pro-proliferative, increases tumour latency
	miR-193a (Up in WNT) miR-224 (Up in WNT)	Not known	*In vitro*	Anti-proliferative, inhibits anchorage independent growth, radiation sensitizer
	miR-128a (Down)	Bmi-1	*In vitro*	Anti-proliferative, Induces cell senescence
	miR-34a (Down)	c-MET, CDK6, MAGE-A, Dll-1	*In vitro*	Anti-proliferative, anti-invasive, pro-apoptotic, induces cell senescence, chemosensitizer
Inhibition of expression of miRNAs	miR-21 (Up)	PDCD4	*In vitro*	Pro-invasive, induces migration
	miR-182 miR-183 (Up in non-WNT)	Not known	*In vitro*	Decreases cell migration

Table 2.3: Experimentally validated up or down-regulated miRNAs with their target genes. Parantheses indicate up or down regulation in subgroup specific manner if mentioned or otherwise. Experimental validation is performed either by over-expression of indicated miRNA or inhibition of endogenous expression of indicated miRNAs and their target genes identified in either *in vitro* or *in vivo* study resulting in indicated functional implication [94].

2.7 Regulators of regulators

2.7.1 Regulation of miRNA transcription

MiRNA coding genes are located either between two genes (intergenic) or in the introns of protein coding genes (intragenic). It is observed that the intragenic miRNAs are mostly transcribed along with their parent gene via their promoters [95]. Most of the miRNAs are transcribed by RNA pol II [73], while some of the miRNAs especially those interspersed between Alu sequences are transcribed by RNA Pol III [77]. Although these findings initiated thrust towards finding promoters of miRNAs, much was not known. However with advances in chromatin biology, chromatin signatures marking active transcription units, like H3K4-tri-methylation, H3K9/14 acetylation were identified. As these chromatin marks are persistent on the genomic regions near TSSs, search for promoter elements and upstream regulatory elements could now be addressed more easily [96]. On similar lines, chromatin Immunoprecipitation sequencing data generated against RNA Pol II in cell lines of different origin has been made available on UCSC genome browser which helps in identification of RNA Pol II binding regions together with chromatin marks discussed earlier. Presence of expressed sequence tags (ESTs), cap analysis gene expression (CAGE) tags and genome wide profiles of DNAseI hypersensitivity sites (DHS) available through ENCODE consortium have proved to be additional surrogate markers for identification of miRNA promoters. 55-64% of all miRNAs are associated with CpG islands in the regions upstream to pri-miRNA sequences. This is particularly important to be viewed in context of regulation of miRNA promoters because of two observations: (1) although most of the miRNAs are transcribed by RNA Pol II promoters, typical RNA Pol II promoter elements like TATA-box elements and TFIIB recognition elements have been observed in only 19% and 21% of total miRNAs respectively[97], and (2) majority of miRNAs have shown to be downregulated in

tumours compared to respective normal tissues due to hyper-methylation at CpG islands in their upstream genomic regions [98].

2.7.2 Epigenetic way of regulation of miRNA promoters

Presence of CpG islands within 4kb of the known promoters of more than half of the total number of miRNAs suggested that the regulation of transcription via promoter DNA methylation may be one of the key mechanisms of transcription regulation of these miRNAs. The first evidence of an epigenetic mechanism involved in silencing of miRNAs in cancer came from study of Saito *et al* who analysed miRNA expression profiles of bladder cancer cells treated with DNMT inhibitor 5-Aza-2'-deoxycytidine (5'-Aza-CdR) and HDAC inhibitor 4-PBA. In addition to miR-127, miR-34 family of microRNAs were the miRNAs whose expression was linked to first for which aberrant DNA methylation and histone deacetylation at their promoters [99]. Subsequently, expression of miRNAs like miR-148a, miR-29 has been shown to be repressed through DNA methylation and/or histone modifications at their promoters in variety of cancers, while these miRNAs have been shown to target DNA methyl-transferases like DNMT1, DNMT3b proteins which are crucial for maintainance of DNA methylation, suggesting presence of feed forward mechanism of regulation. CpG DNA methylation and histone modification are known to be interlinked to each other, where presence of DNA methylation can target repressive histone modifications, which in turn further enhances DNA methylation at that locus [100]. In a study of mammary fibroblasts and epithelial cells, promoters for 232 miRNAs were identified using H3K4me3 profiling, out of which 38% showed tissue specific silencing by promoter methylation. Epigenetic inactivation through histone modifications has been suggested to be more important in tissue specific regulation of miRNAs. In the above mentioned study using mammary fibroblasts and epithelial cells, 58% of tissue specific promoters were silenced by H3K27 trimethylation, while redundancy of both repressive marks i.e. DNA methylation and

H3K27 trimethylation was limited to 21% , indicating different roles of these repressive marks to achieve tissue specific miRNA regulation[97, 101].

2.8 MiRNAs as therapeutic agents or targets

The frequent deregulation of miRNAs in cancer and their interplay with epigenetic regulators make them attractive biomarkers and prospective therapeutic agents/targets for effective cancer treatment.

The epigenetic abnormalities in cancer, unlike genetic lesions, can be reversed by epigenetic-regulated drugs, which provide an opportunity for epigenetic therapy.Two well known DNMT inhibitors, 5-azacytidine (5-AzaC) and 5-aza-2'deoxycytidine (5'-Aza-CdR), were approved by FDA to treat myelodysplastic syndromes (MDS) and AML, while in 2006, FDA also approved the HDAC inhibitor suberoylanilide hydroxamic acid (SAHA) to treat cutaneous T-cell lymphoma (CTCL) [97]. Since many tumour suppressive miRNAs, downregulated in many cancers can be activated by using these drugs, and as miRNAs have been recognised as useful therapeutic targets due to their ability of controlling many genes at a time, HDAC and DNMT inhibitors may gain more importance in cancer therapy in coming years.

The exploration of tumour suppressive or oncogenic miRNAs as therapeutic agents or targets through two ways (1) endogenous miRNA inhibition in case of oncogenic miRNAs and (2) miRNA replacement in case of tumour suppressor miRNAs. The reduction in expression of oncogenic miRs can be achieved by using (1) antagomiRs which are nothing but chemically modified antisense oliginucleotides that are stable in vivo and have greater affinity to target miRNA, (2) miRNA sponges which are oligonucleotides that have complementary sequence for one or more mature miR sequences thus competing with targets of those miRNAs and (3) miR-masks which are oligonucleotides complementary to binding site of miRNA in 3'UTR and prevent binding of miRNA to that 3'UTR. On the other hand, introduction of tumour

suppressor miRNAs that are downregulated in tumour cells can be achieved by synthetic double stranded RNAs into tumour cells [102]. In 2008, the first miRNA based phase I clinical trial was initiated to treat hepatitis C using a Locked Nucleic Acid (LNA) oligonucleotide complementary to miR-122 (Miravirsen) to inhibit expression of this miRNA which normally facilitates viral replication. This was shown to be effective more than anticipated as this antisense oligonucleotide could target pre and pri sequences of miR-122 too [103]. The first miRNA based therapy developed for cancer treatment is MRX34, a synthetic miRNA mimic loaded in liposomal nanoparticles. MiR-34a is tumour suppressor miRNA that acts downstream to p53 and is downregulated in many solid tumours like cervical cancer, ovarian cancer, glioblastoma, hepatocellular carcinoma (liver cancer), colon cancer, non-small cell lung cancer (NSCLC) [104]. MRX34 is in phase I clinical trial initiated by miRNA therapeutics (http://www.mirnatherapeutics.com) and being conducted in patients with unresectable primary liver cancer or solid cancers with liver involvement. The trial also includes a separate cohort of patients with hematological malignancies. These studies therefore indicate that the miRNA based therapy is most likely to be effective in a systemic manner and may be developed against many cancers known to possess similar abnormalities in miRNA expression.

Chapter 3: MATERIALS & METHODS

MATERIALS:

The following chemicals were obtained from **Applied Biosystems, Life technologies,** Carlsbad, CA, USA**:**

2X TaqMan Universal PCR Master Mix (Part No. 4304437); 2X Power SYBR Green PCR Master Mix (Part No. 4367659), 2X TaqMan PreAmp Master Mix (Part No.4384266), TaqMan MicroRNA Assays (Part No. 4427975) - Assay IDs for each miRNA assays are: hsa-miR-193a (000492), hsa-miR-224 (000599), hsa-miR-148a (000470), hsa-miR-204 (000508), hsa-miR-182 (000597), hsa-miR-135b(000461), hsa-miR-592 (001546), RNU48 (001006); MicroAmp optical 384-well Reaction Plate with Barcode (Part No. 4309849) and MicroAmp Optical Adhesive Film Kit (Part No.4313663).

The following chemicals were obtained from **GE Dharmacon,** Lafayette, CO, USA**:**

MiRNA mimics, siGLO RISC-Free Control siRNA, miRIDIAN microRNA mimic and Dharmafect 2 tranfection reagent.

The following chemicals were obtained from **Invitrogen, Life technologies,** Carlsbad, CA, USA**:**

MMLV-RT 200 U/ul (Cat No. 28025-013), Dulbecco's modified Eagle medium (Cat. No.12800-058), DNAse I, amplification grade (Cat No. 18068-015), Fetal bovine serum (CatNo. 16140-071), LMP (low melting point) agarose, Trypsin, L-Glutamine, Formamide (Cat. No.15515)

The following chemicals were obtained from **Sigma-Aldrich,** St Louis, MO, USA**:**

Agarose, Proteinase K, Guanidium Isothiocyanate (GITC), Diethyl pyrocarbonate (DEPC), DMSO, EDTA, Ethidium bromide, BES (B4554-25G), Puromycin (Cat No.P8833-25MG), 5-Aza 2'deoxyctidine (Cat No. A3656-5MG), Trichostatin A (Cat No. #206700), Ammonium persulphate.

The following chemicals were obtained from **Amersham Lifesciences, GE Healthcare Life Sciences,** Pittsburgh, PA, USA**:**

dATP, dGTP, dTTP, dCTP (100 mM each) (Cat. No.27-2035-01), Random hexamers pd(N)6 Sodium salt.

The following chemicals were obtained from **Thermo Scientific, Life technologies,** Carlsbad, CA, USA**:**
10X PCR Buffer, Exonuclease I, Gene Ruler 1 Kb DNA ladder, Shrimp Alkaline Phosphatase (SAP) (Cat. No. EF0511), 25 mM MgCl2, Taq DNA polymerase (1U/ µl) (Cat. No. EP0404). T4-DNA ligase (Cat No.E0011), DpnI (Cat No- ER1701), SuperSignal® West Pico chemiluminescent substrate (Pierce-Thermo scientific, Cat. No.34077)

The following chemicals were obtained from **Merck millipore,** dermstadt, Germany**; Qualigens,** ThermoFischerScientific India Pvt Ltd, Mumbai, India or **s d fine-chem limited,** Mumbai, India**:**
Xylene, Methanol, Glacial Acetic Acid, Potassium Acetate, Sodium Acetate, N-laurylsarcosine. Sulfuric Acid (LR), Potassium dichromate (LR), Tri-Sodium citrate (LR), Citric Acid (LR), Hydrogen peroxide, Methanol.

The following reagents were obtained from **New England Biosciences (NEB),** Ipswich, MA, USA**:** Standard Taq (Cat No.M0273L), T4PNK (M0201)

The following reagents were obtained from **s d fine-chem limited,** Mumbai, India**:**
NaCl (Cat No.20241 AR), $Na_2HPO_4.2H_2O$ (Product no. 20383 AR), $CaCl_2.2H_2O$ (Sigma C-3306)

The following **kits** were obtained from the companies specified in brackets:
Recover All RNA extraction kit (Ambion, Life Technologies, carlsabd, CA, USA; Cat No.AM1975)
EZ DNA Methylation-Gold Kit (Zymo-Research, Irvine, CA, USA; Cat No.D5005)
QiaAmp DNA mini kit (Qiagen, Limburg, Netherlands; Cat No.51304)
Qiagen Plasmid Midi kit (Qiagen, Limburg, Netherlands ; Cat No.12143)
QIAquick Gel Extraction Kit (Qiagen, Limburg, Netherlands; Cat No.28704)

The water used for the preparation of all solutions and reagents was Ultrapure water (Resistivity = 18 MΩ cm) obtained from a Milli-Q water plant (**Millipore,** Billerica, MA,USA).

Disposable plastic ware (certified DNase, RNase, and protease-free) was obtained from **Axygen**, California, USA.

Disposable sterile plastic ware for tissue culture was obtained from **Nunc**, Rochester, NY, USA.

Primers:

All PCR primers were synthesized and obtained from **Sigma Genosys** in the lyophilized form.

METHODS:

3.1 Collection of sporadic medulloblastoma tumour tissues and normal cerebellar tissues

Approval for the project was obtained from the Institutional Review Board and Ethics Committee of Tata Memorial Hospital (T.M.H) and King Edward Memorial (K.E.M.) Hospital, Mumbai. Forty-four fresh tumour tissue specimens of sporadic medulloblastoma were obtained from patients who had undergone surgery at T.M.H and K.E.M. Hospital, Mumbai, after obtaining informed consent. Standard practice of treatment with surgery followed by radiation (with the exception of less than 3 yr old children) and chemotherapy was followed for all the medulloblastoma cases studied. Immediately following surgery, the tumour tissues were snap-frozen in liquid nitrogen and stored at –80°C until use. 96 formalin-fixed paraffin-embedded (FFPE) medulloblastoma tumours tissues from T.M.H and K.E.M Hospital were also included in this study.

Normal cerebellar tissues were obtained from Brain Tissue Repository, NIMHANS, Bangalore that include two normal developing cerebellar tissues from children less than 1 yr of age and six normal adult cerebellar tissues.

3.2. Extraction of nucleic acids

Prior to RNA and DNA extraction, cryosections of fresh frozen tumours and 5µm sections of FFPE tumour tissues were stained for hematoxylin and eosin and examined by light microscopy to ensure at least 80 % tumour content.

3.2.1 Total RNA Extraction

a) RNA from fresh frozen tumour tissues and/or tissue culture cells by acid guanidinium thiocyanate-phenol chloroform extraction[105]

Materials:

1. *Preparation of DEPC-treated Milli-Q water*: Water was collected from the Milli-Q plant directly in sterile 50 ml NUNC tubes. 50 µl DEPC was added to 50ml Milli-Q water mixed vigorously and left overnight at 37°C, with the tubes loosely capped. The tubes were autoclaved on the following day. The DEPC-treated Milli-Q water was used for preparing all the reagents required for RNA extraction.

2. *1 M Sodium citrate, pH 7.0*: 14.7 g Sodium citrate, dihydrate was dissolved in ~35 ml autoclaved Milli-Q water. pH was adjusted to 7.0 with few drops of 1 M citric acid and the volume was made up to 50 ml. (1 M Citric acid was prepared by dissolving 10.5 g powder in 50 ml DEPC-treated water.) 50 µl of DEPC was added to both 1 M citrate and citric acid solution, tubes were mixed vigorously and left at 37°C overnight. The solutions were autoclaved the next day, and stored at room temperature.

3. *10% N-lauryl-sarcosine*: 5 g N-lauryl-sarcosine was dissolved in DEPC-treated water and the final volume was made up to 50 ml. Resulting solution was neither treated with DEPC, nor autoclaved**.** It was kept at 65°C for 1 hr, and stored at room temperature.

4. *4 M Guanidine Isothiocyanate* (GITC): (Prepared in 25 mM Sodium citrate pH 7.0, 0.5% Sarcosyl) 23.6 g of guanidine isothiocyanate was dissolved in 40 ml DEPC-treated water. 1.25 ml of 1 M sodium citrate and 2.5 ml of 10 % sarcosine was added and the final volume

was made up to 50 ml with DEPC-treated water. The final solution was neither treated with DEPC nor autoclaved. Solution D was prepared from GITC by adding β-mercaptoethanol at a final concentration of 0.1 M**.** This solution is stable at room temperature for one month.

5. *Phenol (Saturated with DEPC-treated water)*: 25 ml DEPC-treated water was added to 25 ml distilled phenol at room temperature in a sterile NUNC tube. The tube was mixed vigorously by inverting several times. The phenol was kept at 4°C until the two phases separated (30-60 min). The upper water phase was replaced with fresh DEPC-treated water, mixed once again and stored at 4°C.

6. *2 M Sodium acetate, pH 4.0*: 13.6 g sodium acetate was dissolved in about 25 ml of Milli-Q water and pH was adjusted to 4.0 with glacial acetic acid. Final volume was made up to 50 ml with Milli-Q water. 50 µl DEPC was added to the solution, mixed vigorously and left at 37°C overnight. The solution was autoclaved the following day and stored at room temperature.

7. *Chloroform*

8. *Absolute alcohol*

9. *70 % alcohol*

Only RNase free sterile plastic wares were used.

Method:

1a. approximately 30-50 mg of frozen tumour tissue was collected in a chilled homogenization collection tube. This was homogenized with approximately 2-3 ml of Solution D. The tissue lysate was collected in a microcentrifuge tube and immediately passed through a 26-gauge needle at least ten times. The lysate was triturated until it loses its viscosity, resulting in complete shearing of genomic DNA.

1b. For tissue culture cells, medium was poured off, cells were washed with 1 X PBS twice and 0.5 ml of Solution D was added per well of 24 well plate. The cell lysate was collected

by tilting the plate and was passed immediately through a sterile syringe fitted with a 26 gauge needle. This was done at least ten times until the lysate lost its viscosity, resulting in complete shearing of the genomic DNA. At this stage the lysate was either stored at -20°C or processed further immediately.

2. 50 µl of 2 M Sodium acetate pH 4.0 was added per 0.5 ml lysate and mixed by inverting the tubes.

3. Next, 0.5 ml DEPC-water-saturated phenol and 0.25 ml chloroform was added successively to the tube and the contents of the tube were mixed thoroughly by vortexing for 1 min. The cap of the tube was loosened to release the pressure and then vortexed again for 30 sec.

4. The tube was kept on ice for 15 min and then centrifuged for 15 min at 4°C at 10,000 rpm in a table-top centrifuge. The upper aqueous layer obtained was transferred to a fresh microcentrifuge tube and centrifuged once again to settle any traces of phenol.

5. The aqueous phase was then transferred to a fresh tube and an equal volume of isopropanol (0.5 ml per tube) was added. This was mixed by brief vortexing and kept at -20°C overnight for precipitation of RNA.

6. Next day, the tube was centrifuged at 12,000 rpm at 4°C for 20 min to pellet down the precipitated RNA. The supernatant was decanted carefully without disturbing the RNA pellet.

7. The RNA pellet was washed with 0.5 ml of 70 % ethanol, kept at room temperature for 2 min, and re-centrifuged at 12,000 rpm at 4°C for 10 min. The supernatant was decanted, and the left over alcohol was allowed to dry by keeping the tube open with a clean tissue paper to cover it. The RNA pellet was air-dried, and dissolved in a minimum of 10 µl DEPC-treated water. For dissolving the RNA, it was first kept on ice for about 60 min with intermittent vortexing and spinning, followed by heating at 65°C for 10 min. The dissolved RNA was subsequently stored at -80°C.

8. RNA was quantified spectrophotometrically (O.D. at 260/280 nm) using the NanoDrop UV-Vis spectrophotometer. The integrity of RNA was ascertained by denaturing agarose gel electrophoresis. The ratio of 28s rRNA to 18s rRNA is approximately 2:1 in a good quality RNA.

b) RNA extraction from FFPE tumour tissues by using RecoverAll™ Total Nucleic Acid Isolation kit

In addition to the 45 fresh frozen tumours, 96 FFPE tumour tissues were also included for validation of the miRNA profiling data.

5 to 10, 10 µm sections were taken as starting material to extract RNA. RNA was extracted from these FFPE tissues using Recover All RNA extraction kit. As FFPE RNA is known to be considerably degraded, denaturing gels for quality assessment do not yield significant results. Therefore, RNA quality and quantity was ascertained spectrophotometrically (O.D.260/280 ratio) using the NanoDrop UV-Vis spectrophotometer.

c) Preparation of denaturing gels for RNA separation and quality assessment

Formaldehyde containing agarose gel was used for checking the integrity of RNA from fresh frozen tumour tissues. Unlike DNA, RNA has a high degree of secondary structure, making it necessary to use a denaturing gel. Formaldehyde in the gel disrupts secondary RNA structure enabling the RNA molecules to be separated by charge migration.

Materials:

1. *Agarose*

2. *10X MOPS*: 41.6 g MOPS, 16.7 ml of 3 M sodium acetate pH 5.0, 20 ml of 0.5 M EDTA pH 8.0. Adjust pH to 7.0 with 5 M NaOH and make up the volume to 1 litre with DEPC water. Autoclave the solution and store in an amber colored bottle.

3. *Formaldehyde (37% solution LR grade)*

4. *Formamide*

5. *10X RNA loading dye*: 1 mM EDTA pH 8.0, 50 % v/v glycerol, 0.4 % bromophenol blue.

Method:

1. For a 50 ml volume, 1 % agarose gel was prepared as follows: 0.5 g agarose was weighed into 35 ml of autoclaved Milli-Q water. The slurry was heated in a microwave oven until the agarose dissolved completely. 5 ml 10 X MOPS was added make the final concentration to 1X and the slurry was mixed properly and placed at 60 ºC for 10 min.

2. Next, 10 ml formaldehyde was added and the formaldehyde-agarose slurry was kept at 60ºC for 15 min.

3. Ethidium bromide to a final concentration of 0.5 μg/ml (2.5 μl), was added to the agarose mix, and the mixture was poured in a gel tray and allowed to set at room temperature for 30-45 min.

4. After the gel had completely set, it was placed in the electrophoresis tank filled with 1X MOPS buffer (30 ml MOPS + 30 ml formaldehyde+ 240 ml Milli-Q), just enough to cover the gel.

5. For sample preparation, RNA was mixed with 10 X MOPS (at 1X final concentration) and freshly prepared formamide: formaldehyde (3:1) mixture. For example; for 2 μl of 1 μg RNA, 1 μl of 10 X MOPS and 6 μl formamide: formaldehyde (3:1) was added. This mix was subsequently placed at 60 ºC for 20 - 30 min.

6. 10X RNA loading dye at 1X final concentration was added to the above mix and loaded into the wells of the gel. The gel was electrophoresed at 60 mA constant current, till the dye had migrated almost to the other end of the gel.

7. The gel was then placed in Milli-Q water overnight to wash off excess of ethidium bromide. RNA was visualized by observing the gel under a UV transilluminator.

3.3. Gene expression analysis by real time Reverse transcriptase PCR (Real time-RT-PCR)

3.3.1. Primer Designing

The primers for real time RT-PCR analysis were designed such that they correspond to two adjacent exons of target gene, and are located at exon boundaries, to avoid amplification of genomic DNA. The amplicon size was maintained below 85 bp, to enable amplification of the fragmented RNA from FFPE tissues. Primers were designed using the Oligo Explorer Software v 1.1.2. BLAST (www.ncbi.nlm.nih.gov/BLAST) and e-PCR feature of BiSearch software were performed to ensure primer specificity. The primers were reconstituted in TE Buffer, pH 8.0 to a concentration of 100pmol/µl. For working stock of 10 pmol/µl, the primers were further diluted 1:10 using TE Buffer. All primers were stored at – 20°C. Sequences of the primers used for real time in the present study are listed below in Table 3.1

Gene name	Primer	Sequence
WIF1	FWD	CCTGCCATGAACCCAACAAATGCC
	REV	GAGGCTGGCTTCGTACCTTTTATTGC
NRP1- Total (all isoforms)	FWD	CCGCCTGAACTACCCTGAGAA
	REV	GCCCAAGTCTACCTGTATCCAC
NRP1-3'-UTR	FWD	ACAAGGGAAGTGGAAGGAAGGAA
	REV	AAAATACTTGACCCCCAGGC
NRP1-TM (trans-membrane domain)	FWD	CCTCATCACCATCATAGCCA
	REV	AGCACGACCCCACAGACAGC
GAPDH	FWD	GAAGGTCGGAGTCAACGGATT
	REV	GAGTTAAAAGCAGCCCTGGTG

Table 3.1: Primer sequences used for Real time PCR analysis

3.3.2. Removal of genomic DNA from total cellular RNA

Any genomic DNA contamination if present in the RNA preparation was removed by RNase free DNase I treatment. This procedure was avoided for RNA from FFPE tissues, to avoid further degradation of the already fragmented RNA.

Materials:

1. *10X DNase I buffer*

2. *DNase I (1 U/µl)*

3. *25 mM EDTA*

4. *DEPC treated Milli-Q water*

Method:

1. All the required reagents were thawed and mixed well by tapping and pulse spinning 1 µg RNA was treated with 1 U of DNase I in a 5 µl reaction. The reaction contained the following components:

Constituents	Volume	Final concentration
10X DNase I buffer	0.5 µl	1X
DNase I (1U/µl)	1 µl	1 U/µg of RNA
RNA	1 µg	
DEPC treated Milli-Q water	Make up volume to 5 µl.	

2. The sample was incubated at room temperature for exactly 15 min. Higher temperatures and longer time can lead to Mg++ mediated degradation of the RNA, hence was avoided.

3. The enzyme was inactivated by addition of 0.5µl 25mM EDTA followed by incubation at 65 °C for 10 min.

4. The DNase I treated RNA was then used for cDNA synthesis using M-MLV RT.

3.3.3. Reverse transcriptase reaction for cDNA synthesis

Materials:

1. *5X First Strand Buffer*

2. *M-MLV RT enzyme (200 U/µl)*

3. *0.1 M DTT*

4. *10 mM dNTP mix,*

5. *RNase Inhibitor (20 U/µl),*

6. *Random hexamers p(dN)6 (100 ng/µl)*

Method:

1. A 10 µl reaction was set up for the cDNA synthesis from 1 µg of DNase-treated total RNA

2. First, the following components were added to a nuclease-free microcentrifuge tube:

Constituents	Volume	Final Concentration
DNase-treated total RNA		1 µg
10 mM dNTP mix	0.5 µl	
100 ng/µl random hexamers p(dN)6	0.5 µl	0.5 mM
DEPC treated Milli-Q water		Make up volume to 5 µl
Total Volume	5 µl	

3. RNA was heated at 65 °C for 5 min to denature RNA secondary structures and chilled on ice for 2 minutes.

4. Reaction mix was prepared on ice by adding the following components:

Constituents	Volume	Final Concentration
5X first strand buffer	2 µl	1X
0.1 M DTT	1 µl	0.01 M
RNase inhibitor (20 U/µl)	0.25 µl	5 U
DEPC treated Milli-Q water		Make up volume to 3.5 µl

5. The reaction mix was added to the RNA, mixed by gentle pipetting, and incubated at 37 °C for 5 min to allow annealing of random primers to the RNA.

6. 0.5 µl (100 U) of M-MLV RT was added to the reaction tube and mixed by gentle pipetting. The tubes were transferred to the thermal cycler (Eppendorf) and thereafter the following conditions were followed:

Temperature	Time
25 °C	10 min
37 °C	60 min
70 °C	15 min
4 °C	∞

7. The cDNA synthesized was then used for analyzing gene expression levels by real time PCR or stored at -20 ℃.

3.3.4. Real Time PCR

Materials:

1. *2X Power SYBR Green Master Mix*

2. *10 pmol /µl each gene specific Forward and Reverse primers.*

3. *DEPC- treated Milli-Q water*

Method:

1. The cDNA obtained from the reverse transcription reaction was diluted to 5 ng/µl (fresh frozen tissue) or 50 ng/µl (FFPE tissue) with DEPC-treated Milli-Q water for use in the PCR reaction. The PCR reaction was set up as follows:

Master Mix I:

Constituents	**Volume**	**Final Concentration**
2X SYBR Green Master Mix	2.5 µl	1X
cDNA (5 ng or 50 ng/µl)	2 µl	10 ng or 100 ng
Total Volume	4.5 µl	

Master Mix II:

Constituents	**Volume**	**Final Concentration**
10 pmol/µl Forward primer	0.25 µl	0.5 pmol
10 pmol/µl Reverse primer	0.25 µl	0.5 pmol
Total Volume	0.5 µl	

2. The Master Mix I was then loaded into the wells of a 384-well microtitre optical plate followed by addition of master mix II to each well.

3. The plate was covered with an optical cover sheet and sealed with the help of an applicator. The applicator was pressed evenly over the optical cover sheet and between the goorves separating rows and columns several times to ensure proper sealing of the wells.

4. The sealed plate was then centrifuged briefly at 2000 rpm for 2 min to spin down the reactions and remove air bubbles if any.

5. The plate was loaded in the Real Time PCR machine (ABI Prism 7900HT Sequence Detection System/ QuantStudio 12K Flex, Applied Biosystems, USA) and run on default cycling parameters.

PCR cycling parameters:

Temperature	Time	No. of Cycles
50 °C	10min	Hold
95 °C	10min	Hold
95 °C	15 sec	40
60 °C	1min	

6. The 50 °C incubation is to activate UNG glycosylase enzyme that prevents carry over PCR contamination followed by an initial denaturation step for 10 min with activation of HotStart Taq polymerase and then 40 cycles of denaturation-annealing-extension. In case of SYBR Green Assays after completion of 40 cycles, the dissociation curve step of the amplified products was performed to determine the formation of primer dimers, if any.

7. Amplification data was collected in real time by the machine and stored in the SDS 2.1 or QuantStudio software. After completion of the runs, the data was analyzed using these same softwares.

8. *GAPDH* was used as the housekeeping gene control. The expression of the gene of interest, relative to *GAPDH* levels was quantified and expressed as Relative Quantity (RQ), calculated by the comparative Ct method.

The expression of the gene of interest, relative to *GAPDH (*or *RNU48* in case of miRNAs) levels were quantified and expressed as Relative Quantity (RQ), calculated as Ct (gene of interest) – Ct (*GAPDH*) = ΔCt. The Relative quantity was calculated as $[2^{-(\Delta Ct)} \times 100]$. Ct = Threshold cycle as automatically determined by the SDS 2.1 or QuantStudio software.

3.4.1 Quantification of miRNA expression by Real time PCR

MiRNA quantification involves a stem-loop reverse transcription followed by real time PCR. Mature miRNAs are only 20-23 nucleotides in length. The stem–loop RT primers hybridize to mature miRNA molecule at the 3' end and then get reverse transcribed with the help of a reverse transcriptase enzyme. The RT product is then quantified by conventional TaqMan PCR with miRNA specific forward primer, reverse primer corresponding to part of the stem-loop RT primer (excludes the loop region) and the TaqMan probe.

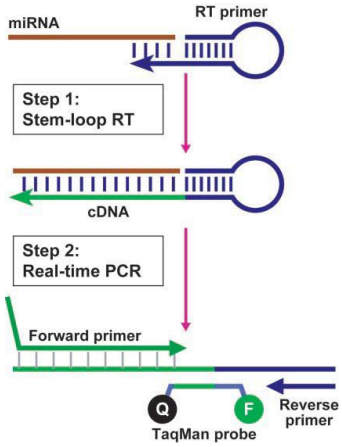

Figure 3.1: Stem- loop RT-PCR for miRNA. Schematic description of stem-loop RT- PCR for miRNA quantification using TaqMan miRNA Assays [106]

Total RNA, 50 ng, was reverse transcribed using stem-loop RT primers pool and Multiscribe Reverse transcriptase as per the manufacturer's instructions. RT primer pool included primers for endogenous small RNAs and concerned microRNAs. The reaction conditions were as follows:

(a) Stem- loop Reverse Transcription for miRNA

Materials:

1. *10X RT Buffer*

2. *100 mM dNTP mix*

3. *Multiplex RT Primer Pool (prepared by using 5X RT Primers for RNU48, miR-148a and/or miR-193a at 0.05X final concentration in 1X T.E) (See section 3.4.2a for details)*

4. *RNase Inhibitor (20 U/µl)*

5. *Multiscribe M-MLV RT enzyme (50 U/µl)*

6. *DEPC- treated Milli-Q water*

Method:

1. All the reagents required were thawed and mixed well by tapping and pulse spinning. MiRNA reverse transcription primers were thawed on ice.

2. A 5 µl reaction was set up from 50 ng of RNA extracted from stable pTRIPZ or pTRIPZ-miR-148a expressing polyclonal populations of medulloblastoma cell lines or Trichostatin A (TSA)/Valproic acid (VPA) treated D425 cells, in case of HDAC inhibitor experiments.

3. The reaction contained the following components:

Components	Volume	Final Concentration
10X RT Buffer	0.5 µl	1X
100mM dNTP mix	0.1 µl	0.5 mM
Multiplex RT primer pool	2 µl	1X
RNase inhibitor (20 U/µl)	0.1µl	2 U
Multiscribe MMLV-RT (ABI)	1 µl	50 U
Total RNA	50 ng/ 200 ng	
DEPC treated MQ water	Make up volume to 5 µl	

4. A master mix was first prepared in a 0.5 ml tube excluding the RNA making up the total volume to 3 µl.

5. Before adding MMLV-RT, the PCR machine was set and kept on hold at 16 °C and the lid temperature was set to 105 °C. The contents of the tube were gently mixed by tapping followed by a pulse spin.

6. 3 µl of master mix was then dispensed into each 0.2 ml tube followed by addition of 2 µl of the diluted RNA sample (5 ng or 100 ng/µl) to the respective tubes. The reaction mix was gently tapped and pulse spun and transferred to a thermal cycler. The reaction conditions were as follows:

Temperature	Time
16 ℃	30 min
42 ℃	30 min
85 ℃	5 min
4 ℃	∞

b) Real time PCR

Materials:

1. *2X Taqman PCR Master Mix*

2. *20X Taqman miRNA Assays (miRNA Primer-Probe)*

3. *DEPC- treated Milli-Q water*

Method:

1. cDNA obtained from the stem- loop reverse transcription reaction was diluted to 5 ng/µl (Fresh frozen tissue) with DEPC-treated Milli-Q water for use in the PCR reaction. The PCR reaction was set up as follows:

Master Mix I:

Components	Volume	Final Concentration
2X Taqman PCR Master mix	2.5 µl	1X
cDNA (5 ng or 20 ng /µl)	2.0 µl	10 ng
Total volume	4.5 µl	

Master Mix II:

Components	Volume	Final Concentration
20X Probe-Primer Mix	0.25 µl	1X
DEPC treated Milli-Q water	0.25 µl	
Total volume	0.5 µl	

The steps following this were same as that in real time PCR for gene expression analysis [*refer Section 3.3.4 steps 2-7*]. RNU48 was used as the housekeeping small RNA internal control for miRNAs. The expression of the miRNA of interest, relative to RNU48 levels was quantified by the comparative Ct method. (*Refer Section 3.3.4 step 8*).

3.4.2 Real time RT-PCR assay for molecular classification of medulloblastoma FFPE tissues [6].

The differential expression of the protein-coding genes (Refer section 3.3.3) and miRNAs across 96 FFPE tissues was analyzed by real-time RT-PCR. Primers used are taken from the study mentioned in [6].

The addition of a pre-amplification step prior to real time PCR is beneficial when working with limiting amounts of RNA. Pre-amplification is particularly recommended for the detection of low-expressing miRNAs. The standard Taqman MicroRNA Assay protocol calls for an individual RT reaction for each target miRNA. By incorporating the preamplification reaction, multiplexed RT step for pools of up to 96 individual RT primers or Taqman miRNA Assays can be performed.

a) Preparation of custom RT pool

Each Taqman MicroRNA Assay contains one 5X RT primer. Up to 96 of these primers can be pooled into one RT reaction as follows:

1) Combine 1µl of each individual 5X RT primer and add 1X T.E to make the final volume to 100 µl.

2) Final concentration of each RT primer in the RT primer pool should be 0.05X each. The RT primer pool can be stored at – 20 °C for up to two months.

b) Preparation of custom pre-amplification (Pre-Amp) primer pool

The Pre-Amp primer pool is prepared similar to the custom RT primer pool. 1 µl of each individual 20X Taqman MicroRNA Assay was combined and 1X T.E. was added to make the final volume to 100µl, with the final concentration of 0.2X for each assay in the pool. Store the Pre-Amp primer pool at – 20 °C.

c) Preparation of the RT reaction mix

The Taqman MicroRNA Reverse Transcription Kit contains all the reagents necessary for the multiplex RT step except the RT primer pool.

1) In a 0.2 µl PCR tube, the following reaction components were added. The reaction mix was prepared on ice. The custom RT pool (thawed on ice) or Multiscribe Reverse Transcriptase should not be vortexed. A single PCR reaction contained the following components:

Components	Volume	Final Concentration
10X RT Buffer	0.5 µl	1X
100 mM dNTP mix	0.1 µl	0.5 mM
Custom RT primer pool	2.0 µl	0.02X each
RNase inhibitor	0.1 µl	2 U
Multiscribe MMLV-RT	1.0 µl	50 U
DEPC treated Milli-Q water	Make up volume to 4 µl	

2) The components were mixed thoroughly by inverting 6 times followed by pulse spin. The reaction mix should not be vortexed.

3) 1 µl of 25 ng total RNA was added to the reaction mix for a total reaction volume of 5 µl. The components were mixed by inverting 6 times followed by pulse spin.

4) The reaction was incubated on ice for 5 min and subsequently transferred into a thermal cycler. The cycling parameters were same as that for stem- loop RT-PCR. The RT product can be stored at - 20°C for up to one week.

d) Preparation of the Pre-Amp reaction mix

1) In a 0.2 µl PCR tube, the following components were added:

Components	Volume	Final Concentration
Taqman Pre-Amp Master Mix	2.5 µl	1X
Pre-Amp primer pool	0.75 µl	0.03X each
RT Product	0.5 µl	2.5 ng
DEPC treated MQ water	Make up volume to 5 µl	

2) The reaction components were mixed thoroughly followed by pulse spin. The tubes were then transferred to a thermal cycler.

PCR cycling parameters:

Temperature	Time	No. of Cycles
95 °C	10 min	Hold
55 °C	2 min	Hold
72 °C	2 min	Hold
95 °C	15 sec	
60 °C	4 min	
99.9 °C	* 10 min	Hold
4 °C	∞	Hold

* For enzyme inactivation

3) After the Pre-Amp PCR the tubes were spun briefly. 2 µl of the Pre-Amp product was diluted to 16 µl (1:8 dilution) using 0.1X T.E., pH 8.0. This is the diluted Pre-Amp product which can be stored at - 20°C for up to one week.

e) Preparation of the real time PCR reaction mix- Refer to 3.4.1

3.5. Bisulphite conversion of genomic DNA and sequencing of PCR amplified gene fragments

Bisulphite conversion of genomic DNA is performed wherein demthylated cytosines from genomic DNA are converted into thymidine, while methylated cytosines remain as cytosine resisting the sodium bisulphite treatment. This Bisulphite converted genomic DNA was used as template to PCR amplify fragment of genomic DNA by using primers. Bisulphite converted DNA sequence was obtained using software called Bisearch by feeding the normal genomic DNA sequence corresponding the concerned genomic region and primers were manually designed such that (1) they do not contain any CpG dinucleotides present in the normal genomic region (2) Amplicon size does not exceed 300 bp and (3) Tm of primers is equal to or greater than 55^0C and should be within 3^0C of each other. Quality and specificity of PCR primers was checked using OligoAnalyser 1.5 (www.genelink.com) and ePCR feature of 'Bisearch' (http://bisearch.enzim.hu/).

3.5.1 Extraction of genomic DNA from Fresh Frozen tissues and cultured cells

Genomic DNA of cultured cells (5x 10^6 cells) and 25-30 mg fresh frozen tissue was isolated by using Qiaamp DNA mini kit as per the manufacturer's instructions.

3.5.2 Bisulphite conversion of DNA

Bisulphite conversion of 500 ng genomic DNA isolated from cultured cells or fresh frozen tumour tissues was performed, using EZ DNA Methylation-Gold Kit from Zymo Research, as per the manufactures instructions. Primer sequences are as given in Table 3.2

Gene name	Primer	Sequence
miR-148a Bisulphite	FWD	ATTAGGAATGGGTTTTAATTTGAGGA
	REV	CCCAACTAAAACAAAAAAAAATAACT

Table 3.2: Primer sequences used for Bisulphite PCR

3.5.3 PCR Amplification

The reaction was made as follows

Components	Volume	Final Concentration
10X standard Taq buffer	1 µl	1X
10 mM dNTP mix	0.2 µl	0.2 mM
Forward primer (10 pmol/µl)	0.3 µl	3 pmol
Reverse primer (10 pmol/µl)	0.3 µl	3 pmol
Taq Polymerase (1 U/ µl)	0.25 µl	0.25 U
Genomic DNA		25 ng
Autoclaved Milli-Q water		Make up volume to 10 µl

PCR Conditions were as follows

Temperature	Time	Cycles
98°C	3 min	1
98°C	30 sec	30
Annealing temperature	45 sec	
72°C	30 sec	
72°C	5min	1

3.5.3. Removal of unused primers and dNTPs from PCR products by Exonuclease I and Shrimp Alkaline Phosphatase

PCR amplified products contain unused primers and dNTPs. If not removed these primers and dNTPs interfere with subsequent reactions. Exonuclease I (Exo) has an exonuclease activity and degrades any single stranded DNA. Shrimp Alkaline Phosphatase (SAP) removes the phosphate groups from dNTPs.

Method:

1. To remove unused primers and dNTPs, 1µl of master mix of Exonuclease I and Shrimp Alkaline Phosphatase was added for every 10µl of PCR product as per table below:

Constituents	Volume	Final Concentration
10X PCR buffer	0.1 µl	1X
Exo I (10 U/µl)	0.05 µl	0.5 U
SAP (1 U/µl)	0.5 µl	0.5 U
Autoclaved MQ water	0.350 µl	
Total Volume	1 µl	

2. 5 µl of the master mix was added to 50 µl of the PCR product. The reaction mixture was mixed by tapping and spun briefly. The reaction was incubated at 37 °C for 2 hr and the enzymes heat inactivated by incubating at 85 °C for 20 min.

3. The reactions were then processed further to remove inactivated enzymes and excess salt.

3.5.4. Clean up of PCR templates for removal of excess salt

1. Autoclaved MQ water was added to Exo-SAP treated PCR products so as to make up the volume to 100 µl. To this, 10 µl of 3M sodium acetate pH 5.2 and 250 µl of chilled absolute ethanol were added.

2. The sample was mixed thoroughly by gentle vortexing and incubated at -20^{0}C overnight.

3. The tube was spun at 14000 rpm for 20 min at 4 °C and the supernatant was discarded carefully. (Note: The pellet may be very small or may not be visible at all. Still proceed with next step.)

4. The pellet was washed with 500 µl of freshly prepared 70 % ethanol and centrifuged at 14,000 rpm for 10 min at room temperature.

5. The supernatant was discarded and step 4 was repeated.

6. The supernatant was discarded and pellet was air dried. Pellet was re-suspended in 8-10 µl of 1 M TE Buffer, pH 8.0.

7. To check the quality and quantity of PCR product, 2 µl of the PCR product was loaded on a 1 % agarose gel and visualized. 10 ng of good quality PCR product was used for sequencing.

3.5.4. Sequencing of the PCR products

In a 0.2 ml PCR tube, 1.5 pmol of either forward or reverse primer and 5-10 ng of Exo-SAP treated PCR amplified product were added. In case sequencing of Vectors, 100 ng DNA was used. The sequencing reactions were carried out in Eppendorf Master Cycler using Big Dye Terminator Kit V 3.1, which has different fluorescent dye for each terminator ddNTP as per manufacturer's instructions. The reactions were cleaned up to remove excess salt. The reactions were run in either a 50 cm or 80 cm capillary filled with POP4 or POP6 polymer (Applied Biosystems, U.S.A) in 3100 Avant Genetic Analyzer (Applied Biosystems, U.S.A). The size of capillary used depended on the PCR product size.

3.6. Construction of miR-148a expressing pTRIPZ vector:

The genomic regions encoding miR-148a were PCR-amplified and cloned in doxycycline inducible pTRIPZ lentiviral vector. Genomic region encoding miR-148a was PCR amplified using High fidelity phusion polymerase and cloned into HpaI site in the vector (blunt-end cloning) (Figure 3.2)

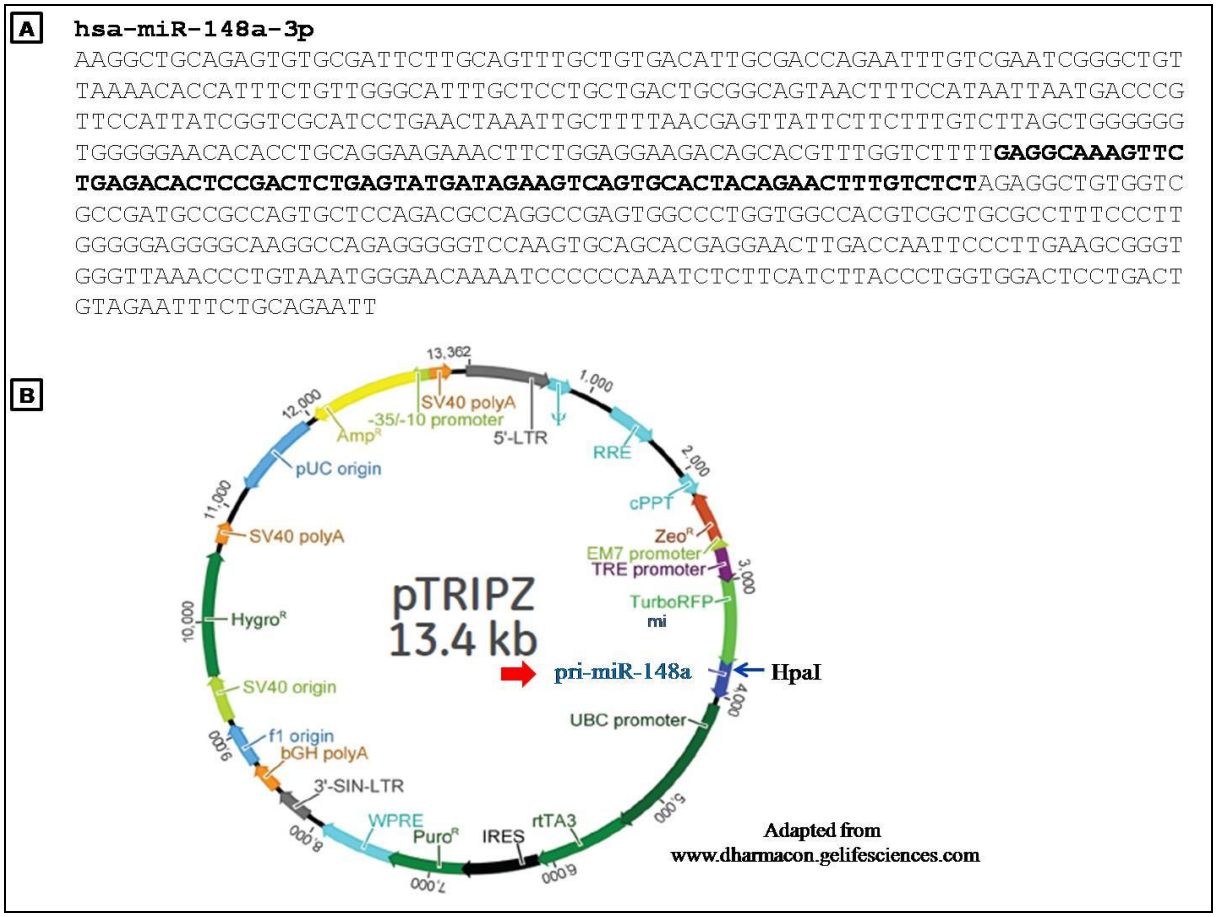

Figure 3.2: Construction of miR-148a expressing pTRIPZ vector
(A) Genomic sequence encoding miR-148a (pri-miR-148a sequence in bold font) that was used for expressing miRNA by cloning in the pTRIPZ vector, (B) Vector map of pTRIPZ vector, a doxycycline inducible lentiviral vector consisting of the tetracycline response element (TRE) fused to minimal CMV promoter which drives turboRFP and miR-148a upon binding of its reverse tetracycline transactivator 3 (rtTA3) in the presence of doxycycline. The expression of TurboRFP enables the user to easily observe expression from the TRE promoter, allowing quick assessment of factors such as expression, viral titre, and transduction efficiency. Constitutively active Ubiquitin C promoter (UBC) drives expression of rtTA3 and puromycin resistance ($Puro^R$).

(a) PCR amplification and Phenol-Choroform method of DNA purification

Reagents: *5X phusion HF buffer, 10mM dNTP mix, Phusion polymerase, Tris saturated phenol*

Tris Saturated Phenol: Distilled phenol kept at –20 ^{0}C was carefully thawed to RT by keeping it at 60 ^{0}C preferably in waterbath. The cap of the bottle was loosened to release any pressure built on thawing the phenol. As phenol is acidic, it needs to be neutralised to avoid degradation of DNA. 25 ml of phenol was taken and equal volume of autoclaved Milli-Q in sterile Nunc tube. It was mixed thoroughly by shaking the tube and allowed to rest until two phases separate. Upper phase was removed. This was repeated once to saturate phenol with water. To the water saturated phenol, equal volume of 1 M Tris, pH 8.0 is added and mixed thoroughly by shaking the tube and allowed two phases to separate. Upper phase was removed and same set of steps were repeated with 0.1 M Tris, pH 8.0. pH of the phenol phase was subsequently achieved to be 7.0 or above. 10-15 ml of 10 mM Tris, pH 8.0 was added on top of the phenol phase for long-term storage in refrigerator and exposure to light was avoided by covering tube with Aluminium foil.

Primers used for amplification of miR-148a coding region from genomic DNA and cloning into pTRIPZ are Forward primer – AAGGCTGCAGAGTGTGCGATTCTTGCAG, Reverse primer – AATTCTGCAGAAATTCTACAGTCAGGAGTC

Method

1. All reagents required for the reaction except for the enzyme were thawed and kept on ice.

2. For each PCR reaction 25 ng of human lymphocytic genomic DNA was added in the end to the 0.2 ml tube containing the PCR components.

3. The PCR Reaction mix was prepared as follows for High Fidelity Phusion polymerase:

Components	Volume	Final Concentration
5X Phusion buffer (HF)	2 µl	1X
10 mM dNTP mix	0.2 µl	0.2 mM
Forward primer (10 pmol/µl)	0.2 µl	2 pmol
Reverse primer (10 pmol/µl)	0.2 µl	2 pmol
Phusion Polymerase (2 U/µl)	0.1 µl	0.2 U
Genomic DNA		25 ng
Autoclaved Milli-Q water		Make up volume to 10 µl

4. Reactions were carried out in Eppendorf MasterCycler 5333 (Eppendorf, Germany). All precautions were taken to avoid PCR related contamination. All reagents and PCR products were handled using filter tips.

5. The PCR cycling parameters were as follows:

Temperature	Time	Cycles
98°C	5 min	1
98°C	30 sec	30
Annealing temperature	45 sec	
72°C	30 sec	
72°C	10 min	1

6. 5 µl of the PCR product was run on 1% agarose gel and visualized using UV transilluminator. The PCR product was further purified using phenol: chloroform, before using it for cloning.

7. Equal volume of Tris Saturated phenol was added to the PCR, mixed and centrifuged at 12,000 rpm, for 15 min, at 20°C.

8. To the supernatant equal volume of phenol: chloroform (1:1) was added, mixed and centrifuged at 12,000 rpm, for 15 min, at 20°C.

9. To the supernatant equal volume of chloroform was added, mixed and centrifuged at 12,000 rpm, for 15 min, at 20°C.

10. Upper layer was separated and 1/10th volume of 3 M sodium acetate pH 5.2 was added and mixed.

11. Then 2.5X volume chilled absolute alcohol (kept at -20°C to chill) was added, mixed well and kept for precipitation overnight at -20°C.

12. Next day, the mixture was centrifuged at high speed (16,000 rpm) for 20 min at 4°C and the pellet was washed with 500 µl of 70% alcohol and centrifuged at 12000 rpm for 10min at 4°C; twice.

13. The pellet was air-dried and dissolved in minimum of 10 µl T.E buffer.

(b) Agarose Gel Electrophoresis

Reagents:

1) 50 X Tris-acetate-EDTA (TAE) buffer: 121 g Tris and 18.6 g EDTA was dissolved in 300 ml of Milli-Q water followed by addition of 28.55 ml glacial acetic acid. Volume was made up to 500 ml and was autoclaved.

2) Ethidium Bromide stock (10 mg/ml): Dissolve 10mg Ethidium Bromide in 1 ml of autoclaved Milli-Q water.

3) 6X DNA loading dye: Dissolve 0.25% bromophenol blue, 40% (w/v) sucrose in Milli-Q water.

Method

1. The appropriate amount of agarose was weighed into a measured volume of 1X TAE buffer to make a 1% gel. The slurry was heated in a microwave oven until the agarose was dissolved completely and ethidium bromide to a final concentration of 0.5 µg/ml (from a 10 mg/ml stock) was added when the gel solution had cooled to about 40°C.

2. A gel tray was cleaned, the gel was poured into the gel tray and a clean comb was inserted in the slot provided in the tray. The gel was allowed to set at room temperature for 30-45 minutes.

3. After the gel had completely set, the gel was placed in the electrophoresis tank filled with 1X TAE buffer. The buffer should be just enough to cover the gel to a depth of about 3 mm and the comb was carefully removed.

4. The DNA samples were mixed with 6X loading buffer at 1X final concentration and loaded into the wells of the gel. The gel was run in electrophoresis chamber at 40mA constant current, till the dye had migrated about three-fourths of the gel.

5. The DNA was visualized by observing the gel on a UV transilluminator.

(c) T4 Polynucleotide kinase reaction:

For blunt-end cloning, Phusion DNA polymerase used for PCR amplification of insert produces blunt ends on the amplified fragment, which lack terminal 5' phosphate groups. T4 Polynucleotide kinase was used to add a phosphate group to the 5' end of the amplicon to facilitate cloning with the vector.

Reagents: *10X T4 Polynucleotide Kinase Reaction buffer, T4 Polynucleotide Kinase (10 U/ µl).*

Method:

1. All reagents required for the reaction except for the enzyme were thawed and kept on ice and reaction was set up as follows:

Components	Volume
10X T4 PNK Reaction buffer	2 µl
DNA	5-10 µl (1- 300 pmol termini)
T4 Kinase (10 U/µl)	1 µl (1U)
Auotclaved Milli-Q water	Make up the volume to 20 µl

2. The reaction was incubated at 37°C for 30min and then heat inactivated at 65°C for 20 min.

(d) Restriction digestion:

Reagents: *10X buffer, Restriction Enzyme*

Method:

1. All reagents required for the reaction except for the enzyme were thawed and kept on ice.

2. For a typical restriction enzyme reaction, 2-3 U of enzyme was used to digest ~1 µg DNA in a reaction volume of 20 µl; at the recommended temperature for at least 4 hr. (If more than one reaction was performed a master mix was prepared containing the buffer, enzyme and Milli-Q water).

3. The reaction was heat inactivated at the recommended temperature for 15-20 min (most enzymes are inactivated at 65°C for 15 min).

4. For cloning the digested product, the volume of the reaction was made to 200 – 300 µl with TE. The mixture was purified by phenol-chloroform method and precipitated with ethanol as described for PCR products. [Refer section 3.6(a)]

(e) Dephosphorylation of Vector using Shrimp Alkaline Phosphatase (SAP):

The digested vector was treated with Shrimp Alkaline Phosphotase to remove the 5'-phosphate from the last base to avoid ligation between the ends of two vector molecules.

Reagents: *10X RE digestion buffer, Shrimp Alkaline Phosphatase (1 U/ µl).*

Method:

1. All reagents required for the reaction except for the enzyme were thawed and kept on ice.

2. The reaction was set up as follows and incubated at 37°C for 60 min.

Components	Volume
10X R.E digestion buffer	3 µl
Shrimp Alkaline Phosphatase (1U/µl)	1 µl (1 U)
RE digested DNA mixture	10-20 µl (1-10pmol termini)
Autoclaved Milli-Q water	Make up volume to 30µl

3. The reaction was terminated by heat inactivation at 65°C for 15 minutes.

(d) Ligation:

Reagents: *10X Ligation buffer, T4 DNA Ligase (5 U/ µl), 50% PEG 4000 solution*.

Method:

1. All reagents required for the reaction except for the enzyme were thawed and kept on ice. The reaction was setup as follows

Components	Blunt-end Ligation	Sticky-end Ligation
	Volume/ amount	Volume/amount
Linear vector DNA	60 fmol vector ends	30 fmol vector ends
Insert DNA (PCR product)	180 fmol insert ends	90 fmol insert ends
10X Ligation buffer	2 µl	2 µl
50% PEG 4000 solution	2 µl	-
T4 DNA Ligase (5U/ µl)	1 µl (5 U)	0.4 µl (2 U)
Autoclaved Milli-Q water	Make up volume to 20 µl	Make up volume to 20 µl

2. The mixture was incubated for 16 hour at 22°C (cold bath) and inactivated by incubating at 65 °C for 10 min.

(e) Preparation of competent cells:

Reagents:

Transformation buffer (TB): 0.3 g PIPES, 0.22 g of $CaCl_2$-$2H_20$, 1.86 g of KCl were dissolved in 95 ml Milli-Q and pH was adjusted to 6.7-6.8 with 5 M KOH. The initial white

precipitate may form at low pH, however once the right pH is adjusted, solution should become clear. 1.09 g of $MnCl_2$ was added in this solution and final volume was made up to 100 ml and filter-sterilised using 0.22 µm filter.

Super Optimal Broth (SOB): 20 g of tryptone, 5 g of yeast extract was dissolved in 995 ml of Milli-Q water. 2 ml of 5 M NaCl and 1.25 ml of 2 M KCl was added to achieve final concentrations of 10 mM and 2.5 mM respectively. Solution was autoclaved and 5 ml of 2 M MgCl2 solution prepared and sterilised separately was added just before use.

Luria Broth (LB): 1 g of tryptone, 0.5 g of yeast extract and 0.5 g of NaCl was dissolved in 100 ml of milli-Q water and autoclaved

SOB agar plates: 1.5-2 g Agar agar was dissolved in 100 ml of SOB (or LB), autoclaved and poured in pre-sterilised plastic plates.

Method-

1. *Eschericia coli* strains DH5α or stbl3 cells were freshly streaked from the glycerol stocks on the SOB agar plates one day prior to inoculation into SOB for competent cells preparation.

2. 200 ml of SOB medium (10% of flask volume) was prepared and autoclaved in wider neck 2L flask. All the steps here onwards are performed in aseptic conditions created by laminar hood.

3. A single colony from freshly streaked SOB plate was inoculated into the 200 ml SOB and flask was incubated at 18^0C at 150-200 rpm till O.D at 600nm reaches to 0.4. O.D at 600 nm was checked at regular intervals by taking out 1ml of growing culture in aseptic conditions by using spectrophotometer.

4. Culture was centrifuged at 3000 rpm for 15 min at 4^0C when O.D reaches 0.4 or in when it's in between 0.4 to 0.7.

5. Supernatent was discarded and one third volume of ice cold transformation buffer (134 ml for 200 ml culture) was added slowly onto the pellet so as to disturb the pellet gently.

6. Cell pellet was resuspended in TB with **gentle pipetting** for 5-10 min and was incubated on ice for additional 10 min. Care was taken to avoid any bubbling during re-suspension of cell pellet.

7. After incubation this was centrifuged at 3000 rpm for 15 min at 4^0C and cell pellet was resuspended in 16 ml of TB(1/12.5 volume of initial culture volume i.e. for 200 ml) as described in earlier step.

8. 1.12 ml of DMSO (final concentration of 7%) was added on walls of suspension tubes slowly and was mixed by shaking or by gentle pipetting once or twice.

9. This solution was then aliquoted in volumes of 100 µl in 1.75 ml prechilled sterilised eppenderoff tubes and snap-freezed in liquid nitrogen as quickly as possible.

10. The competent cell vials were stored at -80^0C and were taken out on ice just before use.

(f) Transformation of competent cells

Reagents: *Stbl3* or DH5α ultra-competent cells, SOC broth, LB broth

Method:

1. Stbl3 or DH5α ultra-competent cells, stored at -80°C was thawed on ice by tap-mixing intermittently and kept on ice.

2. 2-10 µl of the ligation mixture DNA was added to the cells and incubated on ice for 30 min, followed by heat shock for 45 sec at 42°C.

3. Then the transformation mixture was subjected to cold shock by immediately transferring on ice for 5 min.

4. 900 µl of SOC broth was added and incubated on shaker incubator for 1 hr at 37°C.

5. The mixture was spread on LB agar plate containing ampicillin (100 µg/ml) and incubated at 37^oC for 16-18 hr.

6. The colonies obtained were then inoculated in LB broth containing ampicillin (100 µg/ml) and plasmid DNA was extracted from the cultures using alkaline lysis method.

(h) Plasmid extraction by alkaline lysis method:

Reagents:

Solution I: Glucose Tris EDTA solution*:*

Components	Volume	Final concentration
2M Glucose	1.25 ml	50 mM
0.5 M EDTA	1.0 ml	10 mM
2 M Tris, pH 8.0	0.625 ml	25 mM
Final volume	Make up to 50ml with autoclaved Milli-Q water	

Solution II: (**Prepared just before use)**

Components	Volume	Final concentration
5M NaOH	0.2 ml	0.2 N
20% SDS	0.25 ml	1%
Final Volume	Make up to 5ml with autoclaved Milli-Q water	

Solution III/ (3 M Potassium 5 M acetate, pH 4.8):

14.7 g of Potassium acetate was dissolved in 20 ml Milli Q water and volume was made upto 30 ml. To this, 5 M Potassium acetate, 5.5 ml of glacial acetic acid and 10 ml of Milli-Q water was added. pH was checked. If it's not approx 4.8 more acetic acid was added and finally volume was made to 50 ml with MilliQ water and solution was autoclaved.

Method:

1. 1-2 ml of bacterial cultures was centrifuged at 3000 rpm for 5 min at room temperature in 1.5 ml eppenderoff tube. The cell pellet was resuspended in ice cold 100 µl solution I by vortexing and incubated for 5 min at room temperature.

2. 200 µl freshly made solution II was added and mixed by gentle inversion followed by incubation for 5 min on ice.

3. 150 µl solution III was added and immediately mixed by vortexing for 10 sec, followed by incubation for 5 min on ice.

4. The tube was centrifuged at 13000 rpm for 5 min and clear supernatant was removed in a fresh tube without disturbing the pellet.

5. To this supernatant, equal volume of phenol-chloroform (1:1) (for example, 250 µl of Tris-saturated phenol and 250 µl of chloroform was added for 500 µl of supernatant.

6. The tube was vortexed and centrifuged at 12000 rpm for 5 min, aqueous layer was removed carefully to fresh tube.

7. Equal volume of chloroform was added to the aqueous layer and tube was vortexed to thoroughly mix the contents. Step 6 was repeated.

8. 1 ml (or 2X volume) of absolute ethanol was added to the supernatant, mixed by inversion and allowed to precipitate at room temperature for 5 min.

9. The tube was centrifuged at 13000 rpm at room temperature for 5 min, the supernatant decanted carefully; 1 ml of 70% ethanol was added to the DNA pellet and re-spun at 13000 rpm for 5 min. The ethanol was aspirated and the DNA pellet was air dried.

10. The plasmid pellet was dissolved in 10-25 µl TE containing RNase (1 µg/ml) and further screened for insert and orientation by Restriction digestion analysis.

11. The positive miR-expressing constructs were further prepared on a large scale and purified using, Qiagen DNA Midi kit according to manufacturer's protocol.

3.7. Tissue culture media and reagents

1. *Tissue culture medium:* Commercially available powdered medium, Dulbecco's Modified Eagle Medium (DMEM) containing high glucose, pyridoxine hydrochloride and sodium pyruvate or Dulbecco's Modified Eagle Medium: Nutrient mixture (DMEM/F12) was prepared as per the manufacturer's instructions.

The powdered medium was reconstituted by dissolving it in ~ 800 ml autoclaved Milli-Q water under sterile conditions. 3.5 g Sodium bicarbonate was added and the pH was adjusted

to 7.5 using 1N HCl (about 11 ml). The volume was made up to 1 L in a sterile volumetric flask and the medium was filter sterilized through a 0.22 μm pore size filter membrane fitted in a sterile filtration assembly. The filtered medium was stored as 500 ml aliquots at 4ºC. The complete medium contained DMEM supplemented with 10 % fetal bovine serum (FBS). 1 ml of the 100 X antibiotic (Penicillin and streptomycin) stock solution was added per 100 ml of complete medium if required.

2. *100 X antibiotic mix:* 10,000 units penicillin G (Alembic Ltd, Vadodara, India) and 10,000 μg streptomycin sulphate, available as injection vials (Abbott Healthcare Pvt. Ltd, Ahmedabad, India) were dissolved per ml in Milli-Q water, filter sterilized and stored at 4 °C.

3. *10 X phosphate buffered saline (PBS):* 80.8 g NaCl, 2 g KCl, 12.6 g Na_2HPO_4. 2 H_2O, 2 g KH_2PO_4, and 10 g glucose was dissolved in autoclaved Milli-Q water and the volume made up to 1 L. The solution was filter sterilized and stored at 4 °C.

4. *10 X Trypsin (0.25 %):* 2.75 g of trypsin was added to 110 ml of autoclaved Milli-Q water and allowed to dissolve overnight on a magnetic stirrer. The solution was sterilized by filtering through a 0.22 μm pore size Millipore filter. The solution was stored as 10 ml aliquots at -20 ºC. 10 X stocks were diluted to 1 X working solution with 1 X PBS. Working solution was stored at 4 °C.

3.8. Routine maintenance of cell Lines

All glassware and plastic-ware used for tissue culture work were sterile. For maintenance and experimental use, all adherent cells (like HEK 293FT, Daoy) were trypsinized and passaged. While semi adherent cells of D425 and D283 medulloblastoma cell lines were directly collected in medium and did not need trypsinization. The detailed procedure is as follows:

1. Spent medium was aspirated out using a Pasteur pipette and the cells in the plate were rinsed twice with 1 X PBS.

2. 1X trypsin was added to the tissue culture dish, and was removed after the cells started to round up but just before the cells started detaching. The cells were collected in 1X PBS and the cell suspension was transferred to a centrifuge tube containing about 1ml complete medium as serum inhibits trypsin activity and tightly corked.

* In case of D425 and D283 medulloblastoma cells, cells were dislodged, resuspended in medium with the help of Pasteur pipette and cell suspension is transferred to a centrifuge tube.

3. The cell suspension was centrifuged for ~ 2 min at 1000 rpm in REMI bench top centrifuge. The supernatant was discarded and the cell pellet was loosened by tapping the tube gently.

4. The cells were suspended in an appropriate volume of complete medium (DMEM or DMEM-F12 supplemented with 10 % FBS), cell count was taken using a hemocytometer, and the required cell number was seeded in tissue culture dishes, and incubated at 37 °C in a humidified 5 % CO2 incubator. The cultures were passaged twice a week (at around 70-75% confluency) or were frozen when required. The cells were not passaged for too long and fresh vial of frozen cells was revived at regular time intervals.

3.9. Freezing and revival of cell cultures

1. For freezing of cells, 80-90 % confluent cultures were trypsinized as described above. The cell pellet was loosened by tapping the tube gently, and the centrifuge tube was placed on ice for one-two minutes. Pre-chilled freezing medium (90 % FBS + 10 % DMSO) was added drop wise to the cell pellet (~ 1 x 10^6 cells / ml of freezing mixture) on ice, with constant shaking to ensure an even cell suspension and transferred to pre-chilled vials. These vials were cooled gradually and then stored in liquid nitrogen.

2. To revive the frozen cells, a vial containing frozen cells was removed from liquid nitrogen and immediately thawed in a water-bath at 37 °C. As soon as the cell suspension is thawed, it

was transferred to a centrifuge tube containing ~3-4 ml complete medium and centrifuged at 1000 rpm for 2 min. The supernatant was discarded; cell pellet was loosened by tapping the tube gently and re-suspended in 4 ml complete medium and centrifuged again. The supernatant was discarded and the cells were re-suspended in an appropriate volume of complete medium. The medium was replaced after the cells had adhered to the tissue culture dish, preferably on the same day or next day of revival.

3.10. Transient transfection of human medulloblastoma cell line Daoy with miRNA mimics / siGLO control

D283 cells were transfected using synthetic miR-148a mimic and Dharmafect 2 transfection reagent as per manufacturer's protocol. siGLO RISC-Free Control siRNA served as negative control. The siGLO RISC-Free Control siRNA is a stable, fluorescent RNAi control that is chemically modified to impair processing and uptake by RISC, allowing study of cellular effects related only to miRNA transfection.

Method:

1. The lyophilized miRNA mimics were reconstituted in 250 µl nuclease-free water to a final concentration of 20 µM and stored as aliquots in -20 °C.

2. One day prior to transfection, 18,000 Daoy cells / well were seeded in triplicates in a 24-well plate, so that ~ 70-80 % confluency would be achieved at the time of transfection.

3. For each well, miRNA mimics/siGLO at final concentration of 50nM and Dharmafect-2 (1.25 µl) were diluted separately in 50 µl plain DMEM/F12 gently by pipetting up and down.

4. The mix was incubated for 5 min at RT. The diluted miRNA mimics and Dharmafect-2 were then mixed together by gentle pipetting up and down and incubated at room temperature for 20 min.

5. After 20 min of incubation the miRNA mimic and Dharmafect-2 mix was diluted to 0.5 ml with complete medium (1 X DMEM/F12+10 % FBS) and added over the cells replacing the

existing medium. (A master mix was prepared according to the number of wells to be transfected)

6. After 48 hr of transfection, medium was replaced completely with 0.5 ml complete medium, and cells were allowed to recover for a period of 24 hr before analyzing their growth characteristics.

7. Next day, i.e. 72 hr post-transfection, the cells were trypsinized from one or more wells depending on experiment requirements and seeded for invasion assay (Refer section 3.17). RNA lysate was made from the transfected cells from one well of a 24-well plate to check the miRNA levels by real time RT-PCR.

3.11. Transient transfection of 293FT cells using BES buffer for Lentivirus production

Calcium phosphate mediated transfection method was used to transiently transfect plasmid DNA in 293FT cells[107].

Reagents:

2X BBS (BES Buffered Saline) [50 mM BES, 280 mM NaCl, 1.5 mM $Na_2HPO_4.2H_2O$]:

For 50 ml BBS solution, 0.533 g BES, 0.818 g NaCl and 0.0134 g $Na_2HPO_4.2H_2O$ were dissolved in 45 ml autoclaved Milli-Q water and the pH was adjusted exactly to 6.95 using 5M NaOH. Final volume was made up to 50 ml and pH was checked again. Solution was filter sterilized through 0.22 µm filter and stored as 0.5 ml aliquots at -20°C.

0.5 M $CaCl_2$: 3.675 g $CaCl_2.2H_2O$ was dissolved in 45 ml of Milli-Q water. The volume was made up to 50 ml and filter sterilized using 0.22 µm filter. The solution was stored as 0.5 or 1 ml aliquots at -20°C.

The reagents required for transfection were removed from -20^0C and thawed at RT beforehand and all plasmid DNAs used were purified through Qiagen Plasmid Midi Kit.

Method:

1. One day prior to transfection, the cells were trypsinized (the plate should not be over confluent). ~8 x 10^5 HEK293FT cells were seeded in a 55mm plate. The plate should be around 70-80% confluent at the time of transfection.

2. Next day, 4 hr before transfection, medium was replaced with fresh complete medium. The cells were transfected with total of 12µg plasmid DNA using BBS.

3. A total of 12 µg of plasmid DNA (i.e. 6 µg miR-148a expressing pTRIPZ vector/ pTRIPZ empty vector + 4.5 µg pPAX2 + 1.5 µg pMD2.g) was diluted to 100 µl in autoclaved Milli-Q in a sterile tube.

4. 100 µl of 0.5 M $CaCl_2$ was added drop wise to the DNA in a tube (The contents were not mixed).

5. Then, 200 µl 2X BBS was added drop wise and mixed gently by pipetting 3 – 4 times. The DNA-$CaCl_2$ mix was incubated at RT for 20 min.

6. After 20 min, the DNA-$CaCl_2$ complexes were mixed gently by pipetting and added over the cells drop wise, mixed well by gentle swirling the medium in the plate and incubated at 37°C in CO_2 incubator for 16 hr.

7. After 16 hr, the transfection medium was replaced with fresh complete medium.

8. 48 hr post transfection, the virus containing supernatants was harvested and filtered using 0.45 µm filter. The viral supernatant at this point was either used as it is for transduction of medulloblastoma cell lines or concentrated by ultracentrifugation at 25000 rpm, 4 ºC and then used for transduction. Virus containing supernatants were also stored at -80°C until use.

3.12. Transduction with lentiviral particles and stable over-expression of miRNA in Daoy, D425 and D283 cell lines

Stable inducible polyclonal populations of Daoy, D425 and D283 cells expressing miR-148a and empty pTRIPZ vector were generated by infecting these cells with lentiviral particles of pTRIPZ constructs. For checking the viral titer, 1 ml of serially diluted viral supernatant was used to transduce 5 X 10^4 293FT cells per 35mm^2 culture dish.

All lentiviral procedures, were handled in appropriately certified bio-safety level 2 cabinets (Esco Technologies, Hatboro, PA, USA); infected cultures/spent fluids/contaminated disposables were treated with 10% sodium hypochlorite and autoclaved in biohazard bags prior to disposal, following recommended guidelines.

Method:

1. 5 X 10^4 cells of Daoy or 293FT or 1 X 10^6 cells of D425 or D283 cells were seeded in a 35mm^2 dish one day prior to transduction.

2. 1 ml of diluted, neat or concentrated viral supernatant supplemented with Polybrene (4 μg /ml) was used for infecting cells seeded.

3. 16 hr post infection the viral supernatant was replaced with fresh medium.

4. For checking of viral titre, 72 hr post-transduction and 48 hr post doxycycline induction, the number of 293FT RFP-positive cells was estimated using Flow cytometry analysis (FACS Calibur, BD Biosciences, USA). The viral titer was calculated using the formula – (F X C/V) X D, (where, F-frequency of RFP expressing cells, C-Number of cells at the time of seeding, V- Volume of viral supernatant used for transduction and D- Dilution factor of the viral supernatant).

5. The Daoy cells transduced with the miRNA-expressing constructs were trypsinized and seeded in two 55 mm^2 dishes 72 hr post-transduction.

6. For stable transfection, the infected cells were selected in the presence of puromycin (250 ng/ml for Daoy, 200ng/ml for D425 and D283) at least for 6-9 days.

7. The cells were split before they reached 70-80% confluency and always maintained in the presence of puromycin.

8. MiR-148a expression before and 72 hr after doxycycline treatment (4 µg/ml) was checked in these stable polyclonal populations using Real time RT-PCR.

9. The cells induced in the presence of doxycycline for 72 hr were seeded for various experiments.

3.13. Treatment of D425 medulloblastoma cells with HDAC inhibitors Trichostatin A (TSA) and Valproic acid (VPA)

Reagents:

1) *Trichostatin A (TSA, Cat.No-T8552, Sigma-Aldrich)*: 1 mg of powder was dissolved in 500 µl of DMSO to achieve final concentration of 2mg/ml i.e. 6.6 mM. Stock was aliquoted and kept at -20^0C.

2) *Sodium valproate 100 mg/ml (Encorate^{TM}, 5ml Injection, Sun Pharmaceutical Industries Ltd.)*

Method:

1. 3 x 10^5 D425 cells were seeded per 35mm^2 culture dish and appropriate volume of HDAC inhibitors was added 16 hr after seeding.

2. Minimal 2 µl of volume from TSA stock vials of 6.6 mM was diluted to 0.2 mM or 0.4 mM just before use. 2 µl of 0.2 mM or 0.4 mM was added in 2 ml of medium per 35mm^2 dish to achieve final concentration of 200 nM or 400 nM.

3. Sodium Valproate (100 mg/ml or 0.6M) was added directly to 35 mm^2 dish to get final concentration of 3 mM or 5 mM.

4. In case of treatment with both the HDAC inhibitors, cells were incubated for 16 hr with TSA or 24 hr with VPA and RNA was extracted at the end of the treatment.

3.14. MTT Cytotoxicity Assay[7]

Reagents:

Acidified SDS: 10% SDS in 0.01N HCl. 10 g SDS was dissolved in 80 ml autoclaved Milli-Q water, heated at 60°C for 1 hr to assist the dissolution. 88.4 µl of concentrated HCl was added (final concentration at 0.01 N) and the final volume was adjusted to 100 ml. The solution was stored at room temperature.

MTT: 5 mg / ml in 1X PBS. (50 mg MTT powder was dissolved in 10 ml 1X PBS, mixed by vigorous shaking. The solution was stored in dark at 4°C).

The growth kinetics of the stable miR-148a expressing polyclonal populations of Daoy and D425 cells was analyzed by MTT assay over a period of 9 to 12 days.

Method:

1. 500 cells of Daoy or 1500 cells of D425 were seeded in triplicates in a 96 well micro-titre plate in 100 µl complete medium and medium was replenished at three day intervals.
2. At the desired time points, after medium replenishment 20 µl MTT solution was added to each well, after which the plate was incubated at 37°C in CO_2 incubator for a period of 4 hr to let formazan crystals form.
3. The formazan crystals formed were dissolved by adding 100 µl of acidified SDS to each well with overnight incubation at 37°C.
4. Next day, the optical density was read on an ELISA plate reader (SpectraMax- 190, Molecular Devices, USA) at 540 nm against a reference wavelength of 690 nm.

3.15. Clonogenic assay:

Clonogenic assay was performed to study the clonogenic potential and radiation sensitivity of stable miR-148a expressing polyclonal populations of Daoy.

Method:

1. 72 hr post doxycyline induction, cells were trypsinized and 1000 cells were seeded per 55 mm^2 plate. Cells were maintained in presence of puromycin and/or doxycycline.

2. Next day the cells were irradiated at a dose of 4 Gy (Cobalt-60 gamma irradiator, Bhabhatron, BARC) and medium was changed 24 hr later.

3. The cells were allowed to grow for 8-10 days until microscopically visible colonies are formed.

4. The cells were fixed in chilled methanol: acetic acid (3:1), stained with 0.5% crystal violet dye and the colonies were counted using stereomicroscope.

3.16. Soft Agar Colony Formation Assay:

Anchorage-independent growth of Daoy cells stably transduced with miR-expressing pTRIPZ lentiviral vectors was studied by their potential to form colonies in soft agar medium. Since D425 cells grow in semi-adherant fashion, this assay was used to assess clonogenic potential of these cells.

Method: (Note - * denotes conditions D425 cells)

1. For the soft agar medium, 2X DMEM containing 20% FBS was mixed with an equal volume of molten 2 % low melting point (LMP) agarose, and 1 ml of this mixture was poured into a sterile 35mm^2 dish to obtain a basal layer of 1 % agarose in complete medium (DMEM + 10 % FBS or DMEM/F12+20%FBS). The agarose was allowed to set for ~ 1 hr at room temperature before seeding the cells.

2. 7500 Daoy cells were trypsinized and suspended in 1 X DMEM supplemented with 10 % FBS. Similarly, 1000 D425 cells were suspended in 1X DMEM/F12+20% FBS.

3. 2 % LMP molten agarose and 2X DMEM + 20 % FBS or *2X DMEM/F12+40% FBS were added to the cell suspension such that the final concentration of agarose in the suspension was 0.4 % and serum content was 10 % or * 20%

4. The contents were mixed properly using a micropipette and 1 ml of this mixture was added to a 35mm^2 dish pre-coated with the basal layer.

5. The agar was allowed to solidify for about 1 – 2 hr at room temperature and then the plates were incubated at 37 °C in humidified 5 % CO_2 incubator.

6. The cells were fed with 0.1 - 0.2 ml complete medium every 3 days throughout the duration of the experiment.

7. After 3-4 weeks of incubation, colonies (comprising of 10-15 cells per colony) were counted under microscope from the entire plate. Average colony count from plates per group was represented as histograms.

3.17. Invasion Assay

Invasive potential of Daoy and D283 cells stably transduced with miR-148a expressing pTRIPZ vector or pTRIPZ empty vector lentiviral particles was studied by their potential to invade through Matrigel coated transwell inserts.

Materials:

1. Matrigel: (10 mg/ml-5ml pack size, BD Life Sciences, Cat. No- 356234) This was diluted to 1 mg/ml in plain 1X DMEM and aliquoted as 100 µl volume aliquots and was stored at -70^{0}C. Fresh aliquot was taken out and diluted and thawed every time. Repeated freeze-thawing is not advisable.

2. 8-µm pore size transwell inserts (Cat No-353097, BD Biosciences, San Hose, CA, USA)

3. 24 well plate

4. 96well dish

5. Calcein AM (1µg/µl in 100% DMSO) (Cat. No- 206700, Calbiochem)

6. Hickman Buds (local make) or Ear buds(Johnson and Johnson Pvt Ltd)

Method:

1. 8 µm pore size transwell insert was placed into the 24 well-plate custom-designed to accommodate these inserts.

2. Membrane on the inner side of the transwell insert was washed 2-3 times with 1X DMEM or 1X DMEM/F12.

3. Matrigel (stock 1 mg/ml) was diluted to 300 µg/ml on ice and 100 µl of the same (30 µg in total) was added over the inner side of the transwell insert carefully so that bubbles are not formed.

4. Plate was incubated at 37^0C for 1 hr to allow matrigel to polymerize.

5. Un-polymerised matrigel is removed and 50000 cells of Daoy or 75000 cells of D283 were seeded in 200 µl of 1X DMEM. In case of doxycycline treated cells, cells were treated with doxycycline for 72 hr prior to seeding for invasion assay.

6. 750 µl of complete medium was added in lower chamber which served as chemo-attractant. Doxycycline was also added in the upper and lower chamber medium in case of doxycycline induced cells.

7. 5000 cells from the mastermix of cells prepared for seeding in transwell insert were seeded per well of 96 well black plate, in duplicates. This was done to determine initial cell number seeded for invasion assay for each polyclonal population either doxycycline treated or untreated.

8. After ~6-8 hr once these cells have adhered to the plate surface, medium was replaced with fresh medium that is supplemented with Calcein AM (1 µg/µl stock concentration) with final concentration of 2 µg/ml of medium. The plate was incubated for minimum of 30 min at 37^0C.

9. Fluorescence was read with excitation at 485 nm and emission at 535 nm with 0.1 or 0.5 sec as exposure time, Lamp energy 5000, position-top, reading by plate as additional settings,

using Mithras LB940 multimode reader (Berthold Technologies, Germany). The average fluorescence measured for 5000 cells of uninduced vector control or respective polyclonal population was taken as control fluorescence reading to normalize the total fluorescence of invaded cells of respective doxycycline induced vector control or polyclonal populations to account for the differences in cell number resulted while seeding.

10. Daoy and D283 cells were allowed to invade for 36 and 56 hr respectively. 30-60 min prior to the end of this incubation period, Calcein AM at final concentration of 2 µg/ml was added in the lower chamber medium of transwell insert and incubated for minimum of 30 min at 37^0C. For example, 1.6 µl of Calcein AM (1 µg/µl) was first mixed with 50 µl of complete medium, which was then added to lower chamber medium by lifting the insert momentarily.

11. After incubation, membrane of transwell insert was wiped from inside by hickman cotton plug to remove non-invaded cells off the membrane and placed back. Five microscopic images representing all quarters and the centre of each insert were captured using Zeiss Axiovert 200M fluorescence microscope at magnification of 40X (4X objective and 10X of eyepiece).

12. The membrane was then cut with blade gently without disturbing cells on the outer side of the membrane and placed into a well of 96 well plate.100 µl of complete medium was added not to let membrane dry. Fluorescence was read as described in step 9.

13. In case of D283 cells, some proportion of invaded cells does not remain adhered to the membrane but remain in the lower chamber medium. To account for this population of invaded cells, lower chamber medium was centrifuged at 3000 rpm at 5 min to pellet down the cells. Cell pellet was resuspended in 100 µl of complete medium and fluorescence was read as described in step 9. Total fluorescence was calculated from the fluorescence values belonging to lower chamber cells and cells from insert membrane.

14. Total fluorescence measured was normalized to account for the differences in cell seeding as stated in step 9. Difference in normalized fluorescence between doxycycline treated and untreated pTRIPZ-miR-148a population was compared using Student's t test.

3.18. Generation of subcutaneous xenografts in immunodeficient mice for assessment of In vivo tumourigenic potential of miR-148a expressing stable polyclonal populations of Daoy and D425 cells

Inducible stable polyclonal populations of Daoy cells expressing miR-148a or control pTRIPZ vector were studied for their tumourigenic potential *in vivo.*

Animals used: 6 to 8 week old BALB/c Nude mice (CAnN.Cg-*Foxn1nu*/Crl strain) or NODSCID (NOD/NcrCrl-*Prkdc*^{scid}) received from Charles River, USA.

Method:

1. 5 X 10^6 control (un-induced) or doxycycline-induced (for 72 hr) cells of the vector control and miR-148a expressing polyclonal populations of Daoy or D425 cells were suspended in ~0.2 ml 1X PBS. (Refer section 3.8)

2. The cell suspension was then injected subcutaneously in the flank of immunodeficient BALB/c Nude mice using a 21 gauge needle. A single mouse was injected with doxycycline treated pTRIPZ vector control cells in the left flank and doxycycline treated miR-148a expressing cells in the right flank.

3. Mice injected with the induced cell populations were fed with doxycycline (1 mg/ml) through 5% sucrose-water as a carrier solution. Doxycycline supplemented sucrose water was changed every 3 days.

4. Tumour growth was assessed by measuring length and breadth of tumours using vernier calliper at every week up to the 6th week after the injection. Tumour growth was represented in terms of cross sectional area using the formula: (length X breadth) cm^2. At least 6 mice were used in each experiment.

5. Animals were sacrificed at 6^{th} week by using over-exposure to CO_2 or by cervical dislocation as a method of euthanasia as approved by Institutional Animal Ethics Committee (IAEC) and surgically opened to remove tumours. Tumours from two flanks of each animal were photographed together. All the tumours were incubated separately in 10% formalin solution used as fixative overnight, followed by embedding in paraffin to prepare paraffin blocks.

3.19. Generation of orthotopic medulloblastoma xenograft in immunodeficient mice using stereotactic method of intracranial injection for assessment of in vivo tumourigenic potential of miR-148a expressing polyclonal populations of D283 cells.

D283 cells transduced with pTRIPZ-miR-148a construct were transfected with a pcDNA3.1 vector expressing firefly luciferase under CAG (CMV early enhancer/chicken beta-actin promoter) promoter and selected in presence of neomycin. Tumourigenic potential of these firefly luciferase expressing cells with or without doxycycline induced miR-148a expression was studied by generating orthotopic xenograft in immunodeficient mice using sterotactic method of intracranial injection. Following procedure was approved by Institutional Animal Ethics Committee.

Reagents:

1. Anaesthetic agent (Ketamine and Xylazine)

2. Analgesic (Buprenorphine, Neon Laboratories, India)

3. Sterile ocular lubricant (Neosporin, Neon Laboratories, India)

4. Sterile phosphate-buffered saline

5. 70% ethanol

6. Bone wax (Cat. No. W810, Ethicon Inc, Johnson & Johnson Ltd)

7. Tissue adhesive- VetBond^{TM} (n-butyl cyanoacrylate) Cat. No. 1469SB, 3M Animal care products, St Paul, MN, USA)

Equipments:

1. Syringe needle 30G

2.Glass Syringes, 5µl Hamilton Co, Model 75 RN Syringe, 700 Series; volume 5µl; Cat. No. 7634-01)

3. Needles, 26 G, 2" compatible for 5µl syringes (26GA RN 70mm PT3 6PK, Cat. No. 7804-03, Hamilton)

4. Sterile cotton buds

5. Surgical instruments include Fine forceps, Iris Scissors, Blunt forceps, sterile scalpel blades (Local make).

6. Small animal stereotaxic frame (Harvard Apparatus, MA, USA)

7. Electric microdrill and bits (Cat. No.67-1000, Ideal Micro Drill Kit, Cell Point Scientific, Gaithersburg, MD, USA)

8. Heating pad/chamber (with thermometer)

9. Electric clippers

Animals Used: Immunodeficient mice: 6 to 8 week old BALB/c Nude mice (CAnN.Cg-*Foxn1nu*/Crl strain) or NODSCID (NOD/NcrCrl-*Prkdc*^{scid}) received from Charles River, USA.

Method:

A) *Preparation of cells:*

1. D283 cells were collected in medium by triturating using glass pipette. A short spin at 1500 rpm for 1 min was given to remove any dead cells. Cell pellet is resuspended in fresh medium.

2. Cells were counted using haemocytometer and required volume of culture suspension to carry 2 x10^5 cells was spun down at 2000 rpm for 3 min.

3. Cells were washed once with sterile 1X PBS and resuspended in 5 µl final volume of 1X PBS.

4. Cell suspension was kept on ice till the time of injection.

B) Equipment and specimen setup:

1. Small animal stereotaxic frame was assembled as per manufacturer's instructions.

2. Heating chamber necessary for post-procedural care is turned on to maintain temperature of 37^0C.

3. Animals were weighed to decide dosage of anaesthetic agent. Typically 6-8 weeks old animals with minimum of 20 g body weight were used for the intracranial injections.

4. Ketamine and Xylazine were diluted 1:1 in sterile 1X PBS and were mixed to get final concentration of 90-120 mg/kg body weight (ketamine) and 20 mg/kg body weight (xylazine). Diluted stocks of ketamine and xylazine were preserved at 4^0C for up to one week.

C) Surgical procedure:

Preoperative animal preparation:

1. Mouse was anesthetized by administering ketamine-xylazine mixture through intra-peritoneal route by using sterile 30 G syringe needle.

2. Lubricating ophthalmic ointment (Neosporin) was applied on both the eyes of mouse to prevent drying of the cornea.

3. Hair from surgical site was removed with electric clipper or razor in case of NOD-SCID mice.

4. Surgical site was disinfected by wiping the area by cotton tipped buds soaked in 70% ethanol.

5. Anesthetized mouse was positioned appropriately in stereotactic apparatus with incisors locked in mouth fixture at front and ears in ear holders. Ear bars were adjusted in ears at

occiput of head level gently and then were tightened firmly. **Height of mouth fixture and ear bars was adjusted so that head is maintained absolutely steady and flat.**

Preoperative cell preparation:

1. Hamilton syringes and needles (26 G) was washed several times by rinsing it with sterile PBS before aspirating cell culture.

2. Cells in microcentrifuge tube were re-suspended by tapping gently or by pipetting prior to each injection to prevent cell clumping.

3. 5µl of cell suspension was drawn into Hamilton syringe with great care to avoid aspiration of bubbles.

Surgical opening of skull:

1. 1.0-1.5 cm midline sagittal incision was taken with a sterile disposable scalpel blade or iris scissors along the superior aspect of the cranium from intra-aural line towards the anterior aspect of head.

2. Bregma (intersection of coronal and sagital sutures) anteriorly and lambda (conjunction of sagital and lambdoidal sutures) posteriorly was identified as they are used to serve as landmarks for stereotactic localization prior to injection.

3. Fascia over area of skull was removed by using forceps and scalpel blade. This was done to make the injection site easily accessible to drill into skull.

Injection of cells:

1. A guiding needle was attached to the holder attached to dorso-ventral (DV) axis of stereotactic apparatus and was adjusted to 2.5 mm posterior to lambda at midline by using vernier scale on anterio-posterior (AP) axis. DV and AP coordinates required to achieve injection precisely in the cerebellum were chosen by referring to Paxinos and Franklin's the Mouse Brain in Stereotaxic Coordinates: An Atlas of the sterotaxic coordinates of mouse brain.

2. Using microdrill with sterile drill bit, a small burr hole was made as per the coordinates set by guiding needle. Sufficient care was taken so as to keep drilling superficial in order to avoid traumatic injury to brain.

3. 5 µl syringe was attached to stereotactic apparatus holder and put cautiously into drilled burr hole.

4. Needle was maintained perpendicular to skull and slowly inserted 3 mm deep into the brain. After waiting for 1 min, needle was taken aback by 0.5 mm and cell suspension was delivered slowly (5 µl over a total period of 2-3 min).

5. Skull was kept dry during injection, using sterile cotton buds to remove any tissue fluid that may have refluxed out of the burr hole.

6. Syringe was kept in place for 1-2 min upon completion of injection and then slowly withdrawn.

7. Site of burr hole was plugged with bone wax, and skin was closed with the help of tissue adhesive VetBond.

8. Ear holders were unscrewed from the ears of the animal and incisors were removed from mouth fixture.

9. Animal was transferred to heating pad/chamber maintained at 37^0C till it regains consciousness.

10. Animals injected with doxycyline treated D283 pTRIPZ-miR-148a polyclonal population were fed with doxycycline (1 mg/ml) through 5% sucrose-water, while animals injected with doxycycline untreated D283-pTRIPZ-miR-148a polyclonal population were fed with 5% sucrose water.

11. Animals were sacrificed at 5^{th} week by using over-exposure to CO_2 as a method of euthanasia. Whole brain of each animal was collected by surgically opening the skull. Whole brain of each animal was incubated separately in 10% formalin solution overnight and cut in sagittal fashion by using blade to separate two hemispheres. This was then followed by

paraffin embedding of both the hemispheres separately to prepare paraffin blocks. 5 µm sections were taken using microtome and stained for hematoxylin and eosin to visualise tumour cells in cerebellum.

3.20. Bioluminescence imaging

Instruments:

Xenogen IVIS spectrum imaging system (Caliper Life Sciences, MA,USA).

Reagents:

1) D-luciferin, potassium salt (Cat. No.L8220 Biosynth AG, Switzerland) (30 mg/ml): 30 mg of D-luciferin powder is dissolved in 1X PBS and can be stored in -20^{0}C.

2) Isoflorane (Forane 250 ml Inj, Abott laboratories, India)

Method:

1. Mice were anaesthetised with ketamine-xylazine mixture as described earlier. See section 3.19).

2. In case of isoflurane system of gas anaesthesia, exhaust system of isoflurane was switched on, then animals were put in incubation chamber and exposed to 3% isoflurane till animals are anaesthetized and breathing rate is regularised.

3. 100 µl of 30mg/ml of D-luciferin (prepared fresh in 1X PBS) at (150 mg/kg body weight) was administered to anesthetised mice via intra-peritoneal route using sterile 30G syringe needle and animal was placed in the imaging chamber of the IVIS system. In case of isoflurane based anaesthesia, 3% isoflurane was delivered through nose cones provided inside the imaging chamber.

3. Image was acquired ~5 min after injection on auto exposure setting so as to determine optimal exposure time using Living Image 4.0 software provided with the instrument. Images were always captured so that count of photons was detected in the recommended detectable

range for the instrument i.e. 600 to 60000. Exposure time and Camera aperture (f/Stop) settings were adjusted in case required.

4. 8-10 serial images at interval of 2min wherein luminescence counts gradually increase attain peak and reduce subsequently. Image showing peak luminescence counts indicates peak enzyme activity that can be achieved and hence is used as a representative of tumour growth at that time point in a particular animal.

6. Region of interest (ROI) was precisely drawn over site of luminescence (represents site of the tumour) in overlay images using the Living Image 4.0 software (Caliper Life Sciences) and the total normalised photon ouput was represented as average radiance (photons/sec/cm^2/steridian).

6. All the animals were imaged on 1^{st} and 4^{th} week post intracranial injection. Increase in tumour growth from 1^{st} week to 4^{th} week was represented as fold change in radiance. Significance of difference in increase in tumour growth between mice injected with either doxycycline treated or untreated D283 pTRIPZ-miR-148a polyclonal population was calculated using Student's t test.

3.21. Luciferase Reporter Assay

a) Promoter Luciferase assay: Putative promoter regions of respective miRNAs were cloned upstream to firefly luciferase cDNA in a promoter-less luciferase reporter vector pGL3b. cDNAs for *MYC* and mutant *CTNNB1*(mutation at S32, rendering it resistant to phoshorylation mediated degradation) were cloned in pcDNA3.0 expression vector from their respective parent vectors. Co-transfection of promoter constructs with or without mutant β-catenin or MYC expression constructs and EGFP expression plasmid was done using Calcium phosphate BES buffer method in HEK293 cells. Luciferase activity normalised by EGFP flurescence was reported as promoter activity.

b) 3'UTR-reporter Luciferase assay: 3'-UTR (un-translated region) of each of the potential miRNA target genes was amplified from genomic DNA of normal human peripheral blood lymphocytes using Phusion Taq polymerase. The 3'-UTRs were then cloned downstream of firefly luciferase cDNA from pGL3 vector in a pcDNA 3.0 plasmid vector. The genomic region encoding miR-148a was cloned into pcDNA 4.0 plasmid vector wherein miR-148a was expressed under CMV promoter in mammalian cells. HEK 293T cells were transfected with the luciferase reporter plasmid, miR-148a expression vector and EGFP expression vector using calcium phosphate BES buffer method. Luciferase activity was assessed from the total protein extracted from the transfected HEK293T cells and was normalized against the EGFP fluorescence.

3.21.1. Generation of Vector constructs for promoter luciferase reporter assay and 3'UTR luciferase reporter assay.

Reagents:

1) Plasmids: *pcDNA3.0 and pcDNA4 mychisB (Invitrogen, Life Sciences, Carlsbad, CA, USA); pGL3Basic ((Promega, Madison, WI, USA)*

2) Enzymes: *Phusion Taq Polymerase, Klenow Fragment, EcoRV, SmaI, XbaI, BamHI, HindIII, T4 DNA Ligase, standard Taq Polymerase, T4PNK*

3) QIAquick Gel Extraction Kit

1) Promoter constructs – [Refer section 3.6 (a-f) for details of PCR, restriction enzyme digestion, dephosphorylation, ligation reactions]

Putative promoter regions for miR-193a, miR-148a, miR-365 and *GABRE* (miR-224) were amplified using Phusion Taq polymerase and normal human lymphocyte genomic DNA as template. Primers were designed such that they harbour restriction enzyme sites on their 5'ends. Amplified fragments were digested with appropriate restriction enzymes and then cloned in MCS of pGL3basic vector.

Primer sequences for amplification of promoter regions for miRNAs are listed in **table 3.3** below:

Name	Forward/ Reverse	SEQUENCE(5'-3')
miR-365 promoter -1200 to +99	FWD	GGGGTACCCCTTAAAATCACAGTGGAAACTGG
	REV	GAAGATCTTCAAAGAAAGAATGAATGTTAGCC
miR-148a promoter -1749	FWD	GTCCTCGAGAGGTTTCCATTTCGCACTCT
miR-148a promoter -3161	FWD	GGTGGTACCGATGGCAGACAATAACTCCC
miR-148a promoter -1310	FWD	GAGCTCGAGGGAACCTGCTGACTTGACAC
miR-148a promoter -369	REV	TCTAAGCTTTGGCAACTTTTTACCTTCCC
miR-148a mutE-Box1 SDM1	FWD	CCGGGGCGCACGGGACCCCGGGGAG
	REV	CTCCCCGGGGTCCCGTGCGCCCCGG
miR-148a mutE-Box1 SDM2	FWD	CGCCCGGGGCGCCCGGGACCCCGGG
	REV	CCCGGGGTCCCGGGCGCCCCGGGCG
GABRE Promoter -3500	FWD	TTTCTCGAGGTGCTTTCCCCAGTGTCC
GABRE Promoter -1320	FWD	TGTGGGACCGTGTGTGTTTGTCCCTGAGC
GABRE Promoter +28	REV	GACAAGCTTCGCGGAGGTCGCGGCTCA
miR-193a Promoter -4169	FWD	TCTGGTACCCAGGATGCGTATGTCTTCT
miR-193a Promoter -2330	FWD	TCCGGTACCGTCAGGGCATCTTCTTTCT
miR-193a Promoter -1292	FWD	TATGGTACCCGGTACTATGCTTGGCACT
miR-193a Promoter -158	REV	CCAGATATCCAAGGGTTACACGACGCTC

2) pcDNA3-MYC – pBS-MYC cDNA expression vector was gifted by Dr. Joan Massague (Memorial Sloan Kettering cancer centre, New York, USA). MYC cDNA was removed from this plasmid by digesting it with EcoRI and was gel purified using QIAquick Gel Extraction Kit as per manufacturer's instructions. 5'and 3' ends were made blunt using Klenow Fragment and was blunt ended DNA was ligated in EcoRV digested pcDNA3.0 mammalian expression vector.

3) pcDNA3-mutant CTNNB1- pBI-mutant CTNNB1 cDNA expression vector was gifted by Dr. Benjamin Alman (Hospital for Sickkids, Toronto, Ontario, Canada). CTNNB1 cDNA of 2346 bp size was removed from this plasmid by digesting it with SmaI and XbaI and subsequently gel purified using QIAquick Gel Extraction Kit as per manufacturer's instructions. Its 3' end was made blunt using Klenow Fragment and was then blunt end ligated into EcoRV digested pcDNA3.0 mammalian expression vector, using T4 DNA ligase.

4) 3'UTR Luciferase Reporter vector - Firefly Luciferase cDNA was cut from pGL3basic vector by using restriction enzymes HindIII and BamHI and was ligated into pcDNA3.0 cut with similar restriction enzymes. This creates a vector cassette where MCS from pcDNA3.0 lies downstream to the luciferase cDNA cloned. This was used as 3'UTR luciferase reporter vector where 3'UTR of putative gene targets of miR-148a were cloned downstream to firefly luciferase cDNA by exploiting MCS from pcDNA3.0 backbone.

5) 3'UTR Luciferase Reporter constructs for putative gene targets – Primers with desired restriction sites at their 5' end were designed to amplify 3'UTRs of putative miR-148a target genes namely *ARHGAP21, B4GALT5, B4GALT6, DNMT1, ITGA5, MMP15, NRP1, ROBO1, ROCK1* and *TMSB10*. 3'UTRs were amplified using Taq polymerase and cut with appropriate combination of restriction enzymes. Such amplicons were then ligated into 3'UTR luciferase reporter vector digested with similar combination of restriction enzymes, using T4 DNA ligase.

Table 3.4: Primer sequences for PCR amplification of 3'UTRs

Name of the Gene	Forward/ Reverse	**Sequence**
DNMT1 3'UTR	FWD	GACGAATTCTGCCCTCCCGTCACCC
	REV	TAATCTAGACTCATACAGTGGTAGATTTG
ROCK1 3'UTR	FWD	GCGGGATCCCCTACAGGTAGATTAGATTA
	REV	CTCTCTAGATGAGCACAGAGTCATTAGT
ARHGAP21 3'UTR	FWD	ACTGGGGGTATGTCCACTCTA
	REV	ATTTCCAGTGTTTAATTGGGTATGC
TMSB10 3'UTR	FWD	CAGGAATTCAGCAGGAGAAGCGGAGTGAAA
	REV	CCACTCGAGCCATGCCACGAGGTGTGT
NRP1 3'UTR	FWD	ACAAGGGAAGTGGAAGGAAGGAA
	REV	AAAATACTTGACCCCCAGGC
NRP1 3'UTR SDM	FWD	CAACTTTAAAATTTAAAGTATCTTGTCTAGATAAA TATATTTAAAAATATATG
	REV	CATATAATTTTTAAATATATTTATCTAGACAAGAT ACTTTAAATTTTAAGTTG
B4GALT5 3'UTR	FWD	TACACAGCAAGAGAACAGAAATA
	REV	AGTAAATAATGTAATGACAAAGGACTA
MMP15 3'UTR	FWD	ACATCTAGAGGCTGTACAATTTATTCAGTGC
	REV	CCTGAATTCGTACTTGTGTATAATTGCCCGC

ROBO1 3'UTR	FWD	AAACTCGAGACTCAAGATGCCTCCTGTCA
	REV	TATTCTAGATTATGGCTAAAAATAAGGGGCT

6) pcDNA4-miR-148a (miR-148a expression construct) – Primers were designed to amplify miR-148a coding genomic region covering at least 200bp on either side of pri-miR-148a sequence. Amplicon corresponding to 570bp was amplified using Phusion polymerase and was treated using T4 PNK enzyme to phosphorylate 5'ends. This was then ligated with EcoRV digested and dephosphorylated pcDNA4 myc his B expression vector.

7) Mutant NRP1 3'UTR luciferase reporter construct – MiR-148a binding site in NRP1 3'UTR was mutated to yield non-functional binding site by using site directed mutagenesis (SDM) PCR. Nucleotides 5'-CACT- 3' from wild type miR-148a binding site in NRP1 3'UTR were mutated to 5'-TCTA-3' making it incapable of binding to mature miR-148a. Change in nucleotides also resulted in creation of XbaI restriction enzyme site in DNA, which was used to screening procedure for positive colonies post transformation.

Method:

1. Primers were designed to have (a) Tm more than or equal to 78^0C. Tm can be calculated by the formula [Tm = 81.5 + 0.41(%GC) ‑ 675/(length in bases)−%mismatch], (b) Forward primer length between 25 to 45 bases with desired mutation at the centre (c) reverse primer should be exactly complimentary to Forward primer, (d) GC content of more than 40% and terminating in G or C.

2. PCR reaction was set up as follows

Components	Volume per 10µl Reaction	Final Concentration
5XHF/GC buffer	2 µl	1X
10 mM dNTPs	0.2 µl	2 mM
10 pmol/ µl Forward primer	0.2 µl	2 pmol
10 pmol/ µl Reverse Primer	0.2 µl	2 pmol
Template (vector DNA)	10 ng	-
Phusion Taq Polymerase	0.2 µl	
DMSO (optional)	0.3 µl	3%
Autoclaved Milli-Q	Make up to 10 µl	

PCR Reaction conditions were as follows

Temperature	Time	No. Of. Cycles
98^0C	3 min	1
98^0C	1 min	20
56-62^0C (variable)	45 sec	
72^0C	1min per kb	
72^0C	10 min	1
4^0C	∞	

3. PCR product was digested with DpnI enzyme. Reaction conditions were as follows

Components	Volume	Final Concentration
10X Tango buffer	2 µl	1X
PCR product	15 µl	100-200 ng
DpnI (10U/ µl)	1 µl	
Autoclaved Milli-Q	Make up volume to 20 µl	

4. Reaction mixture was incubated at 37^0C for 12-16 hr and was inactivated at 80^0C for 20 min.

5. 5 µl of PCR product before and equivalent PCR product after DpnI digestion was loaded on 1% agarose gel to ensure persistence of full length PCR product post DpnI digestion.

6. 15 µl of DpnI digested DNA was transformed in DH5α competent cells.

7. Plasmid DNA was extracted from 10-20 DH5α colonies formed by alkaline lysis method.

8. DNA was digested with XbaI enzyme as creation of new XbaI restriction enzyme site suggests the successful site directed mutagenesis. It was also given for sequencing with NRP1 3'UTR reverse primer to further confirm the mutation.

3.21.2. Luciferase assay

Reagents:

Cell lysis buffer:

Components	Volume	Final Concentration
1 M Glycine-glycine pH 7.8	1.25 ml	25 mM
1M MgSO4	0.75 ml	15 mM
250 mM EGTA	0.8 ml	4 mM
Triton X-100	0.5 ml	1% (v/v)
100 mM DTT	*	1 mM
Autoclave Milli-Q	Make up to 50 ml	

Luciferase Assay Buffer

Components	Volume	Final Concentration
1 M Potassium phosphate buffer pH 7.8	0.75 ml	15 mM
1 M Glycine-glycine pH 7.8	1.25 ml	25 mM
1 M MgSO4	0.75 ml	15 mM
250 mM EGTA	0.8 ml	4 mM
100 mM ATP	*	2 mM
100 mM DTT	*	1 mM
Autoclave Milli-Q	Make up to 50 ml	

Luciferin Solution

Components	Volume	Final Concentration
1M Glycine-glycine pH 7.8	1.25 ml	25 mM
1M MgSO4	0.75 ml	15 mM
250 mM EGTA	0.8 ml	4 mM
20 mM D-Luciferin	*	0.2 mM
100 mM DTT	*	2 mM
Autoclave Milli-Q	Make up to 50 ml	

(*Note- Add DTT, ATP and D-Luciferin just before use)

Method:

1. HEK293 cells were trypsinised, counted and seeded as $5x10^4$ cells per well of 24 well late or $1x10^4$ cells per well of 96 well plate.

2. 16-24 hr post seeding, transfection of total of 1.5 µg DNA per well of 24 well dish or 0.3 µg DNA per well of 96 well was done using BES buffer method. (Refer section 3.11)

3. DNA mixture was prepared in autoclaved Milli-Q as given below.

For Promoter Luciferase Reporter assay -

Components	Final Amount/ volume	
	24 well plate (for one well)	**96 well plate (for one well)**
pGL3b-Promoter /pGL3b	750 ng	150 ng
pcDNA3/ pcDNA3-mutCTNNB1/ pcDNA3-MYC	500 ng	100 ng
pCS-CG	250 ng	50 ng
Autoclaved Milli-Q (Make up volume to)	12.5 µl	2.5 µl
0.5M CaCl2	12.5 µl	2.5 µl
2X BBS	25 µl	5 µl

For 3'UTR Luciferase Reporter assay -

Components	Final Amount/ volume	
	24 well plate (for one well)	**96 well plate (for one well)**
3'UTR reporter Plasmid	250 ng	50 ng
pcDNA4	500 ng	100 ng
pcDNA4-miR-148a	500 ng	100 ng
pCS-CG	250 ng	50 ng
Autoclaved Milli-Q (Make up volume to)	12.5 µl	2.5 µl
0.5M CaCl2	12.5 µl	2.5 µl
2X BBS	25 µl	5 µl

4. Following addition of 0.5M CaCl2 to the DNA mixture, appropriate volume of 2X BBS was added and then the mixture was mixed by pipetting gently two to three times to ensure thorough mixing of all components.

5. Tubes were incubated for 20 min at RT, following which mixture was added to respective wells or dish.

6. Medium was changed after 16 hr from transfection. Lithium chloride was added at final concentration of 25mM whenever necessary.

7. 72 hr after transfection, medium was removed and cells were washed twice with ice cold 1X PBS.

8. Appropriate volume of cell lysis buffer (200 µl per 35mm dish, 50 µl per well of 24 well plate or 96 well plate was added to the cells. Cells were scraped from the plate and lysis of cells was ensured by pipetting the volume up and down several times.

9. Lysate was transferred to the microcentrifuge tube and centrifuged at 16000 rpm, 4^0C for 5 min.

10. Supernatant was transferred in fresh microcentrifuge tubes and fluorescence and luminescence was measured using Mithras LB940 multimode reader as described below.

11.10 µl of sample was added per well of 384 well Optiplate (Cat No. 6007290, Perkin Elmer), and fluorescence was measured at excitation and emission wavelengths of 485 nm and 515 nm. Each sample was assayed in triplicates.

13. 20 µl of assay buffer and 10 µl of Luciferin solution were added to sample and mixed twice by pipetting.

14. Luminiscence was read immediately at exposure time of 0.1 sec.

3.22. Protein extraction of cultured cells

Reagents:

10X PBS: (1.5 M NaCl, 89.8 mM $Na_2HPO_4.2H_2O$, 28.8 mM $NaH_2PO4.2H_2O$). 90 g NaCl, 16 g $Na_2HPO_4.2H_2O$, 4.5 g $NaH_2PO_4.2H_2O$ per litre; pH adjusted to 7.5 with 5 N NaOH, autoclaved and stored at room temperature. 10X stock was dilute to 1X with autoclaved Milli-Q water and stored at room temperature.

Lamelli buffer or *1X sample buffer:* 62.5 mM Tris-HCl pH 6.8, 2% SDS, 10% glycerol. Total protein was extracted in sample buffer from doxycycline un-induced and induced miR-148a expressing polyclonal populations of Daoy and D283, 72 hr post transfection as described below.

Method:

1. The medium was poured off from the culture dishes and the cells were rinsed twice with 1X PBS gently.

2. The PBS was drained off completely and cells were lysed in 1X sample buffer. About 0.5 – 0.6 ml sample buffer was used for protein extraction from 90 mm^2 dishes with 80-90% confluency. The viscous lysate, due to release of genomic DNA along with proteins from the cells, was collected by swirling the plate several times and transferred into a 1.75 ml microfuge tube.

3. The tubes were immediately kept in a boiling water bath for 7 min, cooled to room temperature and centrifuged in Rota-4 R at 15,000 rpm for 1.5 hr at 20°C to pellet down the genomic DNA. The DNA pellets were discarded.

4. The supernatant lysates containing protein were carefully transferred to fresh tubes and stored at -20°C until further use.

3.23. Estimation of Protein Concentration[108]

The proteins extracted in sample buffer from cells were estimated using this method.

Reagents:

1) 1 mg/ml BSA: 10 mg BSA (sigma) was weighed and dissolved in 1 ml autoclaved Milli-Q water to obtain a stock of 10 mg / ml. This stock was further diluted 1:10 in water to obtain a working stock of 1 mg/ ml. BSA stocks were stored at -20°C.

2) Solution A: Cu-tartrate CO3 (CTC)

a) 20% Na2CO3: 20 g was dissolved in 100 ml Milli-Q water.

b) 0.2 g CuSO4 was dissolved in 40 ml Milli-Q water.

c) 0.4 g potassium tartarate was dissolved in 40 ml Milli-Q water.

CuSO4 and potassium tartarate were mixed (b + c) and the volume was made up to 100 ml with Milli-Q water. Final concentration of CuSO4 is 0.2% and potassium tartarate is 0.4%. To this, 100 ml of 20% Na2CO3 (a) was added slowly with constant stirring. This solution A was stored in dark at room temperature.

3) Solution B: 10% SDS. 10 g of SDS was dissolved in 80 ml Milli-Q water, heated at 60°C to assist dissolution. The final volume was adjusted to 100 ml and stored at room temperature.

4) *Solution C: (0.8 N NaOH)* 16 g of NaOH was dissolved in 100 ml of Milli-Q water, and the volume made up to 500 ml and was stored at room temperature (Note: Do not autoclave).

6) Reagent A: Prepared by mixing solutions A, B, C, and Milli-Q water in a proportion of 1:1:1:1 just before use. (Note: Mixing NaOH with 10% SDS results in a glue like insoluble precipitate. Therefore dilute the 20%SDS first in the required volume of water and then add NaOH and CTC to it.)

7) Reagent B: Folin-Ciocalteau reagent was diluted 1+5 in Milli-Q water just before use.

Method:

1. 2 µl of protein sample to be estimated was diluted in 1 ml of Milli-Q water in duplicates.

2. BSA standards, ranging from 1 µg to 20 µg were prepared in duplicate by appropriately diluting from 1 mg/ml stock of BSA, in 1 ml of Milli-Q water. 2 µl of the sample buffer used for extraction of protein to be estimated was also added. "Blank" tubes were prepared by adding only 2 µl of the sample buffer.

3. 1 ml of freshly prepared reagent A was added to each tube, immediately mixed on a vortex mixer, and kept in dark at room temperature for 10 min. Then 0.5 ml of freshly diluted reagent B was added to each tube, immediately mixed on a vortex mixer and incubated in dark at room temperature for 30 min.

4. The absorbance of the blue colour developed was read at 750 nm against blank in a spectrophotometer (Shimadzu UV-160A, UV-visible recording spectrophotometer), and the concentration of the unknown protein samples was calculated by using the BSA standard plot.

3.24. SDS-Polyacrylamide Gel Electrophoresis (SDS-PAGE)

The proteins extracted in sample buffer from doxycycline treated or untreated vector control and pTRIPZ-miR-148a transduced medulloblastoma cells were separated by SDS-PAGE for western blotting.

Reagents:

1) 30% acrylamide solution: 29.2 g acrylamide, 0.8 g bis-acrylamide were dissolved in approximately 50-60 ml autoclaved Milli-Q water and the final volume was made up to 100 ml. Solution was filtered through ordinary filter paper and stored in an amber colored bottle at 4°C.

2)20% SDS: 20 g SDS was dissolved in 80 ml of Milli-Q water, heated at 60°C to assist the dissolution. The final volume was made up to 100 ml, and stored at room temperature.

3) 1M Tris pH 8.8 and pH 6.8: 60.55 g Tris was dissolved in 400 ml Milli-Q water. pH was adjusted to 8.8 and 6.8 with concentrated HCl, the final volume was made up to 500 ml with Milli-Q water and autoclaved. Solutions were stored at 4°C.

4) 10X electrode buffer: 30 g Tris, 143 g glycine, 20 g SDS were dissolved in approx. 700 ml Milli-Q water and the final volume was made up to 1 L. Stock solution was diluted to 1X with Milli-Q water before use (1X buffer is 25 mM Tris, 190 mM Glycine, 0.2% SDS).

5) 0.5 % Coomassie Blue staining solution: 0.5 g of Coomassie Blue staining dye was dissolved in 50 ml of methanol (LR grade) by constant stirring. The final volume was adjusted to 100 ml by adding 40 ml of Milli-Q water and 10 ml of glacial acetic acid. The staining solution was filtered through filter paper and stored at room temperature for 1 month.

6) Destainer: Methanol (LR), glacial acetic acid (AR) and Milli-Q water mixed in the proportion 5:1:4 and stored at room temperature.

7) Loading Dye: 0.025% Bromophenol Blue was dissolved in 1X Sample Buffer.

Method:

1. Two clean glass plates (one of which was notched), separated by 1.5 mm thick spacers were clamped together. The sides and the bottom of the plates were sealed using 3% agar. The resolving gel of the required percentage (10%) was prepared by mixing the following

Components	Final Concentration of Acryl amide		
	10%	12%	20%
30% Acrylamide	10 ml	12 ml	20 ml
1M Tris-Cl pH8.8	11.2 ml	11.2 ml	11.2 ml
20%SDS	0.15 ml	0.15 ml	0.15 ml
Milli-Q water	8.65 ml	6.65 ml	-
TEMED	20 µl	20 µl	20 µl
20% Ammonium persulfate	50 µl	50 µl	50 µl

2. The gel solution was poured between the two glass plates taking care to avoid air bubbles. Water was carefully layered over the gel and it was allowed to polymerize (approximately 20 – 30 min).

3. Following polymerization, the water layer was removed and a 5% stacking gel was prepared and overlaid over the resolving gel.

5% stacking gel composition

Components	Volume to be added
30% acrylamide solution	1.67 ml
1 M Tris-HCl pH 6.8	1.75 ml
20% SDS	100 µl
Milli-Q water	6.98 ml
TEMED	10 µl
20% ammonium persulphate	25 µl

A comb of 1.5 mm thickness was inserted immediately into the stacking gel solution between the two plates to form wells. After polymerization of the stacking gel, the comb was gently removed and the wells were cleaned by flushing first with water and then with 1X electrode buffer (using a syringe-needle). The gel plates were clamped to the electrophoresis unit and the upper and lower tanks were filled with 1X electrode buffer.

4. The proteins to be resolved were mixed with 1X sample buffer containing 5% v/v BME and 0.01% bromophenol blue, boiled for 3 min and loaded into the wells of the gel along with pre-stained protein ladder.

5. Electrophoresis was carried out at 22 mA constant current till the dye reached the bottom of the gel. The gel was removed carefully and either stained with Coomassie blue to check equal loading of the proteins or processed for western blotting as described later.

3.25. Western Blot Analysis

The proteins separated by SDS-PAGE (Polyacryl Amide Gel Electrophoresis), were transferred to a PVDF membrane by western blotting technique. Various proteins like NRP1, ROCK1, DNMT1, c-Myc and ɣ-tubulin etc were detected on the blot by the immuno-detection method.

Reagents:

1) *1X transfer buffer:* 25 mM Tris, 192 mM Glycine, 20% Methanol. 3 g Tris and 14.4 g Glycine were dissolved in Milli-Q water and volume was made up to 800 ml with Milli-Q water. 200 ml Methanol was added to make 1 L. Buffer was chilled to 4°C before use. (1 L transfer buffer is sufficient for western blotting in Biorad‟s mini trans-blot electrophoretic transfer cell)

2) 10X Tris-buffered saline (TBS): 0.1 M Tris, 1.5 M NaCl 12.1 g Tris and 87.6 g NaCl were dissolved in Milli-Q water, pH was adjusted to 8.0 with concentrated HCl and the final volume was made up to 1 L. Solution was autoclaved and stored at room temperature.

3) 1X Tris-buffered saline with Tween-20 (TBST): 10X TBS was diluted to 1X with Milli-Q water (1 litre), 1 ml Tween-20 was added to the solution and kept on magnetic stirrer for 1 hr.

4) Ponceau-S staining solution: (0.2% Ponceau-S in 1% glacial acetic acid)

5) SuperSignal® West Pico chemiluminescent substrate

6) Antibodies: Catalogue No and companies mentioned in method.

7) X-ray film (Ref no.4908364, Kodak Companies)

8) Whatmann Filter paper 3 (Cat No. 4908364)

Method:

1. The protein samples to be blotted were resolved by SDS-PAGE and the gel was kept in 1X transfer buffer for 15-20 min until the gel was free from the smell of β- mercapto ethanol (BME).

2. The Immobilon PVDF membrane, to be used for blotting, was cut to the size of the gel to be blotted. The membrane was pre-wet in methanol for about 30 seconds, kept in Milli-Q water for 10min. to wash off excess methanol and then placed in 1X transfer buffer for 20 min. Two pieces of a Whatmann 3MM filter paper little bigger than the size of the gel, were also cut.

3. The transfer assembly was prepared according to the manufacturer's instructions. The cassette was assembled in a tray containing 1X transfer buffer by arranging the components in the following sequence: First the cassette was placed, with the gray side down in a tray containing transfer buffer. A Scotch-Brite pad was placed over the grey portion of the cassette, and a piece of Whatman paper was placed over it. Then the transfer buffer equilibrated gel was carefully placed over the Whatman paper and the PVDF membrane was juxtaposed to the gel without trapping any air bubbles between the gel and the PVDF membrane. A small cut was given at one corner of the membrane and the gel for correct orientation. Another piece of Whatman paper and a Scotch-Brite pad were placed over the PVDF membrane. The cassette was closed firmly and locked with the white latch on top of the cassette, and slid into the grooves for holding the cassette in place with the grey portion (gel side) towards the cathode (negative electrode) and the transparent portion (membrane side) towards the anode (positive electrode). This whole assembly was placed inside the tank

containing transfer buffer, and the electrodes were connected to the power supply. Transfer was carried out at 40mA constant current at 4°C for 16 hr.

4. After the transfer, the membrane was carefully removed from the cassette using a pair of forceps, rinsed once with Milli-Q water, and kept in destainer for 30 min (to aide in staining with Ponceau-S). Then the membrane was washed twice with TBST for 5 min each and stained with Ponceau-S till the protein bands were visible. The molecular weight marker positions were marked on the membrane with a soft lead pencil and then the Ponceau-S was completely removed by washing the membrane with TBST. It was either probed immediately or stored at 4°C in TBST, for later use.

5. For probing, the membrane was first blocked with a 5% milk solution prepared in TBST. The membrane was kept in the milk solution for 1 hr at room temperature on a rocker with gentle shaking.

6. The blocking solution was drained off and the membrane was washed 3 times for 5 min each with TBST, on the rocker with vigorous shaking.

7. TBST was drained off completely and the membrane was incubated with appropriately diluted antibody, with gentle shaking on the rocker. The working conditions of various antibodies used are given below.

Name of Antibody	**Company/Catalogue No.**	**Type**	**Dilution**	**Duration**
NRP1	Cell signalling #3725	Rabbit Polyclonal	1:1000 in 1%BSA-TBST	O/N 4^0C
ROCK1	Cell signalling #4035	Rabbit Polyclonal	1:1000 in 1%BSA-TBST	O/N 4^0C
DNMT1	Cell signalling #5119	Rabbit Polyclonal	1:1000 in 1%BSA-TBST	O/N 4^0C
ϒ tubulin	Sigma	Rabbit polyclonal	1:4000 in 1%BSA-TBST	O/N 4^0C
c-Myc	Santacruz 9E10 (sc-40)	Mouse monoclonal	1:1000 in 1%BSA-TBST	1 hr/RT
Goat Anti-rabbit IgG	Thermo Scientific #31460	Goat	1:4000 in 2% milk-TBST	1 hr/RT
Goat Anti-mouse IgG	Thermo Scientific	Goat	1:4000 in 2% milk-TBST	1 hr/RT

8. The antibody solution was drained off and the membrane was washed six times for 5 min each with 1X TBST, on the rocker with vigorous shaking.

9. Then the membrane was incubated with appropriately diluted horseradish peroxidase (HRP) conjugated secondary antibody (anti-IgG) for 1 hr at RT on the rocker with gentle shaking. Anti-rabbit HRP-conjugated antibodies (Thermo-Scientific) were diluted 1:2000 in 1% milk-TBST. The antibody solution was drained off and the membrane was washed vigorously six times for 5 min each with 1X TBST and then three times with 1X TBS.

10. The excess buffer was drained off and the membrane was placed on a clean cling film and covered with commercial chemiluminescent substrate Super Signal West Pico for 5 min at room temperature.

11. Quickly, the detection solution was drained off; the membrane was wrapped in cling film, placed in an X-ray film cassette and exposed to X-ray film for 1-2 min. The signal was visualized after developing the X-ray film.

3.26. Immunohistochemical (IHC) staining of Formalin Fixed Paraffin Embedded (FFPE) Tissue Sections.

Immunohistochemical staining was performed to check NRP1 protein expression in 93 medulloblastoma FFPE sections. The staining was visualised and photographed using Zeiss upright fluorescent microscope Axioimager.Z1 and scored on the basis of intensity and percentage of positive cells. The scoring of staining intensity by pathologist was done in blinded fashion i.e. without prior knowledge of subgroup or survival data.

Reagents:

1. Methanol (LR), Xylene (AR)

2. Sulfuric Acid (LR), Potassium dichromate (LR), Tri-Sodium citrate (LR), Citric Acid (LR), Hydrogen peroxide.

3. Disodium orthophosphate, Sodium dihydrogen orthophosphate, Sodium chloride.

4. DPX

4. Single distilled alcohol (local make)

5. Poly –L-Lysine (Cat. No. P2636, Sigma),

6. Diaminobenzidine/DAB (Cat no: D5637, Sigma)

7. Primary antibodies (details mentioned in method) and Secondary Antibody (Thermo scientific)

9. Streptavidin, Peroxidase-conjugated, Amersham.

Solutions required

1) *Chromic Acid solution***:** 40 g of potassium dichromate was dissolved in 920 ml Mill-Q taken in a glass beaker. 80 ml Conc. Sulfuric Acid. Rubber gloves were worn to prevent any damge due to spillage of strong acid.

2) *Poly –L-Lysine solution:* 50 mg of poly-L-Lysine was dissolved in 50 ml sterile Milli-Q water. Pinch of sodium azide was added to get final concentration of 0.02%.

3) *Stock 1M Citrate Buffer pH 6.0:* 58.82 g of Trisodium citrate was dissolved in about 150 ml of Milli Q water and pH was adjusted to 6.0 with 1 M Citric acid solution. [21. 01 g of Citric acid was added for 100 ml to get 1M citric acid]. Volume was made up to 200 ml. Both the solutions were autoclaved. Before use, 1M Citrate buffer was diluted 100 times in sterile Milli-Q water and pH was adjusted again with 1M citric acid.

4) Phosphate buffered Saline (PBS), 10X: 16 g of disodium orthophosphate, 4.5 g of Sodium dihydrogen orthophosphate, 90 g of Sodium chloride was dissolved in 800 ml of Milli-Q water and pH was adjusted to 7.5 with 5M NaOH. Volume was made up to 1000 ml and solution was filtered through filter paper and autoclaved. 10X PBS was diluted to 1X PBS in fresh sterile MQ water.

5). Hematoxylin solution for counterstaining: Dissolve 5 g haematoxylin in 50 ml alcohol. Add 100 mg potassium aluminium sulphate in water while heating. Cool the solution and add

both the solutions and boil it rapidly. Again cool it and add 2.5 mg mercuric oxide slowly. Heat it till dark purple colour develops. Cool the solution (by placing in cold water). Before use add 2 ml acetic acid to 100 ml of filtered stain.

Method:

Pre-treatment and poly-L-lysine coating of the slides-

1. Microaid glass slides (size 75 X 25 mm + 1 mm, thickness 1.2 mm + 0.1 mm) were dipped in chromic acid solution for 1 hr and then in running tap water for 1 hr to remove chromic acid.

2. They were further boiled in Milli-Q water two-three times with fresh water and drained on tissue paper.

3. These slides then were dipped in Poly-l-lysine solution kept in plastic jar for 15 min. Slides were then dried in 37 ^{0}C incubator in a slide jar overnight.

4. Paraffin sections of 5 µm thickness were taken on dry poly-lysine coated glass slides.

De-paraffinisation of Sections-

5. Slides were dipped sequentially for 10 min each in three koplin jars filled with fresh xylene, followed by two washes of 100% alcohol each of 5 min.

6. Slides were then dipped in a Koplin jar filled with fresh methanol supplemented with 1% of H_2O_2 (500 µl of H_2O_2 was added in 50 ml of methanol) just before use and incubated for 15 min. Jars were covered during incubation.

7. Slides were then transferred to the jars containing 100% alcohol (Alcohol at this step need not be fresh), 70% alcohol and then to 50% alcohol with incubation period of 5 min in each jar.

8. They were further rinsed twice with Milli-Q water for 5 min each.

Antigen retrieval -

9. After rinsing with Milli-Q, slides were transferred immediately to glass vessel with slide rack holding in 400 ml of 10 mM Citrate buffer pH 6.0. (Note that glass vessels or plastic vessels used for this step were microwave heat compatible as stated by manufacturer)

10. Initial buffer level was marked on the box and vessel was heated in microwave oven for 10 min at "High" power setting.

11. The vessel was removed from the microwave oven and lost volume was made up with sterile Milli-Q water. It was then incubated at RT for 1 min, followed by heating in microwave at "low" power setting (90 ^{0}C) for 5 min, twice.

12. The vessel was removed from microwave and kept at RT for 20 min.

13. Slides were transferred to koplin jar and were given three washes with 1X PBS, 5 min each.

Blocking and incubation in primary antibody -

14. Each section was covered with 100 µl of 3% BSA prepared in 1X PBS for 30 min, followed by 3 washes of 1X PBS, 5min each in Koplin jar.

15. Section was then covered with 60-100µl of primary antibody solution and slides were incubated in humidified chamber overnight in refrigerator. Anti-NRP1 (#3725, Cell signalling) or Anti-CD31 (M-20, sc-1506, Santacruz Biotechnology) antibody was diluted 100times in 1% BSA prepared in 1X PBS. Out of two duplicate sections on one slide, one section was incubated in primary antibody solution while other one in 1%BSA. Latter was termed as Secondary control and was used to check for any nonspecific staining because of nonspecific binding of primary antibody.

Incubation in Secondary Antibody and development of signal using DAB

16. Primary antibody solution was drained carefully and sections were washed with two quick rinses of 1X PBS by putting PBS directly onto sections.

17. Slides were then given 5 washes of 5 min in 1X PBS in Koplin jar.

18. Sections were covered with secondary antibody diluted in 1%BSA prepared in 1X PBS and incubated for 1 hr at RT. (1:100 dilution of anti-rabbit HRPO conjugated secondary antibody was used in case of anti-NRP1 staining, while 1:100 dilution of biotinylated anti goat secondary antibody prepared in 1% goat serum was used for anti-CD31 staining).

19. Steps 16 and 17 were repeated.

20. Sections were covered with streptavidin conjugated with HRPO diluted 1:100 in 1X PBS for 1 hr.

21. Step 16 and 17 were repeated.

22. Signal was developed in DAB (1 mg/ml) prepared in 1X PBS, supplemented with 0.1% H_2O_2 (1 μl/ml) by incubating slides in DAB containing koplin jar either for 1min in case of anti-NRP1 staining or 15 sec in case of anti-CD31 staining.

23. Slides were washed with 5-6 quick rinses with Milli-Q water to remove excess DAB and avoid further nonspecific staining.

24. DAB solution used was inactivated by adding 10% sodium hypochloride solution followed by passing through activated charcoal. Give five quick rinses with lots of Milli Q water. Inactivate DAB by adding sodium hypochlorite.

25. Sections were counterstained with hematoxylin solution by covering section in hematoxylin solution for 1 min. Hematoxylin solution were filtered just before use. This was done to stain nuclei in light blue colour. Excess hematoxylin was removed by giving washes of Milli-Q.

Fixation and mounting of sections –

26. Slides were then dipped sequentially in 50% ethanol, 70% ethanol and 100% ethanol for 5 min each. These steps dehydrate sections slowly which is essential for their long preservation time post fixing.

27. Slides were then dipped in xylene for 5 min and then slides were drained on tissue paper. Excess xylene was wiped off carefully without touching sections.

28. Drop of DPX mounting agent was added over section so as to cover section fully and then cover-slip was placed over carefully avoiding air bubble formation.

29. Mounted slides were incubated at 37^0C for 1-2 hr.

Chapter 4: RESULTS

Genome wide expression profiling of medulloblastoma have shown that medulloblastoma is not a single disease, but is comprised of four core molecularly distinct subgroups namely WNT, SHH, Group 3 and Group 4. We have earlier reported that microRNA profile of the medulloblastomas differs across these subgroups and that their expression can be effectively used to classify medulloblastomas into four core molecular subgroups. Highlight of the miRNA profile of medulloblastomas was the distinctive miRNA signature of WNT medulloblastomas. WNT subgroup medulloblastomas showed up-regulation of miR-193a, miR-148a, miR-224, miR-365, miR-23b and miR-10b as compared to medulloblastomas belonging to other subgroups [3, 6]. The present study was aimed to find out (a) whether these WNT subgroup specific miRNAs are regulated directly or indirectly by WNT signalling pathway and, (b) functional role of WNT subgroup specific miR-148a in regulating malignant behaviour of medulloblastoma cells.

4.1 Transcriptional regulation of WNT subgroup specific miRNAs –

4.1.1 Identification of putative promoter regions and transcription factor binding sites.

Most of the miRNA genes are known to be transcribed by RNA polymerase II unlike small noncoding RNAs like tRNAs , U6 snRNAs [73]. Intergenic miRNAs have shown to have been shown to have their own RNA polymerase II promoter while the transcription of intragenic miRNAs is mostly governed by the promoter of their parent gene (See section 2.6.2). In the present study, we primarily sought to identify the core RNA polymerase II promoter regions for WNT subgroup specific miRNAs namely miR-193a, miR-148a, miR-224 and miR-365; and the transcription factor binding sites with the help of four promoter prediction software programmes namely Proscan, Promoter 2, FirstExonFinder and CoreBoost_HM [109-112]. These software programmes are designed to predict putative promoter regions and transcription start sites (TSS) depending upon the density of the transcription factor binding sites (TFBS), presence of CpG island, first splice-donor sites and

histone modifications that mark genomic regions with active chromatin, while the transcription factor binding sites are predicted based on the sequence match found in the genomic region to the consensus binding site sequences. 5 kb genomic region upstream and 500bp genomic region downstream to pri-miRNA sequences were analysed for the presence of putative promoter region, putative transcription start sites and CpG Island. The presence of DNA binding sites for WNT signalling effecter transcription factor complex i.e. β–catenin-Tcf/Lef complex in the promoter region would suggest miRNA to be direct target of WNT signalling. The known direct targets of WNT signalling pathway include a potent transcription factor MYC, which itself activates transcription of number of different genes. Therefore, miRNA expression may also be regulated by MYC in which case it would be an indirect target of WNT signalling pathway. β-Catenin mediates transcriptional activation of its target genes by forming a complex with TCF/LEF1 cofactors which in turn bind to consensus DNA binding motifs (5' A/T A/T CAAAG 3') called as Wnt responsive elements (WREs)[113]. MYC has been shown to bind to two canonical E-Box sequences (5' CACGTG3') and (5'CATGTG3') and few non canonical E-Box sequences through hetero-dimerisation with MAX [114]. UCSC genome browser provides Chromatin immunoprecipitation-sequencing tracks for 161 transcription factors obtained from experiments performed in at least 9 different cell lines, under the ENCODE project (https://genome.ucsc.edu/) that includes MYC and LEF1 DNA binding sites. Presence of these consensus binding sites in miRNA promoters was screened with the help of UCSC genome browser along with manual search.

4.1.2 Evaluation of the promoter activity and its modulation by activated WNT signalling

Putative promoter regions of the miRNAs were PCR amplified from normal human genomic DNA (See section 3.21a) and cloned upstream luciferase cDNA in in a promoter less pGL3basic reporter vector (www.promega.com).

These promoter constructs were co-transfected with GFP expression vector where GFP fluorescence was used as transfection efficiency control. Luciferase activity thus normalised with GFP fluorescence was represented as promoter activity for the respective putative promoter region. To determine whether these miRNAs are direct or indirect targets of WNT signalling pathway, change in promoter activity was evaluated upon co-transfection of the promoter constructs with pcDNA3 expression vectors for mutant β-catenin or c-Myc. Serine at amino acid position 33, 37, 45 and threonine at 41 in case of this mutant β-catenin were mutated to alanine, making it resistant to GSK3β-mediated phosphorylation and in turn proteasomal degradation. This would result in increased nuclear accumulation of β-catenin and thereby enhance transcriptional activity of its target gene promoters. Treatment of HEK 293 cells transfected with promoter constructs with lithium chloride (LiCl), a known WNT signalling pathway agonist, was also used as an alternate approach to see the effect of WNT signalling activation on promoter activities of these constructs. Luciferase based TCF-reporter vector TOP Flash and FOP Flash served as positive and negative controls to check the efficacy of activation of WNT signalling through exogenous expression of mutant β-catenin or upon treatment of LiCl. TOP Flash vector possesses seven consensus Tcf/lef binding sites along with minimal TA viral promoter that drives luciferase expression, while FOP Flash vector possesses mutant Tcf/lef binding sites that cannot respond to WNT signalling activation. Increased expression of MYC upon transfection of MYC expression

vector in HEK293 cells was seen with the help of western blotting technique thereby validating efficacy of MYC expression vector (Fig 4.1D).

MiR-193a –

MiR-193a is an intergenic miRNA. Predictions of the putative promoter regions by all four prediction programmes were found to lie in the 1.2 kb region upstream to pri-miR-193a. While, ~1kb of upstream region was predicted to be CpG-island with more than 4 putative TSSs spread between -700 to -900bp. Four putative GC boxes at -872, -829, -613 and-136 were found, while no TATA box or downstream promoter element (DPE) was found. CpG islands that lack TATA box and DPE are typically known to show multiple GC boxes that are bound by SP1 transcription factors [115]and initiate transcription through multiple weak TSS spread over the region of 100bp. miR-193a hence was found to most likely possess such a CpG-island associated promoter. UCSC derived MYC Chromatin Immunoprecipitation (ChIP) sequencing tracks were found to recognise region upstream to pri-miR-193a (-511 to -943bp) with a single consensus E-Box motif or a DNA binding site for MYC transcription factor, present at -715bp. There were no consensus binding sites found for Tcf/Lef transcription factors in putative promoter region for miR-193a.Genomic regions upstream to pri-miR-193a covering -4169 to -599, -2330 to -158 and -1292 to -158 regions were PCR amplified and cloned in pGL3basic vector (Fig 4.1A). All of these regions showed significantly higher promoter activity ($p < 0.001$) than the empty vector i.e. pGL3b. Upstream region of -4169 to -599 was found to have highest promoter activity amongst other regions, which was ~8 fold higher than the vector control. Upstream regions of -2330 to -158 and -1292 to -158 showed 3.4 to 4.7 fold higher promoter activity than empty vector (Fig 4.1B). Upon co-transfection with MYC expression vector, all the three promoter constructs showed 2-4 fold increase in the basal promoter activity (Fig 4.1C). This effect could possibly be

mediated through MYC binding site present at -715bp. None of the promoter constructs showed any change in promoter activity (Fig 4.1C), upon co-transfection with mutant β-catenin or in presence of LiCl. Although the putative promoter region for miR-193a was not found to have consensus Tcf/Lef binding sites, the indirect activation of promoter through MYC which itself is a direct target of β-catenin-TCF complexes was not observed, upon exogenous expression of mutant β-catenin or treatment with LiCl. This may happen as the indirect effect of β-catenin-Tcf complex through MYC on target promoters will involve primarily the transcriptional activation of *MYC* gene and then its effect on its target gene promoters, which may need longer time than what is offered in short term transient transfection studies.

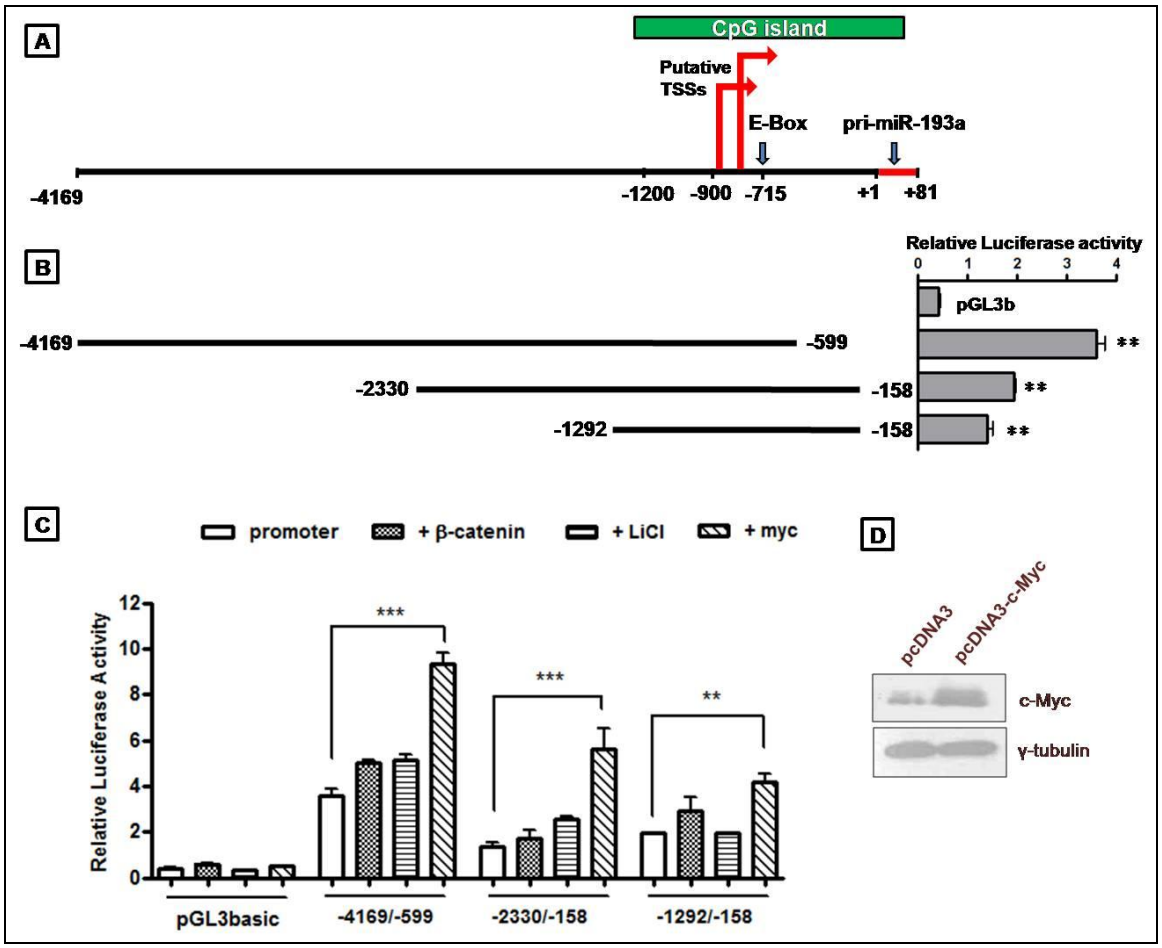

Figure 4.1: Evaluation of the promoter activity of the miR-193a putative promoter constructs and effect of WNT signalling activation and MYC expression on promoter activity

(A) Schematic diagram depicts ~ 4kb genomic region upstream to pri-miR-193a sequence highlighting key features like E-Box, putative TSSs and CpG Island relative to the first nucleotide of pri-miR-193a (+1).

(B &C) schematic diagram shows genomic regions cloned in luciferase reporter vector-pGL3b.Y-axis denotes basal promoter activities (Relative luciferase activity) of the three promoter constructs of miR-193a measured upon transfection in HEK293 cells either alone or along with mutant β-catenin or MYC expression constructs or upon treatment with LiCl. Significance of the difference was calculated by comparing relative luciferase activities of the promoter constructs with that of the pGL3b vector, in case of (B).** indicates $p < 0.001$ as compared to pGL3b. $$ indicates $p < 0.001$ and $$$ indicates $p < 0.0001$. All data points are indicated as mean ± standard error mean based on at least 3 experiments.

(D) Western blot analysis of HEK293 cells transfected with pcDNA3 (vector alone) or pcDNA3-MYC (MYC expression vector) probed for c-Myc and γ-tubulin, where γ-tubulin was used as a housekeeping control.

MiR-148a –

Analysis of 5 kb genomic region upstream and 500bp downstream to pri-miR-148a revealed presence of putative promoter region between -1070 to -1737 and a CpG-island that is spread across 1.5 kb region upstream to pri-miR-148a. Presence of histone modifications like H3K4 trimethylation and monomethylation concentrated in the 500bp region upstream to pri-miR-148a as shown by CoreBoost_HM programme, further suggested presence of active chromatin and in turn active transcription in the corresponding region. Lujambio *et al* have identified transcription start site for miR-148a -518 bp upstream of pri-miR-148a sequence by using 5'RACE (Rapid amplification of cDNA ends) in three cell lines derived from primary tumours belonging to colon cancer, melanoma and head and neck cancers[5]. Two consensus E-Box motifs were found to be present at -1334 and -2208 bp, while there were no Tcf/Lef transcription factor binding sites found in the putative promoter region. Hence -500 to -2000bp region that includes putative promoter region, CpG island and the probable enhancer regions specific to MYC transcription factor was analysed for its promoter activity. Genomic regions upstream to pri-miR-148a namely -3161 to -369, -1749 to -369 and -1310 to -369 that cover the putative promoter region and known TSS of miR-148a were cloned in pGL3b vector (Fig 4.2A,B). The putative promoter constructs (-1749 to -369) contains one MYC binding site or E-Box motif at -1334, while (-3161 to -369) contains one additional MYC binding site that is located at -2208. The genomic region construct for -1310 to -369 did not contain any of the MYC binding sites (Fig 4.2A, B). Promoter constructs corresponding to -3161 to -369 and -1749 to -369 showed almost equivalent basal promoter activity which was found to be 3.6 to 4.5 fold higher than that of empty vector. Promoter construct corresponding to the region -1310 to -369 showed only 1.8 fold higher basal promoter activity than empty vector (Fig 4.2B). This suggests that the region -1749 to -1310 is required

for the basal promoter activity, while the region -3161 to -1749 does not have significant effect on basal promoter activity owing to almost same promoter activities shown by -3161 to -369 and -1749 to -369 promoter constructs. Upon co-transfection with MYC expression vector, promoter constructs corresponding to -3161 to -369 and -1749 to -369 showed 2 fold increase in promoter activity than the respective basal promoter activities, while there was no change in the basal promoter activity of the region -1310 to -369(Fig 4.2C). This suggests that the MYC binding sites present in putative promoter region at -1334 and -2208 may be responsible for the induction in promoter activity seen upon MYC expression. Interestingly, MYC binding site/E-Box motif at -1334 has been reported to bind MYC in a study done using ChIP-PET sequencing on B lymphoid tumours [116]. Hence the MYC binding site at -1334 was mutated from CACGTG to CCCGGG in the putative promoter constructs of -3161 to -369 and -1749 to -369 by using the site directed mutagenesis. The basal promoter activities of MYC binding site mutant promoter constructs corresponding to -3161 to -369 and -1749 to -369 were found to be equivalent to their wild type counterparts (Fig 4.2C). However upon co-transfection with MYC expression vector, MYC binding site mutant promoter constructs failed to show any induction in the promoter activity unlike the parent constructs (Fig 4.2C), suggesting that the MYC binding site at -1334 is primarily responsible for mediating the induction in promoter activity by MYC.

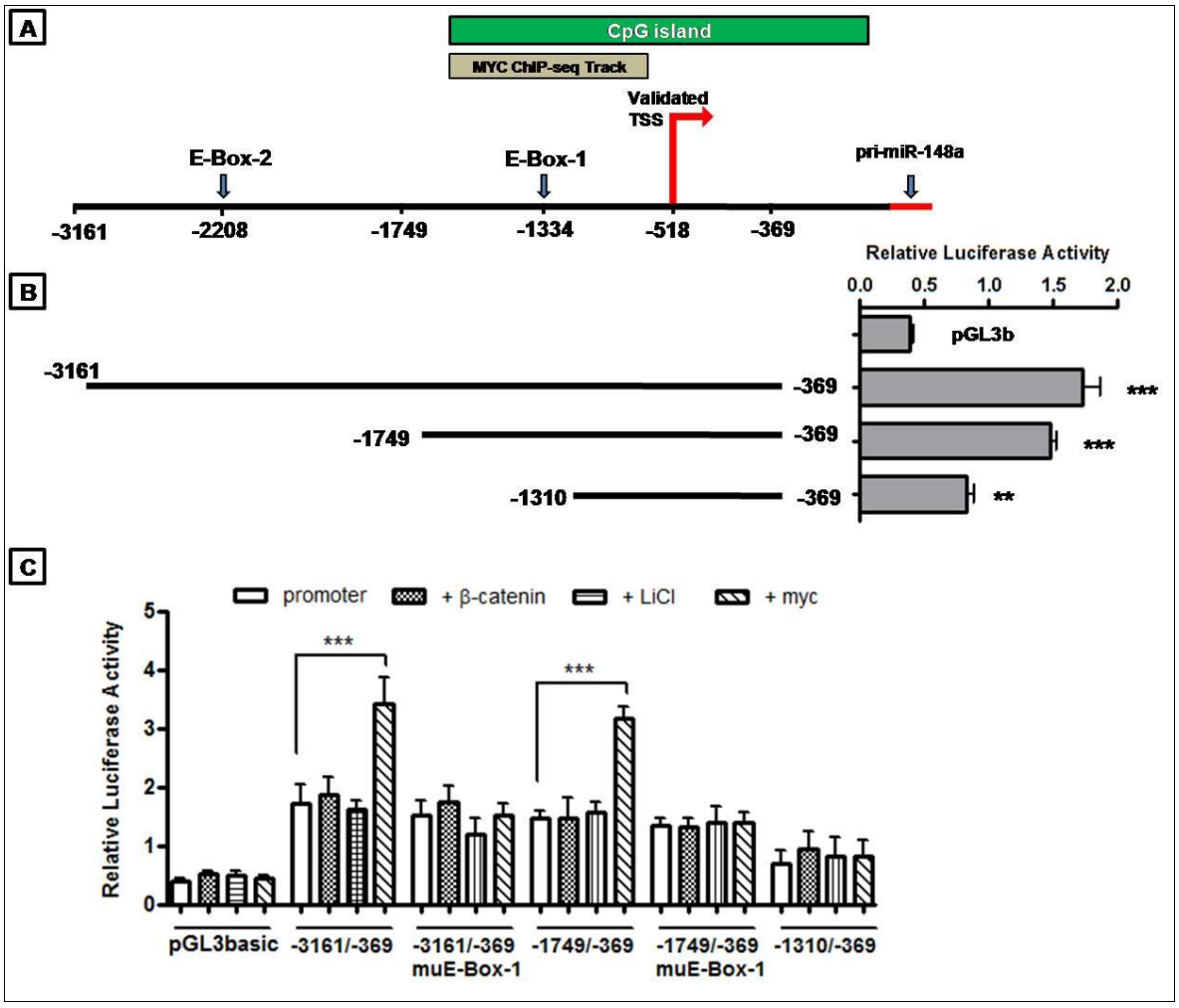

Figure 4.2: Evaluation of the promoter activity of the miR-148a putative promoter constructs and effect of WNT signalling activation and MYC expression on promoter activity
(A) Schematic diagram depicts ~ 3.1kb genomic region upstream to pri-miR-148a sequence highlighting key features like E-Boxes, validated TSSs, Anti-Myc ChIP-Seq track and CpG island relative to the first nucleotide of pri-miR-148a (+1).
(B&C) Schematic diagram shows the genomic region cloned in the two miR-148a promoter contructs in the luciferase reporter vector. Y-axis denotes basal promoter activities (Relative luciferase activity) of the indicated promoter construct of miR-148a as measured when transfected in HEK293 cells either alone or along with mutant beta-catenin or MYC expression constructs or on treatment with LiCl Significance of the difference was calculated by comparing relative luciferase activities of the promoter constructs with that of the pGL3b vector.muE-Box-1 represents mutant E-box-1. Significance of difference in case of (B) was calculated by comparing relative luciferase activities of putative promoter constructs with pGL3b. *** indicates $p < 0.001$. All data points are indicated as mean ± standard error mean based on at least 3 experiments.

MiR-224 (*GABRE*) –

MiR-224 is an intragenic miRNA and lies in intron 6 of GABRE gene. Earlier study from our lab shows that both GABRE and miR-224 are over-expressed in WNT subgroup

medulloblastomas [3].This suggests that like other intragenic miRNAs, miR-224 is most likely to be transcribed along with *GABRE*, its parent gene. Hence, genomic region 5kb upstream and 100bp downstream to known *GABRE* TSS (NCBI ID2564) was screened to check the presence of TFBSs for Tcf/Lef and/or MYC. Three consensus Tcf/Lef binding sites were found in 3.5 kb region upstream to known TSS for *GABRE* at -1210,-2634 and -3183bp positions, while no consensus E-box motif (MYC binding site) was found in this region.

Genomic regions of -3500 to +1 and -1320 to +1 upstream to *GABRE* gene were cloned in pGL3basic vector (Fig 4.3A, B). Both of these promoter constructs showed 50 fold higher promoter activities as compared to that of pGL3basic vector, indicating that the upstream region of -1320 to +28 can be called as the minimal promoter region (Fig 4.3B). Co-transfection of mutant β-catenin expression vector and TOP flash vector resulted in ~ 190 fold higher luciferase activity as compared to pGL3b or with TOP flash when transfected alone. Treatment of HEK293 cells transfected with TOP flash vector with lithium chloride (25mM), known WNT signalling activator also resulted in increase in luciferase activity almost equivalent to that seen in co-transfection with mutant β-catenin expression vector. On the other hand, FOP flash vector which contains mutant Tcf/Lef sites did not show any increase in luciferase activity upon its cotransfection with mutant β-catenin expression vector or in presence of lithium chloride treatment (Fig 4.3C). This suggested that treatment of cells with lithium chloride or exogenous expression of mutant β-catenin resulted in WNT signalling activation.

Both the promoter constructs corresponding to the upstream genomic regions -3500/+28 and -1320/+28, showed no change in the promoter activity upon co-transfection with mutant β-catenin expressing vector or in the presence of Lithium chloride, despite the presence of multiple Tcf/Lef binding sites (Fig 4.3C).

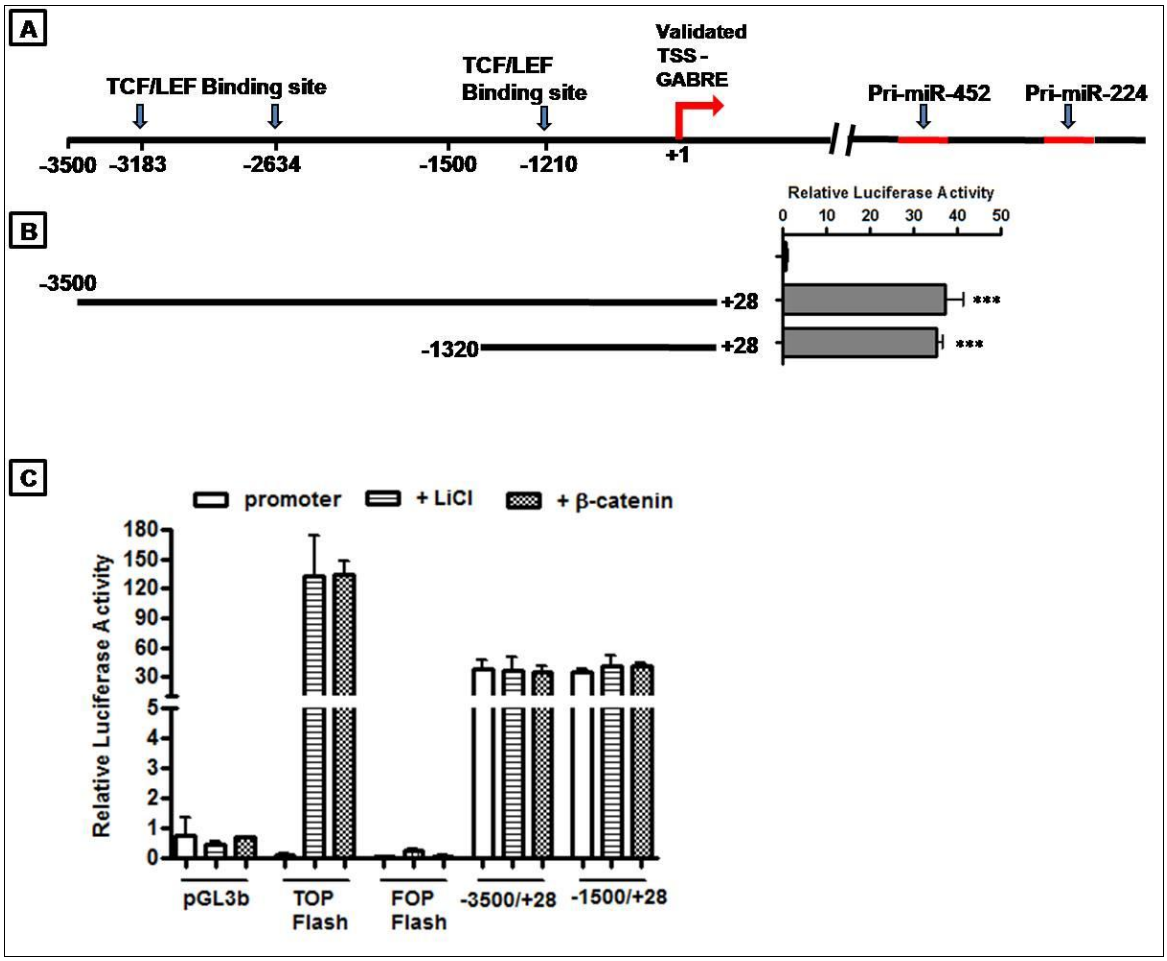

Figure 4.3: Effect of WNT signalling activation on basal promoter activities of GABRE promoter constructs.

(A) Schematic diagram depicts ~ 3.5kb genomic region upstream to known TSS of GABRE gene highlighting three consensus Tcf/Lef binding sites, validated TSS and miR-224-452 cluster lying in intron 6 of GABRE gene.

(B & C). Schematic diagram shows the genomic region cloned in the luciferase reporter vector pGL3b. Y-axis denotes basal promoter activities (Relative luciferase activity) of the indicated promoter construct of GABRE as evaluated on transfection in HEK293 cells either alone or along with mutant beta-catenin or on treatment with LiCl. Significance of the difference was calculated by comparing relative luciferase activities of the promoter constructs with that of the pGL3b vector. Significance of difference was calculated by comparing relative luciferase activity of promoter construct with pGL3b, *** indicates $p < 0.001$. All data points are indicated as mean ± standard error mean based on at least 3 experiments.

MiR-365-

Xu *et al* [117]have reported basal promoter activity in approximately 1.1 kb region upstream TSS reported by miRBase (www.miRbase.org) for the miR-193b-miR-365 cluster miRNAs. Two Tcf/Lef binding sites at -210 and -592 relative to TSS were identified, while there was no MYC binding site found in this region.

Genomic region of -1200 to +99, earlier reported as minimal promoter region for miR-365 was cloned in pGL3basic vector. This promoter construct showed significantly higher promoter activity (~5 fold) than pGL3basic vector (Fig 4.4A, B). However this promoter construct did not show any change in promoter activity upon co-transfection with mutant β-catenin expressing vector or in presence of Lithium chloride, known WNT signaling activator (Fig 4.4B).

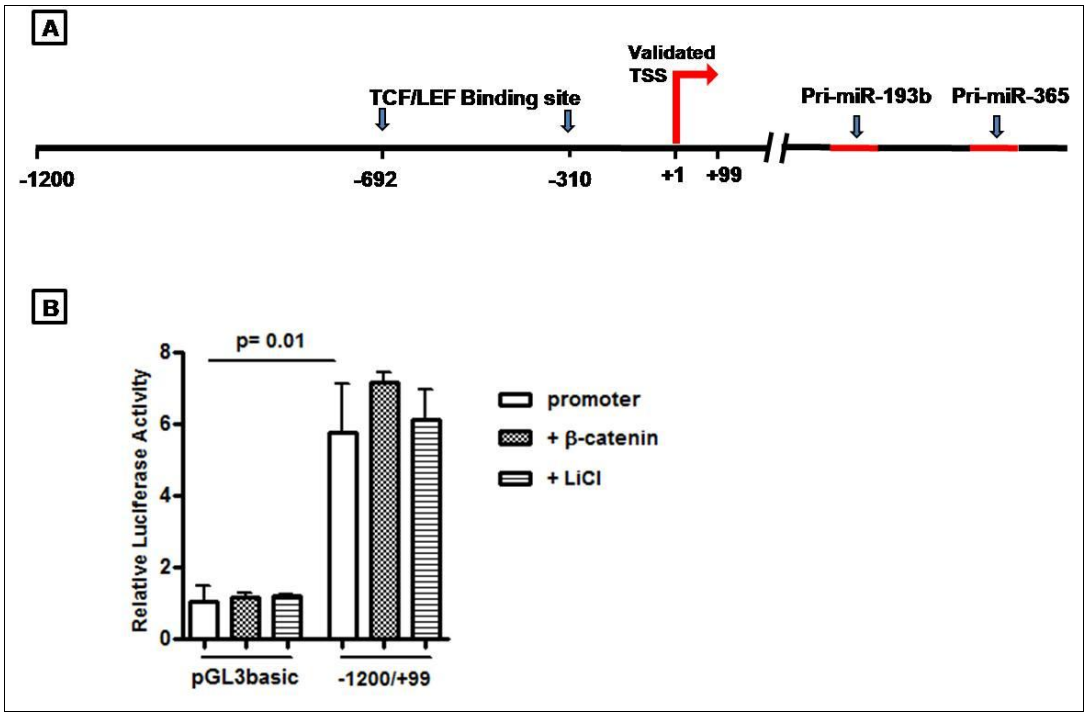

Figure 4.4: Effect of WNT signalling activation on basal promoter activity of miR-365 promoter construct.

(A) Schematic diagram depicts ~ 1.2 kb of the known promoter of miR-365 as reported by Xu *et al*., 2010, highlighting two consensus Tcf/Lef binding sites, validated TSS and miR-365-193b cluster.

(B) Y-axis denotes basal promoter activities (Relative luciferase activity) of the indicated promoter construct of miR-365 as evaluated on transfection in HEK293 cells either alone or along with mutant beta-catenin or on treatment with LiCl. Significance of the difference was calculated by comparing relative luciferase activities of the promoter constructs with that of the pGL3b vector. All data points are indicated as mean ± standard error mean based on at least 3 experiments.

4.1.3 Effect of inhibition of histone deacetylation and CpG methylation on miRNA expression in medulloblastoma cell lines

Based on aforementioned promoter activity studies, the putative promoter activities of miR-148a and miR-193a were found to be induced upon exogenous expression of MYC. Medulloblastoma cell lines belonging to Group 3 medulloblastoma, D425 and D341 are known to have MYC amplification, while expression of MYC is high in another such cell line, D283 [118, 119]. However, these cell lines show very low levels of miR-148a and miR-193a expression. MiR-148a and miR-193a are known to be downregulated as a result of promoter hypermethylation in various cancers. Similar to promoter CpG methylation, transcriptional repression can also happen as a result of histone deacetylation near TSSs through activity of histone deacetylases. Inhibition of Histone deacetylases (HDACs) through HDAC inhibitors has been reported to activate transcription of several genes in different tumour cell lines and has been said to alleviate DNA methylation mediated transcriptional repression[120, 121] Therefore, to identify if these two miRNAs are epigenetically downregulated in non-WNT medulloblastomas, effect of epigenetic modifiers on the expression of these miRNAs in medulloblastoma cell lines was evaluated. Medulloblastoma cell line D425 was treated with with trichostatin A (TSA) and valproic acid (VPA), two well known HDAC inhibitors at 200nM and 3-5mM concentrations respectively. Both the HDAC inhibitors TSA (200-400nM) and VPA (3-5mM) resulted in 120-400 fold higher expression of WIF1, a positive control[122] indicating successful HDAC inhibition (Fig 4.5A) VPA treatment significantly increased endogenous expression of miR-148a by 3.4 fold, while treatment with TSA resulted in modest but significant increase of ~ 1.8-2.4 fold in miR-148a expression (Fig 4.5B). Therefore the under-expression of miR-148a in medulloblastoma cells may be a result of epigenetic inactivation through histone deacetylation at its promoter. MiR-193a expression on the other hand, however was not found to alter upon treatment with TSA

or VPA, suggesting lack of histone deacetylation mediated transcriptional inactivation of miR-193a in medulloblastoma cells (Fig 4.5C)

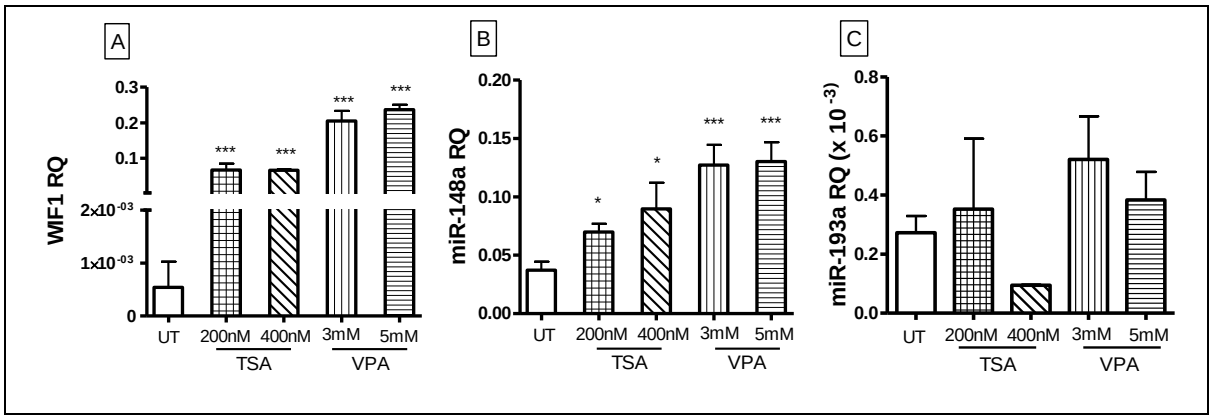

Figure 4.5: Effect of HDAC inhibition on miR-148a and miR-193a expression of D425 medulloblastoma cells.
Real time-RT PCR analysis of expression of *WIF1* (A), miR-148a (B), miR-193a (C) performed on D425 cells either untreated (UT) or treated with HDAC inhibitors Trichostatin A (TSA) and Sodium Valproate (VPA) at concentrations indicated. GAPDH or RNU48 were used as housekeeping control to normalise WIF1 or miR-148a and miR-193a expression respectively.
All the data points are based on three independent experiments. Significance of difference in the expression of the indicated gene/miRNA in the cells treated with TSA/VPA as compared to that in the control untreated cells was calculated by using student's t test. * indicates $p < 0.05$, ** indicates $p < 0.001$ and *** indicates $p < 0.0001$.

5'Aza 2'deoxycytidine (5'Aza-CdR) is used as DNA methylation inhibitor. However it was found to be toxic to D425 medulloblastoma cells at concentrations as low as 0.1 µM. Such a cytotoxic effect of 5'Aza-CdR has been noted on D283 cells, another semi-adherent cell line of medulloblastoma previously. [123]. Therefore to check whether CpG methylation plays role in transcriptional silencing of miR-148a, bisulphite sequencing of the genomic region upstream to pri-miR-148a sequence was performed. Previous studies in various cancers have shown that the CpG methylation of the region -50 to -400bp upstream to pri-miR-148a sequence (first nucleotide of pri-miR-148a taken as +1) brings about transcriptional silencing of miR-148a [5, 8, 124]. Hence upstream region of -300 to -61 was PCR amplified using bisulphite converted genomic DNA of medulloblastoma cell lines Daoy, D283, D425 and D341, and fresh frozen tumour tissues (Fig 4.6A, B). This genomic region includes 10 CpGs

out of which 8 could be faithfully sequenced in most of the samples. None of the 8 CpGs were found to be methylated in WNT tumour tissues. On the other hand, all the 8CpGs were found to be methylated in D283 and D425 medulloblastoma cell lines , while more than 90% of CpGs were found to be either completely methylated or hemi-methylated in Daoy and D341 medulloblastoma cell lines. More than 50% CpGs were found to be partially or completely methylated in 3 out of 5 Group 3 tumours and in 3 out of 3 Group 4 tumours. 25% CpG methylation was found in 2 out of 3 SHH tumours (Fig 4.6A,B). Thus the under-expression of miR-148a in medulloblastoma cell lines and tumour tissues belonging to non-WNT subgroups appears to be as a result of CpG methylation at its upstream genomic region. HDAC inhibitors like VPA and TSA are also known to induce demethylation although not complete at many promoters by either making DNA to be more accessible to DNA demthylases like DNMTs or through histone acetylation induced demethylation through proteins like MBD1[100]. Hence taken together, presence of CpG methylation at genomic region upstream to miR-148a as revealed by bisulphite sequencing in miR-148a under-expressing cell lines and induction of miR-148a expression upon TSA or VPA treatment to medulloblastoma cells, suggests presence of epigenetic inactivation of miR-148a in medulloblastoma tumours and cell lines belonging to non-WNT subgroups.

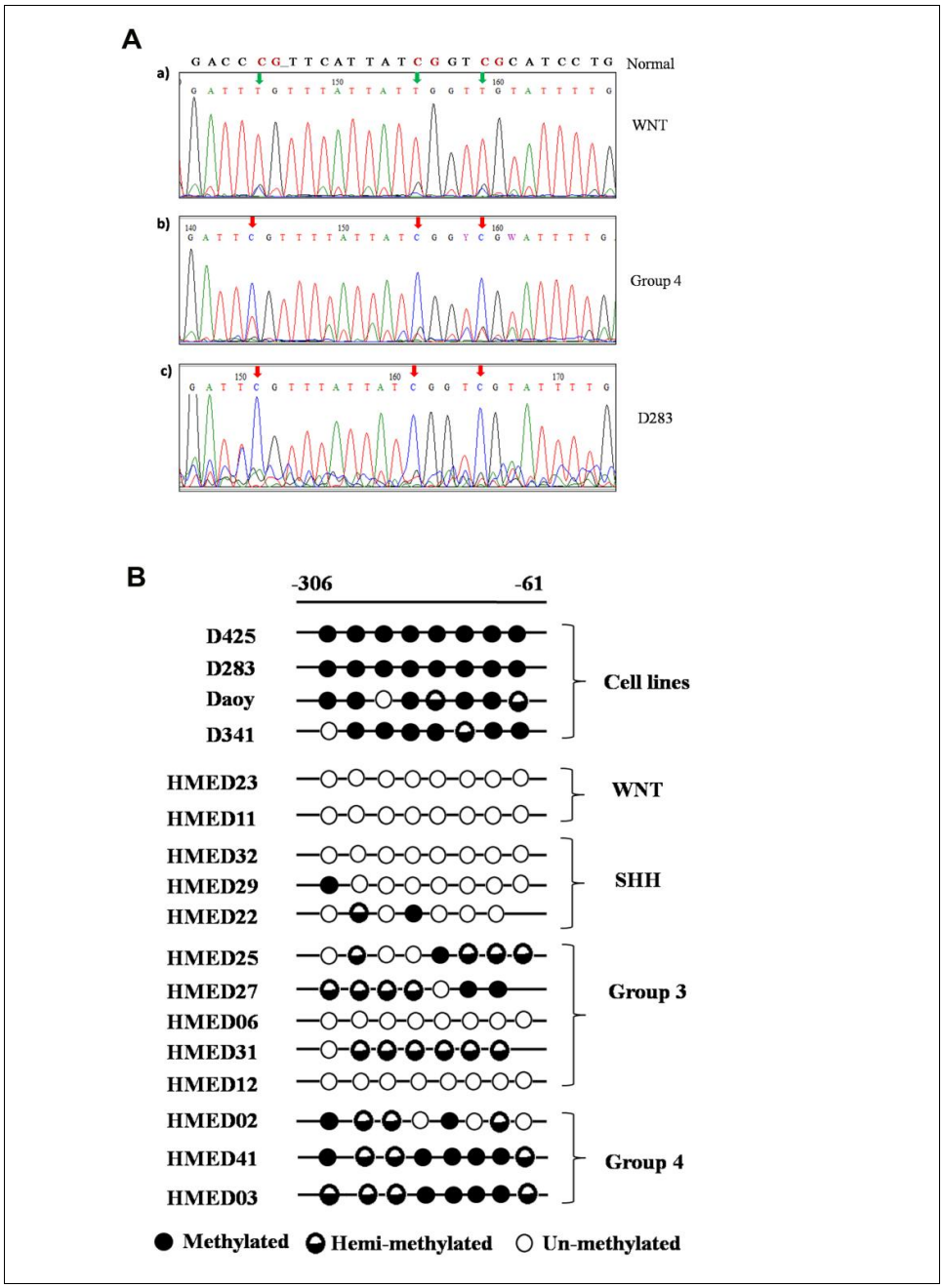

Figure 4.6: Bisulphite sequencing of CpG Island in the genomic region upstream to pri-miR-148a

Genomic region upstream to pri-miR-148a covering -306 to -61bp (first nucleotide of pri-miR-148a sequence taken as +1) was PCR amplified from bisulphite converted genomic DNA of indicated medulloblastoma cell lines and human medulloblastoma tissues (HMED) belonging to different subgroups and sequenced using forward primer. **(A)** Representative electrophoregrams showing nucleotide sequences of miR-148a CpG island region amplified from bisulphite treated genomic DNA belonging to WNT (a), Group 4 (b) medulloblastoma and D283 (c) medulloblastoma cell line. Normal indicates normal human genomic DNA sequence. Red arrows indicate Cs from CpGs retained after bisulphite conversion indicating those that are being methylated in template DNA, while green arrows indicate Cs from CpGs converted into T indicating their un-methylated status in the template DNA. (B) Composite of the CpG methylation profile of miR-148a (-306 to -61bp) upstream region of indicated medulloblastoma cell lines and tumour tissues (HMED) belonging to different subgroups. Each circle represents single CpG dinucleotide.

4.2 Role of WNT subgroup specific miRNA, miR-148a in modulating malignant behaviour of medulloblastoma cell lines –

MiR-148a is one of the up-regulated miRNAs in the WNT subgroup medulloblastomas, while it is known to be down-regulated in various malignancies like gastric cancer, pancreatic cancers etc due to CpG hypermethylation at its promoter [3, 5, 8]. MiR-148a has been shown to play tumour suppressive and anti-metastatic role in head neck cancers, breast cancer, pancreatic cancers and gastric cancers [5, 125]. WNT subgroup medulloblastomas have been reported to have excellent survival rates and lower incidences of metastasis, as compared to other subgroups. Therefore to understand the role of miR-148a in pathogenesis of medulloblastomas, effect of its expression on malignant behaviour of established medulloblastoma cell lines was investigated.

4.2.1 Expression of miR-148a across medulloblastoma cell lines, fresh frozen tumour tissues and FFPE tissues.

Previous work from our group has shown that miR-148a is one of the miRNAs over-expressed in WNT subgroup medulloblastomas. This study included 101 medulloblastoma tissues comprising of 42 fresh frozen and 59 FFPE tissues. In the present study, we further validated the above finding in a larger cohort of 141 medulloblastomas which included 40 FFPE tissues in addition to earlier 101 medulloblastomas. The medulloblastoma tissues were first classified into four molecular subgroups by a real time RT-PCR based assay as stated before [6]. This cohort included 30 WNT, 42 SHH, 31 Group 3 and 38 Group 4 tumours. We also included two normal developing (from the individuals less than one year old) cerebellar tissues and six adult (from the individuals >21 years of age) cerebellar tissues and three medulloblastoma cell lines namely Daoy, D425 and D283. MiR-148a expression was evaluated by real time RT PCR analysis. WNT subgroup medulloblastomas were found to over-express miR-148a by 7-16 fold as compared to other subgroup tumours, 10-20 fold as

compared to normal cerebellar tissues and 7-100 fold as compared to the medulloblastoma cell lines (Fig 4.7).

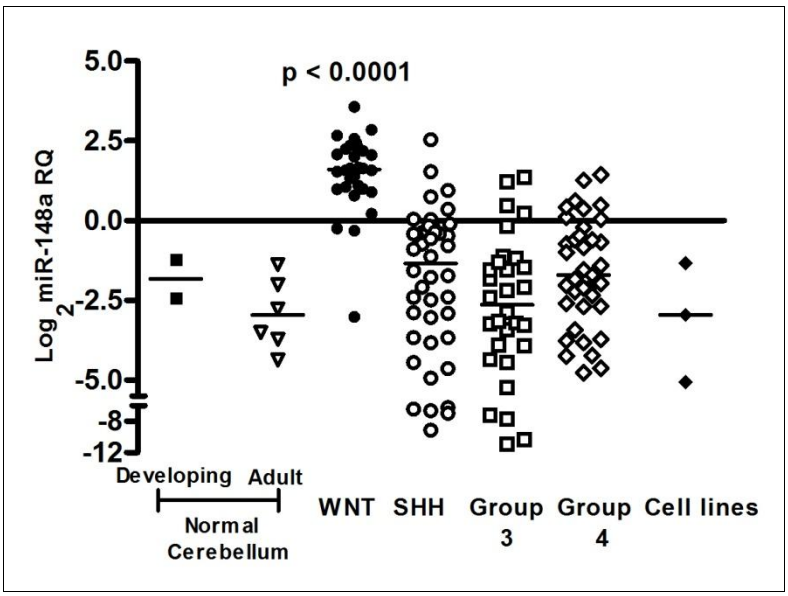

Figure 4.7: Scatter dot lot depicting expression levels of miR-148a across molecular subgroups of medulloblastomas as determined by real time RT-PCR assay.
Y-axis indicates miR-148a expression levels relative to RNU48, a housekeeping control.in Relative Quantity. p value indicates significance of the difference in miR-148a expression in the WNT subgroup as compared to the other subgroups, cell lines and normal cerebellar tissues.

4.2.2 Generation of stable puromycin resistant doxycycline inducible miR-148a expressing polyclonal populations of medulloblastoma cell lines

MiR-148a was expressed either in a stable inducible manner using pTRIPZ constructs carrying the miRNA coding region in three medulloblastoma cell lines Daoy, D425 and D283 or by transfecting miR-148a synthetic mimic in D283 cell line. Synthetic miRNA mimics are 20-23 nucleotides long double stranded oligonucleotides that mimic sequences of mature miRNAs. To express of miR-148a in a stable inducible manner in medullolastoma cell lines, doxycycline inducible lentiviral vector pTRIPZ was used. Genomic region encoding miR-148a along with an additional 200 bp flanking sequence on both 5 and 3' ends was cloned in the pTRIPZ lentiviral vector (Refer section 3.6).

Daoy, D425 and D283 medulloblastoma cells were transduced with the pTRIPZ lentiviral vectors expressing miR-148a at almost 90-100% transduction efficiency. The transduced cells were selected in the presence of puromycin to obtain pooled polyclonal populations that express the desired miRNA in a stable inducible manner. As a negative control, , the cell lines were transduced with an empty pTRIPZ vector or non-targeting (NT) shRNA carrying pTRIPZ lentiviral vector and these pooled puromycin resistant populations were were used as a negative control in all the experiments.

4.2.3 Effect of miR-148a expression on proliferative potential of medulloblastoma cell lines

Inducible stable polyclonal populations expressing miR-148a were generated by lentiviral mediated transduction of Daoy and D425 cells with the pTRIPZ-miR-148a construct. Two cell populations P1 & P2 in both the cell lines were independently transduced and selected in the presence puromycin. Doxycycline treatment of polyclonal population P1 of Daoy cells resulted in induction of miR-148a expression to a level (RQ: 2.0-4.0) comparable to that in the WNT subgroup tumour tissues while doxycycline induction of P2 polyclonal populations resulted in higher miR-148a expression in the range of RQ: 45-62 (Fig 4.8A). Doxycycline induced miR-148a expression resulted in 34 ± 1.7% and 42 ± 3.2 % growth inhibition of P1 and P2 population respectively as compared to their un-induced cells (Fig 4.9A,B). Doxycycline induction of P1 and P2 polyclonal populations of D425 cells resulted in the miR-148a expression levels in the range of 5-10 RQ (Fig 4.8B). MiR-148a expression was found to result in 61 ± 1.8% and 52 ± 5% growth inhibition in P1 and P2 polyclonal populations of D425 cells as compared to un-induced cells (Fig 4.9A, B). Thus, miR-148a expression significantly ($p < 0.0001$) inhibited growth of both the medulloblastoma cell lines studied.

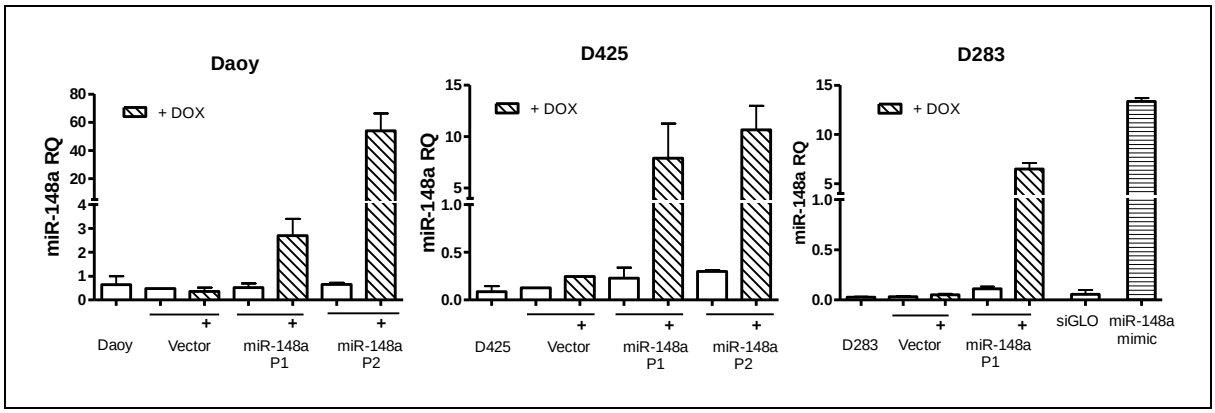

Figure 4.8: Expression levels of miR-148a in miR-148a expressing stable polyclonal populations, as determined by real time RT-PCR assay.

Y-axis indicates miR-148a expression in terms of Relative Quantity in the indicated medulloblastoma cell line and its polyclonal populations transduced with pTRIPZ control lentiviral vector (Vector) or pTRIPZ-miR-148a construct expressing miR-148a in doxycycline inducible manner (P1, P2). + indicates doxycycline induced.

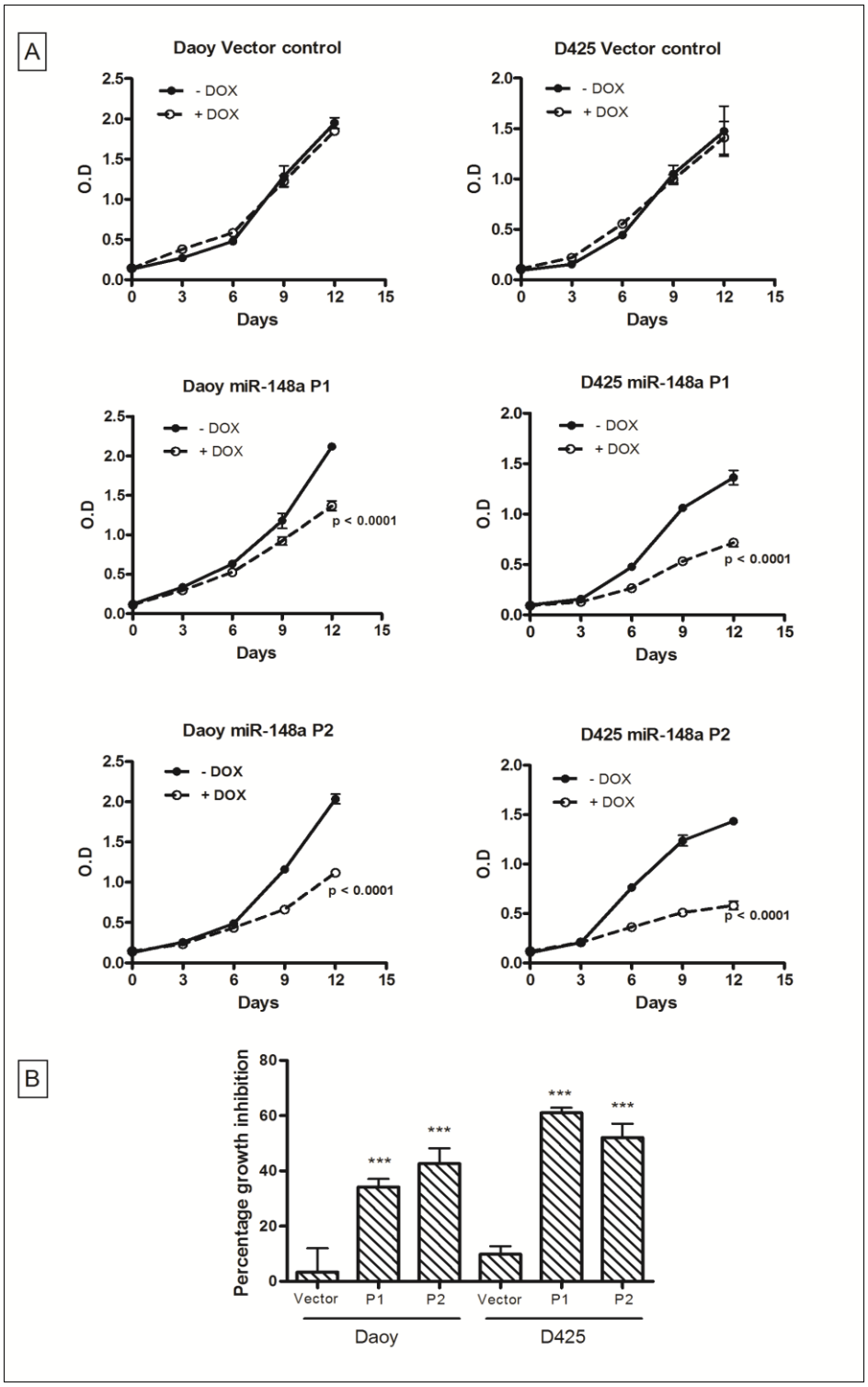

Figure 4.9: Effect of miR-148a expression on growth of medulloblastoma cell lines Daoy and D425 studied using MTT assay. (A) MiR-148a expressing polyclonal population (P1, P2) of Daoy or D425 cells were seeded in triplicate at a density of 500 or 2500 cells / well respectively in a 96 well micro-titre plate for MTT assay. The cells transduced with empty pTRIPZ vector served as a control. The O.D at 540 nm corresponds to the cell density. Each graph represents representative experiment. **(B)** Y axis denotes percentage growth inhibition obtained on doxycycline induction of the vector control and P1, P2 polyclonal population of the indicated cell line as judged by the MTT assay. All the data points are indicated as mean ± standard error mean based on at least three independent experiments.

4.2.4 Effect of miR-148a expression on anchorage independent growth and clonogenic potential of medulloblastoma cell lines

The anchorage independent growth potential of medulloblastoma cell line Daoy was analysed by the ability of cells to form colonies in soft agar, while the clonogenic potential was studied by plating cells in culture plates at low density. However as D425 cell line grows in semi-suspension manner, colony formation potential in soft agar essentially measures clonogenic potential of cells and not the anchorage independent growth per se. Doxycycline induced miR-148a expressing P1 and P2 polyclonal population of Daoy cell line showed 35.82 ± 3.2% and 41.6 ± 6.2% inhibition in colony formation as compared to un-induced control cells (Fig 4.10A).Doxycycline induction of miR-148a expression in P1 and P2 populations of D425 cells resulted in 30.8 ± 0.7% and 43.45 ± 3.1% inhibition in colony formation as compared to un-induced cells (Fig 4.10B). Doxycycline treatment in vector control cells of either Daoy or D425 was not found to have significant effect on colony formation in soft agar as compared to un-induced cells (Fig 4.10A, B). Clonogenic potential of Daoy P1 and P2 cells was found to significantly ($p<0.001$) reduce by 31 ± 2% and 33.4 ± 2.4% when compared to vector control cells (Fig 4.10C,D). Reduction in clonogenic potential (anchorage dependent) and anchorage independent growth potential of Daoy cells was found to be comparable indicating that miR-148a expression did not have significant effect on the anchorage independent growth but reduced clonogenic potential. To check whether miR-148a expression affects radiation sensitivity, clonogenic assay was performed by treating P1 and P2 populations of Daoy cells at 4Gy dose of radiation. Upon irradiation, doxycycline induced vector control cells and P1 or P2 population of cells showed 34-44% reduction in the number of colonies formed as compared to that in the doxycycline induced un-irradiated condition (Fig 4.10D). This suggests that miR-148a expression did not alter radiation sensitivity per se. However, combined effect of miR-148a expression and radiation brought 70-80% reduction in clonogenic potential of Daoy cells.

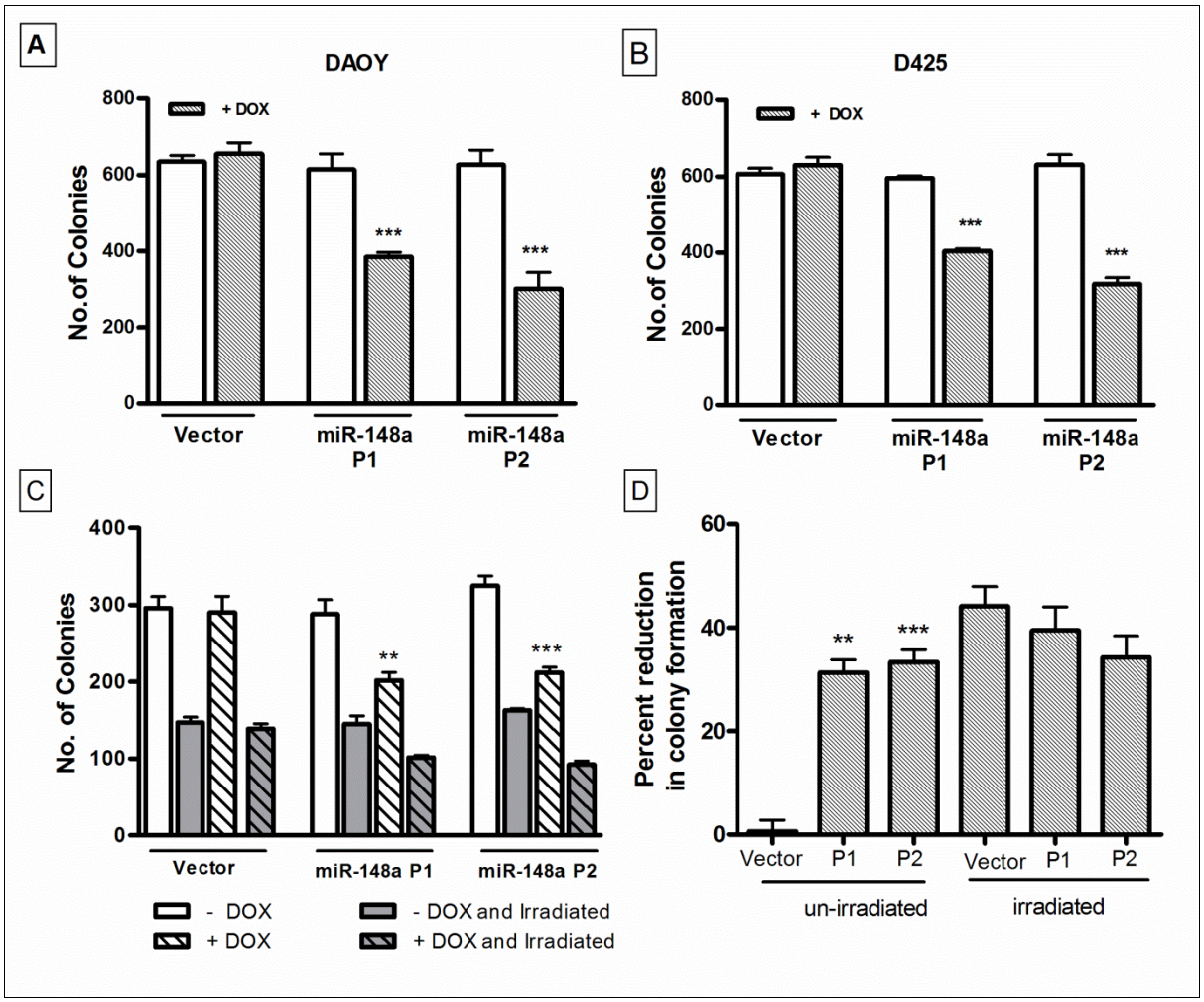

Figure 4.10: Effect of miR-148a expression on anchorage independent growth, clonogenic potential and radiation sensitivity of medulloblastoma cells.

Vector and P1, P2 population of Daoy and D425 cells grown in the presence or absence of doxycycline for 72 hr were seeded at a density of 7500 cells (Daoy) and 1000 (D425) per 35mm^2 culture dish for soft agar assay and 1000 cells (Daoy) per 55mm^2 culture dish for clonogenic assay.

(A, B) Y-axis shows the number of colonies formed in soft agar by vector and P1, P2 polyclonal populations of the indicated cell lines. The significance of the difference in soft agar colony formation observed on doxycycline induction of the polyclonal populations expressing pTRIPZ-miR-148a as compared to that observed in absence of doxycycline induction was determined by Student's t test. ** indicates $p < 0.001$ while *** indicates $p < 0.0001$ as determined using Student's t test.

(C) Clonogenic assay to determine clonogenic potential and radiation sensitivity at dose of 4Gy.Y-axis denotes number of colonies formed in clonogenic assay. The significance of difference in colony formation observed upon doxycycline induction of vector and P1, P2 Daoy cells as compared to that observed in absence of doxycycline induction is calculated by student's t test.

(D) Clonogenic potential was judged by percent reduction in the number of colonies formed on doxycycline induction of the vector control and P1, P2 population cells of Daoy cells, while radiation sensitivity was judged by percent reduction in the number of colonies formed on irradiation of doxycycline induced indicated population, in a clonogenic assay**.**

4.2.5 Effect of miR-148a expression on invasion potential of medulloblastoma cells

Effect of miR-148a expression on invasion potential was evaluated by studying the invasion of cells through matrigel coated membrane of transwell inserts. D425 cells were not found to have significant invasion ability through matrigel coated membranes. Hence, the effect of miR-148a expression on invasion potential was seen using two medulloblastoma cell lines Daoy and D283. Doxycycline treatment of P1 polyclonal population of D283 was found to show miR-148a expression in the range of 6-7, while D283 cells transiently transfected with synthetic miR-148a mimic was found to have miR-148a expression in the range of 12-13.5 RQ respectively (Fig 4.8). Polyclonal populations of Daoy and D283 cells were induced with doxycycline for 72 hr and allowed to invade for 36 and 56 hr respectively. Cells were labelled with Calcein AM, a fluorescent dye prior to the termination of the assay. After wiping the cells off the upper side of the membrane, fluorescence intensity of the lower side of the entire membrane was measured. The fluorescence intensity normalised to the initial number of cells seeded served as a quantitative assessment of the invasion potential. Doxycycline induced miR-148a expression in P1 and P2 populations of Daoy cell line resulted in 57.5 ± 1.4% and 74.7 ± 5.6% inhibition of invasion potential, while miR-148a expression in D283 cells either in stable doxycycline inducible manner or through transient transfection of synthetic mimic resulted in 40 ± 2% reduction in invasion potential (Fig 4.11A,B). Therefore miR-148a expression was found to inhibit invasion potential of medulloblastoma cell lines Daoy and D283.

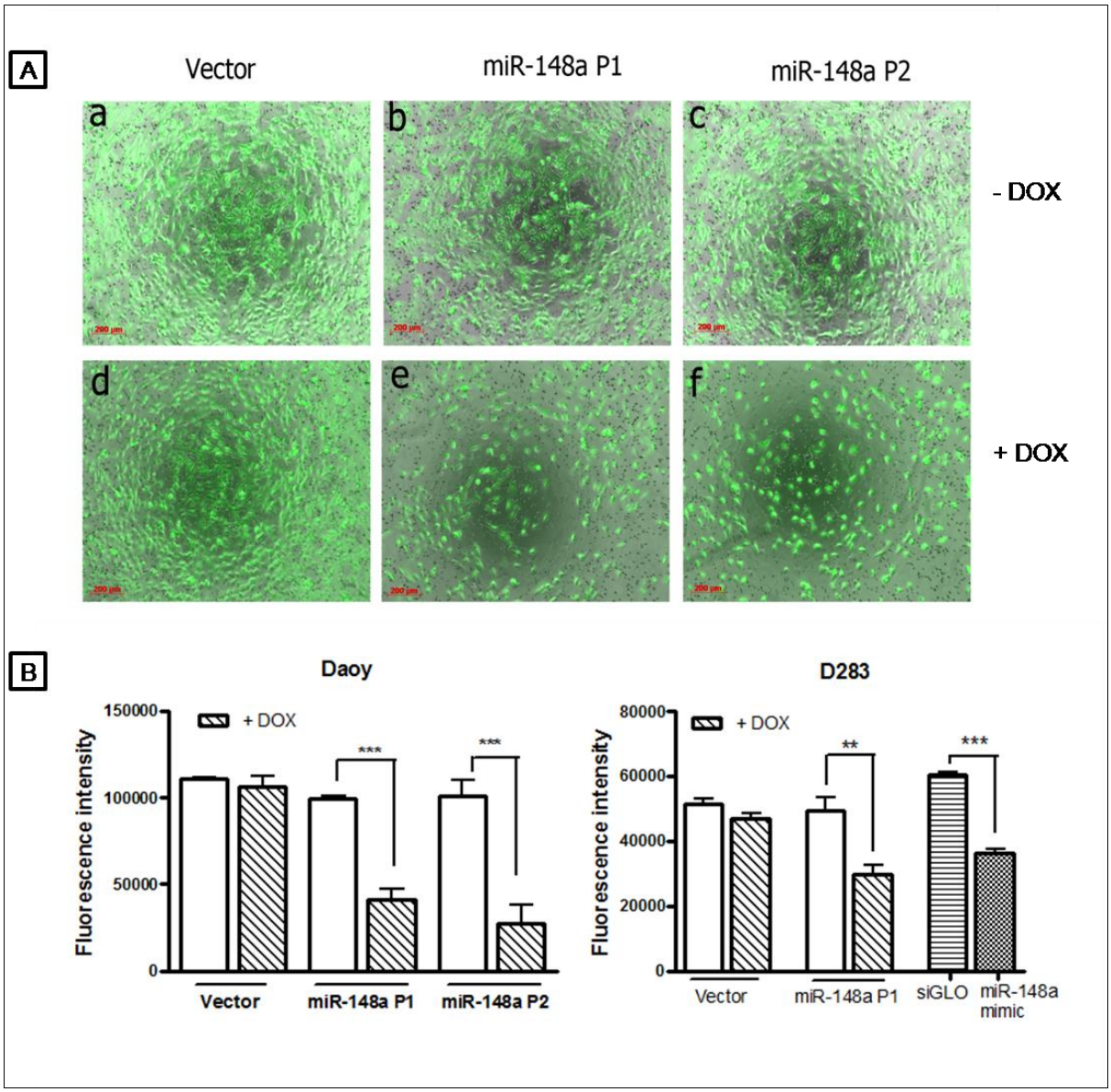

Figure 4.11: Effect of miR-148a expression on *in vitro* invasion potential of medulloblastoma cells

In vitro Invasion potential was determined by studying migration of the cells through matrigel coated 8-µm pore size transwell inserts.

(A) Representative microscopic images of calcein labelled vector, P1 and P2 polyclonal population of Daoy cells with (d, e, f) or without (a, b, c) doxycycline induction, invaded through matrigel coated membrane of transwell inserts.

(B) Y-axis denotes total normalised fluorescence intensity of the invaded cells on the lower side of the transwell membrane 36hr after seeding indicated polyclonal population of Daoy cells into upper chamber of the transwell insert with and without doxycycline induced miR-148a expression.

Total fluorescence intensity of the invaded cells was normalised to the total intensity of the initial cell number seeded of the indicated cell populations. Significance of differencebetween the normalised fluorescence intensities of doxycycline induced polyclonal populations expressing pTRIPZ-miR-148a as compared to that of doxycycline un-induced cells or that in miR-148a mimic transfected cells as compared to siGLO transfected D283 cells, was determined by student's t test. ** indicates $p < 0.001$ while *** indicates $p < 0.0001$.

4.2.6 Effect of miR-148a expression on in vivo tumourigenic potential of medulloblastoma cells

The tumourigenic potential of miR-148a expressing polyclonal population P2 of medulloblastoma cell lines Daoy and D425 was evaluated by generating sub-cutaneous xenografts in immune-compromised BALB/c Nude or NOD-SCID mice. Each mouse was injected subcutaneously with doxycycline induced P2 population of either Daoy or D425 cells in one flank and doxycycline induced vector control cells of respective cell line in the other flank. In vivo tumourigenic potential was quantitated by measuring area of subcutaneous tumour with the help of vernier calliper at regular intervals. Subcutaneous injection of 5×10^6 cells of Daoy or D425 cells resulted in formation of detectable tumours at 2^{nd} or 4^{th} week after injection respectively. Area of tumours formed by doxycycline induced miR-148a expressing P2 population of Daoy at 6^{th} week post-injection was found to be 0.39 ± 0.02 cm^2 which was significantly ($p < 0.001$) smaller than the area of tumours formed by doxycycline induced vector control Daoy cells (0.85 ± 0.07 cm^2) (Fig 4.12A, B). The tumours formed by doxycycline induced miR-148a expressing D425 cells were also found to be significantly ($p < 0.05$) smaller in size (2.8 ± 0.76 cm^2) than those formed by doxycycline induced vector control D425 cells (0.8 ± 0.3 cm^2) (Fig 4.12A, B).

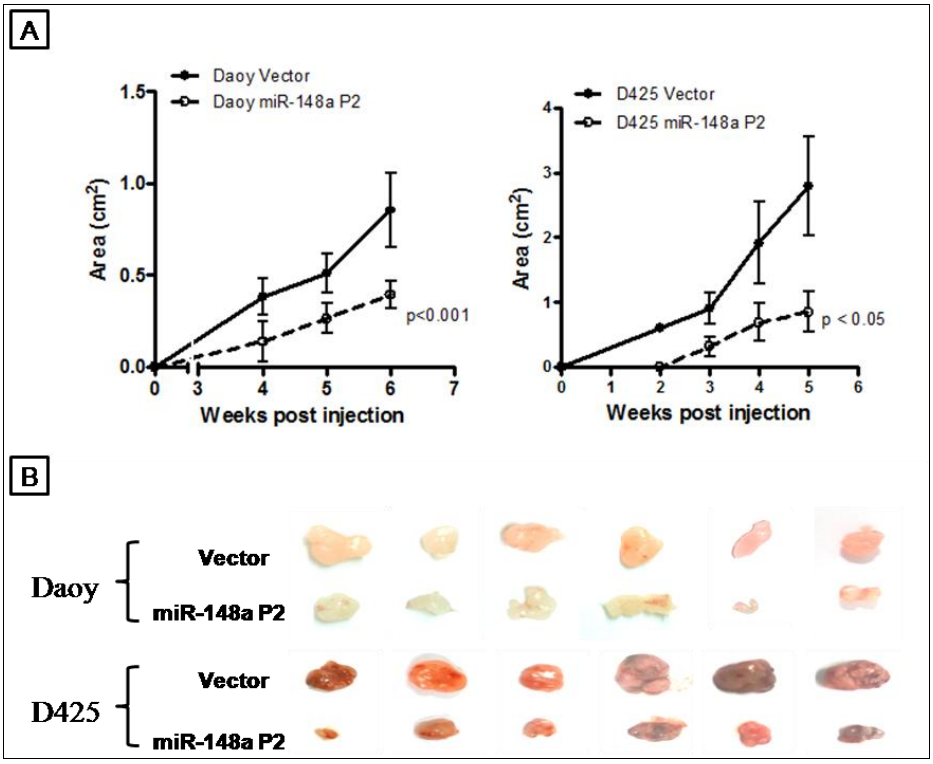

Figure 4.12: Effect of miR-148a expression on tumourigenic potential of Daoy and D425 studied using subcutaneous xenograft mouse model.
(A) Y-axis denotes cross sectional area of the subcutaneous tumours \measured at every week after injection of the indicated doxycycline induced polyclonal population P2 and vector control cells of Daoy or D425 in immunodeficient mice. Significance of the difference between the area of the subcutaneous tumours of vector control cells and that of miR-148a expressing polyclonal population at the week of sacrifice was determined using Student's t test. All the data points are based on experiments done on at least 6 animals.
(B) Representative images of subcutaneous tumours at the day of sacrifice (6^{th} week for Daoy cell line and 5^{th} week for D425 cell line).

Although subcutaneous xenografts in immunodeficient mice have been used as one of the model systems to study in vivo tumourigenic potential of medulloblastoma cell lines, orthotopic intracranial xenograft mouse models have been regarded as better mouse models as cells are injected in brain, the organ of origin that provides appropriate and clinically relevant environment. Further, because these models can be used to study not only tumourigenic potential but also invasion and metastasis at relevant site. However, intracranial xenograft establishment eliminates the ability to monitor tumour growth through direct measurement, such as by use of vernier calipers, the utilization of non-invasive imaging for

assessing tumour burden is therefore needed. Here we utilized the bioluminescence imaging where in cells were engineered to express firefly luciferase (FLuc), then are injected intracranially in cerebellum and tumour growth is monitored by capturing the total luminescence emitted at regular intervals of time by administering D-luciferin, a substrate for luciferase intraperitonially. The normalised luminescence represented as average radiance reflects tumour growth at particular time point in the study. Stable inducible miR-148a expressing D283 polyclonal population P1 was engineered to constitutively express FLuc by transfecting it with pcDNA3.1 vector expressing FLuc followed by selection in the presence of neomycin. These cells ($2x10^5$ cells in 5 µl volume) with or without doxycycline induction were then injected in cerebellum of BALB/c Nude mice with the help of stereotactic injection apparatus. Mice were fed with doxycycline through the 5% sucrose containing water to the group of mice injected with doxycycline induced cells. Tumour growth was monitored at 1^{st} and 4^{th} week post injection and relative increase in average radiance from 1^{st} week to 4^{th} week was represented as measure of tumour growth. A significant reduction ($p < 0.001$) was seen in the average radiance of tumours formed on doxycycline induction of miR-148a in D283 cells as compared to un-induced cells, indicating inhibition in tumour growth by miR-148a expression (Fig 4.13A,B). Therefore miR-148a expression was found to inhibit tumourigenic potential of three medulloblastoma cell lines Daoy, D425 and D283 in either subcutaneous xenograft mouse model or intracranial xenograft mouse model system.

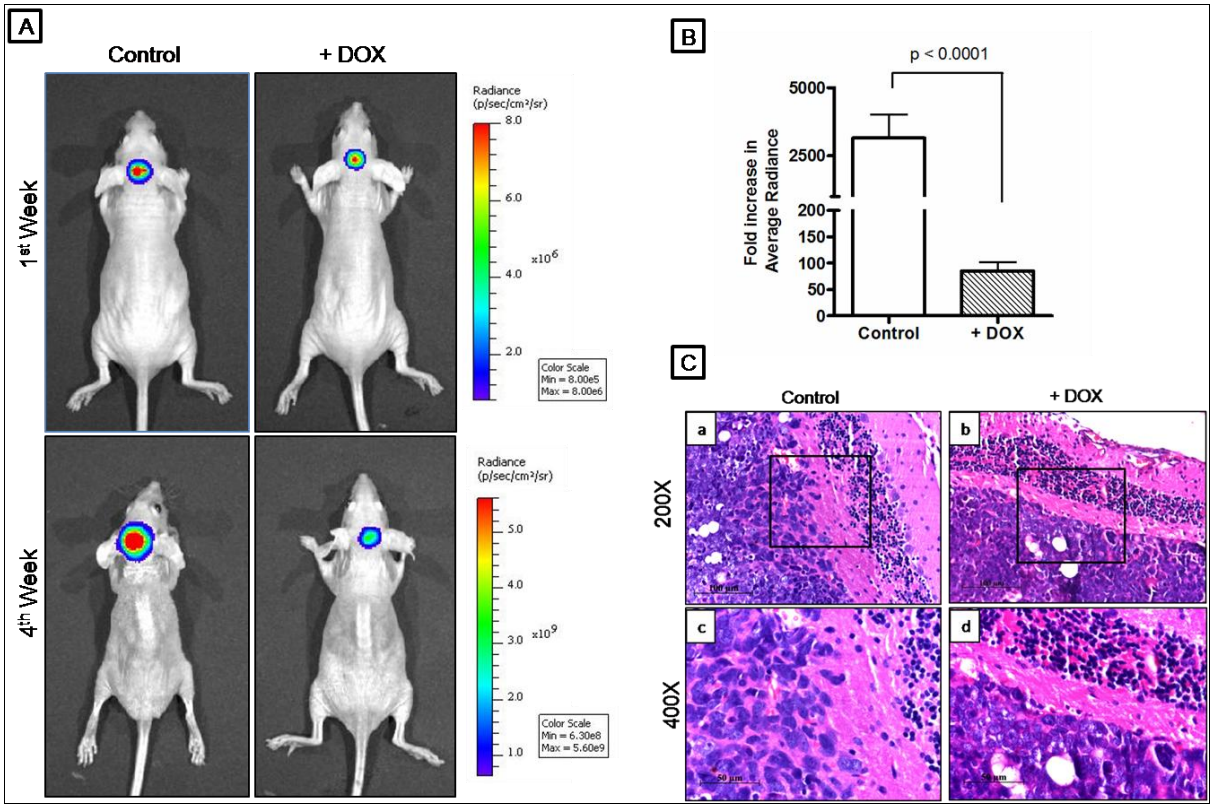

Figure 4.13: Effect of miR-148a expression on tumourigenic potential and *in vivo* invasion potential of D283 cells studied by intracranial xenograft mouse model.
(A) Bioluminescence images of nude mice orthotopically injected with D283 stable polyclonal population P1 expressing miR-148a upon doxycycline (DOX) induction and, firefly luciferse under CAG promoter. The images were captured on 1st and 4th week after the injection.
(B) Y axis shows relative fold increase in the average radiance on 4th week as compared to that on 1st week after injection of D283 cells P1 population with (+DOX) or without doxycycline induction (Control) in 7 mice each.
(C) Representative photographs of hematoxylin-eosin stained paraffin sections of the orthotopic xenografts of control and doxycyclineinduced (+ DOX) D283 cells P1 population. The area marked with rectangle shows invading margins of the tumour cells in the control and doxycycline induced miR-148a expressing cells. c & d show magnified images (400 X) of the invading margins indicated by the rectangles in a & b.

The whole brains of the intracranial xenografted mice were removed at the time of sacrifice and were fixed in 10% formalin. These were then cut at midline in sagital fashion and embedded in paraffin. Serial sagital sections were then taken and H&E staining was performed to confirm the location of tumour in cerebellum and to determine the effect of miR-148a on *in vivo* invasion. On evaluation of H&E stained sagital sections of intracranial tumours, it was found that the tumour margin of doxycycline induced miR-148a expressing D283 cells in cerebellar cortex was much more cohesive than in the case of the un-induced

cells which showed loosely spaced cells at the tumour margin (Fig 4.13C). This suggests that expression of miR-148a did affect the *in vivo* invasive properties of D283 cells.

4.2.7 Effect of miR-148a expression in tumour angiogenesis

MiR-148a expression has been reported to inhibit *in vitro* angiogenesis in breast cancer cells[126]. To see if there is any effect of miR-148a expression on angiogenesis *in vivo*, CD31 staining was performed on subcutaneous tumours formed by miR-148a expressing Daoy cells and vector control Daoy cells. CD31 is a known marker for endothelial cells and immunohistochemical staining for CD31 is commonly used to investigate extent of angiogenesis in tumour tissue sections [127, 128]. Immunohistochemical staining for CD31 was evaluated by pathologist in a blinded study and was represented in terms of macrovascular Density (MVD) which is defined by three factors – (1) number of hotspot areas (areas with maximum number of vessels positive for CD31, (2) total number of CD31 positive vessels in top five fields at 400X magnification and (3) grade of angiogenesis falling in four categories as negative, low, moderate and high. Number of hotspots areas and total number of vessels in top five fields were significantly reduced ($p<0.05$) in tumour sections corresponding to miR-148a expressing Daoy cells compared to that of vector control cells (Fig 4.14A,C,D). Tumour sections with high grade of angiogenesis were seen only in the vector control tumours (~20%), while none of the sections from vector control tumours were graded as negative. On the other hand, ~25% of the tumour sections corresponding to miR-148a expressing Daoy cells were graded as negative while none of the tumour sections showed high level of angiogenesis (Fig 4.14B). These findings suggest that miR-148a expression significantly reduced angiogenesis in subcutaneous tumours of Daoy cells.

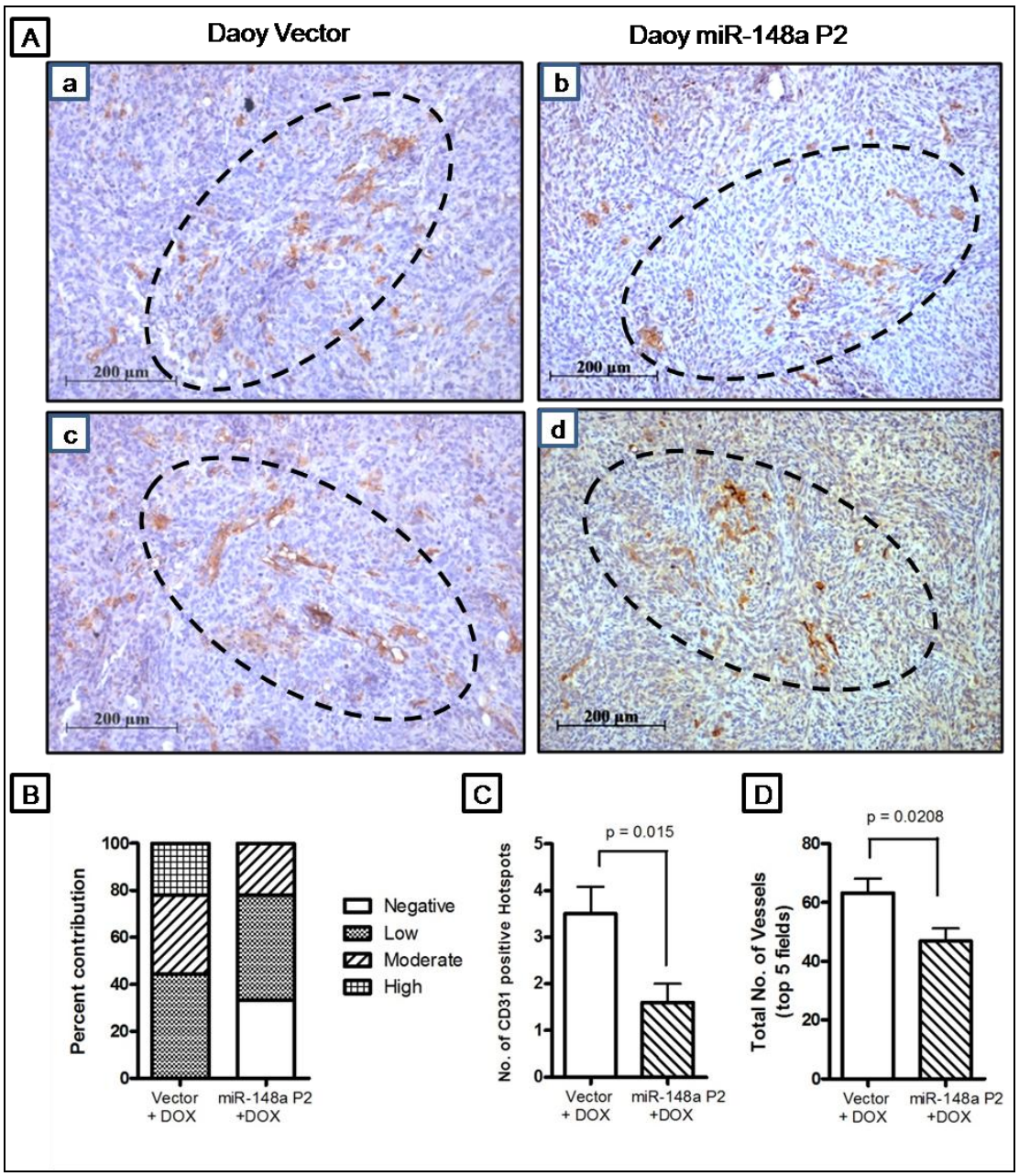

Figure 4.14: Effect of miR-148a expression in tumour angiogenesis studied using immunohistochemical staining for CD31, endothelial cell marker.
(A) Representative microscopic images showing CD31 staining in sections of subcutaneous tumours formed by doxycycline induced vector control (a & c) or P2 population (b & d) of Daoy cells in immune-compromised mice. Black dotted circles indicate hotspot regions in each section. **(B)** Immunohistochemical staining for CD31 is scored subjectively by pathologist through observation of entire section at 5X and 10X into four categories namely negative, low, moderate and high. Y-axis denotes percent contribution of these four categories in vector control or P2 population tumours.
(C) Y-axis denotes number of CD31 positive hotspots (spotted under 100X magnification) in entire section of either vector control or P2 population tumour tissue sections.
(D) Y-axis denotes total number of vessels counted in 5 fields per section with highest number of vessels. Significance of difference between the number of hotspots or total number of vessels between tumour sections belonging to vector control cells and that of miR-148a expressing P2 population cells is determined using Student's t test. All the data points are represented as mean± standard error mean based on experiments performed on tumour sections from 10 animals in each group.

4.2.8 Identification of protein coding gene targets of miR-148a

MicroRNAs function by targeting complementary sequences in 3'Untranslated regions (UTRs) of mRNA transcripts and prevent protein synthesis by inhibiting translation or by inducing target mRNA degradation[129]. Considering the extent of seed sequence match, conservation of seed sequence across species, free energy requirements and target site accessibility, computational target prediction programmes predict the probable mRNA targets for a particular miRNA [80]. In the present study, mRNA target identification for miR-148a was performed using online target prediction tools like targetscan (www.targetscan.org), PicTar (pictar.mdc-berlin.de/), miRANDA (www.microrna.org). The list of predicted mRNA targets of miR-148a was screened to identify the genes that (1) are expressed in normal cerebellum and medulloblastoma tissues and (2) have any known involvement in regulating migration or invasion properties of cells. 3' UTRs of gene targets namely *ARHGAP21, B4GALT5, DNMT1, ROCK1, MMP15, NRP1, ROBO1* and *TMSB10* were cloned downstream to luciferase cDNA in a 3'UTR luciferase reporter vector. Luciferase activity of protein lysates of 293T cells transfected with 3'UTR-luciferase reporter construct with or without exogenous expression of miR-148a expression was evaluated. Luciferase activity of 3'-UTR luciferase reporter constructs for the genes *NRP1, ROCK1, DNMT1 and MMP15* was reduced by 30-40% when co-transfected with miR-148a expression vector as compared to that in the absence of exogenous miR-148a expression (Fig 4.15A). *ROCK1* and *DNMT1* are two known targets of miR-148a and have known role in modulating invasion and tumourigenesis in vivo [124, 130-133]. *NRP1* is one of the novel gene targets of miR-148a identified in the present study and is of particular importance as it is known to play role in multiple signalling pathways that promote growth, invasion and metastasis[134]. Therefore, we further confirmed NRP1 to be miR-148a target by mutating the miR-148a binding site to abolish the binding and checking its luciferase activity. Four nucleotides from seed sequence

in miR-148a binding site from NRP1 3'UTR luciferase reporter construct was mutated from CACT to TCTA with the help of site directed mutagenesis PCR (Fig 4.15B). Upon miR-148a expression, no change in luciferase activity of the mutant construct was seen, unlike parental construct validating NRP1 as miR-148a target (Fig 4.15A). NRP1 as a miR-148a target was further validated by using western blotting (4.15 C, D)

Protein expression of ROCK1, DNMT1 and full length form of NRP1 was found to be reduced in miR-148a expressing Daoy and D283 polyclonal populations and D283 cells transiently transfected with miR-148a mimic than their un-induced control cells as studied by western blotting analysis (Fig 4.15C, D, E, F).

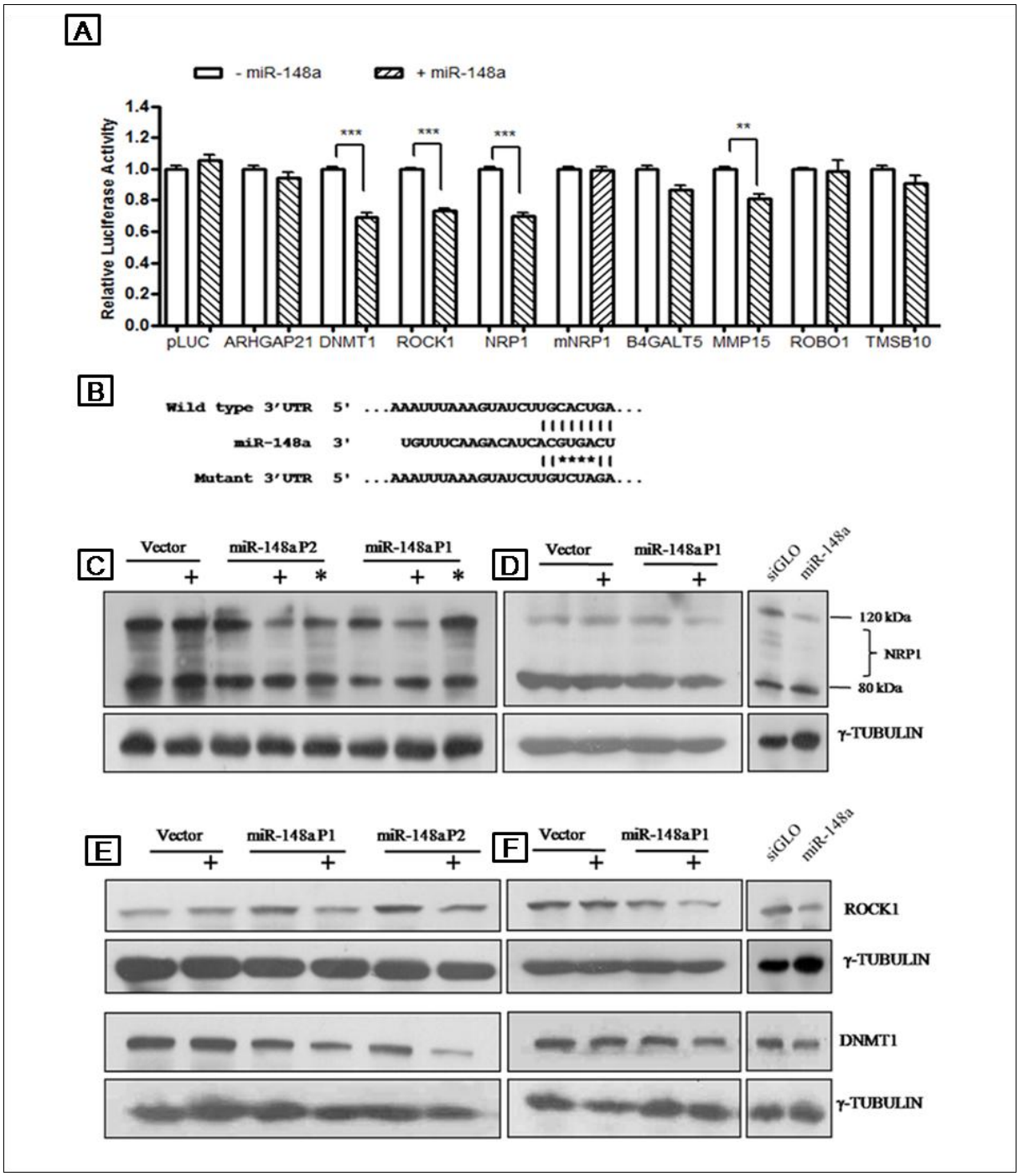

Figure 4.15: Identification of miR-148a target genes

(A) Y-axis denotes Luciferase activity of HEK293 cells transfected with the construct having 3'-UTR region of the indicated gene cloned downstream luciferase cDNA in pcDNA 3.0 vector and EGFP expressing vector with or without pcDNA 3.0 construct expressing miR-148a. The luciferase activity is expressed relative to the GFP fluorescence

(B) Schematic diagram shows miR-148a target site in NRP13'-UTR and position of the mutations (indicated by asterisk) introduced in the target site by site directed mutagenesis.

Western blot analysis shows the expression levels of NRP1 **(C, D)**, ROCK1 and DNMT1 protein **(E, F)** in stable polyclonal populations of Daoy (C, E) and D283 (D, F) cells with (+) or without doxycycline induction of miR-148a expression and in D283 cells transiently transfected with control siGLO or miR-148a mimic **(D, F).** γ-tubulin was used as a loading control. +: Doxycycline induction; * indicates exogenous expression of NRP1 in doxycyline induced cells.

Western blotting analysis for NRP1 detected two isoforms of NRP1, one full length isoform with molecular weight of ~ 120 kDa and other with molecular weight of ~ 80 kDa. Unlike full length isoform, protein levels of ~ 80 kDa isoform were found to be un-altered irrespective of miR-148a expression. To confirm this finding further, we used glioma cell line U373 which has higher expression of full length NRP1 than observed in Daoy and D283. U373 cells were transduced with pTRIPZ-miR-148a viral particles and were selected in the presence of puromycin to generate stable doxycycline inducible miR-148a expressing polyclonal populations. Protein levels of full length NRP1 was found to be reduced in doxycycline induced miR-148a expressing U373 polyclonal populations P1 and P2 as compared to the un-induced cells, while the levels of ~80 kDa NRP1 isoform were unaltered (Fig 4.16D). This suggested that the ~80 kDa isoform is indeed non-responsive towards miR-148a expression. NRP1 gene encodes multiple alternately spliced transcripts. 5882bp CCDS7177 transcript encodes 923 amino acid long full length protein whose 3'-UTR contains the miR-148a target site (ncbi.nlm.nih.gov/gene). Shorter CCDS31179, CCDS31180 transcripts encode 609 and 644 amino acid long proteins respectively, that lack the 3'-UTR as well as the transmembrane domain. These isoforms encode soluble NRP1 forms that have been shown to act as antagonists of the full length membrane bound NRP1 protein [135]. Since miR-148a targets NRP1 3'UTR, it is likely that the ~80kDa NRP1 isoform is not targeted by miR-148a as it lacks 3'UTR. To confirm this possibility, real time RT-PCR analysis was performed using primers for total *NRP1* mRNA expression (all known NRP1 isoforms) as well as primers specific for the 3'- UTR of the full length isoform and primers specific for the transmembrane (TM) region. Relative quantities of NRP1 as estimated using the 3'-UTR specific primers or TM domain specific primers was found to be almost 50% of the total NRP1 expression level in both Daoy and D283 cell line (Fig 4.16A, B). The protein levels of the 120 kDa and ~80 kDa NRP1 isoforms in the endogenous cell were determined

by intensity measurements of bands corresponding to proteins of interest using ImageJ software. The protein levels of 120 kDa were also estimated to be about 50% and 30% of the total NRP1 protein levels in Daoy and D283 cell line respectively (Fig 4.16C). Therefore, miR-148a appears to target only the full length NRP1 isoform and not the 80 kDa isoform as it lacks the 3'-UTR.

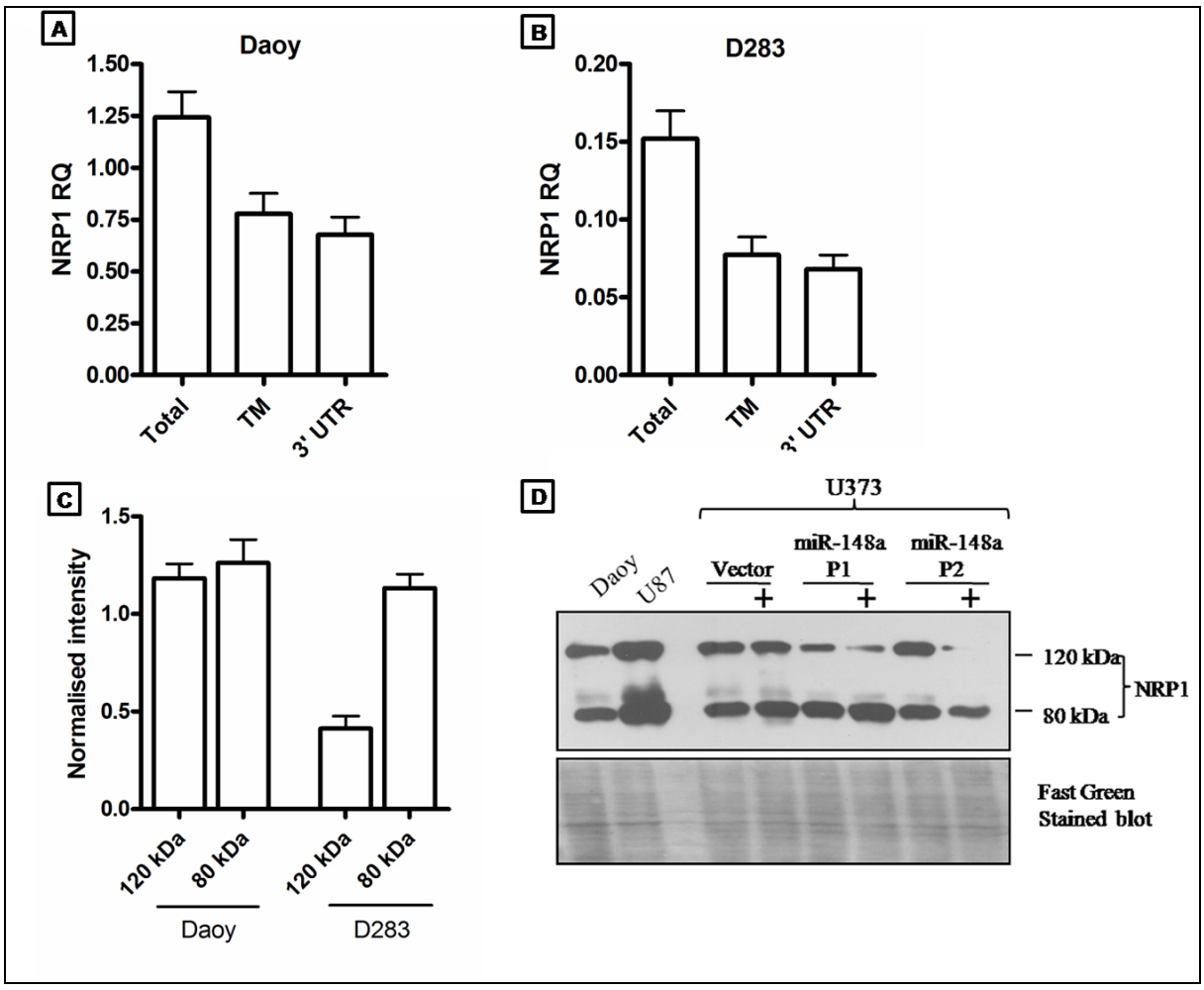

Figure 4.16: The relative levels of NRP1 mRNA and protein levels in Daoy and D283 cells.
(A, B) NRP1 mRNA levels estimated by real time RT-PCR using NRP1 specific primers to amplify all known transcripts (total), primers specific for Transmembrane domain (TM) and primers specific for the 3'-UTR region of the full length NRP1 transcript in Daoy and D283 cells.
(C) Relative proportion of NRP1 protein levels corresponding to the full length 120 kDa and shorter isoform 80 kDa in Daoy and D283 cells as estimated by image analysis of the western blots **(D)** separating total protein extracts of the cell lines and probed with anti-NRP1 antibody.

4.2.9 Effect of Exogenous expression of NRP1 on invasion potential and in vivo tumourigenicity of miR-148a expressing Daoy cells

To further study role of NRP1 downregulation in miR-148a mediated inhibition of tumourigencity and invasion potential experiments were carried out to restore NRP1 expression in miR-148a expressing medulloblastoma cells. Two miR-148a expressing polyclonal populations of Daoy P1 and P2 were transfected with pPGK-NRP1-Neo, a NRP1 expression vector and were selected in the presence of neomycin to achieve stable NRP1 over-expression. Unlike endogenous NRP1, exogenous expression of NRP1 is independent of miR-148a mediated inhibition as the NRP1 cDNA from the expression vector lacks 3'UTR and in turn the miR-148a binding site. Western blot analysis of doxycycline treated exogenously NRP1 expressing cells confirmed the over-expression of full length NRP1 protein expression in exogenously NRP1 expressing Daoy cells of polyclonal populations P1 or P2 (Fig 4.16C). Invasive potential of exogenously NRP1 expressing Daoy cells of polyclonal populations P1 or P2 was studied by matrigel based in vitro invasion assay. Exogenously NRP1 expressing polyclonal populations upon doxycycline induced miR-148a expression showed marginal reduction (~30%) in invasion unlike parental population which showed 60-70% reduction in invasion potential (4.17B, C). Thus restoration of NRP1 expression did rescue the reduction in invasive potential brought about by miR-148a. However, NRP1 expression alone could not rescue the miR-148a mediated inhibition in invasion entirely, indicating the possible role of ROCK1 and DNMT1 as well in regulating the invasion potential of these cells. Further, miR-148a expressing Daoy cells exogenously expressing NRP1 and doxycycline treated vector control cells were injected subcutaneously on each flank of immunodeficient mice to study the effect of NRP1 over-expression on in vivo tumourigenic potential of these cells. Medulloblastoma cells expressing both miR-148a and exogenous NRP1 formed tumours of size comparable to that of the control vector cells

(4.18A, B), indicating that the exogenous NRP1 expression could rescue the reduction in tumourigenicity brought about by miR-148a expression.

Thus downregulation of NRP1 was found to play major role in miR-148a mediated reduction of invasion and tumourigenic potential of medulloblastoma cells.

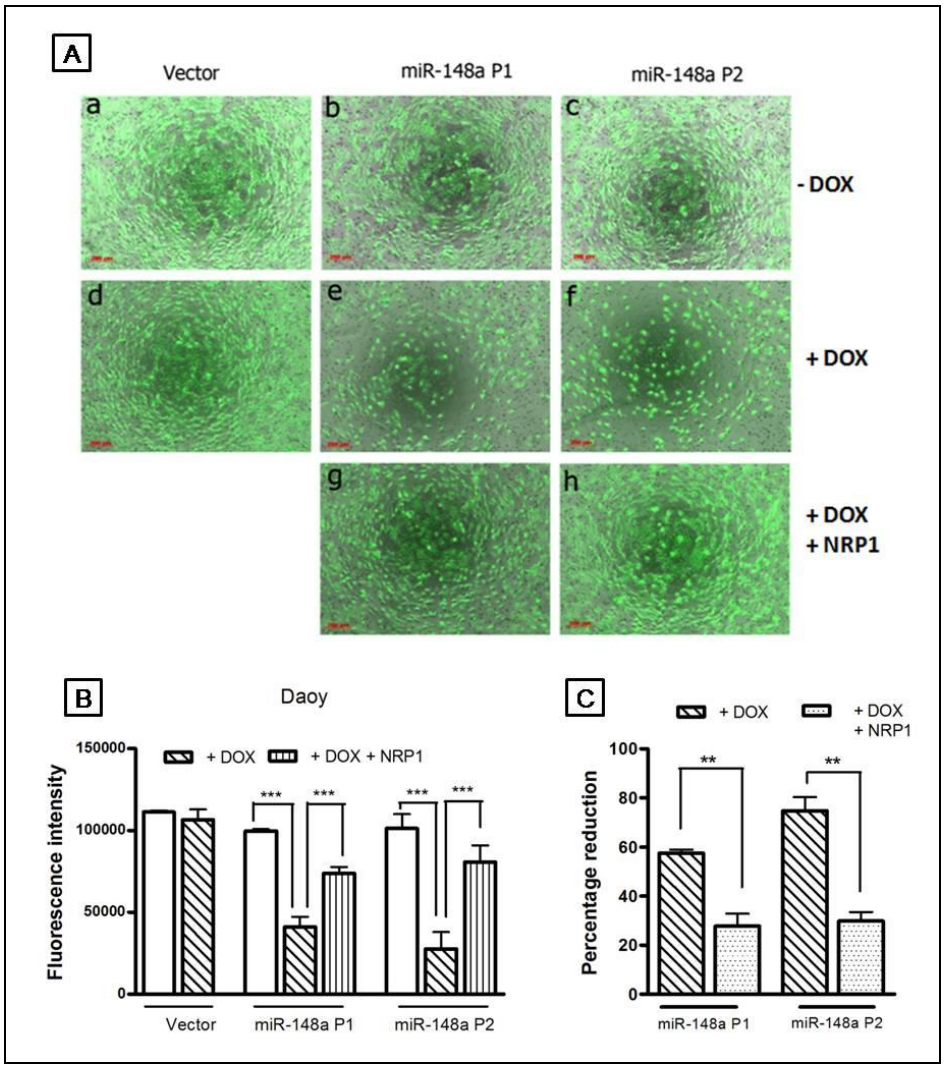

Figure 4.17: Effect of Exogenous expression of NRP1 on invasion potential of miR-148a expressing Daoy cells

(A) Representative images of the Calcein, AM labelled Daoy cells on the lower side of the transwell chamber membrane 36 h after seeding the indicated polyclonal populations of Daoy cells onto the transwell insert, with (d, e & f) or without (a, b & c) induction of miR-148a expression and after restoration of NRP1 expression in doxycycline induced cells (g, h).

(B) Y axis denotes the total fluorescence intensity of the invaded cells normalised to the total intensity of the initial cell number seeded of the indicated cell populations.

(C) Y axis indicates the percent reduction in the fluorescence of the invaded cells of the indicated stable polyclonal populations on doxycycline induction (+DOX) of Daoy P1 and P2 population cells with (+NRP1) or without restoration of NRP1 expression. ** indicates $p < 0.001$; *** indicates $p < 0.0001$.

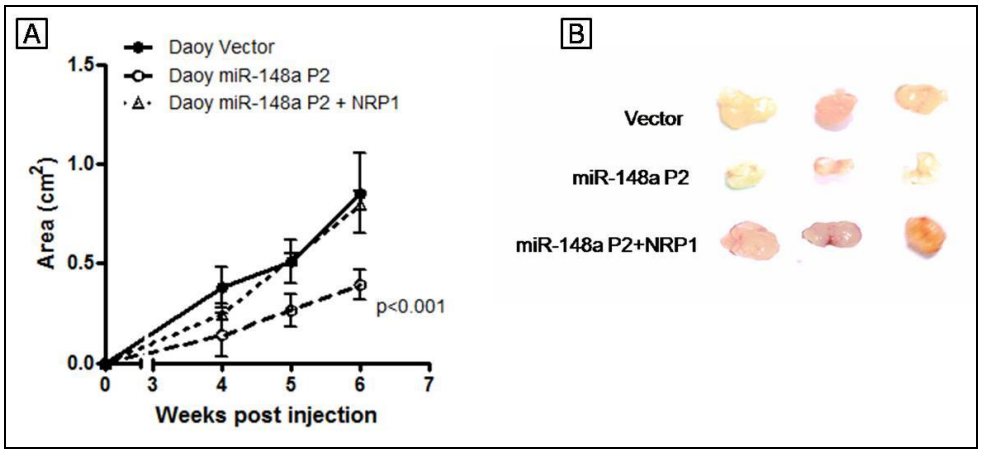

Figure 4.18: Effect of Exogenous expression of NRP1 on *in vivo* tumourigenicity of miR-148a expressing Daoy cells
(A) Y-axis denotes cross sectional area of subcutaneous tumours measured at every week after injection of doxycycline induced vector control cells and polyclonal population P2 of Daoy with or without exogenous NRP1 expression. Significance of the difference in the area of subcutaneous tumours of vector control cells and that of polyclonal population at the week of sacrifice was determined, using Student's t test. All the data points are based on experiments done on at least 6 animals.
(B) Representative images of the subcutaneous tumours at the day of sacrifice (6^{th} week).

4.2.10 NRP1 expression in medulloblastoma tumour tissues and its correlation with molecular subgroups and survival

To study the NRP1 expression in medulloblastoma tumour tissues, immunohistochemical analysis with anti-NRP1 antibody was performed in 93 medulloblastoma FFPE tissues. These medulloblastoma tissues were subgrouped into the four molecular subgroups by using Real time-RT PCR assay as mentioned before[6] and included 20 WNT, 30 SHH, 19 Group 3 and 24 Group 4 tumours. Staining for NRP1 was scored by neuropathologist on the basis of intensity of staining and percentage of positively stained area, into four categories as (1) 'negative' for complete absence of staining, (2) 'low' for weak intensity and focal positive (~10-20% cells positive) areas, (3) 'moderate' for moderate intensity and more than or equal to 50% positive area and (4) 'high' for high intense staining in more than 80% of area. This analysis was done as a blinded study where-in the neuropathologist was unaware of the subgroup of the tumour. Majority of the WNT medulloblastomas (75%) showed no expression of NRP1, consistent with the up-regulation of miR-148a seen in this subgroup.

Group 3 tumours which are known to have the worst prognosis and highest incidence of metastasis showed the least percentage of tumours (23%) lacking the NRP1 expression and was the only subgroup in which tumours (6%) showed high expression of NRP1 (Fig 4.19; 4.20A).

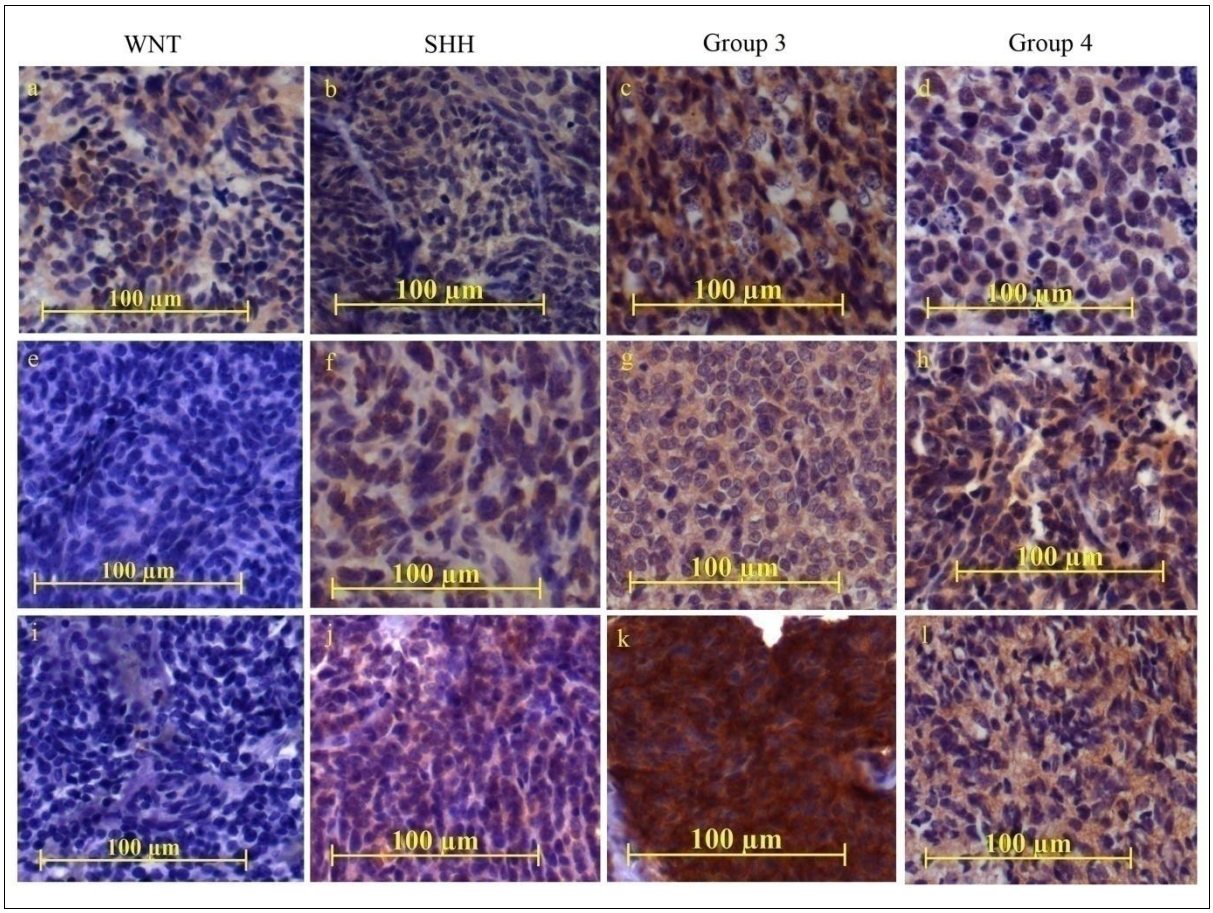

Figure 4.19: Immunohistochemical analysis of NRP1 expression in medulloblastoma tumour tissues.
NRP1 expression was studied in FFPE tissue sections belonging to the four molecular subgroups (WNT, SHH, Group 3, Group 4). The staining was scored as 'negative' for complete absence of staining, 'Low' for weak intensity and focal positive (~10-20% cells positive) areas, 'Moderate' for moderate intensity and more than or equal to 50% positive area while, 'High' for high intense staining in more than 80% of area. Representative images of NRP1 staining in the medulloblastoma tissues scored as negative (e, i), low (a, b, d, f, h), moderate (c, g, j, l) and high intense staining (k) respectively.

The overall survival was available for total of 62 medulloblastoma tissues. The patients who expired within the first month after surgery were excluded from the analysis as the death in peri-surgery period could be due to surgery related causes. The patients were segregated in two groups based on NRP1 expression. 'NRP1 High' expressing group included tumours

with high or moderate NRP1 expression upon immunohistochemical analysis, while 'NRP1 Low' group included tumours with negative or low level of NRP1 expression. The overall survival was found to be significantly (p=0.034) lower in 'NRP1 High' group than the 'NRP1 Low' group (Fig 4.20B). The hazard ratio of 6.06 for 'NRP1 High' group against 'NRP1 Low' group indicated that the 'NRP1 High' group of patients have significantly higher risk than the 'NRP1 Low' group of patients reiterating the importance of NRP1 as a marker for prognostication in medulloblastoma.

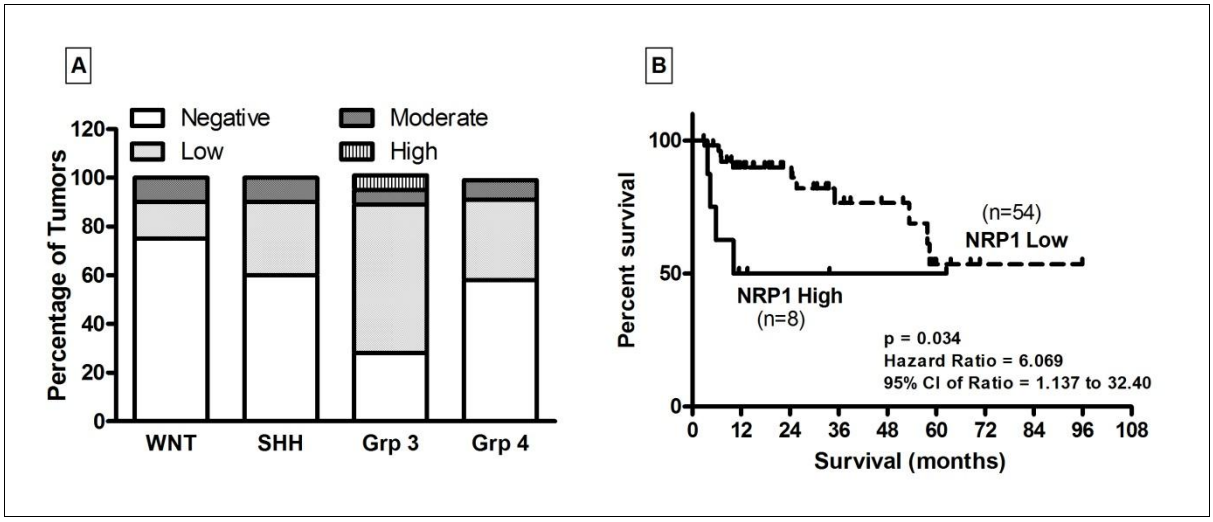

Figure 4.20: Expression of NRP1 across the four molecular subgroups of medulloblastomas.

(A) Percentage distribution of medulloblastoma tissues having NRP1 expressed scored as negative, low, moderate or high is shown across the four subgroups of medulloblastomas.
(B) Kaplan Meier survival analysis of 62 medulloblastoma patients segregated into two groups based on NRP1 expression. "NRP1 low" group includes medulloblastoma tissues with no or low NRP1 expression while "NRP1 high" group includes tumour tissues with moderate or high NRP1 expression.

Chapter 5: DISCUSSION

Medulloblastoma, the most common malignant pediatric brain tumour is known to be composed of four molecularly distinct subgroups. These subgroups not only differ in the expression of protein coding genes and miRNAs but also in demographics, clinical presentation and, most importantly prognosis. WNT subgroup is regarded as subgroup with most favourable prognosis, while Group 3 as the worst prognosis subgroup. The other two subgroups i.e. SHH and Group 4 have an intermediate prognosis. Therefore, understanding the pathogenesis of these tumours becomes important as it may tell us about molecular basis underlying the differential response from different subgroup tumours to the treatment and thereby further evolve into discovery and development of newer and more efficient targeted therapeutic strategies.

MiRNAs act as post transcriptional regulators of gene expression and have been shown to play either oncogenic or tumour suppressor roles in different malignancies. With the potential of targeting many genes at a time, miRNAs can control many different cellular processes via targeting diverse set of genes from different signalling pathways. Aberrant expression of miRNAs has been shown in medulloblastomas and with subgroup specific nature of their expression, miRNAs are most likely to contribute to underlying biology of these tumours. WNT subgroup medulloblastomas that are known to have excellent survival rates have the most distinctive microRNA profile. Therefore this study focused on to address two aspects, firstly, if the transcription of these WNT subgroup specific miRNAs is regulated as a result of WNT signalling activation and secondly, determining the functional role of miR-148a, one of the miRNAs over-expressed in WNT subgroup medulloblastomas.

5.1 Transcription regulation of WNT subgroup specific miRNAs

Our group has earlier shown that WNT subgroup medulloblastomas show distinct profile of up-regulated miRNAs that include miR-193a, miR-148a, miR-224 and miR-365 based on the

microRNA profiling of 101 medulloblastoma tissues[6]. The distinct over-expression of these miRNAs in WNT subgroup as compared to other subgroups and normal cerebellar tissues is similar to the over-expression of many WNT target genes like *MYC, LEF1, DKK1, DKK2, DKK4, AXIN1, RUNX2* [3]. This suggests that the over-expression of miRNAs may possibly be associated with activated WNT signalling pathway and hence possibility of these miRNAs being targets of WNT signalling was evaluated in the present study. Other than being direct targets of WNT signalling effectors β-catenin-TCF complexes, indirect transcriptional regulation of these miRNAs by MYC, a potent transcription factor which itself is a direct target of WNT signalling pathway, was also evaluated.

Present study identified presence of E-Box DNA motif (MYC binding site) close to predicted TSSs for miR-193a and known TSS of miR-148a. Further, the promoter activities of miR-148a and miR-193a promoter constructs were found to be induced upon co-transfection with MYC expression vector in HEK293 cells. MiR-148a promoter was found to possess two E-box motifs with E-Box-1 close to TSS (~ 800bp) and E-Box-2, ~1.7kb away from TSS. Abrogation of MYC induced activation of miR-148a promoter activity upon mutation of E-Box-1 indicated that MYC is most likely to regulate miR-148a promoter activity via E-Box-1. Interestingly, ChIP-PET sequencing data available for MYC in human B cells [116] has reported binding of MYC to E-Box-1 suggesting E-Box-1 motif to play major role in MYC induced activation of miR-148a promoter activity.

Group 3 subgroup tumours are known to show over-expression of MYC or even amplification [9, 37]. However miR-148a and miR-193a, two MYC responsive miRNAs are under-expressed in Group 3 tumours. This suggests presence of alternate regulatory mechanism of transcription of these miRNA coding genes. Both of these miRNAs are known to be downregulated in various malignancies due to CpG DNA methylation in their promoters [5, 12, 13, 136]. Bisulphite sequencing of CpG Island region upstream to pri-miR-

148a performed in the present study showed complete methylation at almost all the CpGs in four medulloblastoma cell lines D283, D425, D341 and Daoy. Presence of Methylation or hemimethylation was found at more than 50% of CpGs in 75% of Group 3 and Group 4 tumours (6 out of 8) and 25% of CpGs found methylated in 2 out of 3 SHH tumours, while WNT tumours did not show any methylation. Since D425, D283 and D341 most likely belong to Group 3 subgroup and Daoy to SHH subgroup [118, 119], the under-expression of miR-148a predominantly in group 3 and 4 tumours and to some extent in SHH tumours is most likely to be as a result of CpG DNA methylation at the promoter. DNA methylation is known to make DNA inaccessible for transcription factors that activate transcription. CpG methylation sites act as nucleation centres for histone deacetylases and polycomb group of proteins to modify chromatin in the surrounding genomic region[100]. DNA methylation and histone deacetylation thus act together to cause transcriptional repression and the repression can be relieved upon treatment of HDAC inhibitors or demethylating agent [100, 137]. Indeed upon treatment with HDAC inhibitors, modest induction in miR-148a expression was seen in D425 medulloblastoma cells. However, miR-193a expression was not found to be induced upon treatment with HDAC inhibitors. Treatment of cancer cell lines with HDAC inhibitors has been shown to cause partial reversion of DNA methylation and combined treatment of 5-Aza deoxycytidine and TSA has been used to completely reverse the DNA methylation at CpG islands [121]. Since DNA methylase inhibitor 5'Aza deoxycytidine was found to be toxic to D425 medulloblastoma cells, change in expression of miR-148a or miR-193a could not be evaluated upon DNA demethylation. Nevertheless, taken together these findings suggest the role of both CpG DNA methylation and histone deacetylation in transcriptional repression of miR-148a.

MiR-224-452 cluster lies in intron 6 of *GABRE* gene. Expression profile of WNT subgroup tumours shows over-expression of *GABRE* and miR-224-425 cluster [3]. Since intragenic

miRNAs are known to be transcribed along with their parent gene, it is therefore most likely that miR-224 is transcribed along with *GABRE* through its promoter. Minimal promoter region driving expression of miR-193b-miR-365 cluster has also been previously reported and was used for the present study [117]. Multiple consensus DNA binding sites for β-catenin-TCF complexes were found to be present within distance of 1kb from known TSS of *GABRE* (miR-224) and miR-365. However no change in promoter activity was seen upon WNT signalling activation either upon treatment with lithium chloride or upon forced expression of constitutively active mutant β-catenin. Such lack of response in promoter activity despite presence of consensus DNA binding sites may occur as a result of β-catenin-TCF complexes alone not being sufficient to activate these promoter regions and need presence of additional cell type specific cofactors or chromatin regulating proteins that cooperate with these complexes for transcriptional activation of target genes. However lack of medulloblastoma cell line belonging to WNT subgroup medulloblastoma impedes the further investigation.

5.2 Functional role of WNT subgroup specific miR-148a and its target genes:

In the present study we have shown tumour suppressive role of miR-148a in three medeulloblastoma cell lines Daoy, D425 and D283 that belong to SHH , Group 3/Group 4 subgroups. Expression of miR-148a to the levels comparable to that in WNT tumours was found to inhibit proliferation, clonogenic, invasion and tumourigenic potential of these cells. MiR-148a expression has been shown to inhibit growth, invasion potential and tumourigenic properties of various cancer cells including gastric cancer cells, hepatocellular cancer cells, pancreatic cancer cells and prostate cancer cell lines[138, 139]. Recently miR-148a has been shown to inhibit glioma stem cell like properties and tumourigenicity [140, 141]. Thus the tumour suppressive role of miR-148a in medulloblastoma is consistent with its known functional role in other malignancies. 3'UTRs of select set of genes with known role in

modulating invasion and tumourigenic properties of tumour cells like NRP1, ROCK1, DNMT1 and MMP15 were found to be targeted by miR-148a in a 3'UTR luciferase reporter assay. Few of these targets i.e. NRP1, ROCK1 and DNMT1 were further confirmed to be downregulated on miR-148a expression by studying their expression using western blotting in miR-148a expressing medulloblastoma cell lines.

ROCK1 and DNMT1 are two known target genes of miR-148a. ROCK1 is an essential effector kinase that acts downstream of Rho-GTPases and participates in regulation of cytoskeletal rearrangement and cell motility[142]. In gastric cancer and non small cell lung cancer cells, ROCK1 was found to be a direct target of miR-148a and downregulation of ROCK1 was shown to inhibit motility and invasion of these cells [130, 140]. In a similar study involving glioma cell lines, downregulation of ROCK1 via miR-124 was found to reduce invasion potential and motility of cells [143]. ROCK1 is therefore likely to contribute towards miR-148a mediated inhibition of invasion in medulloblastoma cell lines.

DNMT1, the major enzyme responsible for maintenance of the DNA methylation pattern, is known to be downregulated upon miR-148a expression in breast cancer, gastric cancer and IDH1 mutant gliomas [124, 125, 140]. Downregulation of DNMT1 expression has been shown to reduce tumour incidence in *Ptch1* heterozygous knock-out mice, a mouse model of SHH subgroup medulloblastomas [144]. Although mechanistic details of how DNMT1 regulates tumourigenic and/or invasion ability of cells are not elucidated by any of these studies, considering its role in maintainance of DNA methylation it is likely that downregulation of DNMT1 may regulate these processes through its target genes, which are yet not known. In addition to being target of miR-148a, as mentioned earlier downregulation of DNMT1 has been shown to cause demethylation at miR-148a promoter associated CpG Island, thereby inducing miR-148a expression. Hence such a feedback regulatory loop between miR-148a and DNMT1 is likely to be present in WNT subgroup medulloblastomas.

Downregulation of DNMT1 may also result in global hypomethylation which is consistent with the low CpG methylation rate observed in WNT tumours. Interestingly, DNMT3b which is overexpressed in many cancer tissues and cell lines [145] is also found out to be the direct target of miR-148a [146], suggesting that targeting of DNMT family of proteins by miR-148a may have larger implications than known till now.

A well known DNMT inhibitor 5'Azadeoxycytidine (decitabine) and 5'Azacytidine has been approved by Food and drug administration for the treatment of myelodysplastic syndromes, while these have also been used for forced expression of Estrogen receptor in triple negative breast cancer[147]. These inhibitors are of particular importance if tested against non-WNT medulloblastomas. These inhibitors are likely to activate transcriptionally repressed tumour suppressor miRNAs like miR-148a and others via inhibiting DNMTs. Similar strategy deploying HDAC inhibitors like valproic acid which are already approved FDA drugs may also be tested for the treatment of non-WNT medulloblastomas.

Neuropilin 1(NRP1) was identified as a novel target of miR-148a in the present study. 3'-UTR of the full length NRP1 transcript contains a single 8-mer miR-148a target site which is conserved among vertebrates (www.targetscan.org). Using 3'UTR luciferase reporter constructs of wild type NRP1 and miR-148a binding site mutant constructs, NRP1 was identified as a direct target of miR-148a. Western blot analysis showed downregulation of full length NRP1 protein (120 kDa isoform) on miR-148a expression in multiple cell lines including Daoy, D283, medulloblastoma cell lines and U373 glioblastoma cell line, further confirming NRP1 as a miR-148a target. NRP1 gene encodes multiple alternately spliced transcripts. 5882 bp CCDS7177 transcript encodes 923 amino acid long full length protein whose 3'-UTR contains the miR-148a target site (www.ncbi.nlm.nih.gov/gene). Shorter CCDS31179, CCDS31180 transcripts encode 609 and 644 amino acid long proteins lack the 3'-UTR as well as the transmembrane domain. These isoforms encode soluble NRP1 forms

that have been shown to act as antagonist of the full length membrane bound NRP1 protein [148]. The 80 kDa NRP1 protein detected in the western blot analysis showed no change in the levels upon miR-148a expression. Therefore, it most likely belongs to the soluble NRP1 isoforms based on both its size and the real time RT-PCR analysis that shows the contribution of the shorter soluble isoforms to the total NRP1 expression levels. Thus, miR-148a targets only the functionally active full length NRP1 isoform and not the soluble isoforms that act as antagonist of NRP1 activity.

5.3 Neuropilin1: A novel target of miR-148a and its functional implications

NRP1 is a single pass trans-membrane protein, which was first identified as a ligand binding coreceptor of Semaphorin 3A that plays a role in axon patterning in nervous system development [149]. Subsequently, it was shown to act as a co-receptor of VEGF-A165 and other isoforms of VEGF that promote blood vessel growth during normal vasculature development and during angiogenesis in tumour progression[150]. NRP1 has also been reported to act as a co-receptor of multiple growth factors like TGF-beta 1, HGF, FGF2, EGF and PDGF [151-156]. NRP1 has been reported to be over-expressed in various cancers including that of breast, prostate, pancreatic, colon, gliomas and its expression has been reported to correlate with poor prognosis[149, 154, 157]. In the present study, majority (75%) of the WNT subgroup medulloblastomas lacked detectable NRP1 expression. This observation was consistent with the high miR-148a expression in the WNT subgroup medulloblastomas as well as the low incidence of metastasis and excellent survival of the WNT subgroup patients [4, 6]. Majority of the Group 3 tumours which are known to have the worst survival among the four medulloblastoma subgroups expressed NRP1. Further, Kaplan-Meier survival analysis showed NRP1 expression in medulloblastomas to be associated with worse survival. Hence, NRP1 expression may prove to be useful marker for prognostication in medulloblastomas.

Recently, Snuderl *et al* have reported that Placental Growth Factor (PIGF)-NRP1 signalling is necessary for growth and spread of medulloblastomas [158]. Inhibition of PIGF-NRP1 signaling was found to result in regression of medulloblastoma xenografts, decreased metastasis and increased survival of mice. NRP1 has been shown to promote epithelial mesenchymal transition and increase motility of endothelial cells as well as that of cancer cells by regulating TGF-beta, integrin and HGF/c-Met signaling [151, 152]. NRP1 expression has been shown to inhibit motility of medulloblastoma cells from *Ptch1* (+/-) mice [159]. NRP1 has also been reported to promote cancer stem cell maintenance in glioblastoma cells by inhibiting VEGF-VEGFR2-NRP1 signaling and in breast cancer cells by inhibiting NF-kB signaling [160, 161]. NRP1 has been shown to act as a co-receptor in multiple signaling pathways that promote tumour growth and progression [162]. In the present study as well, NRP1 expression was found to bring about almost complete rescue of miR-148a mediated inhibition of the invasion potential and tumourigenicity of medulloblastoma cells. This indicates major role for NRP1 in miR-148a's tumour suppressive effect on medulloblastoma cells. NRP1 therefore has been identified as an attractive therapeutic target for various cancers.

In addition, role of NRP1 in promoting tumour angiogenesis is also well established [163]. In the present study, subcutaneous tumours formed by miR-148a expressing Daoy medulloblastoma cells were found to show significant reduction in overall microvascular density as evaluated by reduction in total number of CD31 positive microvessels and microvessel hotspots, in comparison to tumour formed by vector control cells. Therefore, it is likely that NRP1 may play role in miR-148a mediated inhibition in angiogenesis, however this needs to be validated further. Taken together, miR-148a mediated down-regulation of NRP1 therefore could be an effective therapeutic strategy for the treatment of medulloblastomas as well as other cancers.

A number of approaches have been explored for targeting NRP1 which include siRNAs against NRP1, anti-NRP1 antibodies, peptides targeting NRP1 and soluble NRP1 antagonists[164, 165]. NRP1 siRNAs or anti-NRP1 peptides have been shown to inhibit tumour growth, angiogenesis and metastasis in several cancers including hepatocellular carcinoma and glioblastoma [166-168]. Anti-NRP1 humanized monoclonal antibody MNRP1685A has been introduced in clinical trial for the treatment of various advanced solid tumours in combination with bevacizumab, an angiogenesis inhibitor [169]. Circulating NRP1 is abundantly found in human plasma that is contributed by soluble NRP1 as well as the extracellular domain shed from the membrane bound full length isoform [170]. Therefore, any inhibitor that targets NRP1 protein would also target these soluble isoforms and hence would be required in large amounts for therapeutic effectiveness. However, since miR-148a targets only the NRP1 full length mRNA and not the soluble isoforms, it is likely to serve as a more effective strategy for targeting NRP1.

5.4 Role of WNT subgroup specific miRNAs in pathogenesis of WNT subgroup medulloblastomas

In an earlier study by our group, we have reported that some of the highly over-expressed WNT subgroup specific miRNAs like miR-193a and miR-224, when expressed exogenously inhibit proliferation, increase radiation sensitivity and decrease anchorage independent growth of cell line[3]. MiR-224 has been reported to promote apoptosis by targeting apoptosis inhibitor-5 (API5) in hepatocellular cancer cells. In congruence to these reports, our lab has previously showed that miR-224 expression in glioma cells increases radiation sensitivity of glioma cells too and brings about reduction of API5 expression [171]. MiR-193a has been shown to play tumour suppressive role in oral sqamous cell carcinoma, acute myleiod leukaemia, Breast cancer, colon cancer and non small cell lung cancer cells and has been shown to target c-kit, PTK2, KRAS, PLAU, ERBB4 and S6K2 protein expression [12,

172-174]. The present study highlights tumour suppressive action of miR-148a in medulloblastoma cells that is consistent with a number of reports indicating the anti-metastatic and tumour suppressive role of miR-148a in other cancers[5, 130, 139]. Taken together the tumour suppressive and anti-metastatic role of these miRNAs overexpressed in WNT subgroup may contribute towards less invasive nature, lower metastatic rates and better responsiveness of WNT subgroup tumours to the treatment and ultimately to their excellent prognosis as compared to other subgroups of medulloblastoma. Therefore further preclinical studies are required to test these miRNAs as therapeutic agents for the treatment of non-WNT medulloblastomas.

5.5 MiRNAs: therapeutic agents for cancers

In 2008, the first miRNA based phase I clinical trial was initiated to treat hepatitis C using a Locked Nucleic Acid (LNA) oligonucleotide complementary to miR-122 (Miravirsen) to inhibit expression of this miRNA which normally facilitates viral replication. This was shown to be effective more than anticipated as this antisense oligonucleotide could target pre and pri sequences of miR-122 too [103]. The first miRNA based therapy developed for the treatment of cancer is MRX34, a synthetic miRNA mimic loaded in liposomal nanoparticles. MiR-34a is tumour suppressor miRNA that acts downstream to p53 and is downregulated in many solid tumours like cervical cancer, ovarian cancer, glioblastoma, hepatocellular carcinoma (liver cancer), colon cancer, non-small cell lung cancer (NSCLC)[104]. MRX34 is in phase I clinical trial initiated by miRNA therapeutics (http://www.mirnatherapeutics.com) and being conducted in patients with unresectable primary liver cancer or solid cancers with liver involvement. The trial also includes a separate cohort of patients with hematological malignancies.

MiR-148a, is expressed in normal tissues and its expression is known to be lost in several cancers often as a result of promoter hypermethylation [5]. It has also been shown to have

tumour suppressive roles in various malignancies[139]. In the present study, we found that MiR-148a expression at physiological levels showed tumour suppressive effect on medulloblastoma cells. Therefore, miR-148a as a therapeutic agent is unlikely to be toxic to normal tissues. MiR-148a was further found to bring tumour suppressive effect by targeting NRP1, ROCK1 and DNMT1. These targets are distinct from those of other tumour-suppressive miRNAs like miR-34a and let-7a that are being explored for their therapeutic potential (http://www.mirnatherapeutics.com)[93]. MiR-148a may therefore be an attractive therapeutic agent for the treatment of non-WNT medulloblastomas as well as other cancers.

Chapter 6: SUMMARY &CONCLUSIONS

Genome wide expression profiling studies have unequivocally demonstrated four molecular subgroups of medulloblastoma that not only differ in their genetic makeup but are also distinct in their clinical characteristics. Previous study from our lab showed that the four subgroups also differ in their miRNA profile with the most distinctive microRNA profile of the WNT subgroup tumors. MicroRNA profile is expected to play major role in excellent survival rates of this subgroup. The present study addressed two key questions (1) Does WNT signalling pathway has direct or indirect role in transcriptional regulation of WNT subgroup specific expression of miRNAs and (2) whether miR-148a, a WNT subgroup specific miRNA affects the growth and malignant behaviour of medulloblastoma cells.

Briefly, the salient findings of the present study are:

- Promoter regions of the WNT subgroup specific miRNAs viz miR-148a, miR-193a were found to possess two and one MYC binding sites respectively, while that of miR-224 (*GABRE*) and miR-365 were found to have two and three binding sites respectively for the WNT signalling effector protein β-catenin/TCF complex.
- **Promoter activities for miR-193a and miR-148a were shown to be induced by 3-4 fold upon exogenous expression of MYC.** Almost complete abrogation of the MYC induced activation upon mutation in the MYC binding site in the miR-148a promoter region further validated transcriptional regulation of miR-148a promoter by MYC. **Therefore, miR-148a appears to be a direct target of MYC.**
- Genomic region upstream to pri-miR-148a was found to be CpG methylated in medulloblastoma cell lines and most (~60%) of the non-WNT medulloblastoma tissues. MiR-148a expression was also found to be significantly induced ($p < 0.05$) in medulloblastoma cells upon treatment with HDAC inhibitors Trichostatin A and Valproic acid. **Thus, miR-148a expression in non-WNT medulloblastomas appears to be downregulated as a result of epigenetic inactivation.**

- Expression of miR-148a at levels comparable to those in the WNT subgroup medulloblastomas or higher was found to bring about significant ($p < 0.0001$) reduction in growth (35-60%), clonogenic potential (~30-40%), invasion potential (40-70%) and tumorigenicity of medulloblastoma cells belonging to the three subgroups *viz.* SHH, Group 3 or Group 4. **Thus, miR-148a expression has tumor suppressive activity in medulloblastoma cells.**
- **Neuroplin 1 was identified as a novel miR-148a target gene in medulloblastoma**. Mir-148a mediated growth inhibition of medulloblastoma cells was found to be accompanied by downregulation of NRP1 and ROCK1, DNMT1, two known miR-148a targets. Restoration of NRP1 expression brought about almost complete rescue of miR-148a mediated inhibition of invasion potential and *in vivo* tumorigenicity of medulloblastoma cells. Thus, NRP1 downregulation appears to play major role in miR-148a mediated tumor suppression of medulloblastoma cells.
- Furthermore, NRP1 expression in medulloblastomas was found to be higher in Group 3 medulloblastomas having the highest incidence of metastasis and poor survival while majority (75%) of the WNT subgroup tumors showed little or no expression. **Kaplan Meier analysis showed high NRP1 expression to be significantly ($p < 0.05$) correlated with poor survival.**

In conclusion, the present study identified the possible association of expression of some WNT subgroup specific miRNAs with the WNT signalling pathway activation and further showed that miR-148a, one of the WNT subgroup specific miRNA to act as a tumour suppressor miRNA in medulloblastoma by targeting NRP1. Earlier studies from the lab have shown that two other WNT subgroup specific miRNAs viz. miR-193a and miR-224 to also have tumor suppressive and radiation sensitizing activity. **Thus, miRNA over-expression**

appears to make the WNT subgroup tumors less aggressive and more responsive to treatment that is consistent with the excellent survival of the WNT subgroup patients.

The present study not only identified NRP1 as a novel target of miR-148a but also showed to be a major player in miR-148a's tumour-suppressive activity. NRP1 is already in clinical trial as a target for the treatment of various cancers due its known role in tumour growth, metastasis and angiogenesis. Various strategies to target NRP1 are being attempted that include NRP1 antibodies, NRP1 siRNAs etc. However, the presence of high levels of circulating NRP1 antagonist isoforms in human blood makes it difficult to effectively target pathogenic NRP1 full length isoform. **MiR-148a targets specifically the full-length isoform that contains miR-148a binding site in its 3-UTR region, making miR-148a as possibly the most effective NRP1 targeting agent.**

With the capability of targeting multiple oncogenes at a time, miRNAs are powerful tools for effective treatment of cancer. Clinical trial of MRX34 and Miravirsen that are primarily based on the concept of replacement of tumour suppressor miRNA in tumours by delivering through liposomal or nanoparticle based formulation are underway. Early success of these trials is encouraging to consider miR-148a for the treatment of non-WNT medulloblastomas. Future studies should therefore be directed towards development of miRNA based treatment strategies for medulloblastomas as well as other cancers.

BIBLIOGRAPHY

1. Polkinghorn WR, Tarbell NJ: **Medulloblastoma: tumorigenesis, current clinical paradigm, and efforts to improve risk stratification**. *Nature clinical practice Oncology* 2007, **4**(5):295-304.
2. Rossi A, Caracciolo V, Russo G, Reiss K, Giordano A: **Medulloblastoma: from molecular pathology to therapy**. *Clinical cancer research : an official journal of the American Association for Cancer Research* 2008, **14**(4):971-976.
3. Gokhale A, Kunder R, Goel A, Sarin R, Moiyadi A, Shenoy A, Mamidipally C, Noronha S, Kannan S, Shirsat NV: **Distinctive microRNA signature of medulloblastomas associated with the WNT signaling pathway**. *Journal of cancer research and therapeutics* 2010, **6**(4):521-529.
4. Kool M, Korshunov A, Remke M, Jones DT, Schlanstein M, Northcott PA, Cho YJ, Koster J, Schouten-van Meeteren A, van Vuurden D *et al*: **Molecular subgroups of medulloblastoma: an international meta-analysis of transcriptome, genetic aberrations, and clinical data of WNT, SHH, Group 3, and Group 4 medulloblastomas**. *Acta neuropathologica* 2012, **123**(4):473-484.
5. Lujambio A, Calin GA, Villanueva A, Ropero S, Sanchez-Cespedes M, Blanco D, Montuenga LM, Rossi S, Nicoloso MS, Faller WJ *et al*: **A microRNA DNA methylation signature for human cancer metastasis**. *Proceedings of the National Academy of Sciences of the United States of America* 2008, **105**(36):13556-13561.
6. Kunder R, Jalali R, Sridhar E, Moiyadi A, Goel N, Goel A, Gupta T, Krishnatry R, Kannan S, Kurkure P *et al*: **Real-time PCR assay based on the differential expression of microRNAs and protein-coding genes for molecular classification of formalin-fixed paraffin embedded medulloblastomas**. *Neuro-oncology* 2013, **15**(12):1644-1651.
7. Mosmann T: **Rapid colorimetric assay for cellular growth and survival: application to proliferation and cytotoxicity assays**. *Journal of immunological methods* 1983, **65**(1-2):55-63.
8. Hanoun N, Delpu Y, Suriawinata AA, Bournet B, Bureau C, Selves J, Tsongalis GJ, Dufresne M, Buscail L, Cordelier P *et al*: **The silencing of microRNA 148a production by DNA hypermethylation is an early event in pancreatic carcinogenesis**. *Clinical chemistry* 2010, **56**(7):1107-1118.
9. Northcott PA, Korshunov A, Witt H, Hielscher T, Eberhart CG, Mack S, Bouffet E, Clifford SC, Hawkins CE, French P *et al*: **Medulloblastoma comprises four distinct molecular variants**. *Journal of clinical oncology : official journal of the American Society of Clinical Oncology* 2011, **29**(11):1408-1414.
10. Gerber NU, Mynarek M, von Hoff K, Friedrich C, Resch A, Rutkowski S: **Recent developments and current concepts in medulloblastoma**. *Cancer treatment reviews* 2014, **40**(3):356-365.
11. Zhang B, Pan X, Cobb GP, Anderson TA: **microRNAs as oncogenes and tumor suppressors**. *Developmental biology* 2007, **302**(1):1-12.
12. Kozaki K, Imoto I, Mogi S, Omura K, Inazawa J: **Exploration of tumor-suppressive microRNAs silenced by DNA hypermethylation in oral cancer**. *Cancer research* 2008, **68**(7):2094-2105.
13. Lv L, Deng H, Li Y, Zhang C, Liu X, Liu Q, Zhang D, Wang L, Pu Y, Zhang H *et al*: **The DNA methylation-regulated miR-193a-3p dictates the multi-chemoresistance of bladder cancer via repression of SRSF2/PLAU/HIC2 expression**. *Cell death & disease* 2014, **5**:e1402.
14. Raffel C: **Medulloblastoma: molecular genetics and animal models**. *Neoplasia* 2004, **6**(4):310-322.

15. Ferguson S, Lesniak MS: **Percival Bailey and the classification of brain tumors**. *Neurosurgical focus* 2005, **18**(4):e7.
16. Crawford JR, MacDonald TJ, Packer RJ: **Medulloblastoma in childhood: new biological advances**. *The Lancet Neurology* 2007, **6**(12):1073-1085.
17. Roussel MF, Hatten ME: **Cerebellum development and medulloblastoma**. *Current topics in developmental biology* 2011, **94**:235-282.
18. Pomeroy SL, Tamayo P, Gaasenbeek M, Sturla LM, Angelo M, McLaughlin ME, Kim JY, Goumnerova LC, Black PM, Lau C *et al*: **Prediction of central nervous system embryonal tumour outcome based on gene expression**. *Nature* 2002, **415**(6870):436-442.
19. de Bont JM, Packer RJ, Michiels EM, den Boer ML, Pieters R: **Biological background of pediatric medulloblastoma and ependymoma: a review from a translational research perspective**. *Neuro-oncology* 2008, **10**(6):1040-1060.
20. Pfister S, Remke M, Benner A, Mendrzyk F, Toedt G, Felsberg J, Wittmann A, Devens F, Gerber NU, Joos S *et al*: **Outcome prediction in pediatric medulloblastoma based on DNA copy-number aberrations of chromosomes 6q and 17q and the MYC and MYCN loci**. *Journal of clinical oncology : official journal of the American Society of Clinical Oncology* 2009, **27**(10):1627-1636.
21. Cowan R, Hoban P, Kelsey A, Birch JM, Gattamaneni R, Evans DG: **The gene for the naevoid basal cell carcinoma syndrome acts as a tumour-suppressor gene in medulloblastoma**. *British journal of cancer* 1997, **76**(2):141-145.
22. Hamilton SR, Liu B, Parsons RE, Papadopoulos N, Jen J, Powell SM, Krush AJ, Berk T, Cohen Z, Tetu B *et al*: **The molecular basis of Turcot's syndrome**. *The New England journal of medicine* 1995, **332**(13):839-847.
23. Nusse R, Varmus H: **Three decades of Wnts: a personal perspective on how a scientific field developed**. *The EMBO journal* 2012, **31**(12):2670-2684.
24. Li F, Chong ZZ, Maiese K: **Vital elements of the Wnt-Frizzled signaling pathway in the nervous system**. *Current neurovascular research* 2005, **2**(4):331-340.
25. Clevers H, Nusse R: **Wnt/beta-catenin signaling and disease**. *Cell* 2012, **149**(6):1192-1205.
26. Ellison DW, Onilude OE, Lindsey JC, Lusher ME, Weston CL, Taylor RE, Pearson AD, Clifford SC: **beta-Catenin status predicts a favorable outcome in childhood medulloblastoma: the United Kingdom Children's Cancer Study Group Brain Tumour Committee**. *Journal of clinical oncology : official journal of the American Society of Clinical Oncology* 2005, **23**(31):7951-7957.
27. Moon RT, Kohn AD, De Ferrari GV, Kaykas A: **WNT and beta-catenin signalling: diseases and therapies**. *Nature reviews Genetics* 2004, **5**(9):691-701.
28. Varjosalo M, Taipale J: **Hedgehog: functions and mechanisms**. *Genes & development* 2008, **22**(18):2454-2472.
29. Rubin LL, de Sauvage FJ: **Targeting the Hedgehog pathway in cancer**. *Nature reviews Drug discovery* 2006, **5**(12):1026-1033.
30. Pasca di Magliano M, Hebrok M: **Hedgehog signalling in cancer formation and maintenance**. *Nature reviews Cancer* 2003, **3**(12):903-911.
31. Thompson MC, Fuller C, Hogg TL, Dalton J, Finkelstein D, Lau CC, Chintagumpala M, Adesina A, Ashley DM, Kellie SJ *et al*: **Genomics identifies medulloblastoma subgroups that are enriched for specific genetic alterations**. *Journal of clinical oncology : official journal of the American Society of Clinical Oncology* 2006, **24**(12):1924-1931.
32. Northcott PA, Dubuc AM, Pfister S, Taylor MD: **Molecular subgroups of medulloblastoma**. *Expert review of neurotherapeutics* 2012, **12**(7):871-884.
33. Cho YJ, Tsherniak A, Tamayo P, Santagata S, Ligon A, Greulich H, Berhoukim R, Amani V, Goumnerova L, Eberhart CG *et al*: **Integrative genomic analysis of medulloblastoma identifies a molecular subgroup that drives poor clinical outcome**. *Journal of clinical oncology : official journal of the American Society of Clinical Oncology* 2011, **29**(11):1424-1430.
34. Gajjar AJ, Robinson GW: **Medulloblastoma-translating discoveries from the bench to the bedside**. *Nature reviews Clinical oncology* 2014, **11**(12):714-722.

35. Robinson G, Parker M, Kranenburg TA, Lu C, Chen X, Ding L, Phoenix TN, Hedlund E, Wei L, Zhu X *et al*: **Novel mutations target distinct subgroups of medulloblastoma**. *Nature* 2012, **488**(7409):43-48.
36. Risinger JI, Berchuck A, Kohler MF, Boyd J: **Mutations of the E-cadherin gene in human gynecologic cancers**. *Nature genetics* 1994, **7**(1):98-102.
37. Northcott PA, Shih DJ, Peacock J, Garzia L, Morrissy AS, Zichner T, Stutz AM, Korshunov A, Reimand J, Schumacher SE *et al*: **Subgroup-specific structural variation across 1,000 medulloblastoma genomes**. *Nature* 2012, **488**(7409):49-56.
38. Schroeder K, Gururangan S: **Molecular variants and mutations in medulloblastoma**. *Pharmacogenomics and personalized medicine* 2014, **7**:43-51.
39. Gibson P, Tong Y, Robinson G, Thompson MC, Currle DS, Eden C, Kranenburg TA, Hogg T, Poppleton H, Martin J *et al*: **Subtypes of medulloblastoma have distinct developmental origins**. *Nature* 2010, **468**(7327):1095-1099.
40. Leary SE, Olson JM: **The molecular classification of medulloblastoma: driving the next generation clinical trials**. *Current opinion in pediatrics* 2012, **24**(1):33-39.
41. Wu X, Northcott PA, Croul S, Taylor MD: **Mouse models of medulloblastoma**. *Chinese journal of cancer* 2011, **30**(7):442-449.
42. Yang ZJ, Ellis T, Markant SL, Read TA, Kessler JD, Bourboulas M, Schuller U, Machold R, Fishell G, Rowitch DH *et al*: **Medulloblastoma can be initiated by deletion of Patched in lineage-restricted progenitors or stem cells**. *Cancer cell* 2008, **14**(2):135-145.
43. Hallahan AR, Pritchard JI, Hansen S, Benson M, Stoeck J, Hatton BA, Russell TL, Ellenbogen RG, Bernstein ID, Beachy PA *et al*: **The SmoA1 mouse model reveals that notch signaling is critical for the growth and survival of sonic hedgehog-induced medulloblastomas**. *Cancer research* 2004, **64**(21):7794-7800.
44. Hatton BA, Villavicencio EH, Tsuchiya KD, Pritchard JI, Ditzler S, Pullar B, Hansen S, Knoblaugh SE, Lee D, Eberhart CG *et al*: **The Smo/Smo model: hedgehog-induced medulloblastoma with 90% incidence and leptomeningeal spread**. *Cancer research* 2008, **68**(6):1768-1776.
45. Taylor MD, Northcott PA, Korshunov A, Remke M, Cho YJ, Clifford SC, Eberhart CG, Parsons DW, Rutkowski S, Gajjar A *et al*: **Molecular subgroups of medulloblastoma: the current consensus**. *Acta neuropathologica* 2012, **123**(4):465-472.
46. DeSouza RM, Jones BR, Lowis SP, Kurian KM: **Pediatric medulloblastoma - update on molecular classification driving targeted therapies**. *Frontiers in oncology* 2014, **4**:176.
47. Northcott PA, Jones DT, Kool M, Robinson GW, Gilbertson RJ, Cho YJ, Pomeroy SL, Korshunov A, Lichter P, Taylor MD *et al*: **Medulloblastomics: the end of the beginning**. *Nature reviews Cancer* 2012, **12**(12):818-834.
48. Pan E, Pellarin M, Holmes E, Smirnov I, Misra A, Eberhart CG, Burger PC, Biegel JA, Feuerstein BG: **Isochromosome 17q is a negative prognostic factor in poor-risk childhood medulloblastoma patients**. *Clinical cancer research : an official journal of the American Association for Cancer Research* 2005, **11**(13):4733-4740.
49. Ryan SL, Schwalbe EC, Cole M, Lu Y, Lusher ME, Megahed H, O'Toole K, Nicholson SL, Bognar L, Garami M *et al*: **MYC family amplification and clinical risk-factors interact to predict an extremely poor prognosis in childhood medulloblastoma**. *Acta neuropathologica* 2012, **123**(4):501-513.
50. Northcott PA, Lee C, Zichner T, Stutz AM, Erkek S, Kawauchi D, Shih DJ, Hovestadt V, Zapatka M, Sturm D *et al*: **Enhancer hijacking activates GFI1 family oncogenes in medulloblastoma**. *Nature* 2014, **511**(7510):428-434.
51. Pei Y, Moore CE, Wang J, Tewari AK, Eroshkin A, Cho YJ, Witt H, Korshunov A, Read TA, Sun JL *et al*: **An animal model of MYC-driven medulloblastoma**. *Cancer cell* 2012, **21**(2):155-167.
52. Kawauchi D, Robinson G, Uziel T, Gibson P, Rehg J, Gao C, Finkelstein D, Qu C, Pounds S, Ellison DW *et al*: **A mouse model of the most aggressive subgroup of human medulloblastoma**. *Cancer cell* 2012, **21**(2):168-180.
53. Roussel MF, Robinson GW: **Role of MYC in Medulloblastoma**. *Cold Spring Harbor perspectives in medicine* 2013, **3**(11).

54. Jones DT, Jager N, Kool M, Zichner T, Hutter B, Sultan M, Cho YJ, Pugh TJ, Hovestadt V, Stutz AM *et al*: **Dissecting the genomic complexity underlying medulloblastoma**. *Nature* 2012, **488**(7409):100-105.
55. Swartling FJ, Grimmer MR, Hackett CS, Northcott PA, Fan QW, Goldenberg DD, Lau J, Masic S, Nguyen K, Yakovenko S *et al*: **Pleiotropic role for MYCN in medulloblastoma**. *Genes & development* 2010, **24**(10):1059-1072.
56. Swartling FJ, Savov V, Persson AI, Chen J, Hackett CS, Northcott PA, Grimmer MR, Lau J, Chesler L, Perry A *et al*: **Distinct neural stem cell populations give rise to disparate brain tumors in response to N-MYC**. *Cancer cell* 2012, **21**(5):601-613.
57. Dubuc AM, Remke M, Korshunov A, Northcott PA, Zhan SH, Mendez-Lago M, Kool M, Jones DT, Unterberger A, Morrissy AS *et al*: **Aberrant patterns of H3K4 and H3K27 histone lysine methylation occur across subgroups in medulloblastoma**. *Acta neuropathologica* 2013, **125**(3):373-384.
58. Hovestadt V, Jones DT, Picelli S, Wang W, Kool M, Northcott PA, Sultan M, Stachurski K, Ryzhova M, Warnatz HJ *et al*: **Decoding the regulatory landscape of medulloblastoma using DNA methylation sequencing**. *Nature* 2014, **510**(7506):537-541.
59. Zhang X, Wen H, Shi X: **Lysine methylation: beyond histones**. *Acta biochimica et biophysica Sinica* 2012, **44**(1):14-27.
60. Ecker J, Oehme I, Mazitschek R, Korshunov A, Kool M, Hielscher T, Kiss J, Selt F, Konrad C, Lodrini M *et al*: **Targeting class I histone deacetylase 2 in MYC amplified group 3 medulloblastoma**. *Acta neuropathologica communications* 2015, **3**:22.
61. Lee SJ, Lindsey S, Graves B, Yoo S, Olson JM, Langhans SA: **Sonic hedgehog-induced histone deacetylase activation is required for cerebellar granule precursor hyperplasia in medulloblastoma**. *PloS one* 2013, **8**(8):e71455.
62. Pugh TJ, Weeraratne SD, Archer TC, Pomeranz Krummel DA, Auclair D, Bochicchio J, Carneiro MO, Carter SL, Cibulskis K, Erlich RL *et al*: **Medulloblastoma exome sequencing uncovers subtype-specific somatic mutations**. *Nature* 2012, **488**(7409):106-110.
63. Schwalbe EC, Williamson D, Lindsey JC, Hamilton D, Ryan SL, Megahed H, Garami M, Hauser P, Dembowska-Baginska B, Perek D *et al*: **DNA methylation profiling of medulloblastoma allows robust subclassification and improved outcome prediction using formalin-fixed biopsies**. *Acta neuropathologica* 2013, **125**(3):359-371.
64. Jin B, Li Y, Robertson KD: **DNA methylation: superior or subordinate in the epigenetic hierarchy?** *Genes & cancer* 2011, **2**(6):607-617.
65. Wightman B, Ha I, Ruvkun G: **Posttranscriptional regulation of the heterochronic gene lin-14 by lin-4 mediates temporal pattern formation in C. elegans**. *Cell* 1993, **75**(5):855-862.
66. Lee RC, Feinbaum RL, Ambros V: **The C. elegans heterochronic gene lin-4 encodes small RNAs with antisense complementarity to lin-14**. *Cell* 1993, **75**(5):843-854.
67. Reinhart BJ, Slack FJ, Basson M, Pasquinelli AE, Bettinger JC, Rougvie AE, Horvitz HR, Ruvkun G: **The 21-nucleotide let-7 RNA regulates developmental timing in Caenorhabditis elegans**. *Nature* 2000, **403**(6772):901-906.
68. Pasquinelli AE, Reinhart BJ, Slack F, Martindale MQ, Kuroda MI, Maller B, Hayward DC, Ball EE, Degnan B, Muller P *et al*: **Conservation of the sequence and temporal expression of let-7 heterochronic regulatory RNA**. *Nature* 2000, **408**(6808):86-89.
69. Johnson SM, Grosshans H, Shingara J, Byrom M, Jarvis R, Cheng A, Labourier E, Reinert KL, Brown D, Slack FJ: **RAS is regulated by the let-7 microRNA family**. *Cell* 2005, **120**(5):635-647.
70. Griffiths-Jones S, Grocock RJ, van Dongen S, Bateman A, Enright AJ: **miRBase: microRNA sequences, targets and gene nomenclature**. *Nucleic acids research* 2006, **34**(Database issue):D140-144.
71. Hammond SM: **An overview of microRNAs**. *Advanced drug delivery reviews* 2015, **87**:3-14.
72. Kim VN: **MicroRNA biogenesis: coordinated cropping and dicing**. *Nature reviews Molecular cell biology* 2005, **6**(5):376-385.
73. Lee Y, Kim M, Han J, Yeom KH, Lee S, Baek SH, Kim VN: **MicroRNA genes are transcribed by RNA polymerase II**. *The EMBO journal* 2004, **23**(20):4051-4060.

74. Finnegan EF, Pasquinelli AE: **MicroRNA biogenesis: regulating the regulators**. *Critical reviews in biochemistry and molecular biology* 2013, **48**(1):51-68.
75. Baskerville S, Bartel DP: **Microarray profiling of microRNAs reveals frequent coexpression with neighboring miRNAs and host genes**. *RNA* 2005, **11**(3):241-247.
76. Rodriguez A, Griffiths-Jones S, Ashurst JL, Bradley A: **Identification of mammalian microRNA host genes and transcription units**. *Genome research* 2004, **14**(10A):1902-1910.
77. Borchert GM, Lanier W, Davidson BL: **RNA polymerase III transcribes human microRNAs**. *Nature structural & molecular biology* 2006, **13**(12):1097-1101.
78. Sassen S, Miska EA, Caldas C: **MicroRNA: implications for cancer**. *Virchows Archiv : an international journal of pathology* 2008, **452**(1):1-10.
79. Martinez-Sanchez A, Murphy CL: **MicroRNA Target Identification-Experimental Approaches**. *Biology* 2013, **2**(1):189-205.
80. Bartel DP: **MicroRNAs: target recognition and regulatory functions**. *Cell* 2009, **136**(2):215-233.
81. Calin GA, Ferracin M, Cimmino A, Di Leva G, Shimizu M, Wojcik SE, Iorio MV, Visone R, Sever NI, Fabbri M *et al*: **A MicroRNA signature associated with prognosis and progression in chronic lymphocytic leukemia**. *The New England journal of medicine* 2005, **353**(17):1793-1801.
82. He L, Thomson JM, Hemann MT, Hernando-Monge E, Mu D, Goodson S, Powers S, Cordon-Cardo C, Lowe SW, Hannon GJ *et al*: **A microRNA polycistron as a potential human oncogene**. *Nature* 2005, **435**(7043):828-833.
83. O'Donnell KA, Wentzel EA, Zeller KI, Dang CV, Mendell JT: **c-Myc-regulated microRNAs modulate E2F1 expression**. *Nature* 2005, **435**(7043):839-843.
84. Pierson J, Hostager B, Fan R, Vibhakar R: **Regulation of cyclin dependent kinase 6 by microRNA 124 in medulloblastoma**. *Journal of neuro-oncology* 2008, **90**(1):1-7.
85. Ferretti E, De Smaele E, Po A, Di Marcotullio L, Tosi E, Espinola MS, Di Rocco C, Riccardi R, Giangaspero F, Farcomeni A *et al*: **MicroRNA profiling in human medulloblastoma**. *International journal of cancer Journal international du cancer* 2009, **124**(3):568-577.
86. Northcott PA, Fernandez LA, Hagan JP, Ellison DW, Grajkowska W, Gillespie Y, Grundy R, Van Meter T, Rutka JT, Croce CM *et al*: **The miR-17/92 polycistron is up-regulated in sonic hedgehog-driven medulloblastomas and induced by N-myc in sonic hedgehog-treated cerebellar neural precursors**. *Cancer research* 2009, **69**(8):3249-3255.
87. Weeraratne SD, Amani V, Teider N, Pierre-Francois J, Winter D, Kye MJ, Sengupta S, Archer T, Remke M, Bai AH *et al*: **Pleiotropic effects of miR-183~96~182 converge to regulate cell survival, proliferation and migration in medulloblastoma**. *Acta neuropathologica* 2012, **123**(4):539-552.
88. Bai AH, Milde T, Remke M, Rolli CG, Hielscher T, Cho YJ, Kool M, Northcott PA, Jugold M, Bazhin AV *et al*: **MicroRNA-182 promotes leptomeningeal spread of non-sonic hedgehog-medulloblastoma**. *Acta neuropathologica* 2012, **123**(4):529-538.
89. Zhang Z, Li S, Cheng SY: **The miR-183 approximately 96 approximately 182 cluster promotes tumorigenesis in a mouse model of medulloblastoma**. *Journal of biomedical research* 2013, **27**(6):486-494.
90. Li Y, Guessous F, Zhang Y, Dipierro C, Kefas B, Johnson E, Marcinkiewicz L, Jiang J, Yang Y, Schmittgen TD *et al*: **MicroRNA-34a inhibits glioblastoma growth by targeting multiple oncogenes**. *Cancer research* 2009, **69**(19):7569-7576.
91. de Antonellis P, Medaglia C, Cusanelli E, Andolfo I, Liguori L, De Vita G, Carotenuto M, Bello A, Formiggini F, Galeone A *et al*: **MiR-34a targeting of Notch ligand delta-like 1 impairs CD15+/CD133+ tumor-propagating cells and supports neural differentiation in medulloblastoma**. *PloS one* 2011, **6**(9):e24584.
92. Weeraratne SD, Amani V, Neiss A, Teider N, Scott DK, Pomeroy SL, Cho YJ: **miR-34a confers chemosensitivity through modulation of MAGE-A and p53 in medulloblastoma**. *Neuro-oncology* 2011, **13**(2):165-175.
93. Bader AG: **miR-34 - a microRNA replacement therapy is headed to the clinic**. *Frontiers in genetics* 2012, **3**:120.

94. Vidal DO, Marques MM, Lopes LF, Reis RM: **The role of microRNAs in medulloblastoma**. *Pediatric hematology and oncology* 2013, **30**(5):367-378.
95. Ozsolak F, Poling LL, Wang Z, Liu H, Liu XS, Roeder RG, Zhang X, Song JS, Fisher DE: **Chromatin structure analyses identify miRNA promoters**. *Genes & development* 2008, **22**(22):3172-3183.
96. Schanen BC, Li X: **Transcriptional regulation of mammalian miRNA genes**. *Genomics* 2011, **97**(1):1-6.
97. Baer C, Claus R, Plass C: **Genome-wide epigenetic regulation of miRNAs in cancer**. *Cancer research* 2013, **73**(2):473-477.
98. Lu J, Getz G, Miska EA, Alvarez-Saavedra E, Lamb J, Peck D, Sweet-Cordero A, Ebert BL, Mak RH, Ferrando AA *et al*: **MicroRNA expression profiles classify human cancers**. *Nature* 2005, **435**(7043):834-838.
99. Saito Y, Liang G, Egger G, Friedman JM, Chuang JC, Coetzee GA, Jones PA: **Specific activation of microRNA-127 with downregulation of the proto-oncogene BCL6 by chromatin-modifying drugs in human cancer cells**. *Cancer cell* 2006, **9**(6):435-443.
100. Rountree MR, Bachman KE, Herman JG, Baylin SB: **DNA methylation, chromatin inheritance, and cancer**. *Oncogene* 2001, **20**(24):3156-3165.
101. Vrba L, Garbe JC, Stampfer MR, Futscher BW: **Epigenetic regulation of normal human mammary cell type-specific miRNAs**. *Genome research* 2011, **21**(12):2026-2037.
102. Schoof CR, Botelho EL, Izzotti A, Vasques Ldos R: **MicroRNAs in cancer treatment and prognosis**. *American journal of cancer research* 2012, **2**(4):414-433.
103. Gebert LF, Rebhan MA, Crivelli SE, Denzler R, Stoffel M, Hall J: **Miravirsen (SPC3649) can inhibit the biogenesis of miR-122**. *Nucleic acids research* 2014, **42**(1):609-621.
104. Hayes J, Peruzzi PP, Lawler S: **MicroRNAs in cancer: biomarkers, functions and therapy**. *Trends in molecular medicine* 2014, **20**(8):460-469.
105. Chomczynski P, Sacchi N: **Single-step method of RNA isolation by acid guanidinium thiocyanate-phenol-chloroform extraction**. *Analytical biochemistry* 1987, **162**(1):156-159.
106. Chen C, Ridzon DA, Broomer AJ, Zhou Z, Lee DH, Nguyen JT, Barbisin M, Xu NL, Mahuvakar VR, Andersen MR *et al*: **Real-time quantification of microRNAs by stem-loop RT-PCR**. *Nucleic acids research* 2005, **33**(20):e179.
107. Kingston RE, Chen CA, Okayama H: **Calcium phosphate transfection**. *Current protocols in immunology / edited by John E Coligan [et al]* 2001, **Chapter 10**:Unit 10 13.
108. Lowry OH, Rosebrough NJ, Farr AL, Randall RJ: **Protein measurement with the Folin phenol reagent**. *The Journal of biological chemistry* 1951, **193**(1):265-275.
109. Knudsen S: **Promoter2.0: for the recognition of PolII promoter sequences**. *Bioinformatics* 1999, **15**(5):356-361.
110. Prestridge DS: **Predicting Pol II promoter sequences using transcription factor binding sites**. *Journal of molecular biology* 1995, **249**(5):923-932.
111. Davuluri RV, Grosse I, Zhang MQ: **Computational identification of promoters and first exons in the human genome**. *Nature genetics* 2001, **29**(4):412-417.
112. Wang X, Xuan Z, Zhao X, Li Y, Zhang MQ: **High-resolution human core-promoter prediction with CoreBoost_HM**. *Genome research* 2009, **19**(2):266-275.
113. Jho EH, Zhang T, Domon C, Joo CK, Freund JN, Costantini F: **Wnt/beta-catenin/Tcf signaling induces the transcription of Axin2, a negative regulator of the signaling pathway**. *Molecular and cellular biology* 2002, **22**(4):1172-1183.
114. Blackwell TK, Huang J, Ma A, Kretzner L, Alt FW, Eisenman RN, Weintraub H: **Binding of myc proteins to canonical and noncanonical DNA sequences**. *Molecular and cellular biology* 1993, **13**(9):5216-5224.
115. Butler JE, Kadonaga JT: **The RNA polymerase II core promoter: a key component in the regulation of gene expression**. *Genes & development* 2002, **16**(20):2583-2592.
116. Zeller KI, Zhao X, Lee CW, Chiu KP, Yao F, Yustein JT, Ooi HS, Orlov YL, Shahab A, Yong HC *et al*: **Global mapping of c-Myc binding sites and target gene networks in human B cells**. *Proceedings of the National Academy of Sciences of the United States of America* 2006, **103**(47):17834-17839.

117. Xu Z, Xiao SB, Xu P, Xie Q, Cao L, Wang D, Luo R, Zhong Y, Chen HC, Fang LR: **miR-365, a novel negative regulator of interleukin-6 gene expression, is cooperatively regulated by Sp1 and NF-kappaB**. *The Journal of biological chemistry* 2011, **286**(24):21401-21412.
118. Aldosari N, Wiltshire RN, Dutra A, Schrock E, McLendon RE, Friedman HS, Bigner DD, Bigner SH: **Comprehensive molecular cytogenetic investigation of chromosomal abnormalities in human medulloblastoma cell lines and xenograft**. *Neuro-oncology* 2002, **4**(2):75-85.
119. Bigner SH, Friedman HS, Vogelstein B, Oakes WJ, Bigner DD: **Amplification of the c-myc gene in human medulloblastoma cell lines and xenografts**. *Cancer research* 1990, **50**(8):2347-2350.
120. Ropero S, Esteller M: **The role of histone deacetylases (HDACs) in human cancer**. *Molecular oncology* 2007, **1**(1):19-25.
121. Milutinovic S, D'Alessio AC, Detich N, Szyf M: **Valproate induces widespread epigenetic reprogramming which involves demethylation of specific genes**. *Carcinogenesis* 2007, **28**(3):560-571.
122. Vibhakar R, Foltz G, Yoon JG, Field L, Lee H, Ryu GY, Pierson J, Davidson B, Madan A: **Dickkopf-1 is an epigenetically silenced candidate tumor suppressor gene in medulloblastoma**. *Neuro-oncology* 2007, **9**(2):135-144.
123. Harada K, Toyooka S, Maitra A, Maruyama R, Toyooka KO, Timmons CF, Tomlinson GE, Mastrangelo D, Hay RJ, Minna JD *et al*: **Aberrant promoter methylation and silencing of the RASSF1A gene in pediatric tumors and cell lines**. *Oncogene* 2002, **21**(27):4345-4349.
124. Zhu A, Xia J, Zuo J, Jin S, Zhou H, Yao L, Huang H, Han Z: **MicroRNA-148a is silenced by hypermethylation and interacts with DNA methyltransferase 1 in gastric cancer**. *Med Oncol* 2012, **29**(4):2701-2709.
125. Xu Q, Jiang Y, Yin Y, Li Q, He J, Jing Y, Qi YT, Li W, Lu B, Peiper SS *et al*: **A regulatory circuit of miR-148a/152 and DNMT1 in modulating cell transformation and tumor angiogenesis through IGF-IR and IRS1**. *Journal of molecular cell biology* 2013, **5**(1):3-13.
126. Yu J, Li Q, Xu Q, Liu L, Jiang B: **MiR-148a inhibits angiogenesis by targeting ERBB3**. *Journal of biomedical research* 2011, **25**(3):170-177.
127. Nico B, Benagiano V, Mangieri D, Maruotti N, Vacca A, Ribatti D: **Evaluation of microvascular density in tumors: pro and contra**. *Histology and histopathology* 2008, **23**(5):601-607.
128. Wang D, Stockard CR, Harkins L, Lott P, Salih C, Yuan K, Buchsbaum D, Hashim A, Zayzafoon M, Hardy RW *et al*: **Immunohistochemistry in the evaluation of neovascularization in tumor xenografts**. *Biotechnic & histochemistry : official publication of the Biological Stain Commission* 2008, **83**(3-4):179-189.
129. Bartel DP: **MicroRNAs: genomics, biogenesis, mechanism, and function**. *Cell* 2004, **116**(2):281-297.
130. Zheng B, Liang L, Wang C, Huang S, Cao X, Zha R, Liu L, Jia D, Tian Q, Wu J *et al*: **MicroRNA-148a suppresses tumor cell invasion and metastasis by downregulating ROCK1 in gastric cancer**. *Clinical cancer research : an official journal of the American Association for Cancer Research* 2011, **17**(24):7574-7583.
131. Gailhouste L, Gomez-Santos L, Hagiwara K, Hatada I, Kitagawa N, Kawaharada K, Thirion M, Kosaka N, Takahashi RU, Shibata T *et al*: **miR-148a plays a pivotal role in the liver by promoting the hepatospecific phenotype and suppressing the invasiveness of transformed cells**. *Hepatology* 2013, **58**(3):1153-1165.
132. Li J, Song Y, Wang Y, Luo J, Yu W: **MicroRNA-148a suppresses epithelial-to-mesenchymal transition by targeting ROCK1 in non-small cell lung cancer cells**. *Molecular and cellular biochemistry* 2013, **380**(1-2):277-282.
133. Liffers ST, Munding JB, Vogt M, Kuhlmann JD, Verdoodt B, Nambiar S, Maghnouj A, Mirmohammadsadegh A, Hahn SA, Tannapfel A: **MicroRNA-148a is down-regulated in human pancreatic ductal adenocarcinomas and regulates cell survival by targeting CDC25B**. *Laboratory investigation; a journal of technical methods and pathology* 2011, **91**(10):1472-1479.

134. Prud'homme GJ, Glinka Y: **Neuropilins are multifunctional coreceptors involved in tumor initiation, growth, metastasis and immunity**. *Oncotarget* 2012, **3**(9):921-939.
135. Gagnon ML, Bielenberg DR, Gechtman Z, Miao HQ, Takashima S, Soker S, Klagsbrun M: **Identification of a natural soluble neuropilin-1 that binds vascular endothelial growth factor: In vivo expression and antitumor activity**. *Proceedings of the National Academy of Sciences of the United States of America* 2000, **97**(6):2573-2578.
136. Ma K, He Y, Zhang H, Fei Q, Niu D, Wang D, Ding X, Xu H, Chen X, Zhu J: **DNA methylation-regulated miR-193a-3p dictates resistance of hepatocellular carcinoma to 5-fluorouracil via repression of SRSF2 expression**. *The Journal of biological chemistry* 2012, **287**(8):5639-5649.
137. Cameron EE, Bachman KE, Myohanen S, Herman JG, Baylin SB: **Synergy of demethylation and histone deacetylase inhibition in the re-expression of genes silenced in cancer**. *Nature genetics* 1999, **21**(1):103-107.
138. Fujita Y, Kojima K, Ohhashi R, Hamada N, Nozawa Y, Kitamoto A, Sato A, Kondo S, Kojima T, Deguchi T *et al*: **MiR-148a attenuates paclitaxel resistance of hormone-refractory, drug-resistant prostate cancer PC3 cells by regulating MSK1 expression**. *The Journal of biological chemistry* 2010, **285**(25):19076-19084.
139. Chen Y, Song YX, Wang ZN: **The microRNA-148/152 family: multi-faceted players**. *Molecular cancer* 2013, **12**:43.
140. Li S, Chowdhury R, Liu F, Chou AP, Li T, Mody RR, Lou JJ, Chen W, Reiss J, Soto H *et al*: **Tumor-suppressive miR148a is silenced by CpG island hypermethylation in IDH1-mutant gliomas**. *Clinical cancer research : an official journal of the American Association for Cancer Research* 2014, **20**(22):5808-5822.
141. Lopez-Bertoni H, Lal B, Li A, Caplan M, Guerrero-Cazares H, Eberhart CG, Quinones-Hinojosa A, Glas M, Scheffler B, Laterra J *et al*: **DNMT-dependent suppression of microRNA regulates the induction of GBM tumor-propagating phenotype by Oct4 and Sox2**. *Oncogene* 2014.
142. Schmitz AA, Govek EE, Bottner B, Van Aelst L: **Rho GTPases: signaling, migration, and invasion**. *Experimental cell research* 2000, **261**(1):1-12.
143. An L, Liu Y, Wu A, Guan Y: **microRNA-124 inhibits migration and invasion by down-regulating ROCK1 in glioma**. *PloS one* 2013, **8**(7):e69478.
144. Ecke I, Petry F, Rosenberger A, Tauber S, Monkemeyer S, Hess I, Dullin C, Kimmina S, Pirngruber J, Johnsen SA *et al*: **Antitumor effects of a combined 5-aza-2'deoxycytidine and valproic acid treatment on rhabdomyosarcoma and medulloblastoma in Ptch mutant mice**. *Cancer research* 2009, **69**(3):887-895.
145. Subramaniam D, Thombre R, Dhar A, Anant S: **DNA methyltransferases: a novel target for prevention and therapy**. *Frontiers in oncology* 2014, **4**:80.
146. Duursma AM, Kedde M, Schrier M, le Sage C, Agami R: **miR-148 targets human DNMT3b protein coding region**. *RNA* 2008, **14**(5):872-877.
147. Conte M, Altucci L: **Molecular pathways: the complexity of the epigenome in cancer and recent clinical advances**. *Clinical cancer research : an official journal of the American Association for Cancer Research* 2012, **18**(20):5526-5534.
148. Rossignol M, Gagnon ML, Klagsbrun M: **Genomic organization of human neuropilin-1 and neuropilin-2 genes: identification and distribution of splice variants and soluble isoforms**. *Genomics* 2000, **70**(2):211-222.
149. Jubb AM, Strickland LA, Liu SD, Mak J, Schmidt M, Koeppen H: **Neuropilin-1 expression in cancer and development**. *The Journal of pathology* 2012, **226**(1):50-60.
150. Klagsbrun M, Takashima S, Mamluk R: **The role of neuropilin in vascular and tumor biology**. *Advances in experimental medicine and biology* 2002, **515**:33-48.
151. Glinka Y, Stoilova S, Mohammed N, Prud'homme GJ: **Neuropilin-1 exerts co-receptor function for TGF-beta-1 on the membrane of cancer cells and enhances responses to both latent and active TGF-beta**. *Carcinogenesis* 2011, **32**(4):613-621.
152. Hu B, Guo P, Bar-Joseph I, Imanishi Y, Jarzynka MJ, Bogler O, Mikkelsen T, Hirose T, Nishikawa R, Cheng SY: **Neuropilin-1 promotes human glioma progression through**

potentiating the activity of the HGF/SF autocrine pathway. *Oncogene* 2007, **26**(38):5577-5586.

153. Mamluk R, Gechtman Z, Kutcher ME, Gasiunas N, Gallagher J, Klagsbrun M: **Neuropilin-1 binds vascular endothelial growth factor 165, placenta growth factor-2, and heparin via its b1b2 domain**. *The Journal of biological chemistry* 2002, **277**(27):24818-24825.
154. Rizzolio S, Tamagnone L: **Multifaceted role of neuropilins in cancer**. *Current medicinal chemistry* 2011, **18**(23):3563-3575.
155. Pellet-Many C, Frankel P, Evans IM, Herzog B, Junemann-Ramirez M, Zachary IC: **Neuropilin-1 mediates PDGF stimulation of vascular smooth muscle cell migration and signalling via p130Cas**. *The Biochemical journal* 2011, **435**(3):609-618.
156. Zhang L, Parry GC, Levin EG: **Inhibition of tumor cell migration by LD22-4, an N-terminal fragment of 24-kDa FGF2, is mediated by Neuropilin 1**. *Cancer research* 2013, **73**(11):3316-3325.
157. Osada H, Tokunaga T, Nishi M, Hatanaka H, Abe Y, Tsugu A, Kijima H, Yamazaki H, Ueyama Y, Nakamura M: **Overexpression of the neuropilin 1 (NRP1) gene correlated with poor prognosis in human glioma**. *Anticancer research* 2004, **24**(2B):547-552.
158. Snuderl M, Batista A, Kirkpatrick ND, Ruiz de Almodovar C, Riedemann L, Walsh EC, Anolik R, Huang Y, Martin JD, Kamoun W *et al*: **Targeting placental growth factor/neuropilin 1 pathway inhibits growth and spread of medulloblastoma**. *Cell* 2013, **152**(5):1065-1076.
159. Hayden Gephart MG, Su YS, Bandara S, Tsai FC, Hong J, Conley N, Rayburn H, Milenkovic L, Meyer T, Scott MP: **Neuropilin-2 contributes to tumorigenicity in a mouse model of Hedgehog pathway medulloblastoma**. *Journal of neuro-oncology* 2013, **115**(2):161-168.
160. Glinka Y, Mohammed N, Subramaniam V, Jothy S, Prud'homme GJ: **Neuropilin-1 is expressed by breast cancer stem-like cells and is linked to NF-kappaB activation and tumor sphere formation**. *Biochemical and biophysical research communications* 2012, **425**(4):775-780.
161. Hamerlik P, Lathia JD, Rasmussen R, Wu Q, Bartkova J, Lee M, Moudry P, Bartek J, Jr., Fischer W, Lukas J *et al*: **Autocrine VEGF-VEGFR2-Neuropilin-1 signaling promotes glioma stem-like cell viability and tumor growth**. *The Journal of experimental medicine* 2012, **209**(3):507-520.
162. Ellis LM: **The role of neuropilins in cancer**. *Molecular cancer therapeutics* 2006, **5**(5):1099-1107.
163. Miao HQ, Klagsbrun M: **Neuropilin is a mediator of angiogenesis**. *Cancer metastasis reviews* 2000, **19**(1-2):29-37.
164. Chaudhary B, Khaled YS, Ammori BJ, Elkord E: **Neuropilin 1: function and therapeutic potential in cancer**. *Cancer immunology, immunotherapy : CII* 2014, **63**(2):81-99.
165. Geretti E, Klagsbrun M: **Neuropilins: novel targets for anti-angiogenesis therapies**. *Cell adhesion & migration* 2007, **1**(2):56-61.
166. Jia H, Cheng L, Tickner M, Bagherzadeh A, Selwood D, Zachary I: **Neuropilin-1 antagonism in human carcinoma cells inhibits migration and enhances chemosensitivity**. *British journal of cancer* 2010, **102**(3):541-552.
167. Nasarre C, Roth M, Jacob L, Roth L, Koncina E, Thien A, Labourdette G, Poulet P, Hubert P, Cremel G *et al*: **Peptide-based interference of the transmembrane domain of neuropilin-1 inhibits glioma growth in vivo**. *Oncogene* 2010, **29**(16):2381-2392.
168. Raskopf E, Vogt A, Standop J, Sauerbruch T, Schmitz V: **Inhibition of neuropilin-1 by RNA-interference and its angiostatic potential in the treatment of hepatocellular carcinoma**. *Zeitschrift fur Gastroenterologie* 2010, **48**(1):21-27.
169. Patnaik A, LoRusso PM, Messersmith WA, Papadopoulos KP, Gore L, Beeram M, Ramakrishnan V, Kim AH, Beyer JC, Mason Shih L *et al*: **A Phase Ib study evaluating MNRP1685A, a fully human anti-NRP1 monoclonal antibody, in combination with bevacizumab and paclitaxel in patients with advanced solid tumors**. *Cancer chemotherapy and pharmacology* 2014, **73**(5):951-960.

170. Lu Y, Xiang H, Liu P, Tong RR, Watts RJ, Koch AW, Sandoval WN, Damico LA, Wong WL, Meng YG: **Identification of circulating neuropilin-1 and dose-dependent elevation following anti-neuropilin-1 antibody administration**. *mAbs* 2009, **1**(4):364-369.
171. Upraity S, Kazi S, Padul V, Shirsat NV: **MiR-224 expression increases radiation sensitivity of glioblastoma cells**. *Biochemical and biophysical research communications* 2014, **448**(2):225-230.
172. Gao XN, Lin J, Li YH, Gao L, Wang XR, Wang W, Kang HY, Yan GT, Wang LL, Yu L: **MicroRNA-193a represses c-kit expression and functions as a methylation-silenced tumor suppressor in acute myeloid leukemia**. *Oncogene* 2011, **30**(31):3416-3428.
173. Iliopoulos D, Rotem A, Struhl K: **Inhibition of miR-193a expression by Max and RXRalpha activates K-Ras and PLAU to mediate distinct aspects of cellular transformation**. *Cancer research* 2011, **71**(15):5144-5153.
174. Yu T, Li J, Yan M, Liu L, Lin H, Zhao F, Sun L, Zhang Y, Cui Y, Zhang F *et al*: **MicroRNA-193a-3p and -5p suppress the metastasis of human non-small-cell lung cancer by downregulating the ERBB4/PIK3R3/mTOR/S6K2 signaling pathway**. *Oncogene* 2015, **34**(4):413-423.

PUBLICATIONS

MiR-148a, a microRNA upregulated in the WNT subgroup tumors, inhibits invasion and tumorigenic potential of medulloblastoma cells by targeting Neuropilin 1

Kedar Yogi[1], Epari Sridhar[2], Naina Goel[6], Rakesh Jalali[4], Atul Goel[7], Aliasgar Moiyadi[3], Rahul Thorat[5], Pooja Panwalkar[1], Atul Khire[1], Archya Dasgupta[4], Prakash Shetty[3], and Neelam Vishwanath Shirsat[1]

[1] Shirsat Laboratory, Advanced Centre for Treatment, Research and Education in Cancer, Tata Memorial Centre, Kharghar, Navi Mumbai, India

[2] Department of Pathology, Advanced Centre for Treatment, Research and Education in Cancer, Tata Memorial Centre, Kharghar, Navi Mumbai, India

[3] Department of Surgical Oncology, Advanced Centre for Treatment, Research and Education in Cancer, Tata Memorial Centre, Kharghar, Navi Mumbai, India

[4] Department of Radiation Oncology, Tata Memorial Hospital, Tata Memorial Centre, Parel, Mumbai, India

[5] Laboratory Animal Facility, Advanced Centre for Treatment, Research and Education in Cancer, Tata Memorial Centre, Kharghar, Navi Mumbai, India

[6] Department of Pathology, Seth G. S. Medical College and K. E. M. Hospital, Parel, Mumbai, India

[7] Department of Neurosurgery, Seth G. S. Medical College and K. E. M. Hospital, Parel, Mumbai, India

Correspondence to: *Neelam Vishwanath Shirsat,* ***email***: *nshirsat@actrec.gov.in*

Keywords: Medulloblastoma, miR-148a, Neuropilin 1, invasion, WNT subgroup

Received: *November 17, 2014* ***Accepted***: *February 27, 2015* ***Published***: *March 2, 2015*

ABSTRACT

Medulloblastoma, a common pediatric malignant brain tumor consists of four molecular subgroups viz. WNT, SHH, Group 3 and Group 4. MiR-148a is over-expressed in the WNT subgroup tumors, which have the lowest incidence of metastasis and excellent survival among all medulloblastomas. MiR-148a was expressed either in a transient manner using a synthetic mimic or in a stable doxycycline inducible manner using a lentiviral vector in non-WNT medulloblastoma cell lines. Expression of miR-148a to levels comparable to that in the WNT subgroup tumors was found to inhibit proliferation, clonogenic potential, invasion potential and tumorigenicity of medulloblastoma cells. MiR-148a expression in medulloblastoma cells brought about reduction in the expression of NRP1, a novel miR-148a target. Restoration of NRP1 expression in medulloblastoma cells was found to rescue the reduction in the invasion potential and tumorigenicity brought about by miR-148a expression. NRP1 is known to play role in multiple signaling pathways that promote tumor growth, invasion and metastasis. NRP1 expression in medulloblastomas was found to be associated with poor survival, with little or no expression in majority of the WNT tumors. The tumor suppressive effect of miR-148a expression accompanied by the down-regulation of NRP1 makes miR-148a an attractive therapeutic agent for the treatment of medulloblastomas.

INTRODUCTION

Brain tumors are the most common solid tumors in children. Medulloblastomas account for about 20% of all primary brain tumors in children. Standard treatment includes surgical resection, followed by cranio-spinal radiation and chemotherapy. Advances in surgical and radiation techniques have improved the 5-year survival rate to about 80% for average risk patients and 55-76% for high risk patients [1]. Genome wide expression profiling

studies have identified four core molecular subgroups of medulloblastomas called WNT, SHH, Group 3 and Group 4 [2]. WNT and SHH subgroup tumors appear to result from the constitutive activation of WNT and SHH signaling pathways respectively, based on their expression profiles as well as their mutational landscape [2, 3]. Group 3 and Group 4 tumors have overlapping gene expression profiles. MYC over-expression/amplification and expression of the photoreceptor signaling pathway genes is a characteristic of most Group 3 tumors while Group 4 tumors are characterized by the expression of various neuronal differentiation related genes [2, 4]. The four molecular subgroups also vary in clinical characteristics like age related incidence, presence of metastasis and survival. Group 3 tumors have the highest incidence of metastasis at diagnosis and poor overall survival. WNT subgroup medulloblastomas on the other hand have the lowest incidence of metastasis at diagnosis (< 10%) and highest survival (90% - 95% ten year overall survival) among all the four subgroups [5].

We have earlier reported that WNT subgroup tumors have a distinctive microRNA profile with a number of miRNAs over-expressed in these tumors as compared to other medulloblastoma subgroups as well as normal cerebellar tissues [4]. Further, over-expression of miR-193a-3p, miR-224, miR-148a, miR-23b, and miR-365 in the WNT subgroup tumors was validated in a study done on 103 medulloblastomas [6]. While miR-148a is upregulated in the WNT subgroup medulloblastomas, it is known to be downregulated as a result of promoter hypermethylation in various cancers and has been shown to act as tumor-suppressive/ metastasis suppressive miRNA [7, 8]. It is therefore likely that miR-148a contributes to lower metastatic incidence and excellent survival of the WNT subgroup medulloblastomas. In order to understand role of miR-148a in medulloblastoma biology, effect of miR-148a expression on the growth and malignant behavior of established medulloblastoma cell lines was investigated in the present study.

RESULTS

MiR-148a expression was studied in a total of 141 medulloblastoma tumor tissues (including 103 cases reported earlier) by real time RT-PCR analysis. The tumor tissues were molecularly classified using a panel of 12 protein-coding genes and 9 miRNAs for molecular classification as described before [6]. WNT subgroup medulloblastomas were found to over express miR-148a by 6-12 fold ($p < 0.0001$) as compared to

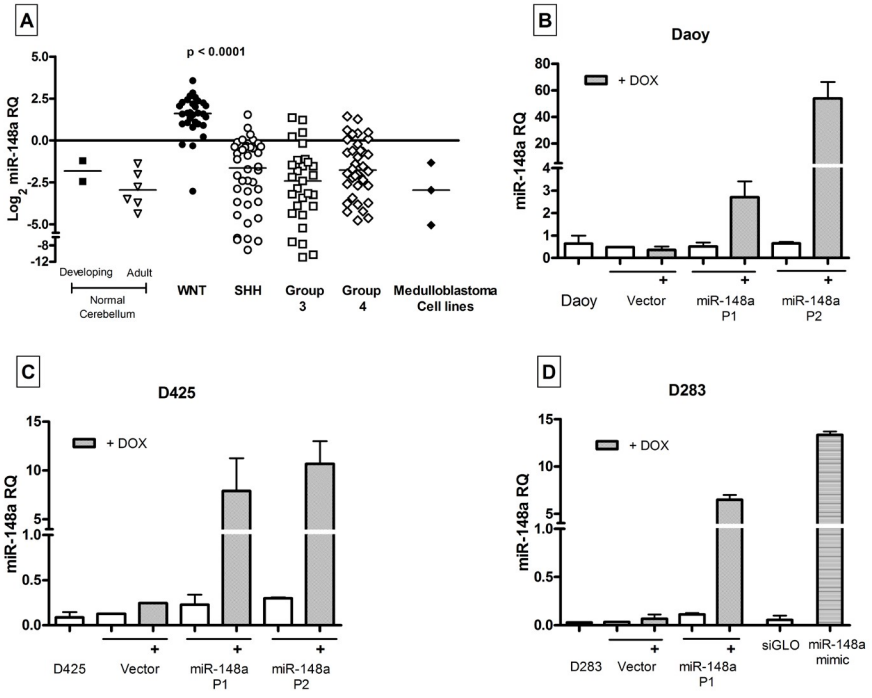

Figure 1: Expression levels of miR-148a across four molecular subgroups of medulloblastoma, cell lines and miR-148a expressing stable polyclonal populations, as determined by real time RT-PCR assay. (A) miR-148a levels were evaluated in 141 medulloblastoma tissues classified in the four molecular subgroups, normal developing (from less than 1year old infants) cerebellar tissues and adult (from individuals >21 yr of age) cerebellar tissues. (B, C, D) Relative Quantity of miR-148a in the indicated medulloblastoma cell line and its polyclonal populations transduced with pTRIPZ control lentiviral vector (Vector) or pTRIPZ-miR-148a construct expressing miR-148a in doxycycline inducible manner (P1, P2) and in the cells transiently transfected with control siGLO or miR-148a mimic . + DOX: doxycycline induced.

the other subgroup tumors, 10-20 fold as compared to normal cerebellar tissues and 7-100 fold as compared to the established medulloblastoma cell lines (Figure 1A). In order to understand the role of miR-148a in medulloblastoma biology, medulloblastoma cell lines were transduced with pTRIPZ lentiviral vector expressing miR-148a in doxycycline inducible manner. D425 and D283 cell lines belong to Group 3, Group 3/Group 4 medulloblastoma subgroup respectively while Daoy cell line belongs to SHH subgroup based on their cytogenetic profiles [9, 10] and expression profiles (data not shown).

Effect of miR-148a expression on the growth of medulloblastoma cells studied using MTT assay

Stable polyclonal populations (P1, P2) of medulloblastoma cell lines Daoy and D425 expressing miR-148a in doxycycline inducible manner were selected in the presence of puromycin. Doxycycline treatment of polyclonal population P1 of Daoy cells resulted in the induction of miR-148a expression to a level (RQ: 2.0-4.0) comparable to that in the WNT subgroup tumor tissues while doxycycline induction of P2 polyclonal populations resulted in higher miR-148a expression in the range of RQ: 45-55 (Figure 1B). The effect of miR-148a expression on the growth of the medulloblastoma cell lines was studied over a period of 12 days by MTT assay. Doxycycline induced miR-148a expression resulted in 30-35% and 42-45% growth inhibition of P1 and P2 population respectively (Figure 2A, Supplementary Fig. S1A). Doxycycline induction of P1 and P2 polyclonal populations of D425 cells resulted in the miR-148a expression levels in the range of 5-10 RQ (Figure 1C). MiR-148a expression was found to result in 57-64% growth inhibition of D425 cells (Figure 2A, Supplementary Figure S1B). Thus, miR-148a expression significantly ($p < .0001$) inhibited growth of both the medulloblastoma cell lines studied.

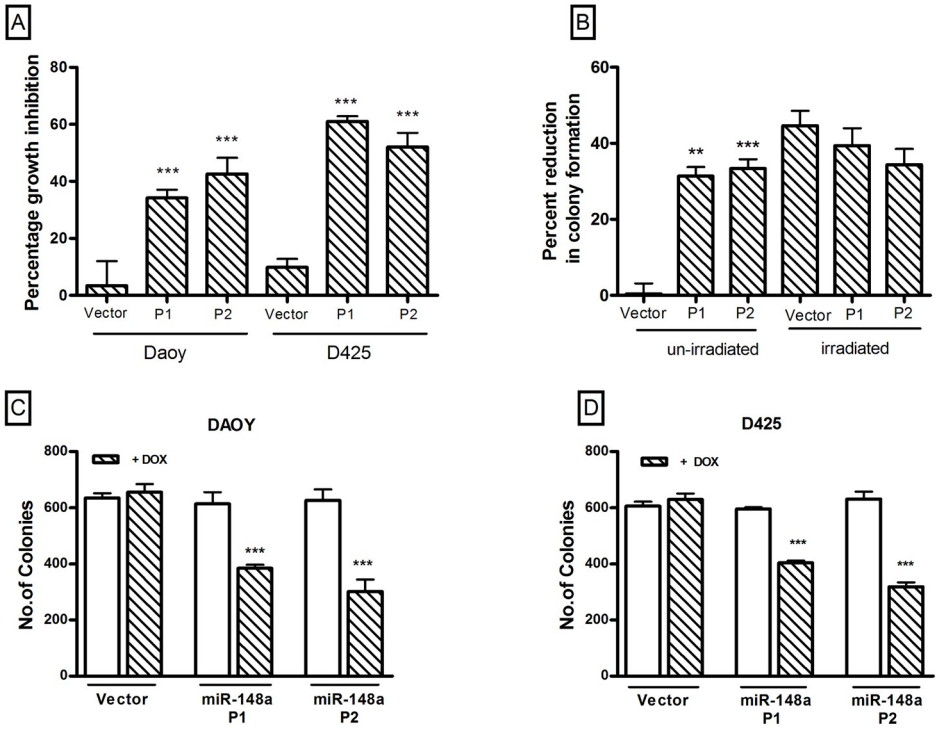

Figure 2: Effect of miR-148a expression on growth, clonogenic potential and, anchorage independent growth of medulloblastoma cell lines studied using stable polyclonal populations (P1, P2) of Daoy and D425 cells expressing miR-148a on doxycycline induction. (A) Y axis denotes percentage growth inhibition obtained on doxycycline induction of the vector control and P1, P2 polyclonal populations of the indicated cell line as judged by the MTT assay. (B) Y axis indicates percent reduction in the number of colonies formed on doxycycline induction of the vector control and P1, P2 population cells of Daoy cells and percent reduction in the number of colonies formed on irradiation of doxycycline induced indicated population, in a clonogenic assay. (C, D) Y axis denotes the number of colonies formed in a soft agar assay by the vector control and P1, P2 population of the indicated cell line. The significance of the difference in the growth inhibition or soft agar colony formation observed on doxycycline induction of the polyclonal populations expressing pTRIPZ-miR-148a as compared to that observed in the polyclonal population transfected with control pTRIPZ vector was calculated by the student's t test. ** indicates $p < 0.001$ while *** indicates $p < 0.0001$ as determined using Student's t test.

Effect of miR-148a expression on clonogenic potential, radiation sensitivity, and anchorage-independent growth of medulloblastoma cell lines.

The effect of miR-148a expression on the clonogenic potential and radiation sensitivity was studied using clonogenic assay. MiR-148a expression in Daoy cells was found to reduce clonogenic potential of Daoy cells by 35-40% as studied using both the P1 and P2 polyclonal populations (Figure 2B). Irradiation of vector control cells at a dose of 4 Gy reduced their clonogenic potential by 40-50% with or without doxycycline treatment. Irradiation of Doxycycline induced P1 and P2 population was found to reduce clonogenic potential further by 33-47% (Figure 2B). Thus, miR-148a expression although did not increase radiation sensitivity per se, the combined effect of miR-148a and radiation brought about 80-90% reduction in the clonogenic potential of Daoy cells.

The effect of miR-148a expression on the anchorage-independent growth of medulloblastoma cells was studied by soft agar colony formation assay. The

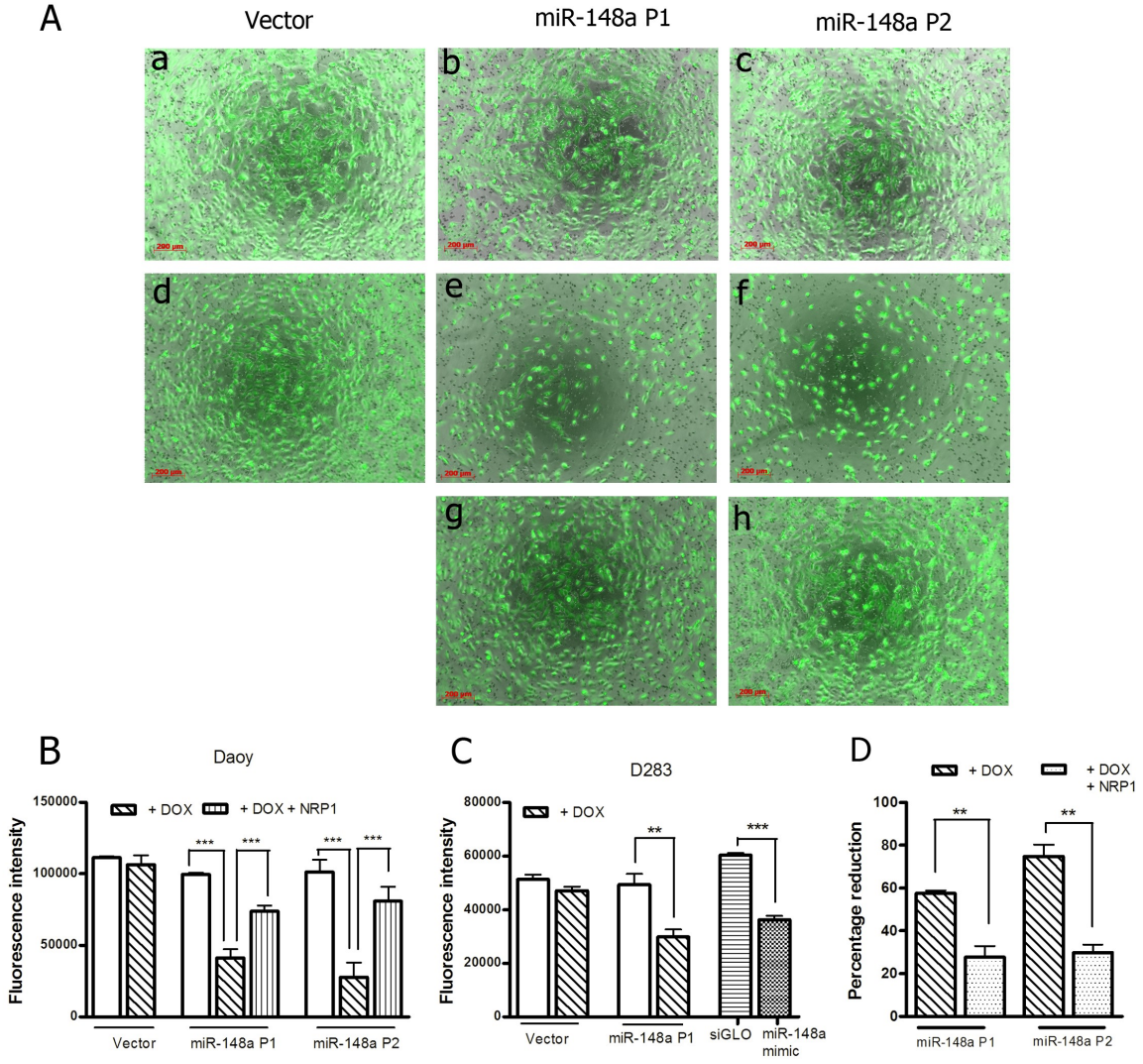

Figure 3: Effect of miR-148a expression on the invasive potential of Daoy and D283 cell lines. Invasion potential was determined by studying migration through matrigel coated 8-µm pore size transwell inserts. The study was done using the stable polyclonal populations (P1, P2) of Daoy and D283 cells expressing miR-148a on doxycycline induction. (A) Representative images of the Calcein, AM labeled cells on the lower side of the transwell chamber membrane 36 h after seeding the indicated polyclonal populations of Daoy cells onto the transwell insert, with (d, e & f) or without (a, b & c) induction of miR-148a expression and after restoration of NRP1 expression (g, h) in doxycycline induced cells. (B-C) Y axis denotes the total fluorescence intensity of the invaded cells normalized to the total intensity of the initial cell number seeded of the indicated cell populations. (D) Y axis indicates the percent reduction in the fluorescence of the invaded cells of the indicated stable polyclonal populations on doxycycline induction (+DOX) of Daoy P1 and P2 population cells with (+NRP1) or without restoration of NRP1 expression. ** indicates $p < 0.001$; *** indicates $p < 0.0001$.

number of soft agar colonies formed by P1 and P2 Daoy cell populations was found to be reduced by 30-45% upon doxycycline induction of miR-148a expression (Figure 2C). The reduction in the soft agar colony formation is comparable to the reduction in the clonogenic potential upon miR-148a expression in Daoy cells. Therefore, miR-148a expression was not found to have significant effect on the anchorage-independent growth potential.

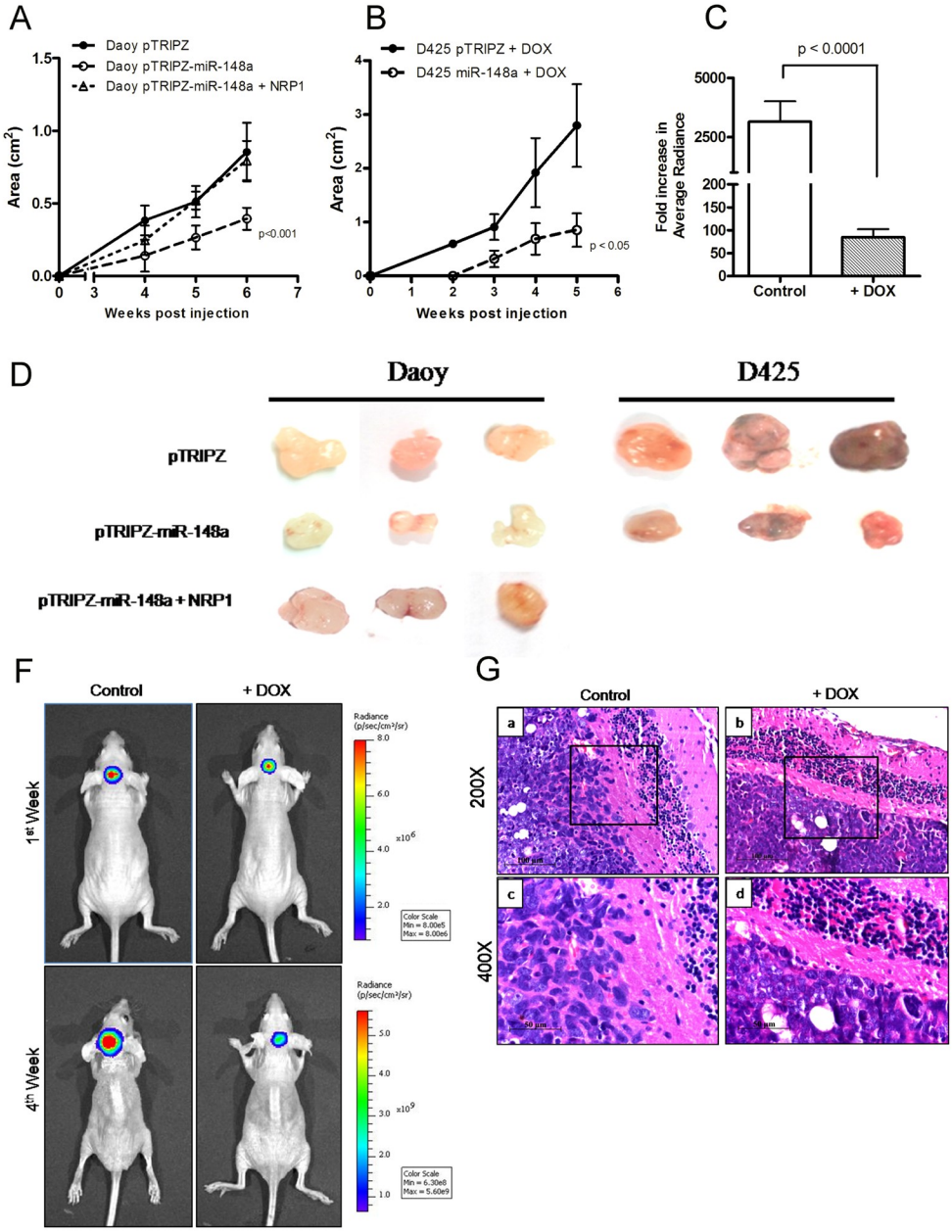

Figure 4: Effect of miR-148a expression on tumorigenicity of medulloblastoma cells. (A-B) Y axis denotes the area of subcutaneous tumors formed over a period of 4-6 weeks in nude mice, post injection of doxycycline induced Daoy or D425 P2 polyclonal population (pTRIPZ-miR-148a) and vector (pTRIPZ) control population and after restoration of NRP1 expression in doxycycline induced P2 population of Daoy cells (n = 6 each). (D) shows photographs of these subcutaneous tumors. (F) shows bioluminescence images of nude mice orthotopically injected with D283 stable polyclonal population P1 expressing miR-148a upon doxycycline (DOX) induction and, firefly luciferse under CAG promoter. The images were captured on 1st and 4th week after the injection. (C) Y axis shows relative fold increase in the average radiance on 4th week as compared to that on 1st week after injection of D283 cells P1 population with (+DOX) or without doxycycline induction (Control) in 7 mice each. (G) shows photographs of hematoxylin-eosin stained paraffin sections of the orthotopic xenografts of control and doxycycline induced D283 cells P1 population. The area marked with rectangle in a & b shows invading margins of the tumor cells in the control and doxycycline induced miR-148a expressing cells; c & d show magnified images (400 X) of the invading margins indicated by rectangles in a & b.

Clonogenic potential of D425 cells was studied by soft agar assay as they grow in a semi-suspension manner. Polyclonal populations P1 and P2 of D425 cells showed reduction in the soft agar colony formation by 30-50% upon miR-148a expression (Figure 2D). Thus, miR-148a expression was found to bring about significant ($p < 0.0001$) reduction in the clonogenic potential of both the medulloblastoma cell lines studied.

Effect of miR-148a expression on *in vitro* invasion potential of medulloblastoma cell lines

Effect of miR-148a expression on the invasion potential of medulloblastoma cells was evaluated by studying invasion of the cells through Matrigel™ coated membranes in transwell inserts. MiR-148a expressing polyclonal populations P1 and P2 of Daoy cell line

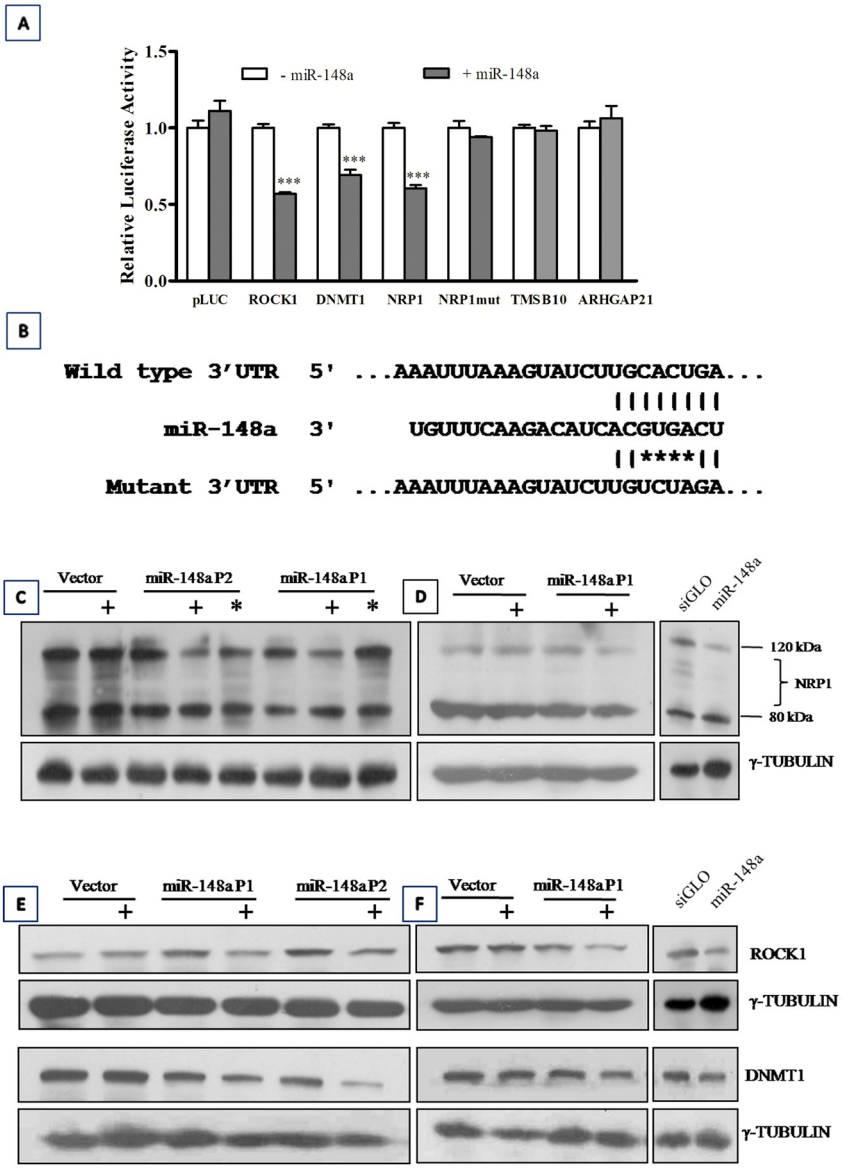

Figure 5: Identification of miR-148a targets. Y-axis denotes Luciferase activity of 293 FT cells transfected with the construct having 3'-UTR region of the indicated gene cloned downstream luciferase cDNA in a pcDNA 3.0 vector and EGFP expressing vector with or without pcDNA 3.0 construct expressing miR-148a. The luciferase activity is expressed relative to the GFP fluorescence. *** indicates $p < 0.0001$. (B) Schematic diagram shows miR-148a target site in NRP1 3'-UTR and position of the mutations (indicated by asterisk) introduced in the target site by site directed mutagenesis. (C, D, E, F) Western blot analysis shows reduction in the expression levels of NRP1, ROCK1 and DNMT1 protein in stable polyclonal populations of Daoy (C, E) and D283 (D, F) cells on doxycycline induction of miR-148a expression. γ-tubulin was used as a loading control. +: Doxycycline induction; * indicates exogenous expression of NRP1 in doxycyline induced cells.

showed 60-70% reduction in the invasion potential upon doxycycline induced miR-148a expression (Figure 3A, B, D). D425 cells were not found to have significant invasion ability through Matrigel™ as studied over a period of 48 h. Therefore, the effect of miR-148a expression on the invasion potential was studied using D283 cells. Stable polyclonal population P1 of D283 cells expressing pTRIPZ-miR-148a was found to express miR-148a at RQ 6-7 on doxycycline induction while transient transfection with miR-148a mimic in D283 cells resulted in miR-148a expression at RQ 12-13.5 (Figure 1D). MiR-148a expression either in a stable inducible manner or in a transient manner using a synthetic miR-148a mimic, showed a reduction in the invasion potential of D283 cells by about 35-43% (Figure 3C).

Effect of miR-148a expression on *in vivo* tumorigenicity and *in vivo* invasion potential of medulloblastoma cells

In order to study the effect of miR-148a expression on tumorigenicity of medulloblastoma cells, miR-148a expressing polyclonal populations of Daoy and D425 cells were injected subcutaneously in immunodeficient BALB/c Nude mice. Subcutaneous injection of 5 X 10^6 D425/Daoy cells resulted in tumors of measurable size by 2nd and 4th week of injection respectively. MiR-148a expression brought about 45-60% reduction ($p < 0.05$) in the tumor forming ability of Daoy cell P2 population (Figure 4A, D). Doxycycline induction of miR-148a expression in P2 population of D425 cells was found to bring about 50-80% reduction ($p < 0.05$) in the size of the tumors formed (Figure 4B, D).

D283 polyclonal population P1 cells, engineered to express firefly luciferase, were injected stereotactically in cerebellum of nude mice with or without doxycycline induction of miR-148a expression. Figure 4C, 4F show ~25 fold reduction ($p < 0.0001$) in the bioluminescence (average radiance) of the tumors formed on induction of miR-148a expression as determined by *in vivo* imaging. Therefore, miR-148a expression was found to decrease tumorigenicity in all the three medulloblastoma cell lines studied. The tumor margin of doxycycline induced (+DOX) miR-148a expressing D283 cells in the cerebellar cortex was cohesive and distinct from the adjacent

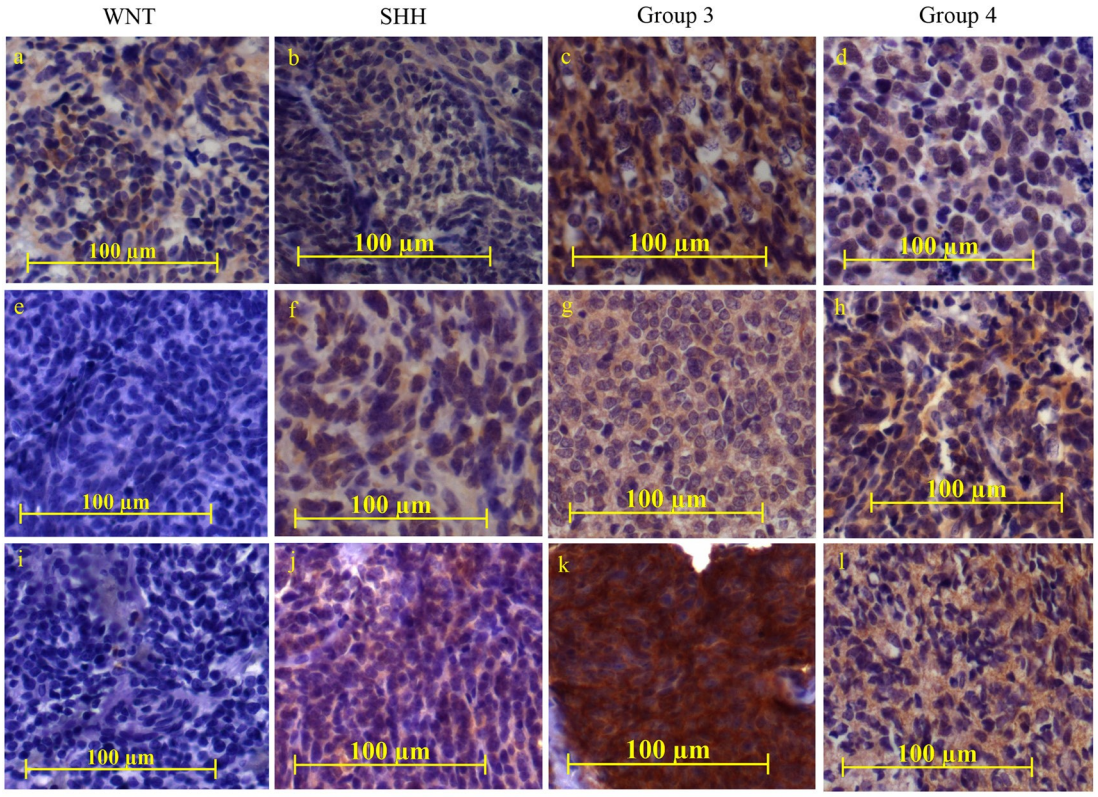

Figure 6: Immunohistochemical analysis of NRP1 expression in medulloblastoma tumor tissues. NRP1 expression was studied in FFPE tissue sections belonging to the four molecular subgroups (WNT, SHH, Group 3, Group 4). The staining was scored as 'negative' for complete absence of staining, 'Low' for weak intensity and focal positive (~10-20% cells positive) areas, 'Moderate' for moderate intensity and more than or equal to 50% positive area while, 'High' for high intense staining in more than 80% of area. Representative images of NRP1 staining in the medulloblastoma tissues scored as negative (e, i), low (a, b, d, f, h), moderate (c, g, j, l) and high intense staining (k) respectively.

cerebellar cortex (Figure 4G, B, D). On the other hand, tumor margin of the control D283 cells was much more non-cohesive having loosely spaced cells indicating invasive phenotype (Figure 4G, A, C). Thus, miR-148a expression not only reduced tumorigenicity but also *in vivo* invasion potential of D283 medulloblastoma cells.

Identification of protein-coding gene targets of miR-148a by Luciferase reporter assay and validation by western blot analysis

In order to identify miR-148a target genes instrumental in bringing about miR-148a mediated inhibition of invasion and tumorigenic potential, three protein coding genes *viz. NRP1*, *ARHGAP21*, *TMSB10* were investigated as potential miR-148a targets. These genes were predicted as miR-148a targets by the target prediction program, TargetScan 5.01 and were short-listed for experimental validation based on the presence of conserved target site, expression of the target gene in normal cerebellum and medulloblastoma tissues and their known role in invasion/metastasis. 3'-Untranslated regions (3'-UTR) of the putative target genes *viz*. *NRP1*, *ARHGAP21*, *TMSB10* and two known miR-148a target genes *ROCK1* and *DNMT1* were cloned downstream to luciferase cDNA in the reporter vector. Luciferase activity of the cells expressing *ROCK1*, *DNMT1* and *NRP1* constructs was found to be reduced by 30-50% ($p < 0.0001$) in the presence of miR-148a expression (Figure 5A) while there was no significant reduction in the luciferase activity of the cells expressing *ARHGAP21*, *TMSB10* constructs. To further confirm *NRP1* as a miR-148a target, miR-148a binding site in the *NRP1* 3'UTR region was mutated by site directed mutagenesis as shown in Figure 5B. The cells expressing *NRP1* 3'UTR mutant construct failed to show reduction in the luciferase activity in the presence of miR-148a.

Western blot analysis showed reduction in the protein levels of NRP1, ROCK1 and DNMT1 in miR-148a expressing P1, P2 populations of Daoy cells and P1 polyclonal population of D283 cells as well as in D283 cells transiently transfected with miR-148a mimic (Figure 5C, D, E, F). The protein levels of the full length 120 kDa NRP1 isoform decreased on miR-148a expression. However, protein levels of the ~ 80 kDa NRP1 isoform were not altered on miR-148a expression. This observation was confirmed in a human glioma cell line U373 that expresses both 120 kDa and 80 kDa NRP1 isoforms at higher levels (Supplementary Figure S2). Since miR-148a targets the 3'-UTR of NRP1 it is likely that the ~80 kDa isoform is not targeted by miR-148a since it lacks the 3'-UTR. Real time RT-PCR analysis was performed using primers for total *NRP1* mRNA expression (all known NRP1 isoforms) as well as primers specific for the 3'-UTR of the full length isoform and primers specific for the transmembrane (TM) region. Relative quantities of NRP1 as estimated using the 3'-UTR specific primers or TM domain specific primers was found to be almost 50% of the total NRP1 expression level in both Daoy and D283 cell line (Supplementary Figure S3A, B). The protein levels of the 120 kDa isoform were also estimated to be about 50% and 30% of the total NRP1 protein levels in Daoy and D283 cell line respectively (Supplementary Figure S3C). Therefore, miR-148a appears to target only the full length NRP1 isoform and not the 80 kDa isoform as it lacks the 3'-UTR.

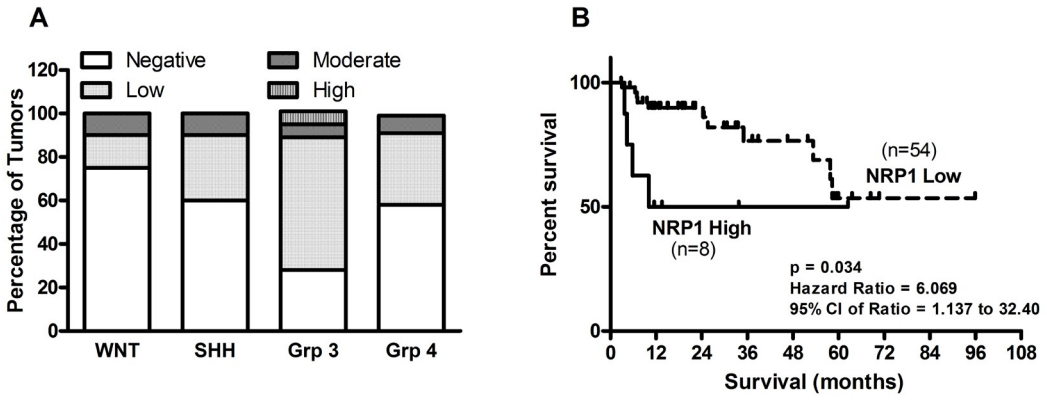

Figure 7: Expression of NRP1 across the four molecular subgroups of medulloblastomas. (A) Percentage distribution of medulloblastoma tissues having NRP1 expressed scored as negative, low, moderate or high is shown across the four subgroups of medulloblastomas. (B) Kaplan Meier survival analysis of 62 medulloblastoma patients segregated into two groups based on NRP1 expression. "NRP1 low" group includes medulloblastoma tissues with no or low NRP1 expression while "NRP1 high" group includes tumor tissues with moderate or high NRP1 expression .

Reversal of miR-148a mediated reduction in invasion potential and tumorigenicity of medulloblastoma cells upon exogenous NRP1 expression.

MiR-148a expressing polyclonal populations P1 and P2 of Daoy cell line were transfected with a construct expressing NRP1 under Phosphoglycerate kinase 1 (PGK1) promoter (a kind gift from Dr. Lena Claesson-Welsh, Uppsala Universitet, Uppsala, Sweden). The parental P1, P2 miR-148a expressing populations showed 60-80% reduction in the invasion potential as judged by the invasion of the cells through matrigel coated transwell inserts. On the other hand, the P1, P2 polyclonal population cells with exogenous NRP1 expression showed only marginal (~20%) reduction in the invasion potential upon doxycycline induced miR-148a expression (Figure 3A, B, D, G, H). Thus, restoration of NRP1 expression rescued the reduction in the invasion potential brought about by miR-148a expression, indicating the role of NRP1 in the invasion ability of medulloblastoma cells. Further, on subcutaneous injection, P2 polyclonal population of Daoy cells transfected with the NRP1 cDNA construct formed tumors of size comparable to that of the control vector cells after doxycycline induction of miR-148a expression (Figure 4A, D). Thus, NRP1 expression was found to rescue the reduction in tumorigenicity brought about by miR-148a expression indicating major role for NRP1 in miR-148a mediated tumorigenicity inhibition.

NRP1 expression in medulloblastomas and its correlation with molecular subgroups and, survival

NRP1 expression was studied in a total of 93 medulloblastoma formalin fixed paraffin embedded (FFPE) tumor tissues by immunohistochemical analysis. Figure 6 shows representative photographs of NRP1 expression in medulloblastoma tissues belonging to the four molecular subgroups. Majority (75%) of the WNT subgroup medulloblastomas showed no detectable NRP1 expression, while only 23% Group 3 tumors lacked NRP1 expression (Figure 7A). Kaplan Meier survival analysis of 62 medulloblastoma cases, showed that tumors with moderate or high NRP1 expression had significantly poorer overall survival ($p = 0.0349$; hazard ratio 6.06) than those having no detectable or low NRP1 expression (Figure 7B).

DISCUSSION

MiR-148a expression has been shown to be downregulated in various cancers including hepatocellular carcinoma, breast cancer, prostate cancer, pancreatic cancer, gastric cancer, non-small cell lung cancer, advanced colorectal cancer, adult acute lymphoblastic leukemia as well as in cancer associated fibroblasts in endometrial cancer [7, 8, 11]. Hypermethylation of CpG island in the miR-148a promoter region has been found to bring about downregulation of miR-148a expression in many cancers [7]. Expression of miR-148a at levels comparable to those in the WNT subgroup medulloblastomas or higher was found to inhibit growth and bring about reduction in the clonogenic potential, invasion potential and tumorigenicity of medulloblastoma cells belonging to the three subgroups *viz*. SHH, Group 3 and Group 4. MiR-148a expression has been reported to reduce growth, tumorigenic potential and invasion potential of various cancer cells including HBx expressing hepatocarcinoma cells, gastric cancer cells, pancreatic cancer cell lines and prostate cancer cell lines [11-14]. Recently miR-148a has also been reported to inhibit glioma stem cell-like properties and tumorigenicity [15, 16]. Thus, tumor suppressive effect of miR-148a expression in medulloblastoma cells is consistent with its role in other cancers.

Expression of ROCK1 and DNMT1, two known miR-148a targets, was found to be downregulated upon miR-148a expression in medulloblastoma cells [17, 18]. Rho-ROCK signaling cascade plays a major role in the re-organization of cytoskeleton during cell migration, adhesion, and cytokinesis [18]. Downregulation of DNMT1 expression has been shown to reduce tumor incidence in the *Ptch1* heterozygous knock-out mice, a mouse model of SHH subgroup medulloblastomas [19]. Downregulation of ROCK1 and DNMT1 upon miR-148a expression is therefore likely to contribute to miR-148a's tumor-suppressive effect on medulloblastoma cells.

Neuropilin 1 (NRP1) was identified as a novel target of miR-148a in the present study. 3'-UTR of the full length NRP1 transcript contains a single 8-mer miR-148a target site which is conserved among vertebrates (www.targetscan.org). Luciferase reporter assay validated NRP1 as a miR-148a target. Western blot analysis showed downregulation of full length NRP1 protein (120 kDa isoform) on miR-148a expression in multiple cell lines including Daoy, D283, medulloblastoma cell lines and U373 glioblastoma cell line, further confirming NRP1 as a miR-148a target. NRP1 gene encodes multiple alternately spliced transcripts. 5882 bp CCDS7177 transcript encodes 923 amino acid long full length protein whose 3'-UTR contains the miR-148a target site (ncbi.nlm.nih.gov/gene). Shorter CCDS31179, CCDS31180 transcripts encode 609 and 644 amino acid long proteins respectively, that lack the 3'-UTR as well as the transmembrane domain. These isoforms encode soluble NRP1 forms that have been shown to act as antagonists of the full length membrane bound NRP1 protein [20]. The 80 kDa NRP1 protein levels did not change upon miR-148a expression as judged

by the western blot analysis. Therefore, it most likely belongs to the soluble NRP1 isoforms based on both its size and the real time RT-PCR analysis that shows the contribution of the shorter soluble isoforms to the total NRP1 expression levels. Thus, miR-148a targets only the functionally active full length NRP1 isoform and not the soluble isoforms that act as antagonist of NRP1 activity.

NRP1 is a single pass trans-membrane protein, which was first identified as a ligand binding co-receptor of Semaphorin 3A that plays a role in axon patterning in nervous system development [21, 22]. Subsequently, it was shown to act as a co-receptor of VEGF-A_{165} and other isoforms of VEGF that promote blood vessel growth during normal vasculature development and during angiogenesis in tumor progression [23]. NRP1 has also been reported to act as a co-receptor of multiple growth factors like TGF-beta 1, HGF, EGF and PDGF [24-28]. NRP1 has been reported to be over-expressed in various cancers including breast, prostate, pancreatic, colon, gliomas and its expression has been reported to correlate with poor prognosis [21, 29, 30]. In the present study, majority (75%) of the WNT subgroup medulloblastomas lacked detectable NRP1 expression. This observation is consistent with the high miR-148a expression in the WNT subgroup medulloblastomas as well as the low incidence of metastasis and excellent survival of the WNT subgroup patients [5, 6]. Majority of the Group 3 tumors which are known to have the worse survival among the four medulloblastoma subgroups expressed NRP1. Further, Kaplan-Meier survival analysis showed NRP1 expression in medulloblastomas to be associated with worse survival. Hence, NRP1 expression is a useful marker for prognostication in medulloblastomas.

Recently, Snuderl *et al* have reported that Placental Growth Factor (PIGF)-NRP1 signaling is necessary for growth and spread of medulloblastomas [31]. Inhibition of PIGF-NRP1 signaling was found to result in regression of medulloblastoma xenografts, decreased metastasis and increased survival of mice. NRP1 has been shown to promote epithelial mesenchymal transition and increase motility of endothelial cells as well as cancer cells by regulating TGF-beta, integrin and HGF/c-Met signaling [25, 32]. Downregulation of NRP1 expression has been shown to inhibit motility of medulloblastoma cells from *Ptch1* (+/-) mice [33]. Autocrine VEGF-VEGFR2-NRP1 signaling has also been reported to promote cancer stem cell maintenance in glioblastoma while NRP1 expression in breast cancer stem cells has been shown to be linked with the activation of NF-kB signaling [34, 35]. NRP1 has been shown to act as a co-receptor in multiple signaling pathways that promote tumor growth and progression [36]. Besides, the role of NRP1 in promoting tumor angiogenesis is very well established [37]. NRP1 has therefore been identified as an attractive therapeutic target for various cancers. In the present study as well, NRP1 expression was found to bring about almost complete rescue of miR-148a mediated inhibition of the invasion potential and tumorigenicity of medulloblastoma cells. This indicates major role for NRP1 in miR-148a's tumor-suppressive effect on medulloblastoma cells. Therefore, miR-148a mediated down-regulation of NRP1 could be an effective therapeutic strategy for the treatment of medulloblastomas as well as other cancers.

A number of approaches have been explored for targeting NRP1 including siRNAs against NRP1, anti-NRP1 antibodies, peptides targeting NRP1, and soluble NRP1 antagonists [38, 39]. NRP1 siRNAs or anti-NRP1 peptides have been shown to inhibit tumor growth, angiogenesis and metastasis in several cancers including hepatocellular carcinoma and glioblastoma [40-42]. Anti-NRP1 humanized monoclonal antibody MNRP1685A has been introduced in clinical trial for the treatment of various advanced solid tumors in combination with bevacizumab [43]. Circulating NRP1 is abundantly found in human plasma that is contributed by soluble NRP1 as well as the extracellular domain shed from the membrane bound full length isoform [44]. Therefore, any inhibitor that targets NRP1 protein would also target these soluble isoforms and hence would be required in large amounts for therapeutic effectiveness. However, since miR-148a targets only the NRP1 full length mRNA and not the soluble isoforms, it is likely to serve as a more effective strategy for targeting NRP1.

MiR-148a is expressed in normal tissues and its expression is known to be lost in several cancers often as a result of promoter hypermethylation [7]. MiR-148a expression at physiological levels showed tumor suppressive effect on medulloblastoma cells. Therefore, miR-148a as a therapeutic agent is unlikely to be toxic to normal tissues. MiR-148a was found to bring about tumor-suppressive effect by targeting NRP1, ROCK1 and DNMT1. These targets are distinct from those of other tumor-suppressive miRNAs like miR-34a and let-7a that are being explored for their therapeutic potential (www.mirnarx.com) [45]. MiR-148a is therefore an attractive therapeutic agent for the treatment of medulloblastomas as well as other cancers.

MATERIALS AND METHODS

Cell culture

Human medulloblastoma cell lines Daoy and D283 were obtained from ATCC, Manassas, VA, USA. Authenticity of the cell lines was confirmed by the Short Tandem Repeat (STR) marker profiling. Medulloblastoma cell line D425 was a kind gift from Dr. Darell Bigner (Duke University Medical Centre, Durham, NC, USA). The cells were grown in Dulbecco's Modified Eagle Medium: Nutrient Mixture F-12 (DMEM/ F-12)

supplemented with 10% Fetal Bovine Serum (FBS) (Life Technologies, Carlsbad, CA, USA) in a humidified atmosphere of 5% CO2. HEK293 FT cells were obtained from Life Technologies, Carlsbad, CA, USA and were grown in Dulbecco's Modified Eagle Medium (DMEM) supplemented with 10% FBS.

Tumor tissues

Medulloblastoma tumor tissues were obtained with the approval of the Institutional Review Board. All the medulloblastoma cases studied were treated as per the standard practices with surgery followed by radiation (with the exception of less than 3 yr old children) and chemotherapy. The normal human cerebellar tissues were obtained from the Human Brain Tissue Repository at the National Institute of Mental Health and Neurosciences (NIMHANS), Bangalore, India.

Transfection of medulloblastoma cells with synthetic miRNA mimics

D283 cells were transfected with 50 nM of miR-148a mimic, or siGLO (a RISC-free control siRNA) or siRNA negative control (Dharmacon, Thermo Scientific, Lafayette, CO, USA) as per the manufacturer's protocol for a period of 48 h using Dharmafect-2 transfection reagent. The transfected cells were seeded for various assays after 72 h. MiRNA levels in the transfected cells were estimated by real time Reverse Transcription-Polymerase Chain Reaction (RT-PCR) analysis using *RNU48* as an endogenous control.

Transduction of medulloblastoma cells with miRNA expressing lentiviral vectors

Genomic region encoding miR-148a was amplified from normal human lymphocyte DNA by Polymerase Chain reaction (PCR) and cloned in a pTRIPZ lentiviral vector (Open Biosystems, Thermo Scientific, Lafayette, CO, USA) downstream of doxycycline-inducible minimal Cytomegalo virus (CMV) promoter. The nucleotide sequences of the primers used for amplification are given in Supplementary Table 1. Daoy, D425 and D283 medulloblastoma cell lines were transduced with pTRIPZ-miR-148a lentiviral particles and stable polyclonal populations were selected in the presence of puromycin. The cells transduced with lentiviral particles of empty pTRIPZ vector or pTRIPZ-NT vector expressing non-targeting shRNA (Open Biosystems, Thermo Scientific, Lafayette, CO, USA) were used as a control.

Real time RT-PCR analysis and Molecular Classification of Medulloblastomas

MiR-148a expression in the transfected cells was determined by real time RT-PCR analysis using the Taqman assay (Applied Biosystems, Thermo Scientific, Lafayette, CO, USA) with *RNU48* as a control house-keeping small RNA. Relative quantification of the expression levels of *NRP1* was done by SYBR Green real time RT-PCR assay using *GAPDH* as a house-keeping control gene. Relative Quantity (RQ) was estimated as $RQ = 2^{-(Ct_{test} - Ct_{control})} X\ 100$. The primers for real time PCR were designed such that they corresponded to two adjacent exons of the gene (Supplementary Table 1). In case the primers belonged to a single exon, the RNA was treated with RNase-free DNase before reverse transcription. Molecular classification of FFPE tumor tissues was carried out using real time RT-PCR as described before [6].

MTT reduction assay

Growth of miRNA expressing cells and control cells was studied by MTT [2-(4,5-dimethyl-2-thiazolyl)-3,5-diphenyl-, bromide] reduction assay. 500 or 1500 cells of Daoy and D425 cell lines respectively, were seeded per well of a 96-well micro-titer plate [46]. Cell growth was followed over a period of 12 days with replenishment of the medium every 3rd day. 20 µl of MTT (5 mg/ml) was added to each well at the end of the incubation period and the cells were incubated further for a period of 4 h. 100 µl of 10% SDS in 0.01 M HCl was added per well to dissolve the dark blue formazan crystals. Optical density was estimated using an Enzyme-linked immunosorbent assay (ELISA) reader at a wavelength of 540 nm with a reference wavelength of 690 nm.

Clonogenic Assay for assessing clonogenic potential and radiation sensitivity

1000 cells were plated per 55 mm plate and were allowed to grow for 6-8 days until microscopically visible colonies formed. The cells were fixed by incubation in chilled methanol:acetic acid mixture (3:1) and the colonies were visualized by staining with 0.5% crystal violet. For radiation sensitivity determination, the cells were irradiated at a dose of 4 Gy (Cobalt-60 gamma irradiator, developed by Bhabha Atomic Research Centre, India) 16 h after seeding for the clonogenic assay.

Soft agar colony formation assay

7500 Daoy cells or 1000 D425 cells were seeded in DMEM /F-12 medium supplemented with 10% FBS

containing 0.3% agarose over a basal layer of 1% agarose in DMEM/F-12/10%FBS. The cells were incubated for about 3-4 weeks and the colonies formed were counted.

In vitro invasion assay

50,000-75000 cells were seeded in 200 µl of plain DMEM in the upper chamber of 8-µm pore size transwell inserts (BD Biosciences, San Hose, CA, USA) coated with Matrigel™, placed in a 24 well micro-titer plate. 750 µl of DMEM supplemented with 10% FBS was added to the lower chamber. The cells were allowed to migrate for 36-56 h and were labeled with Calcein AM (Life technologies, Carlsbad, CA, USA), a fluorescent dye, 1h prior to terminating the invasion. Non -invaded cells from the upper chamber were removed by wiping the upper portion of the insert with a cotton bud. The inserts were photographed using a Zeiss Axiovert 200M fluorescence microscope. Fluorescence intensity of the Calcein AM-labeled cells on the lower side of the insert was measured using a fluorescence reader using excitation wavelength of 488 nm and emission wavelength of 525 nm.

In vivo tumorigenicity assay using subcutaneous xenografts in immunodeficient mice

The experimental protocol was approved by the Institutional Animal ethics committee. 5 X 10^6 Daoy/D425 cells transduced with pTRIPZ-miR-148a construct were injected subcutaneously in the flanks of BALB/c Nude mice (CAnN.Cg-*Foxn1nu*/Crl strain received from Charles River, USA) following doxycycline induction for 72 h. Control cells transduced with pTRIPZ-NT construct were injected into the other flanks of the mice following doxycycline induction. Size of the tumors developed was measured using Vernier caliper at regular intervals over a period of 1-2 months.

In vivo tumorigenicity assay using orthotopic xenografts in immunodeficient mice

D283 polyclonal populations transduced with pTRIPZ-miR-148a construct were transfected with a pcDNA3.1 vector expressing firefly luciferase under CAG (CMV early enhancer/chicken beta-actin promoter) promoter. 2 X 10^5 cells were injected into the cerebellum of BALB/c Nude mice through 0.5 mm burr hole in the midline, 2 mm posterior to lambda at 2 mm depth, using small animal stereotaxic frame (Harvard Apparatus, Holliston, MA, USA). The tumor growth was monitored by *in vivo* bioluminescence imaging. At the time of imaging mice were anesthetized using Ketamine (90 mg/kg body weight) and, Xylazine (20 mg/kg body weight). Serial images of the mice were captured after intraperitoneal injection of D-Luciferin (150 mg/kg body weight) using IVIS Spectrum (Perkin-Elmer, Waltham, MA) *in vivo* imaging system until the peak luciferase activity was attained. The photon output from the image with peak luciferase activity was quantified by manually drawing region of interest (ROI) around the luminescent source using "Living Image" software and expressed in radiance (photons/sec/cm^2/steridian). A pseudo-color image representing light intensity (blue least intense and red most intense) was generated and superimposed over the gray scale reference image. All the animals were imaged on first and fourth week post intracranial injection.

Luciferase reporter Assay

3'-UTR (untranslated region) of each of the potential miRNA target genes was amplified from genomic DNA of normal human peripheral blood lymphocytes using Phusion Taq polymerase (Thermo scientific, Pittsburgh, PA, USA). The 3'-UTRs were then cloned downstream of firefly luciferase cDNA from PGL3 vector (Promega, Madison, WI, USA) in a pcDNA 4.0 plasmid vector (Invitrogen, Life Sciences, Carlsbad, CA, USA). The genomic region encoding miR-148a was cloned into pcDNA 3.0 plasmid vector wherein the miRNA was expressed under CMV promoter in mammalian cells. HEK 293T cells were transfected with the luciferase reporter plasmid, miRNA expressing plasmid and a plasmid vector expressing EGFP fluorescent protein by Calcium phosphate BES buffer method. Luciferase activity was assessed from the total protein extracted from the transfected HEK293T cells and was normalized against the EGFP fluorescence measured using Mithras LB940 multimode reader (Berthold Technologies, Bad Wildbad, Germany).

Western blotting

Total protein extracts of the medulloblastoma cell lines before and after expression of miR-148a, were separated by SDS-PAGE electrophoresis and blotted onto a PVDF membrane (Amersham-GE Healthcare Life Sciences, Mumbai, India). The membrane was then incubated with anti-NRP1 (#3725), anti-DNMT1 (#5119), anti-ROCK1 (#4035) antibody (Cell signaling technologies, Boston, MA, USA) or anti-γ-tubulin (T3559) antibody (Sigma-Aldrich, MO, USA) as per the manufacturer's instructions, followed by incubation with anti-rabbit IgG conjugated with Horse Radish Peroxidase and developed using SuperSignal West Pico chemiluminescent substrate (Pierce, Thermo Fischer scientific, Waltham, MA, USA). Protein expression levels were determined by intensity measurements of the bands corresponding to the proteins of interest using ImageJ software (imajeJ.nih.gov.in).

Immunohistochemical Analysis

5 µm sections of FFPE medulloblastoma tissues were deparaffinized, rehydrated and the antigen retrieval was done as per the protocol (www.cellsignal.com). Non-specific binding to the sections was blocked using 3% Bovine serum albumin (BSA) for 1 h. The sections were incubated in 1:100 diluted anti-NRP1 antibody (Cell signaling technologies, Boston, MA, USA) in 1% BSA overnight at 4ºC , followed by incubation with the peroxidase conjugated secondary anti-rabbit IgG (Pierce, Thermo Fischer scientific, Waltham, MA, USA). As a negative control, the sections were treated identically but without the primary antibody. The bound peroxidase signal was detected using 3, 3-' Diaminobenzidine as a substrate. The staining was visualized and photographed using Zeiss Upright fluorescent microscope Axioimager. Z1 and scored on the basis of the intensity and percentage of positive cells. . The scoring of the staining intensity by a neuropathologist blinded to the molecular subgroup or survival data.

Correlation of miR-148a and NRP1 expression with molecular sub-grouping and Survival

MiR-148a levels determined by real time RT-PCR analysis as described before were correlated with molecular sub-grouping of 141 FFPE medulloblastoma tumour tissues studied. The significance of the difference in miR-148a expression in the WNT subgroup tumors as compared to other medulloblastomas was evaluated by the Student's t test. NRP1 expression evaluated by immunohistochemical analysis was correlated with molecular sub-grouping. Kaplan-Meier survival analysis was done using GraphPad Prism version 5.01 software and the significance of the difference in the NRP1 high and NRP1 low groups was determined by Log-Rank test.

All the above experiments were performed at least in triplicate. Student's t test was performed to check for statistical significance of the difference in the performance of miR-148a expressing cells as compared to the control cells.

ACKNOWLEDGEMENTS

This work was financially supported by the Department of Biotechnology and Terry Fox Foundation, New Delhi, India. We thank Dr. Ratika Kunder for assistance in the manuscript preparation, Dr. Abhijit De for the CAG-luciferase construct and assistance in *in vivo* imaging analysis, Mr. Anant Sawant & Mr. Umesh Kadam for the technical assistance.

CONFLICT OF INTEREST

The authors have no conflict of interest.

REFERENCES

1. Rossi A, Caracciolo V, Russo G, Reiss K and Giordano A. Medulloblastoma: from molecular pathology to therapy. Clin Cancer Res. 2008; 14(4):971-976.
2. Taylor MD, Northcott PA, Korshunov A, Remke M, Cho YJ, Clifford SC, Eberhart CG, Parsons DW, Rutkowski S, Gajjar A, Ellison DW, Lichter P, Gilbertson RJ, Pomeroy SL, Kool M and Pfister SM. Molecular subgroups of medulloblastoma: the current consensus. Acta Neuropathol. 2012; 123(4):465-472.
3. Northcott PA, Jones DT, Kool M, Robinson GW, Gilbertson RJ, Cho YJ, Pomeroy SL, Korshunov A, Lichter P, Taylor MD and Pfister SM. Medulloblastomics: the end of the beginning. Nat Rev Cancer. 2012; 12(12):818-834.
4. Gokhale A, Kunder R, Goel A, Sarin R, Moiyadi A, Shenoy A, Mamidipally C, Noronha S, Kannan S and Shirsat NV. Distinctive microRNA signature of medulloblastomas associated with the WNT signaling pathway. J Cancer Res Ther. 2010; 6(4):521-529.
5. Kool M, Korshunov A, Remke M, Jones DT, Schlanstein M, Northcott PA, Cho YJ, Koster J, Schouten-van Meeteren A, van Vuurden D, Clifford SC, Pietsch T, von Bueren AO, Rutkowski S, McCabe M, Collins VP, et al. Molecular subgroups of medulloblastoma: an international meta-analysis of transcriptome, genetic aberrations, and clinical data of WNT, SHH, Group 3, and Group 4 medulloblastomas. Acta Neuropathol. 2012; 123(4):473-484.
6. Kunder R, Jalali R, Sridhar E, Moiyadi A, Goel N, Goel A, Gupta T, Krishnatry R, Kannan S, Kurkure P, Deopujari C, Shetty P, Biyani N, Korshunov A, Pfister SM, Northcott PA, et al. Real-time PCR assay based on the differential expression of microRNAs and protein-coding genes for molecular classification of formalin-fixed paraffin embedded medulloblastomas. Neuro Oncol. 2013; 15(12):1644-1651.
7. Lujambio A, Calin GA, Villanueva A, Ropero S, Sanchez-Cespedes M, Blanco D, Montuenga LM, Rossi S, Nicoloso MS, Faller WJ, Gallagher WM, Eccles SA, Croce CM and Esteller M. A microRNA DNA methylation signature for human cancer metastasis. Proc Natl Acad Sci U S A. 2008; 105(36):13556-13561.
8. Chen Y, Song YX and Wang ZN. The microRNA-148/152 family: multi-faceted players. Mol Cancer. 2013; 12:43.
9. Friedman HS, Burger PC, Bigner SH, Trojanowski JQ, Wikstrand CJ, Halperin EC and Bigner DD. Establishment and characterization of the human medulloblastoma cell line and transplantable xenograft D283 Med. J Neuropathol Exp Neurol. 1985; 44(6):592-605.

10. Aldosari N, Wiltshire RN, Dutra A, Schrock E, McLendon RE, Friedman HS, Bigner DD and Bigner SH. Comprehensive molecular cytogenetic investigation of chromosomal abnormalities in human medulloblastoma cell lines and xenograft. Neuro Oncol. 2002; 4(2):75-85.

11. Xu X, Fan Z, Kang L, Han J, Jiang C, Zheng X, Zhu Z, Jiao H, Lin J, Jiang K, Ding L, Zhang H, Cheng L, Fu H, Song Y, Jiang Y, et al. Hepatitis B virus X protein represses miRNA-148a to enhance tumorigenesis. J Clin Invest. 2013; 123(2):630-645.

12. Zhang R, Li M, Zang W, Chen X, Wang Y, Li P, Du Y, Zhao G and Li L. MiR-148a regulates the growth and apoptosis in pancreatic cancer by targeting CCKBR and Bcl-2. Tumour Biol. 2014; 35(1):837-844.

13. Zheng B, Liang L, Wang C, Huang S, Cao X, Zha R, Liu L, Jia D, Tian Q, Wu J, Ye Y, Wang Q, Long Z, Zhou Y, Du C, He X, et al. MicroRNA-148a suppresses tumor cell invasion and metastasis by downregulating ROCK1 in gastric cancer. Clin Cancer Res. 2011; 17(24):7574-7583.

14. Fujita Y, Kojima K, Ohhashi R, Hamada N, Nozawa Y, Kitamoto A, Sato A, Kondo S, Kojima T, Deguchi T and Ito M. MiR-148a attenuates paclitaxel resistance of hormone-refractory, drug-resistant prostate cancer PC3 cells by regulating MSK1 expression. J Biol Chem. 2010; 285(25):19076-19084.

15. Lopez-Bertoni H, Lal B, Li A, Caplan M, Guerrero-Cazares H, Eberhart CG, Quinones-Hinojosa A, Glas M, Scheffler B, Laterra J and Li Y. DNMT-dependent suppression of microRNA regulates the induction of GBM tumor-propagating phenotype by Oct4 and Sox2. Oncogene. 2014.

16. Li S, Chowdhury R, Liu F, Chou AP, Li T, Mody RR, Lou JJ, Chen W, Reiss J, Soto H, Prins R, Liau LM, Mischel PS, Nghiemphu PL, Yong WH, Cloughesy TF, et al. Tumor-Suppressive miR148a Is Silenced by CpG Island Hypermethylation in IDH1-Mutant Gliomas. Clin Cancer Res. 2014; 20(22):5808-5822.

17. Xu Q, Jiang Y, Yin Y, Li Q, He J, Jing Y, Qi YT, Xu Q, Li W, Lu B, Peiper SS, Jiang BH and Liu LZ. A regulatory circuit of miR-148a/152 and DNMT1 in modulating cell transformation and tumor angiogenesis through IGF-IR and IRS1. J Mol Cell Biol. 2013; 5(1):3-13.

18. Zhang J, Ying ZZ, Tang ZL, Long LQ and Li K. MicroRNA-148a promotes myogenic differentiation by targeting the ROCK1 gene. J Biol Chem. 2012; 287(25):21093-21101.

19. Ecke I, Petry F, Rosenberger A, Tauber S, Monkemeyer S, Hess I, Dullin C, Kimmina S, Pirngruber J, Johnsen SA, Uhmann A, Nitzki F, Wojnowski L, Schulz-Schaeffer W, Witt O and Hahn H. Antitumor effects of a combined 5-aza-2'deoxycytidine and valproic acid treatment on rhabdomyosarcoma and medulloblastoma in Ptch mutant mice. Cancer Res. 2009; 69(3):887-895.

20. Rossignol M, Gagnon ML and Klagsbrun M. Genomic organization of human neuropilin-1 and neuropilin-2 genes: identification and distribution of splice variants and soluble isoforms. Genomics. 2000; 70(2):211-222.

21. Jubb AM, Strickland LA, Liu SD, Mak J, Schmidt M and Koeppen H. Neuropilin-1 expression in cancer and development. J Pathol. 2012; 226(1):50-60.

22. Pellet-Many C, Frankel P, Jia H and Zachary I. Neuropilins: structure, function and role in disease. Biochem J. 2008; 411(2):211-226.

23. Klagsbrun M, Takashima S and Mamluk R. The role of neuropilin in vascular and tumor biology. Adv Exp Med Biol. 2002; 515:33-48.

24. Mamluk R, Gechtman Z, Kutcher ME, Gasiunas N, Gallagher J and Klagsbrun M. Neuropilin-1 binds vascular endothelial growth factor 165, placenta growth factor-2, and heparin via its b1b2 domain. J Biol Chem. 2002; 277(27):24818-24825.

25. Hu B, Guo P, Bar-Joseph I, Imanishi Y, Jarzynka MJ, Bogler O, Mikkelsen T, Hirose T, Nishikawa R and Cheng SY. Neuropilin-1 promotes human glioma progression through potentiating the activity of the HGF/SF autocrine pathway. Oncogene. 2007; 26(38):5577-5586.

26. Glinka Y and Prud'homme GJ. Neuropilin-1 is a receptor for transforming growth factor beta-1, activates its latent form, and promotes regulatory T cell activity. J Leukoc Biol. 2008; 84(1):302-310.

27. Pellet-Many C, Frankel P, Evans IM, Herzog B, Junemann-Ramirez M and Zachary IC. Neuropilin-1 mediates PDGF stimulation of vascular smooth muscle cell migration and signalling via p130Cas. Biochem J. 2011; 435(3):609-618.

28. Rizzolio S, Rabinowicz N, Rainero E, Lanzetti L, Serini G, Norman J, Neufeld G and Tamagnone L. Neuropilin-1-dependent regulation of EGF-receptor signaling. Cancer Res. 2012; 72(22):5801-5811.

29. Osada H, Tokunaga T, Nishi M, Hatanaka H, Abe Y, Tsugu A, Kijima H, Yamazaki H, Ueyama Y and Nakamura M. Overexpression of the neuropilin 1 (NRP1) gene correlated with poor prognosis in human glioma. Anticancer Res. 2004; 24(2B):547-552.

30. Rizzolio S and Tamagnone L. Multifaceted role of neuropilins in cancer. Curr Med Chem. 2011; 18(23):3563-3575.

31. Snuderl M, Batista A, Kirkpatrick ND, Ruiz de Almodovar C, Riedemann L, Walsh EC, Anolik R, Huang Y, Martin JD, Kamoun W, Knevels E, Schmidt T, Farrar CT, Vakoc BJ, Mohan N, Chung E, et al. Targeting placental growth factor/neuropilin 1 pathway inhibits growth and spread of medulloblastoma. Cell. 2013; 152(5):1065-1076.

32. Glinka Y, Stoilova S, Mohammed N and Prud'homme GJ. Neuropilin-1 exerts co-receptor function for TGF-beta-1 on the membrane of cancer cells and enhances responses to both latent and active TGF-beta. Carcinogenesis. 2011; 32(4):613-621.

33. Hayden Gephart MG, Su YS, Bandara S, Tsai FC, Hong J, Conley N, Rayburn H, Milenkovic L, Meyer T and Scott MP. Neuropilin-2 contributes to tumorigenicity in a

mouse model of Hedgehog pathway medulloblastoma. J Neurooncol. 2013; 115(2):161-168.

34. Hamerlik P, Lathia JD, Rasmussen R, Wu Q, Bartkova J, Lee M, Moudry P, Bartek J, Jr., Fischer W, Lukas J, Rich JN and Bartek J. Autocrine VEGF-VEGFR2-Neuropilin-1 signaling promotes glioma stem-like cell viability and tumor growth. J Exp Med. 2012; 209(3):507-520.

35. Glinka Y, Mohammed N, Subramaniam V, Jothy S and Prud'homme GJ. Neuropilin-1 is expressed by breast cancer stem-like cells and is linked to NF-kappaB activation and tumor sphere formation. Biochem Biophys Res Commun. 2012; 425(4):775-780.

36. Ellis LM. The role of neuropilins in cancer. Mol Cancer Ther. 2006; 5(5):1099-1107.

37. Miao HQ and Klagsbrun M. Neuropilin is a mediator of angiogenesis. Cancer Metastasis Rev. 2000; 19(1-2):29-37.

38. Chaudhary B, Khaled YS, Ammori BJ and Elkord E. Neuropilin 1: function and therapeutic potential in cancer. Cancer Immunol Immunother. 2014; 63(2):81-99.

39. Geretti E and Klagsbrun M. Neuropilins: novel targets for anti-angiogenesis therapies. Cell Adh Migr. 2007; 1(2):56-61.

40. Raskopf E, Vogt A, Standop J, Sauerbruch T and Schmitz V. Inhibition of neuropilin-1 by RNA-interference and its angiostatic potential in the treatment of hepatocellular carcinoma. Z Gastroenterol. 2010; 48(1):21-27.

41. Jia H, Cheng L, Tickner M, Bagherzadeh A, Selwood D and Zachary I. Neuropilin-1 antagonism in human carcinoma cells inhibits migration and enhances chemosensitivity. Br J Cancer. 2010; 102(3):541-552.

42. Nasarre C, Roth M, Jacob L, Roth L, Koncina E, Thien A, Labourdette G, Poulet P, Hubert P, Cremel G, Roussel G, Aunis D and Bagnard D. Peptide-based interference of the transmembrane domain of neuropilin-1 inhibits glioma growth in vivo. Oncogene. 2010; 29(16):2381-2392.

43. Patnaik A, LoRusso PM, Messersmith WA, Papadopoulos KP, Gore L, Beeram M, Ramakrishnan V, Kim AH, Beyer JC, Mason Shih L, Darbonne WC, Xin Y, Yu R, Xiang H, Brachmann RK and Weekes CD. A Phase Ib study evaluating MNRP1685A, a fully human anti-NRP1 monoclonal antibody, in combination with bevacizumab and paclitaxel in patients with advanced solid tumors. Cancer Chemother Pharmacol. 2014; 73(5):951-960.

44. Lu Y, Xiang H, Liu P, Tong RR, Watts RJ, Koch AW, Sandoval WN, Damico LA, Wong WL and Meng YG. Identification of circulating neuropilin-1 and dose-dependent elevation following anti-neuropilin-1 antibody administration. MAbs. 2009; 1(4):364-369.

45. Bader AG. miR-34 - a microRNA replacement therapy is headed to the clinic. Front Genet. 2012; 3:120.

46. Mosmann T. Rapid colorimetric assay for cellular growth and survival:application to proliferation and cytotoxic assays. J Immunol Methods. 1983; 65(1-2):55-63.